Universidade do Minho
Escola de Engenharia

Cátia Sofia Neves Braga

(nano)Materials for accelerating syntrophic fatty acids degradation to methane

Abril 2023

(nano)Materials for accelerating syntrophic fatty acids degradation to methane
Cátia Sofia Neves Braga
UMinho | 2023

Universidade do Minho
Escola de Engenharia

Cátia Sofia Neves Braga

(nano)Materials for accelerating syntrophic fatty acids degradation to methane

Tese de Doutoramento
Doutoramento em Engenharia Química e Biológica

Trabalho efetuado sob a orientação da
Doutora Andreia Filipa Ferreira Salvador Doutora Luciana José Ribeiro Pereira
E da
Professora Doutora Inês Antunes Cardoso Pereira

Abril 2023

DIREITOS DE AUTOR E CONDIÇÕES DE UTILIZAÇÃO DO TRABALHO POR TERCEIROS

ACKNOWLEDGEMENTS

During this journey, many people contributed with knowledge, inspiration, encouragement and support, making me grow professionally and personally. To all of them, I offer my gratitude.

To Professor Madalena Alves, for giving me the opportunity to join her incredible team (BRIDGE group), for pushing me out of my comfort zone and for the scientific inspiration that she gave in all the meetings where we discussed science. And thank you for the support during the development of this PhD project.

To my supervisors, Doctor Andreia Salvador, Doctor Luciana Pereira, and Professor Inês Pereira, for accepting being part of this project, and for helping and supporting me to accomplish the conclusion of this thesis. Thank you for sharing your scientific knowledge, for dedicating your time and for all the suggestions that contributed to this work.

To Andreia Salvador, for being more than my supervisor. For being a friend, for believing in my work and for not letting me fall when things went less well. Thank you for inspiring me in science and for being a person with such a big heart.

To Gilberto Martins, for all his expertise and contributions for the work developed. To Salomé Duarte and João Sequeira for gladly contributing with their expertise in different phases of this work. Thank you for your help and for being part of this project.

To all external collaborators that contributed to my PhD work, namely Professor Fernando Pereira (FEUP), Doctor Salomé Soares (FEUP), Professor Isabel Neves (UMinho) and Rui Fernandes (HEMS, i3S), thank you for the availability and the cooperation over this work.

To my colleagues and friends from BRIDGE, for the constant support, help and friendship. In particular to Salomé, Rita, Carla, Sónia and Sérgio, thank you for being such good friends and always being there for me at any time. Thank you to Ana Júlia Cavaleiro for also contributing with her expertise and for the advices given during the development of this project. And thank you to CEB and all the technical staff.

To my family, specially my mom and my sister, and my friends, specially Fi, Daniela Martins, Rita Sousa, and João Campos. Thank you for being always there for me. To Nelson, for being my partner, and for believing, supporting and encouraging me all the time. Thank you for being there for me too.

This PhD was supported by the Portuguese Foundation for Science and Technology (FCT) through the grants SFRH/BD/132003/2017 and COVID/BD/152431/2022, and by European Union, through the Portuguese State Budget and the European Social Fund under the scope of Norte2020 - Programa Operacional Regional do Norte. Entities supporting this work: FCT under the scope of the strategic funding of UIDB/04469/2020 unit, and LABBELS - associate laboratory in biotechnology and bioengineering and microelectromechanical systems. This research was also supported under the scope of the CM4Methane project (Ref: PTDC/BTA-BTA/2249/2021) financed by national funds through FCT, I.P.

STATEMENT OF INTEGRITY

I hereby declare having conducted this academic work with integrity. I confirm that I have not used plagiarism or any form of undue use of information or falsification of results along the process leading to its elaboration.

I further declare that I have fully acknowledged the Code of Ethical Conduct of the University of Minho.

RESUMO

O metano é produzido a partir de uma ampla diversidade de resíduos orgânicos por comunidades microbianas anaeróbias, onde as relações sintróficas desempenham um papel determinante na eficiência do processo. Os mecanismos de transferência de eletrões interespécies (IET) podem envolver a troca de transportadores de eletrões (hidrogénio, formato), mas também a transferência direta de eletrões entre espécies (DIET). Os materiais condutores melhoram as taxas de produção de metano (MPR), mas os mecanismos envolvidos nessa IET mediada pelos materiais ainda são controversos e não totalmente conhecidos. Nesta tese, investigou-se o efeito de vários (nano)materiais, nomeadamente carvão ativado (AC), magnetite (Mag), nanotubos de carbono (CNT), AC/CNT modificados, zeólito (Zeo), areia e esferas de vidro, na produção de metano (MP). Apesar das diferenças a nível físico-químico, em geral, os (nano)materiais aumentaram as atividades metanogénicas, diminuindo as fases de latência que antecedem a MP e aumentando as MPR. As diversas características físico-químicas dos (nano)materiais, como a área de superfície específica, a área dos mesoporos, o volume dos microporos, a condutividade elétrica, a acidez/basicidade do material e as impurezas presentes na sua composição (por exemplo, S e N), isoladamente não conseguem explicar as melhorias observadas na MP. O silício foi um elemento encontrado em todos os materiais testados e melhorou a MP por mecanismos ainda desconhecidos, que merecem ser investigados. As mudanças observadas no potencial redox do meio de crescimento na presença de (nano)materiais não se correlacionaram diretamente com a melhoria na MP. Além disso, diferentes (nano)materiais podem afetar de forma diferente o mesmo microrganismo metanogénico. Por exemplo, o *Methanobacterium formicicum* foi bastante estimulado pelo AC e drasticamente inibido pela Mag. Contudo, o mesmo (nano)material não afetou outras espécies da mesma forma. Por exemplo, o Zeo melhorou a MPR do *M. formicicum* (a crescer em H_2/CO_2) e da *Methanothrix harundinacea* (a crescer em acetato), mas não teve efeito sobre a MP do *Methanospirillum hungatei* (a crescer em H_2/CO_2) e da *M. barkeri* (a crescer em acetato). Os resultados sugerem ainda que as espécies microbianas são afetadas diferencialmente, independentemente do tipo de substrato. O efeito dos (nano)materiais também varia dependendo da cocultura sintrófica, uma vez que o AC aumentou a atividade metanogénica da cocultura sintrófica *Syntrophomonas zehnderi* e *M. formicicum*, mas a Mag causou uma drástica inibição. Já noutra cocultura, constituída por *Syntrophomonas wolfei* e *M. hungatei*, o AC e a Mag não causaram impacto significativo. A atividade microbiana também parece influenciar o efeito dos (nano)materiais, já que melhorias significativas foram observadas principalmente por culturas menos ativas. Por exemplo, o AC melhora as MPR do *M. formicicum* quando adicionado na altura da inoculação, mas não teve efeito quando adicionado a culturas ativas deste microrganismo durante a fase de crescimento exponencial. Esta relação entre a atividade microbiana e o efeito dos (nano)materiais também foi observada em enriquecimentos microbianos e no bioreator operado em contínuo. A composição microbiana dos enriquecimentos especializados na degradação de butirato e desenvolvidos com e sem (nano)materiais foi diferente, e não foram enriquecidas espécies eletroativas (tais como *Geobacter* spp.) na presença dos materiais. Análises microscópicas, taxonómicas e de expressão genética sugerem que a conversão de butirato a hidrogénio e acetato foi efetuada por microrganismos do género *Syntrophomonas*, e nenhum gene relacionado com DIET foi detetado.

Palavras-chave: Ácidos gordos; Interações sintróficas; Metano; (nano)Materiais; Transferência de electrões interespécies.

ABSTRACT

Methane is produced from a wide diversity of organic wastes by anaerobic microbial communities, where syntrophic relationships play a key role in the efficiency of the process. Interspecies electron transfer (IET) mechanisms may involve the exchange of electron carriers (hydrogen, formate), but also direct interspecies electron transfer (DIET). Conductive materials improve methane production rates (MPR), but the mechanisms involved in this material mediated IET are still controversial and not fully known. In this thesis, the effect of several (nano)materials, namely activated carbon (AC), magnetite (Mag), carbon nanotubes (CNT), modified AC/CNT, zeolite (Zeo), sand and glass beads, on methane production (MP) was investigated. Despite their physicochemical differences, generally, (nano)materials enhanced methanogenic activities, by decreasing lag phases preceding MP and increasing MPR. The various physicochemical characteristics of (nano)materials, such as the specific surface area, area of mesopores, volume of micropores, electrical conductivity, material acidity/basicity, and impurities present on material composition (e.g., S and N) could not explain per se the enhancement observed on MP. Silicon was an element found in all materials tested and, per se, improved MP by mechanisms yet unknown, which deserve to be further explored. The changes observed on redox potential of the growth medium in the presence of (nano)materials were not directly correlated with the improvement of MP. Besides, different (nano)materials can impact differently the same methanogen. For example, *Methanobacterium formicicum* was greatly stimulated by AC and drastically inhibited by Mag. However, the same (nano)material did not impact all species in the same way. For instance, Zeo improved MPR by *M. formicicum* (growing on H_2/CO_2) and *Methanothrix harundinacea* (growing on acetate) but had no effect on MP by *Methanospirillum hungatei* (growing on H_2/CO_2) and *M. barkeri* (growing on acetate). These results likewise suggest that microbial species are differentially affected, independently of the type of substrate. The effect of (nano)materials also varies depending on the syntrophic coculture, since AC enhanced the methanogenic activity of the syntrophic coculture *Syntrophomonas zehnderi* and *M. formicicum*, but Mag caused severe inhibition. Yet, in another coculture, composed by *Syntrophomonas wolfei* with *M. hungatei,* AC and Mag did not cause significant impact. The microbial activity also seems to dictate the effect of (nano)materials, as significant improvements were mainly observed by less active cultures. For instance, AC generally improved MPR of *M. formicicum* cultures, but had no effect when added to highly active *M. formicicum* cultures during the exponential growth phase. This relation between microbial activity and the effect of (nano)materials was also observed in enrichment cultures and in the continuous bioreactor. Microbial composition of butyrate-degrading enrichments developed with and without (nano)materials was different, but electroactive species (e.g., *Geobacter*) were not enriched in the presence of any material. Microscopic, taxonomic and gene expression analyses suggested that butyrate conversion to hydrogen and acetate occurred by microorganisms closed related to *Syntrophomonas*, and no genes related to DIET were detected.

Keywords: Fatty acids; Interspecies electron transfer; Methane; (nano)Materials; Syntrophic interactions.

TABLE OF CONTENTS

LIST OF FIGURES

List of Figures - Appendix

LIST OF TABLES

List of Tables - Appendix

LIST OF ABBREVIATIONS

AC	Activated carbon
AC_{b1}	Activated carbon from batch 1
AC_{b2}	Activated carbon from batch 2
AC_{b3}	Activated carbon from batch 3
Ack	Acetate kinase
Acs	Acetyl-CoA decarbonylase/synthetase
Act	Acetyl-CoA acetyltransferase
AC-b1	Stable and well-adapted butyrate-degrading enrichment with activated carbon from the first batch of experiments
AC_HNO_3	Activated carbon oxidized with nitric acid
AC_HNO_3_400	Activated carbon oxidized with nitric acid at 400 °C
AC_HNO_3_600	Activated carbon oxidized with nitric acid at 600 °C
AC_HNO_3_900	Activated carbon oxidized with nitric acid at 900 °C
AC_H_2SO_4	Activated carbon treated with sulfuric acid
AC_H_2SO_4_ HNO_3	Activated carbon treated with H_2SO_4 and HNO_3
AC_N	Activated carbon thermal treated with nitrogen flow
AC@2%Fe	Activated carbon impregnated with 2 % of iron, calcinated and reduced at 400 °C
AD	Anaerobic digestion
AGS	Anaerobic granular sludge
Ak	Acetate kinase
ANOVA	Single factor analysis of variances
ASi	Silicic acid in aqueous solution
At	Phosphate acetyltransferase
AtoB	Acetyl-CoA C-acetyltransferase
ATPase	ATP synthase
Bcd	Butyryl-CoA dehydrogenase
BET	Brunauer-Emmett-Teller
B-AC-1	Enrichment culture with activated carbon, first incubation
B-AC-2	Enrichment culture with activated carbon, second incubation (1st transfer)
B-Mag-1	Enrichment culture with magnetite, first incubation
B-Mag-2	Enrichment culture with magnetite, second incubation (1st transfer)
B-without-AC-Mag-1	Enrichment culture without activated carbon or magnetite, first incubation
B-without-AC-Mag-2	Enrichment culture without activated carbon or magnetite, second incubation (1st transfer)
B-without-Zeo-1	Enrichment culture without zeolite, first incubation
B-without-Zeo-2	Enrichment culture without zeolite, second incubation (1st transfer)
B-Zeo-1	Enrichment culture with zeolite, first incubation

B-Zeo-2	Enrichment culture with zeolite, second incubation (1st transfer)
Bty-b1	Stable and well-adapted butyrate-degrading enrichment without materials from the first batch of experiments
Bty-b2	Stable and well-adapted butyrate-degrading enrichment without materials from the second batch of experiments
C	Concentration
C_{H2}	Initial concentration of hydrogen
c1	Low concentration of substrate
c2	High concentration of substrate
CIET	Conductive material mediated interspecies electron transfer
CM	Conductive materials
CNT	Carbon nanotubes
CNT@2%Fe	Carbon nanotubes impregnated with 2 % of iron, calcinated and reduced at 400 °C
CoA	Coenzyme A
CoB	Coenzyme B
COD	Chemical oxygen demand
Codh	Carbon-monoxide dehydrogenase
Codh-Acs	Carbon monoxide dehydrogenase/acetyl-CoA decarbonylase/synthase complex
CODrem	Chemical oxygen demand removal
CoM	Coenzyme M
Ctr	Crotonyl-CoA hydratase
CV	Cyclic voltammetry
DIET	Direct interspecies electron transfer
EA	Elemental analysis
EC	Enzyme commission number
Ech	Energy-converting hydrogenase
EDS	Energy dispersive spectrometry
EET	Extracellular electron transfer
EGSB	Expanded granular sludge bed
Eha	Energy-converting hydrogenase A
EIS	Electrochemical impedance spectroscopy
EMPR	Exponential methane production rates
Etf	Electron transfer flavoprotein
EtfAB	Electron transfer flavoproteins A and B
e-pili	Electrically conductive pili
Fd	Ferredoxin
FD_{ox}	Oxidized ferredoxin
Fd_{red}	Reduced ferredoxin
Fdh	Formate dehydrogenase
Fdh1, Fdh3	Formate dehydrogenases (1 and 3)

Fdh2, Fdh4	NADH dependent formate dehydrogenases (membrane bound, quinone reducing)
FeS	Complex membrane bound FeS-oxidoreductase
FID	Flame ionization detector
FISH	Fluorescence *in situ* hybridizing
Fnt	Formate transporter
Fpo	$F_{420}H_2$ dehydrogenase
Frh	Coenzyme F_{420}-reducing hydrogenase
Ftr	Formyl-methanofurantetrahydromethanopterin formyl-transferase
Fwd	Formyl-methanofuran dehydrogenase
GAC	Granular activated carbon
GC	Gas chromatography
HbdH	3-hydroxybutyryl-CoA dehydrogenase
Hdr	Soluble heterodisulfide reductase
HdrDE	Membrane-bound heterodisulfide reductase (acetoclastic metabolism)
Hmd	H_2-dependent methylenetetrahydromethanopterin dehydrogenase
HPLC	High performance liquid chromatography
HRT	Hydraulic retention time
Hyd1	Electron confurcating (NADH-dependent) hydrogenase
Hyd2	Membrane-bound [FeFe]-hydrogenase
Hyd3	Ferredoxin dependent hydrogenase
H_4MPT	Tetrahydromethanopterin
IET	Interspecies electron transfer
IFT	Interspecies formate transfer
IHT	Interspecies hydrogen transfer
IMPR	Initial methane production rates
Inoc-b1	Inoculum for the first batch of experiments with enrichment cultures
Inoc-b2	Inoculum for the second batch of experiments with enrichment cultures
LCFA	Long chain fatty acids
LessAct	Less active
LessAct-B-AC-1a	Less active enrichment developed with activated carbon during 2nd transfer, bottle a
LessAct-B-AC-1b	Less active enrichment developed with activated carbon during 2nd transfer, bottle b
LessAct-B-AC-2a	Less active enrichment developed with activated carbon during 3rd transfer, bottle a
LessAct-B-AC-2b	Less active enrichment developed with activated carbon during 3rd transfer, bottle b
LessAct-B-Mag-1a	Less active enrichment developed with magnetite during 2nd transfer, bottle a
LessAct-B-Mag-1b	Less active enrichment developed with magnetite during 2nd transfer, bottle b

LessAct-B-Mag-2a	Less active enrichment developed with magnetite during 3rd transfer, bottle a
LessAct-B-Mag-2b	Less active enrichment developed with magnetite during 3rd transfer, bottle b
LessAct-B-without-AC-Mag-1a	Less active enrichment developed without activated carbon or magnetite during 2nd transfer, bottle a
LessAct-B-without-AC-Mag-1b	Less active enrichment developed without activated carbon or magnetite during 2nd transfer, bottle b
LessAct-B-without-AC-Mag-2a	Less active enrichment developed without activated carbon or magnetite during 3rd transfer, bottle a
LessAct-B-without-AC-Mag-2b	Less active enrichment developed without activated carbon or magnetite during 3rd transfer, bottle b
LessAct-B-without-Zeo-1b	Less active enrichment developed without zeolite during 4th transfer, bottle b
LessAct-B-Zeo-1a	Less active enrichment developed with zeolite during 4th transfer, bottle a
Mag	Magnetite
Mag-b1	Stable and well-adapted butyrate-degrading enrichment with magnetite from the first batch of experiments
Mcr	Methyl-coenzyme M reductase
McrABG	Methyl-coenzyme M reductase ABG
Mch	Methenyl-tetrahydromethanopterin cyclohydrolase
Mer	5,10- methylenetetrahydromethanopterin reductase
MFR	Methanofuran
MoreAct	More active
MoreAct-B-AC-3	Well adapted butyrate-degrading enrichment culture developed with activated carbon after 9 transfers (methane only produced via hydrogenotrophic pathway)
MoreAct-B-Mag-3	Well adapted butyrate-degrading enrichment culture developed with magnetite after 8 transfers (methane only produced via hydrogenotrophic pathway)
MoreAct-B-without-AC-Mag-3	Well adapted butyrate-degrading enrichment culture developed without activated carbon or magnetite after 9 transfers (methane only produced via hydrogenotrophic pathway)
MP	Methane production
MPh	Methanophenazine
MPR	Methane production rates
MQ	Menaquinone (or methylnaphthoquinone)
Mtd	Methylene-tetrahydromethanopterin dehydrogenase
Mtr	Methyl-H_4MPT:CoM methyltransferase (hydrogenotrophic metabolism)
MtrA-H	Tetrahydromethanopterin S-methyltransferase (acetoclastic metabolism)
Mvh	F_{420}-non-reducing hydrogenase
MWCNT	Multiwalled carbon nanotubes
n	Number of transfers performed in microbial enrichment studies

nc	Not calculated
nd	Not detected
Non-CM	Non-conductive materials
OLR	Organic loading rate
ORP	Oxidation reduction potential (redox potential)
PAC	Powdered activated carbon
pH_{pzc}	pH at the zero point charge
Pta	Phosphate acetyltransferase
rGO	Reduced graphene oxide
S_{BET}	Specific surface area
SEM	Scanning electron microscope
SMA	Specific methanogenic activity
S_{meso}	Mesopore surface area
STP	Standard temperature and pressure conditions
t	Time of incubation
TEM	Transmission electron microscopy
TS	Total solids
VFA	Volatile fatty acids
Vh0	Nickel-iron-sulfur haemoprotein
V_{micro}	Micropore volume
Vp	Pore volume
VS	Volatile solids
VSS	Volatile suspended solids
$V_{p\ P/P0=0.95}$	Total pore volume
Zeo	Zeolite
Zeo-b2	Stable and well-adapted butyrate-degrading enrichment with zeolite from the second batch of experiments
ZVI	Zero-valent iron
ΔG^0	Gibbs free energy
λ	Lag phase

CHAPTER 1

1. THESIS SCOPE

1.1. CONTEXT

The application of (nano)materials is a promising strategy to boost methane production (MP) in anaerobic digestion (AD), by accelerating the anaerobic conversion of waste into methane. This strategy should contribute for the emergent energy transition occurring in European Union, which aims a clean energy system, and the independence from external gas providers. High capital investments are being applied to improve biogas production and biogas upgrading to biomethane, in order to reach 35 billion cubic meters of biomethane by 2030, to mitigate the impact of the current rising energy prices (Comission, 2022a, 2022b). AD offers innumerous advantages, beginning by the valorization of organic waste, which is the low-cost carbon source, used for biogas generation. Sustainable feedstocks such as animal manure, domestic or agricultural organic wastes, or industrial wastewaters are continuously generated and thus do not represent a limitation to reach the European Union target (Alberici et al., 2022). The waste conversion rates however, might be low, and strategies to enhance AD efficiency are needed. Therefore, research on biogas production and specifically on new emerging technologies that can significantly accelerate the transformation of biowaste to biomethane is paramount to contribute to a green transition in Europe. Because some conductive materials (CM) were found to accelerate anaerobic reactions and MP, their application in AD may be the key for providing a faster and efficient energy transition. On the other hand, methane is a powerful greenhouse gas, being naturally produced in anaerobic environments, like freshwater sediments, where CM are also naturally present (Amelia-Elena et al., 2018; Stams and Plugge, 2009). For example, minerals, like iron oxides, or black carbons are naturally present in nature, and the anthropogenic activity can even increase the input of CM in sediments (e.g., nutrient management of soils with conductive chars) (Amelia-Elena et al., 2018). Consequently, CM might also contribute for the increase of atmospheric methane emissions (Amelia-Elena et al., 2018). Small alterations in methane emissions can result in significant impacts on climate change, influencing the dynamics of ecosystems (Morris et al., 2013). Thus, having methanogenesis a central role in the geomicrobial cycle of carbon in nature, the potential acceleration in the methane production rates (MPR) is also a matter of global awareness.

There are several knowledge gaps in the global understanding of CM in methane production in natural and engineered AD processes. For example, the environmental implications of applying such materials in AD processes are not known, and it is still not clear the mechanisms by which some CM enhance MP. One possible mechanism is the shift of the interspecies electron transfer (IET) from the typical exchange of soluble molecules, such as H_2 and formate, to interspecies electron transfer mediated via CM which could be more efficient. However, changes in IET cannot completely explain MP improvements, since the

methanogenic activity of pure cultures of methanogens is also enhanced by carbon nanotubes (CNT) (Salvador et al., 2017). The effect of (nano)materials in the electron transfer mechanisms is an emerging and fascinating field of research that has been pushed exponentially in the last years, and deserves to be further investigated, focusing on both applied and fundamental issues. This thesis is focused on respond to the following research questions:

1) Which type of (nano)materials affect most MP from butyrate, acetate, and H_2/CO_2?
2) What are the main reasons for the acceleration of MPR by (nano)materials?

   Hypothesis 1: The influence of physicochemical properties like surface area, porosity, electrical conductivity, material acidity/basicity, or of some impurities present on material composition that can be used by the microbial cultures?

   Hypothesis 2: The alteration of the growth medium parameters (e.g., redox potential (ORP)) by the presence of (nano)materials?

   Hypothesis 3: None of the above? Or all?
3) Which groups of methanogens experience an improvement on their methanogenic activity by exposure to (nano)materials?

   Hypothesis 1: Is the effect related, or not, with the type of methanogenic group (i.e., acetoclastic or hydrogenotrophic)?

   Hypothesis 2: The effect of (nano)materials is species specific?

   Hypothesis 3: Different types of (nano)materials will affect differently the methanogenic activity of the same microorganism?
4) How microbial communities evolve in the presence or absence of (nano)materials?

   Hypothesis 1: Will electroactive bacteria be enriched in contact with CM?

   Hypothesis 2: Would fatty acids conversion to methane be more efficient in the presence of (nano)materials?

   Hypothesis 3: The IET mechanisms will be affected in the presence of CM?
5) Continuous anaerobic bioreactors treating synthetic fatty acid-rich wastewater will be enhanced in the presence of CM?

1.2. AIMS

The main goal of this PhD work was to assess the influence of (nano)materials with distinct physicochemical properties on the MPR by pure cultures of hydrogenotrophic and acetoclastic methanogens, syntrophic cocultures, enriched microbial cultures and even complex microbial

communities in anaerobic bioreactors. For that, the effect of different materials – CNT, activated carbon (AC), magnetite (Mag), zeolite (Zeo), sand, glass beads - in anaerobic systems of increasing complexity was investigated. The objectives were to accelerate the MP, while identifying the main mechanisms involved in the improvement of volatile fatty acids (VFA) conversion to methane. Metabolic changes and interspecies microbial interactions, as well as microbial-material interactions were investigated using different approaches, such as by measuring the methanogenic activities and by using metatranscriptomics analysis and electronic microscopy techniques.

1.3. THESIS OUTLINE

This thesis is divided into 7 chapters, starting with Chapter 1, where the contextualization and the motivations to pursue this research topic is presented, the objectives are exposed, the thesis outline is presented, and the scientific outputs are listed as well. A literature review is given in Chapter 2, emphasizing on IET mechanisms, biochemistry and microbiology of syntrophic butyrate degradation, effects of (nano)materials in systems of different complexity, and a brief summary of methodologies that could be used to study microbial interactions with (nano)materials. In Chapter 3, the pure culture *Methanobacterium formicicum* was incubated with several types of (nano)materials to investigate the influence of different physicochemical properties of materials towards its methanogenic activity. The selection of materials and concentrations to be used in the other experiments were based on the results obtained in this chapter. In Chapter 4, the effect of AC, Mag and Zeo was investigated in different pure cultures of hydrogenotrophic (*M. formicicum*, *Methanospirillum hungatei*) and acetoclastic (*Methanosaeta harundinacea*, *Methanosarcina barkeri*) methanogens, to investigate if the effect of (nano)materials is related or not with the type of methanogenic group. This chapter also include the study of these materials towards the syntrophic metabolism of *Syntrophomonas zehnderi* and *M. formicicum* coculture growing on oleate, and *Syntrophomonas wolfei* with *M. hungatei* coculture growing on butyrate. In Chapter 5, the activity of microbial communities is shown as a factor determinant for the impact of (nano)materials towards MP. In Chapter 6, anaerobic complex microbial communities were enriched in specialized butyrate-degrading microorganisms with different (nano)materials (i.e., AC, Mag and Zeo). The microbial interactions and enzyme's activities in AC-enrichment cultures were assessed by metatranscriptomics analysis. In Chapter 7, the main findings and conclusions of this work are highlighted, and suggestions for future work with (nano)materials in anaerobic systems are given.

1.4. SCIENTIFIC OUTPUTS

The important achievements obtained during the experimental and research work presented in this thesis were (and will be further) disseminated through publication of manuscripts in ISI peer reviewed journals as well as through presentation in national and international scientific conferences.

Manuscripts submitted:

1. C.S.N. Braga, M. Martins, O.S.G. Soares, M.F.R. Pereira, I.A.C. Pereira, L. Pereira, M.M. Alves, A.F. Salvador. (2023). Methane production rate by pure cultures of methanogens and by syntrophic cocultures is regulated by activated carbon, magnetite and one type of a zeolite. Submitted on 29 march 2023 in the Journal of Environmental Chemical Engineering.

Manuscripts in preparation:

1. Braga, Cátia S.N., Salvador, Andreia F., Sequeira, João C., Duarte, M. Salomé., Martins, Gilberto, Pereira, Soares, O. Salomé G. P., M. Fernando R., Pereira, Inês A. C., Pereira, Luciana, Alves, M. Madalena. (2023). The activity of microbial communities dictates the effect of activated carbon, magnetite and zeolite on boosting methane production.
2. Braga, Cátia S.N., Salvador, Andreia F., Duarte, M. Salomé., Martins, Gilberto, Pereira, Soares, O. Salomé G. P., M. Fernando R., Pereira, Inês A. C., Pereira, Luciana, Alves, M. Madalena. (2023). Conductive materials modulate microbial communities and accelerate methane production from butyrate without changing interspecies electron transfer mechanisms.

Papers in peer-reviewed ISI journals as co-author:

1. A.R. Silva, A.J. Cavaleiro, O.S.G.P. Soares, C.S.N. Braga, A.F. Salvador, M.F.R. Pereira, M.M. Alves, L. Pereira. (2021). Detoxification of Ciprofloxacin in an Anaerobic Bioprocess Supplemented with Magnetic Carbon Nanotubes: Contribution of Adsorption and Biodegradation Mechanisms. International Journal of Molecular Sciences, 22, 2932. doi:10.3390/ijms22062932.

Oral communications in international conferences as a speaker:

1. Braga, Cátia S.N.; Salvador, Andreia F.; Duarte, M. Salomé; Martins, Gilberto; Pereira, Luciana; Pereira, M. Fernando R.; Soares, O. Salomé G. P.; Pereira, Inês C.; Alves, M. Madalena. Differential effects of carbon-based and iron-based conductive materials in anaerobic butyrate-degrading enrichments. 4th International Conference on Biogas Microbiology. Braga, Portugal, May 9th-11th, Oral communication within Biotransformations theme (OC-BT-09), 2022.
2. Braga, Cátia S.N.; Salvador, Andreia F.; Martins, Gilberto; Pereira, Luciana; Soares, O. Salomé G. P.; Pereira, M. Fernando R.; Pereira, Inês C.; Alves, M. Madalena. Effects of conductive and

non-conductive materials on the activity of a hydrogenotrophic methanogen. ISAM 2021 Online - International Symposium on Anaerobic Microbiology. No. 104, Innsbruck, Austria, June 16-17, 2021.

Oral communications in scientific meetings as a speaker:

1. Pitch oral communication: "Acceleration of methane production with conductive materials". CEB Scientific Biennial Meeting, Campus de Gualtar, Braga, Portugal, May 16, 2022.
2. Oral communication invitation: Nano scale investigation - "Effects of carbon nanotubes and magnetite on the activity of the methanogen *Methanobacterium formicicum*". Jornadas de Engenharia Biológica XXIII, Centre of Biological Engineering, University of Minho (Braga, Portugal) (Online event), December 04, 2020.

Oral communications in international conferences as co-author:

1. Alves, M. Madalena; Braga, Cátia S.N.; Martins, Gilberto; Pereira, Luciana; Pereira, M. Fernando R.; Soares, O. Salomé G. P.; Pereira, Inês C., Salvador, Andreia F. Race on electron transfer in anaerobic processes. Keynote lecture within the theme "Inspiring Anaerobic Biotechnologies through Microbiology Research". 17th World Congress on Anaerobic Digestion. Ann Arbor, Michigan, USA, 17-22 June, 2022.

Posters in national and international conferences:

1. Braga, Cátia S.N.; Salvador, Andreia F.; Martins, Gilberto; Pereira, Luciana; Pereira, M. Fernando R.; Soares, O. Salomé G. P.; Pereira, Inês C.; Alves, M. Madalena. Pure cultures of hydrogenotrophic methanogens are affected by modified activated carbons, zeolite, sand and glass beads. Electromicrobiology 2021. Aarhus, Denmark, November 3rd-5th, P54, 2021.
2. Martins, Gilberto; Braga, Cátia S.N.; Salvador, Andreia F.; Pereira, Luciana; Pereira, M. Fernando R.; Soares, O. Salomé G. P.; Pereira, Inês C.; Alves, M. Madalena. Zeolite stimulates the activity of microbial enrichments converting butyrate to methane. Electromicrobiology 2021. Aarhus, Denmark, November 3rd-5th, P53, 2021.
3. Salvador, Andreia F.; Braga, Cátia S.N.; Duarte, Maria Salomé; Martins, Gilberto; Pereira, Luciana; Pereira, M. Fernando R.; Soares, O. Salomé G. P.; Pereira, Inês C.; Alves, M. Madalena. Modulation of butyrate-degrading methanogenic communities by conductive materials. Electromicrobiology 2021. Aarhus, Denmark, November 3rd-5th, P52, 2021.
4. Braga, Cátia S.N.; Salvador, Andreia F.; Martins, Gilberto; Pereira, Luciana; Soares, O. Salomé G. P.; Pereira, M. Fernando R.; Pereira, Inês C.; Alves, M. Madalena. Activated carbon and magnetite affect the methanogenic activity of acetoclastic and hydrogenotrophic methanogens.

DCE21 - Doctoral Congress in Engineering - 4th Symposium on Chemical and Biological Engineering. Porto, Portugal, June 28-29, 189-190, 2021. ISBN: 978-972-752-282-8.

5. Faria, Juliana; Rocha, Ana; Duarte, Maria Salomé; Braga, Cátia S.N.; Fonseca, António M.; Neves, Isabel C.; Alves, M. Madalena. Effect of zeolite nanomaterials in methanogenic communities. XXVII Encontro Nacional da Sociedade Portuguesa de Química. No. P27, Braga, Portugal, July 14-16 julho, 232, 2021.
6. Alves, M. Madalena; Braga, Cátia S.N.; Martins, Gilberto; Salvador, Andreia F.; Pereira, M.F.R.; Pereira, Luciana; Soares, O.S.G.P.; Cavaleiro, Ana Júlia; Pereira, M. Alcina; Stams, Alfons J.M. Conductive materials affect methanogenic activity of pure cultures of methanogens and syntrophic cocultures. Electromicrobiology 2019. No. P1, Aarhus, Denmark, March 21-22, 36, 2019.

CHAPTER 2

2. General Introduction

Conductive (nano)materials, like activated carbon (AC), magnetite (Mag), and carbon nanotubes (CNT), have been applied in anaerobic digestion (AD) processes with the aim of enhancing the efficiency of methane production (MP) during the degradation of organic wastes. Previous research suggested that interspecies electron transfer (IET) mechanisms may change in the presence of conductive materials (CM), but this cannot explain the improvements observed in methanogenic pure cultures. This chapter provides a contextualization about the syntrophic relationships in AD processes and the mechanisms known for IET. A literature review is also presented for the application and the effects of CM in systems of different complexity, i.e., from pure cultures of methanogens to complex microbial communities. A general overview is given for the main possible mechanisms reported in the literature when carbon- and iron-based materials, and also zeolites (Zeo), are applied in anaerobic environments. Finally, some methodologies considered important to study anaerobic systems in the presence of (nano)materials are presented.

2.1. SYNTROPHIC INTERACTIONS IN ANAEROBIC DIGESTION PROCESSES

Anaerobic digestion is a biotechnology process where biomethane, a renewable biofuel, is produced during the treatment of organic wastes. The conversion of wastes to methane is accomplished through a sequence of four steps, namely hydrolysis, acidogenesis, acetogenesis and methanogenesis (Borja et al., 2011). It is a complex biological process that involves the activity of different microbial groups, i.e., hydrolytic, acidogenic and acetogenic bacteria, and methanogenic archaea (Figure 2.1) (Borja et al., 2011; Stams et al., 2012). Methanogens are dependent on acetogenic bacteria which convert a wide range of organic compounds to their simple substrates, i.e., H_2/CO_2, formate and acetate, which are used by methanogens to produce methane (Whitman et al., 2006). But acetogens are dependent on methanogens as well. The acetogenic reactions, like the oxidation of volatile fatty acids (VFA) to acetate and H_2/CO_2, are thermodynamically unfavourable (Table 2.1) (Moraes et al., 2015; Zhang et al., 2023). For instance, the Gibbs free energy change of butyrate reaction is positive (+48 kJ per mole of butyrate oxidized) under standard conditions (pH 7, 1 atm of H_2 and 1 mmol·L^{-1} of acetate and butyrate (Sieber et al., 2012)). Butyrate degradation becomes thermodynamically favourable only when hydrogen and formate concentrations are maintained at low levels as they are consumed by methanogens, with a Gibbs free energy change of -39 kJ per mole of butyrate (1 Pa of H_2 partial pressure and 0.1 mmol·L^{-1} of butyrate and acetate) (Sieber et al., 2012). This mutualistic interaction is known as syntrophy, where the intermediates that are exchanged between the syntrophic partners must be maintained at very low concentrations to keep occurring an efficient cooperation among partners (Sieber et al., 2012). By removing hydrogen from the system, methanogens maintain the hydrogen partial pressure at low levels, which is a favourable condition to keep acetogenic reactions to occur, while the acetogenic bacteria provide the methanogenic substrates as a product of their metabolism (Shen et al., 2016). This is a mutual dependent relationship, since specific organic compounds cannot be degraded by neither the bacterium nor the archaeon alone (J R Sieber et al., 2010; Stams and Plugge, 2009).

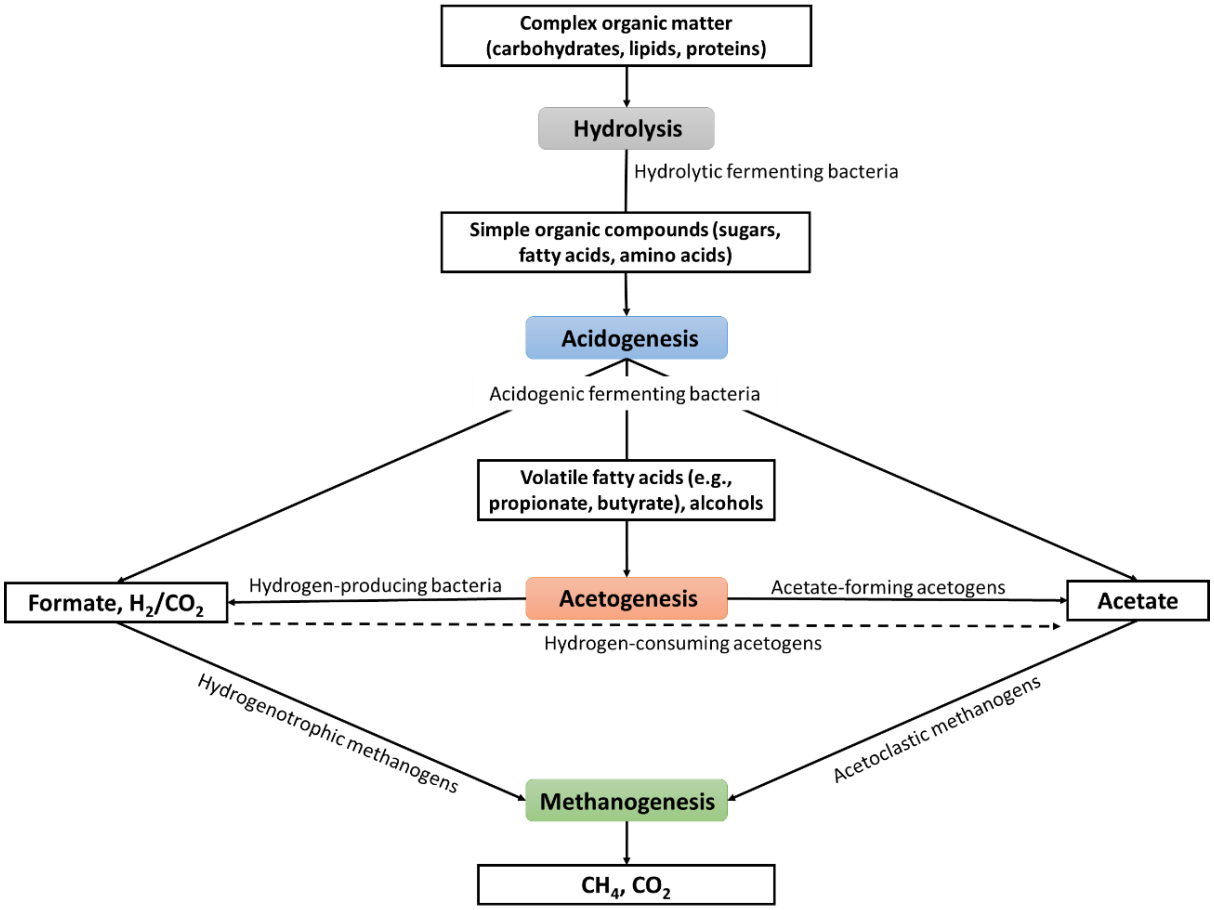

Figure 2.1. Schematic representation of the complex organic matter degradation during AD process and the microbial groups involved.

The cooperation between syntrophic partners is established by transferring electrons from one species to the other, in a process called interspecies electron transfer (IET) (Stams and Plugge, 2009; Zhang et al., 2023). For instance, typical fatty-acids degrading syntrophic bacteria store the electrons (present in VFA) in hydrogen molecules and the resulting H_2 is then transferred to hydrogenotrophic methanogens that use it for methane production (MP) via CO_2 reduction (J.-H. Park et al., 2018). For many years, electron transfer via H_2/formate carriers between syntrophic bacteria and methanogens were the only known mechanisms for IET (Barua and Dhar, 2017; Martins et al., 2018). However, mechanisms for IET in microbial communities can also include IET directly via biological electrical connections (e.g., nanowires), or by the mediation of electrons via CM (Barua and Dhar, 2017; Lovley, 2017a; Rotaru et al., 2021). Direct interspecies electron transfer (DIET) and conductive materials mediated interspecies electron transfer (CIET) can be alternative mechanisms to IET or can exist coupled to the formation of H_2/formate electron carriers. The mechanisms for external electron exchange between syntrophic partners will be presented in more detail in the following subsections.

Table 2.1. Standard free Gibbs energies of some VFA and methanogenic reactions involved in fatty acid oxidation and MP (adapted from Stams and Plugge (2009))

	Substrates	Reactions	ΔG°'/ (kJ·mol^{-1})
Fatty acids oxidation	Propionate	$C_3H_5O_2^- + 2H_2O \rightarrow C_2H_3O_2^- + 3H_2 + CO_2$	+72
	Butyrate	$C_4H_7O_2^- + 2H_2O \rightarrow 2C_2H_3O_2^- + H^+ + 2H_2$	+48
Acetoclastic methanogenesis	Acetate	$C_2H_3O_2^- + H^+ \rightarrow CH_4 + CO_2$	-36
Hydrogenotrophic methanogenesis	Hydrogen	$4H_2 + CO_2 \rightarrow CH_4 + 2H_2O$	-131

2.1.1. Mechanisms of interspecies electron transfer

In methanogenic environments, the mechanisms responsible for IET can be diverse. Electrons can be transferred between electron-donating bacteria and electron-accepting methanogens through the following mechanisms: a) interspecies hydrogen transfer (IHT) or interspecies formate transfer (IFT); b) direct interspecies electron transfer (DIET), via electrically conductive pili (*e*-pili) and/or *c*-type cytochromes; or c) conductive material mediated interspecies electron transfer (CIET) (Figure 2.2) (Lovley, 2017b; Martins et al., 2018; Rotaru et al., 2021).

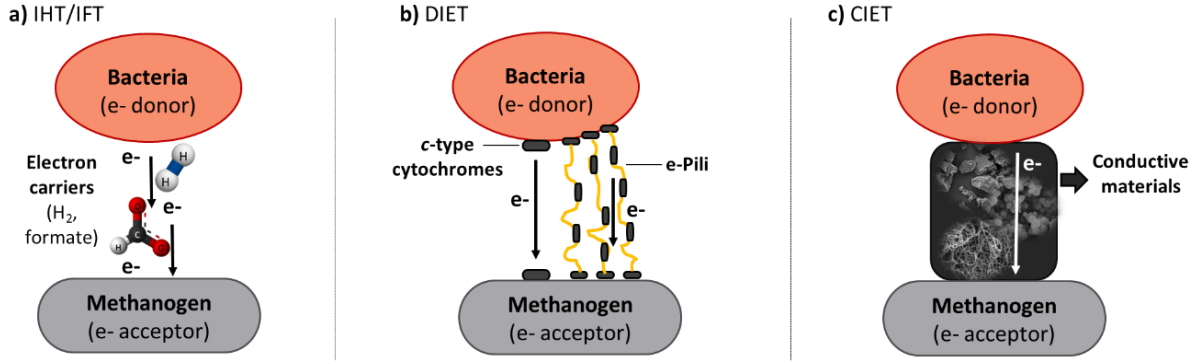

Figure 2.2. Schematic representation of IET mechanisms occurring in methanogenic environments (adapted from Martins *et al.* (2018)).

2.1.1.1. Indirect interspecies electron transfer

The IHT/IFT (Figure 2.2a) are mechanisms that involve the production and consumption of electron carriers (i.e., hydrogen and formate), being classified as an indirect mechanism for IET (Stams and Plugge, 2009). The electron-donating bacteria are able to produce soluble molecules (H_2 and formate) as a way to dissipate the electrons generated from the degradation of organic compounds (Martins et al., 2018; Shen et al., 2016). Then, electrons are transferred via diffusible electron-carrying molecules between the electron-donating species (syntroph – the acetogenic bacteria) and the electron-accepting partner (methanogenic archaea) (J.-H. Park et al., 2018). In IHT, protons are reduced to H_2 which can be

oxidized by hydrogenotrophic methanogens producing methane via CO_2 reduction (Rotaru et al., 2014a). Some hydrogenotrophic methanogens are also capable to produce methane using formate as electron donor (J. H. Park et al., 2018; Rotaru et al., 2014b). Comparing both molecules in terms of diffusivity, hydrogen can diffuse 30 times faster than formate and IHT becomes more favourable when interspecies distances are low (Shen et al., 2016; Stams, 1994). Moreover, the IHT rate is significantly improved when bacteria and methanogens form aggregates, because microorganisms are packed together and the small distance between cells facilitates hydrogen diffusion (Shen et al., 2016; Stams and Plugge, 2009). In contrast, formate is about 1 000 times more soluble than hydrogen, so IFT could be the dominant mechanism when interspecies distances are high (Shen et al., 2016; Stams, 1994). This way, under certain conditions IFT may prevail over IHT, and vice-versa (Shen et al., 2016; Zhang et al., 2023). Examples of syntrophic relationships involving IHT and IFT are the *Syntrophomonas wolfei* (a facultative syntrophic bacteria) in coculture with *Methanospirillum hungatei* (Schmidt et al., 2013; Sieber et al., 2015) and the syntrophic coculture *Syntrophomonas zehnderi* (an obligatory syntrophic bacteria) with *Methanobacterium formicicum* (Sousa et al., 2007). In the case of the first example, *S. wolfei* can grow axenically in pure culture on unsaturated fatty acids, such as crotonate (Schmidt et al., 2013; Sieber et al., 2015). However, to grow with other fatty acids, such as butyrate, *S. wolfei* needs the presence of a suitable hydrogen- and/or formate-utilizing partner, like *M. hungatei* (Schmidt et al., 2013; Sieber et al., 2015). The role of the methanogenic partner will be to maintain hydrogen and formate (the electron carriers produced during butyrate degradation) at low levels, allowing butyrate degradation to be thermodynamically favourable (Schmidt et al., 2013; Sieber et al., 2015, 2014). This way, IHT and/or IFT is required for butyrate oxidation (Schmidt et al., 2013; Sieber et al., 2015). On the other hand, the bacterium *S. zehnderi* is not able to grow axenically with any substrate tested so far, although it degrades a wide range of medium to long-chain fatty acids (LCFA) with different degrees of saturation (e.g., butyrate, caproate, palmitate, stearate, oleate), when in cooperation with a syntrophic partner (Sousa et al., 2009, 2007). Therefore, in certain methanogenic environments, syntrophic relationships may be the key factor for the complete biodegradation of fermentation products, like fatty acids, by microorganisms that live in conditions close to thermodynamic equilibrium (Desmond-Le Quéméner et al., 2021; Sousa et al., 2009; Xu et al., 2019).

In addition, IET can also occur by other indirect mechanisms, like via extracellular insoluble compounds, such as humic acids that can mediate electrons transfer between humics-reducing and humics-oxidizing microorganisms. Also, humic acids can be used as redox mediators in the anaerobic substrate degradation coupled to the abiotic reduction of metal oxides (e.g., Fe(III)), being reoxidized and

participating in many cycles (Martins et al., 2018). Other examples of insoluble compounds are flavin, sulfide, cysteine and riboflavin, and phenazine that can be used in the reduction of sulphate or insoluble electron acceptors (Shen et al., 2016). In contrast to soluble electron carriers, such as hydrogen and formate (they can diffuse in and out of the cell), the insoluble compounds cannot penetrate the cell surface (Martins et al., 2018).

2.1.1.2. Direct interspecies electron transfer

The mechanism of DIET relies on direct cell-to-cell electrical contacts by *e*-pili and/or *c*-type cytochromes (membrane-bound electron transport proteins), which are the main biological structures known to participate in this type of IET (Figure 2.2b) (Lovley, 2017b; Rotaru et al., 2021). This mechanism is shuttle-free, which means it does not involve the exchange of electron carriers like hydrogen or formate (Martins et al., 2018). For this reason, DIET has the potential to transfer electrons at higher rates than IHT/IFT, once it does not rely on molecules diffusion between syntrophic partners (Desmond-Le Quéméner et al., 2021).

Conductive *e*-pili are biological cellular structures that possess the flexibility and length to connect the syntrophic partners and have electrical conductivity to support physiologically relevant rates of extracellular electron transfer (EET) (Lovley, 2017b). These filamentous protein appendages in the cell surface can only be produced by bacteria with genes encoding pili protein, such as the gene *pil*A (Barua and Dhar, 2017; Shen et al., 2016). So far, *Geobacter* species are the ones known to produce *e*-pili and to participate in DIET, but other microorganisms may also have the capacity to produce pili (Lovley, 2017b). The conductivity of pili must be assessed (by direct measurement) in order to verify if the structure is capable of supporting long-range electron transport (Lovley, 2017b). The outer membrane cytochromes enable the electrons to be transferred from within a cell to another cell outside (Shen et al., 2016). There may be occasions that electrical contacts are made between cytochromes associated with the outer membranes of the syntrophic partners, instead via *e*-pili (Lovley, 2017b).

DIET was first demonstrated in artificial cocultures of *Geobacter metallireducens* and *Geobacter sulfurreducens* degrading ethanol, with fumarate as the electron acceptor (Liu et al., 2015; Lovley, 2017b; Rotaru et al., 2021). These energy sources could not be used by neither the partners alone, and together they established a metabolically co-dependent coculture (Rotaru et al., 2021). *G. metallireducens* was capable of oxidizing ethanol, but could not use fumarate as an electron acceptor, while *G. sulfurreducens* could reduce fumarate to succinate but could not consume ethanol (Chen et al., 2014b; Liu et al., 2015). The possibility of IHT/IFT by the coculture was excluded, because *G. metallireducens* is unable to degrade

ethanol with the production of H_2 or formate and, the fact that when a *G. sulfurreducens* strain (lacking the genes encoding hydrogenases and formate dehydrogenases, being incapable of hydrogen and formate uptake) was used, the IET kept occurring (Chen et al., 2014b). These species have the genes to produce *e*-pili capable of long-range electron transfer (Liu et al., 2015; Lovley, 2017b), and to produce cytochromes that can participate in EET (either associated with pili or alone) (Xu et al., 2019). It was proposed that the electrons would be released extracellularly via *e*-pili and outer-membrane multiheme *c*-type cytochromes by *G. metallireducens*, and *G. sulfurreducens* only need an outer membrane multiheme cytochrome (like OmcS, which can form electrically conductive cytochrome-chains) to accept the electrons (Liu et al., 2015; Rotaru et al., 2021). The conductivity of the pili is not due to the presence of OmcS along the length of pili, but it is thought that its presence facilitates electron transfer between the pili and extracellular acceptors or donors (Liu et al., 2015; Summers et al., 2010). Nevertheless, the importance and the functional role of each type of electrical connection in different syntrophic interactions are not completely understood. The work developed by Liu *et al*. (2018) highlighted the importance of extracellular cytochromes in DIET performed by *Geobacter* cocultures, which contradicts the previous assumption that both *e*-pili and extracellular cytochromes were essential for DIET (Liu et al., 2018). The authors reported that two pilus-free *Geobacter* species in coculture (*G. metallireducens* with *G. sulfurreducens*) formed aggregates and grown syntrophically via DIET. These results suggested that *e*-pili were not necessary to facilitate DIET and that cytochromes alone could establish the IET (Liu et al., 2018). However, *e*-pili would be required during EET between *Geobacter* species to reduce extracellular insoluble electron acceptors (e.g., anodes) (Liu et al., 2018). The opinion of the authors is that the actual functional role of the pili in DIET is uncertain, because when *pil*A is deleted there was a change on the distribution of outer-surface cytochromes (OmcZ and OmcS required for DIET), while the repression of *pil*B (which motors the assembly of type IV pili) in both *Geobacter* species inhibited the pilus assembly but did not alter the distribution of extracellular cytochromes (Liu et al., 2018).

Furthermore, syntrophic interactions via DIET between *G. metallireducens* and methanogens assigned to order *Methanosarcinales* were also observed. Electron-donating bacteria released electrons extracellularly which are accepted by the electron-accepting methanogen that use these electrons to produce methane from the reduction of CO_2 (Barua and Dhar, 2017; Martins et al., 2018; J. H. Park et al., 2018). In methanogenic environments, methanogens would be the electron-accepting partner for syntrophs like *G. metallireducens* (Rotaru et al., 2021). Only few microorganisms, namely *G. metallireducens* with acetoclastic methanogens (*Methanosaeta* or *Methanosarcina* species), were unequivocally demonstrated as performing DIET (Holmes et al., 2018; Lovley, 2017a; Rotaru et al.,

2014b, 2014a). The capability of *Methanosaeta harundinacea* (Rotaru et al., 2014b) and *Methanosarcina barkeri* (Rotaru et al., 2014a) of receiving electrons via DIET to reduce the CO_2 was discovered when these methanogens could only grow in coculture with strains of ethanol-utilizing, as *G. metallireducens*, capable of producing *e*-pili (Rotaru et al., 2014b, 2014a). Note that till then, *Methanosaeta* species were thought to be obligate acetoclastic methanogens, only capable of using acetate as substrate for MP (Xu et al., 2019). The conductive *e*-pili produced by bacteria was considered to be very important for the EET when in coculture with methanogens, but the cell machinery involved in electrons uptake by the methanogen remains unknown (Martins et al., 2018; Rotaru et al., 2014a). In other words, the extracellular electron contacts that might allow some methanogenic archaea to accept electrons via DIET are not known yet (Martins et al., 2018; Rotaru et al., 2014a). Firstly, it was hypothesized that if cytochromes were a requirement for DIET, only the genera *Methanosaeta* and *Methanosarcina* would be more likely to play a role in DIET due to their high *c*-type cytochromes content, which hydrogenotrophs lack (Rotaru et al., 2018, 2014a). But it is also possible that unprecedented electron uptake mechanisms may be employed by members of *Methanosarcinales* that are unknown so far (Rotaru et al., 2021). It was recently found that *Methanosarcina* did not need the multiheme *c*-type cytochromes to establish DIET or to interact directly with electrodes (Rotaru et al., 2021; Yee and Rotaru, 2020). This was demonstrated when the multiheme *c*-type cytochromes of *Methanosarcina mazei* was deleted, and this methanogen kept participating in DIET or retrieving electrons from a cathode (Yee and Rotaru, 2020). On the other hand, the cellular envelopes of *Methanothrix* and *Methanosarcina* have multiple redox proteins and external proteins (e.g., ferredoxin) that may be involved in obtaining electrons from electron-donating bacteria (Castilho et al., 2022). Other hypothesis is that flagellar appendages of methanogens might be involved in extracellular electron uptake once they are similar to conductive pili (Castilho et al., 2022). Regarding hydrogenotrophic methanogens, experiments point out to the inability of *M. formicicum*, *M. hungatei*, and *Methanoculleus marisnigri* to perform DIET with *G. metallireducens* (Rotaru et al., 2014b; Yee and Rotaru, 2020), but a *Methanobacterium* strain growing on formate was reported to perform DIET with *G. metallireducens* (Zheng et al., 2020).

Other results in this research field have shown that depending on the species, the electron uptake mechanism might be different, even when they belong to the same genus (Yee et al., 2019). For example, Yee *et al.* (2019) tested two methanogens belonging to *Methanosarcina* genus (*M. barkeri* and *M. horonobensis*) for their ability to accept electrons directly from insoluble electron donors (intrinsic electroactivity) (Yee et al., 2019). Comparative genome analysis revealed differences between the two *Methanosarcina* species in energy metabolism, extrachromosomal functions and ion transporters (Yee et

al., 2019). The results also showed that while both *Methanosarcina* species grew syntrophically using DIET, only *M. barkeri* grew on a cathode (Yee et al., 2019). So, electron uptake routes from cathodes, or from other cells, might be different between *Methanosarcina* species and not all DIET-methanogens are electroactive (Yee et al., 2019). Besides, the diversity of microorganisms capable of participating in DIET may include other organisms aside from the typical electroactive bacteria (i.e., *Geobacter* spp.). For instance, Walker *et al.* (2020) showed that *Syntrophus aciditrophicus,* a typical hydrogen-producing syntroph, can also produce *e*-pili and can grow via DIET (Walker et al., 2020). This species is one of the most studied pure culture models for IHT/IFT, which was not previously characterized as an electrogen (Rotaru et al., 2021; Walker et al., 2020). It was formerly thought that this species would be unlikely to participate in DIET because it lacked a gene homologous to the pilin monomer that assembles *e*-pili in *Geobacter* (Walker et al., 2020). Therefore, it cannot be ruled out that other typical syntrophic fatty-acids degrading bacteria might have the capacity for DIET (Walker et al., 2020).

2.1.1.3. Conductive materials and interspecies electron transfer

IET can be accelerated in the presence of CM, such as iron-based and carbon-based materials, through a mechanism known as CIET (Figure 2.2c) (Rotaru et al., 2021). CM can function as electrical conduits, allowing the attachment of syntrophic partners on the surface of CM through which electron exchange occurs (Barua and Dhar, 2017). This external cell-to-cell electron transfer can enhance the syntrophic conversion of different organic compounds to methane, without the need for cells to form agglomerates or to be in direct contact as it occurs in DIET (Barua and Dhar, 2017; Rotaru et al., 2021). A significant downregulation of the typical genes involved in DIET occurs when CM are present (Rotaru et al., 2021). Conductive based-carbon materials, such as carbon cloth (Chen et al., 2014b), biochar (Chen et al., 2014a), and granular activated carbon (GAC) (Liu et al., 2012), have been shown as IET mediators in defined cocultures of *G. metallireducens* with *G. sulfurreducens* by replacing the biological electrical connections required for DIET (Table 2.2). For example, in the incubations with mutant strains, which could not express *e*-pili, CIET replaced DIET (Chen et al., 2014b, 2014a; Liu et al., 2012; Lovley, 2017b). In addition, CIET was observed in syntrophic cocultures of *G. metallireducens* with *M. barkeri* in the presence of GAC (0.05 mmol·L^{-1}) (Liu et al., 2012; Rotaru et al., 2014a), carbon cloth (20 g·L^{-1}) (Chen et al., 2014b) or biochar (around 25 g·L^{-1}) (Chen et al., 2014a). In general, wild-type strains in the presence of CM produced methane at higher rates and down-regulated the genes involved in DIET (Chen et al., 2014b, 2014a; Liu et al., 2012; Lovley, 2017b).

The addition of iron-based materials like magnetite (Mag) in anaerobic environments has also been reported to facilitate microbial electron exchange. Mag mediated electron transfer by replacing the pili-associated cytochrome OmcS in *G. sulfurreducens* (Liu et al., 2015). In the presence of Mag, this species downregulated the expression of the OmcS gene (Liu et al., 2015). Also, a strain of *G. sulfurreducens,* in which the OmcS gene was deleted, could only grow in coculture when Mag was present (Liu et al., 2015). It was suggested that cocultures in the presence of CM instead of wasting their energy on producing biological structures, may use it for cells growth, which is advantageous (Barua and Dhar, 2017). Thus, the application of CM as mediators for IET could be metabolically more favourable, since there is a range of electrical CM that can replace biological structures required for DIET (Lovley, 2017b).

Table 2.2. Summary of the studies with defined cocultures where CM act as mediators in IET

Syntrophic coculture	Electron donor	Electron acceptor	CM	Impacts	References
G. sulfurreducens strain DL1, (ATCC 51573) and *G. metallireducens* strain GS-15 (ATCC 53774)	Ethanol (10 mmol·L^{-1})	Fumarate (40 mmol·L^{-1})	Mag (10 mmol·L^{-1})	(+) The rate of ethanol metabolism increased in the presence of Mag (+) Mag could substitute for the electron transfer function of OmcS in IET	(Liu et al., 2015)
G. metallireducens strain GS-15 (ATCC 53774) and *G. sulfurreducens* strain DL1 (ATCC 51573)	Ethanol (10 mmol·L^{-1})	Fumarate (40 mmol·L^{-1})	Carbon cloth (20 g·L^{-1})	(+) Higher metabolic rates with carbon cloth (+) Carbon cloth mediated IET between the distant syntrophic partners	(Chen et al., 2014b)
G. metallireducens strain GS-15 (ATCC 53774) and *M. barkeri* type strain DSM 800 (ATCC 43569)	Ethanol (10 mmol·L^{-1})	CO_2	Carbon cloth (20 g·L^{-1})	(+) Reduction in 75 % of the time to begin ethanol consumption with carbon cloth (+) Carbon cloth mediated IET between the distant syntrophic partners	(Chen et al., 2014b)
G. metallireducens strain GS-15 (ATCC 53774) and *G. sulfurreducens* strain PCA (ATCC 51573)	Ethanol (10 mmol·L^{-1})	Fumarate (40 mmol·L-1)	Biochar (25 g·L^{-1})	(+) Higher metabolic rates with biochar	(Chen et al., 2014a)
G. metallireducens and *M. barkeri* type strain DSM 800 (ATCC 43569)	Ethanol (20 mmol·L^{-1})	CO_2	Biochar (25 g·L^{-1})	(+) Biochar mediated IET between syntrophic partners	(Chen et al., 2014a)
G. metallireducens strain ATCC 53774 and *M. barkeri* (DSM 800)	Ethanol (20 mmol·L^{-1})	CO_2	GAC (0.05 mmol·L^{-1})	(+) The presence of GAC allowed the pilin-deficient *G. metallireducens* to share electrons with *M. barkeri*, demonstrating that GAC could substitute for e-pili	(Rotaru et al., 2014a)
G. metallireducens strain GS-15 (ATCC 53774) and *G. sulfurreducens* strain DL1 (ATCC 51573)	Ethanol (10 mmol·L^{-1})	Fumarate (40 mmol·L^{-1})	GAC (0.05 mmol·L^{-1})	(+) The presence of GAC improved the metabolism of the coculture	(Liu et al., 2012)
G. metallireducens and *M. barkeri* strain DSM 800 (ATCC 43569)	Ethanol (20 mmol·L^{-1})	CO_2	GAC (0.05 mmol·L^{-1})	(+) Little or no lag phase was observed with GAC, which enhanced the conversion of ethanol to methane	(Liu et al., 2012)

.

2.1.2. The microbiology of syntrophic butyrate degradation

Butyrate is a 4-carbon saturated VFA (C4:0), which is a common intermediate in AD, resulting from the anaerobic fermentation of sugars and amino acids (Stams et al., 2012; Ziels et al., 2019). Butyrate degradation by syntrophic bacteria is well documented, turning butyrate a good VFA model for studying syntrophic interactions.

Under unfavorable thermodynamic conditions ($\Delta G^{\circ\prime} > 0$), butyrate accumulation in bioreactors leads to the acidification and instability of the process, or even to the failure of the system (Barua et al., 2018). Thus, syntrophic interactions are required between syntrophic bacteria and hydrogen- and acetate-scavenging partners (Figure 2.3), to maintain the favorable thermodynamic conditions for butyrate conversion to acetate and hydrogen (Table 2.2) (Stams et al., 2012; Ziels et al., 2019). In Figure 2.3 is illustrated the metabolic pathways involved for the complete conversion of butyrate to methane and these pathways will be addressed in more detail in the next subsections.

List of abbreviations used in the scheme of Figure 2.3: CoA - coenzyme A; CoB - coenzyme B; CoM - coenzyme M; Fd - ferredoxin; Fd_{ox} - oxidized ferredoxin; Fd_{red} - reduced ferredoxin; ATPase - ATP synthase. Syntrophic butyrate metabolism: Act - acetyl-CoA acetyltransferase; Bcd - butyryl-CoA dehydrogenase; Ctr - crotonyl-CoA hydratase; HbdH - 3-hydroxybutyryl-CoA dehydrogenase; AtoB - acetyl-CoA C-acetyltransferase; Pta - phosphate acetyltransferase; Ak - acetate kinase; Hyd1 - electron confurcating hydrogenase; Hyd2 - membrane-bound [FeFe]-hydrogenase; Hyd3 - ferredoxin dependent hydrogenase; Fdh1, Fdh3 - formate dehydrogenases; Fdh2, Fdh4 - formate dehydrogenase (membrane bound, quinone reducing); Fnt – formate transporter; MQ - menaquinone; EtfAB - Electron transfer flavoproteins A and B; FeS – complex membrane bound FeS-oxidoreductase. Hydrogenotrophic metabolism: Mtr - tetrahydromethanopterin S-methyl-transferase; Mcr - methyl-coenzyme M reductase; Hdr - soluble heterodisulfide reductase; Fdh - formate dehydrogenase; Mvh - F_{420}-non-reducing hydrogenase; Frh - coenzyme F_{420}-reducing hydrogenase; Fwd - formyl-methanofuran dehydrogenase; Eha - energy-converting hydrogenase A; MFR - methanofuran; Ftr - Formyl-methanofurantetrahydromethanopterin formyl-transferase; H_4MPT – tetrahydromethanopterin; Mch - Methenyl-tetrahydromethanopterin cyclohydrolase; Mtd - methylene-tetrahydromethanopterin dehydrogenase; Mer - 5,10- methylenetetrahydromethanopterin reductase. Acetoclastic metabolism: Ack - Acetate kinase; At - phosphate acetyltransferase; Acs - acetyl-CoA decarbonylase/synthetase; Codh - carbon-monoxide dehydrogenase; Codh-Acs - carbon monoxide dehydrogenase/acetyl-CoA decarbonylase/synthase complex; MtrA-H - tetrahydromethanopterin S-methyltransferase; McrABG - methyl-coenzyme M reductase; HdrDE - membrane-bound heterodisulfide reductase; Ech - energy-converting hydrogenase; MPh – methanophenazine; Fpo - $F_{420}H_2$ dehydrogenase.

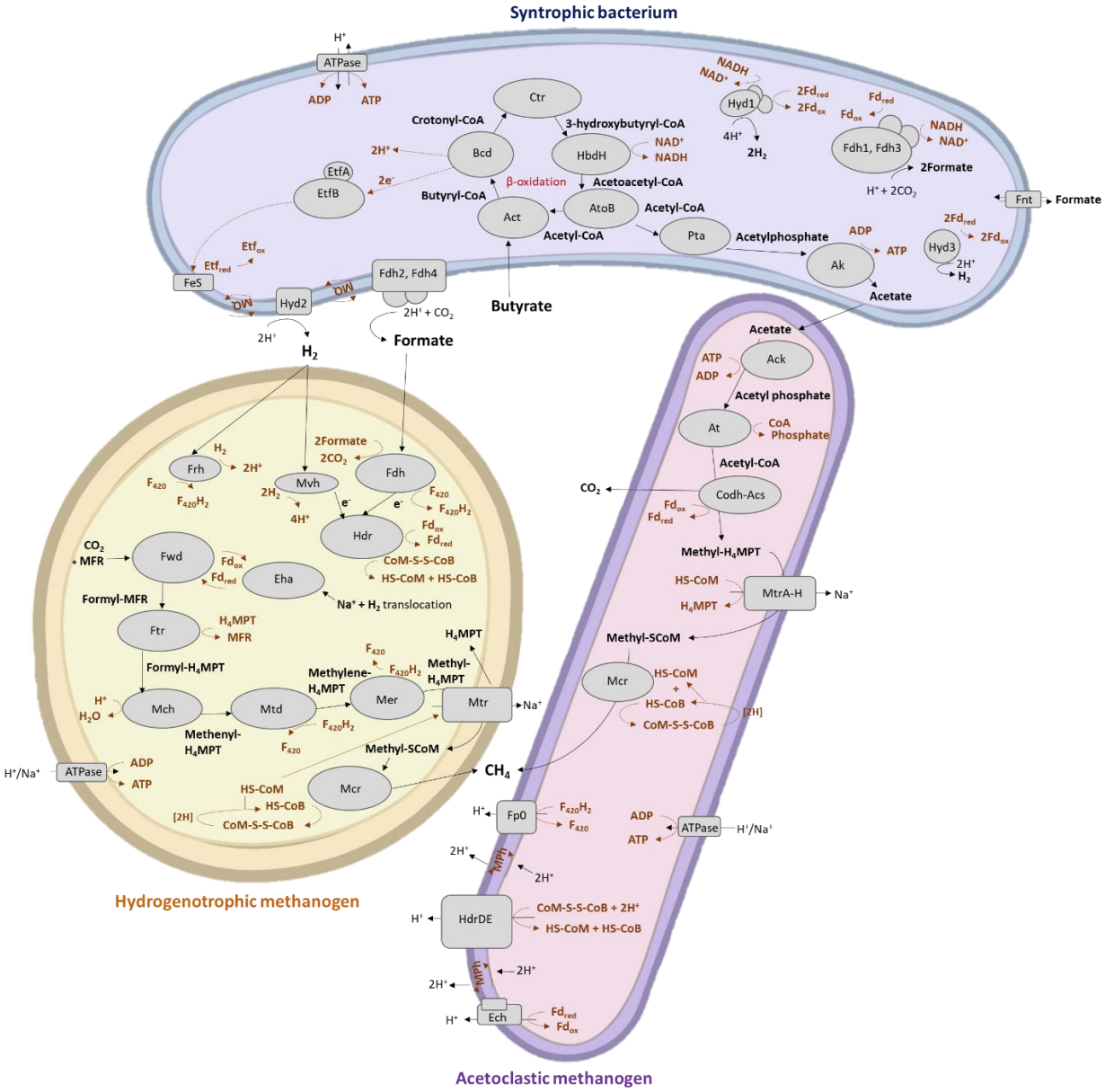

Figure 2.3. Illustrative representation of the metabolic pathways involved in anaerobic butyrate-degradation by syntrophic communities (support references: (Enzmann et al., 2018; Kurth et al., 2020; Lie et al., 2012; Jessica R. Sieber et al., 2010; Stams et al., 2012; Stams and Plugge, 2009; Ziels et al., 2019)).

2.1.2.1. Butyrate-degrading syntrophic bacteria

Obligate syntrophs are a specialized group of bacteria that oxidize compounds like butyrate typically via IHT/IFT (Whitman et al., 2006). Key microorganisms in syntrophic butyrate degradation include members of *Syntrophomonadaceae*, such as the butyrate-degrading *S. wolfei* (J R Sieber et al., 2010; Stams et al., 2012; Stams and Plugge, 2009; Ziels et al., 2019). Syntrophic butyrate metabolism occurs via β-oxidation pathway (J R Sieber et al., 2010), and *Syntrophomonas* genome encode enzymes required for β-oxidation

of butyrate and several hydrogenases, formate dehydrogenases and electron transfer flavoproteins (Ziels et al., 2019).

The β-oxidation cycle starts with butyrate being activated to butyryl-CoA by the transfer of the coenzyme A (CoA) group from acetyl-CoA, and it is β-oxidized to two acetyl-CoA molecules (Figure 2.3) (J R Sieber et al., 2010; Jessica R. Sieber et al., 2010). One of them is used to activate butyrate and the other one is used for ATP synthesis by the action of phosphotransacetylase (Pta) and acetate kinase (Ak) (J R Sieber et al., 2010; Jessica R. Sieber et al., 2010). The butyryl-CoA is oxidized to crotonyl-CoA that promotes the reduction of electron transfer flavoproteins (EtfAB) (and two protons are released into the cytoplasm), and the oxidation of L-3-hydroxylbutyryl-CoA to 3-oxobutyryl-CoA generates NADH (Müller et al., 2010; J R Sieber et al., 2010). Hydrogen production will occur through a NADH-dependent hydrogenase (Hyd1) or NADH dependent formate dehydrogenase (Fdh1, Fdh3) using the electrons derived from NADH (J R Sieber et al., 2010).

The hydrogenases are enzymes that catalyse the reversible conversion of H_2 into protons and electrons, and common redox mediators involved in hydrogen production are NADH, $FaDH_2$, and ferredoxins (Fd) (Stams and Plugge, 2009; Zhang et al., 2023). The NADH oxidation occurs through the NADH-linked hydrogenases or formate dehydrogenases, which are present in many fermentative bacteria (Whitman et al., 2006). However, the oxidation of NADH is thermodynamically favourable only under low concentrations of hydrogen or formate (Whitman et al., 2006). In the same way, the production of hydrogen or formate will be only favoured at low hydrogen partial pressures, which can be obtained thanks to hydrogen or formate removal by methanogens (J R Sieber et al., 2010). The hydrogenase activity is inhibited when hydrogen concentration is high (Martins et al., 2018). If butyrate-oxidizing bacterium, like *S. wolfei*, can produce either formate or H_2, the production of one or the other electron carrier will be determined by the environmental conditions. For example, the identity of the methanogenic partner (whether it can produce both electron carriers or not), or the distance between cells (which may favoured the exchange of one electron carrier over another, based on their distinct rates of diffusion) are some factors that dictate the relative abundance of these carriers during butyrate conversion (J R Sieber et al., 2010; Whitman et al., 2006). Yet, it is suggested that hydrogen and formate are energetically equivalent at least in anaerobic digesters (Schink et al., 2017).

On the other hand, reversed electron transport is required to produce H_2 from electrons derived from the oxidation of butyryl-CoA to crotonyl-CoA (J R Sieber et al., 2010). This process is an input of energy that allows the production of hydrogen and formate in concentrations that support the energy metabolism of methanogens (J R Sieber et al., 2010). Membrane-bound ATPase generates a transmembrane proton

potential (ion gradient) which is, most likely, the source for this energy input (J R Sieber et al., 2010; Stams and Plugge, 2009). A redox loop system is formed by a membrane-bound iron-sulfur oxidoreductase redox-linked to a membrane-bound hydrogenase (Hyd2) or formate dehydrogenase (Fdh2, Fdh4) via menaquinone (MQ) (J R Sieber et al., 2010; Sieber et al., 2015). MQ (abbreviation for methylnaphthoquinone) is an electron carrier in the cytoplasmatic membrane of bacteria and of methanogenic archaea (Thauer et al., 2008). The iron-sulfur oxidoreductase will reoxidized the reduced electron transfer flavoprotein (Etf) at the membrane (J R Sieber et al., 2010). The two protons available into the cytoplasm will drive the reduction of MQ to menaquinol using the two electrons from butyryl-CoA oxidation located on the membrane-bound iron-sulfur oxidoreductase (J R Sieber et al., 2010). The oxidation of menaquinol can occur by a membrane-bound hydrogenase or formate dehydrogenase, depending on the syntrophic partner or the incubation conditions, in order to release H_2 or formate, respectively (J R Sieber et al., 2010). The two protons released into the cytoplasm during oxidation of butyryl-CoA are counterbalanced by the two protons used from the exoplasmic space to produce the H_2 or formate (J R Sieber et al., 2010). Thus, only two protons are need to be transported across the membrane per mol of butyryl-CoA oxidized, once two protons are released into the cytoplasm during the reoxidation of menaquinol (J R Sieber et al., 2010). As a result, 2/3 of an ATP equivalent is used to overcome this energy barrier, which leaves about 1/3 of an ATP available to support growth (J R Sieber et al., 2010). Besides, in a series of reactions, the acetyl groups are also cleaved off, then producing acetate (Stams et al., 2012).

As syntrophic communities grow in conditions close to thermodynamical equilibrium, the syntrophic bacteria are commonly found in low abundance since they present low growth rates and yields (Hao et al., 2020; Stams et al., 2012).

2.1.2.2. Methanogenic partners in syntrophic fatty acids degradation

In methanogenic environments, methanogens belonging to the orders *Methanobacteriales*, *Methanomicrobiales*, and *Methanosarcinales*, are commonly found and they can serve as syntrophic partners for VFA-oxidizing bacteria (Stams and Plugge, 2009). In mesophilic digesters, hydrogenotrophic and acetoclastic methanogens prevail once the organic matter degradation provides mainly acetate, formate, and H_2/CO_2 (Enzmann et al., 2018). At mesophilic temperatures, the growth of methanogens like *Methanosarcina*, *Methanobacterium*, or *Methanococcus* is favoured (Enzmann et al., 2018). The hydrogen consumption by hydrogenotrophic methanogens allows the maintenance of H_2 concentration at low levels ($< 10^{-4}$ atm), being the syntrophy established between hydrogen-producing bacteria and

hydrogenotrophic methanogens essential for their survival (J. H. Park et al., 2018). While methanogens from almost all methanogenic orders can perform hydrogenotrophic methanogenesis to produce methane from H_2/CO_2, the MP from acetate (acetoclastic methanogenesis) is only performed in the order *Methanosarcinales* by two genera, *Methanothrix* and *Methanosarcina* (Borja et al., 2011; Enzmann et al., 2018; Whitman et al., 2006). The dominant species may vary, and *Methanothrix* may be dominant at low acetate concentrations, as they have higher affinity for acetate when compared with *Methanosarcina* species (Enzmann et al., 2018; Harirchi et al., 2022). Examples of methanogens commonly found in anaerobic digesters are *M. formicicum*, *Methanococcus maripaludis*, and *M. hungatei*, involved in MP from H_2/CO_2, and *M. barkeri*, *M. mazei* and *Methanothrix concilli* involved in MP from acetate (Borja et al., 2011; Wainaina et al., 2019). Methanogens like *M. hungatei* are known to cooperate with syntrophs, such as *S. wolfei*, to perform syntrophic butyrate degradation (Schmidt et al., 2013; Sieber et al., 2015). Despite methanogenesis being biochemically complex (involving the structure and synthesis of many coenzymes), the methanogens only use simple compounds to produce methane (Whitman et al., 2006). In hydrogenotrophic metabolism (Figure 2.3), CO_2 is firstly reduced by using the reduced ferredoxin (Fd_{red}) as electron donor, and activated to formyl-methanofuran (Enzmann et al., 2018). Methanofuran (MFR) acts as a formyl carrier, it can present different forms among methanogens, and it activates CO_2 to formyl-MFR (Whitman et al., 2006). Then, the formyl group is transferred to tetrahydromethanopterin (H_4MTP) originating formyl-H_4MTP (Enzmann et al., 2018). H_4MTP is a one-carbon carrier, in which the formyl group is dehydrated and reduced to methylene-H_4MTP, and then to methyl-H_4MTP by using the reduced F_{420} ($F_{420}H_2$) as electron donor (Enzmann et al., 2018; Whitman et al., 2006). Coenzymes are electron donors in methanogenesis, and the coenzyme F_{420} participates in two-electron transfer reactions, being coupled to hydrogenase, formate dehydrogenase, or other enzymes (Whitman et al., 2006). The transference of the methyl group to coenzyme M (HS-CoM) forms the methyl-CoM, which is then reduced to methane using as electron donor the coenzyme B (HS-CoB) (Enzmann et al., 2018). Thus, HS-CoM is a one-carbon carrier unique to methanogens, being the terminal carbon carrier (as methyl-S-CoM is reduced to CH_4) (Whitman et al., 2006). Finally, the reduction of the resulting heterodisulfide (CoM-S-S-CoB) with H_2 allows to recycle the coenzymes (Enzmann et al., 2018). The electrons required for CO_2 reduction can also be derived from formate instead of H_2 (Enzmann et al., 2018). Formate can be converted to hydrogen by formate hydrogen lyase, which is a membrane-associated enzyme complex, or it can be excreted and consumed by methanogens (Stams and Plugge, 2009). In methanogens using formate, firstly, four formate molecules are oxidized to CO_2 by formate dehydrogenases (Fdh), and then one CO_2 molecule is reduced to methane (Enzmann et al., 2018).

In acetoclastic methanogenesis (Figure 2.3), acetate is activated using ATP and CoA, and converted to acetyl-CoA (Enzmann et al., 2018). Then, the carbon monoxide dehydrogenase (Codh)/acetyl-CoA synthase split the acetyl-CoA (Enzmann et al., 2018). The methyl group is transferred to H_4MTP (noting that in *Methanosarcina* it will be tetrahydrosarcinapterin (H_4SPT)) and the conversion to methane follows the same steps of the CO_2 reduction pathway as explained above in hydrogenotrophic methanogenesis (Enzmann et al., 2018). Ferredoxins are especially abundant in acetoclastic methanogens (Whitman et al., 2006).

Methanogens also need a number of vitamins, such as thiamine, riboflavin, pyridoxine, corrinoids, biotin, niacin, and pantothenate (Whitman et al., 2006). For instance, flavins can function as electron carriers for hydrogenases, NADH reductases and formate dehydrogenases in *Methanobacterium* (Whitman et al., 2006). On the other hand, corrinoids can function as methyl carriers, being important during MP (Whitman et al., 2006).

According with the mode of energy conservation, methanogens can be divided in methanogens with and without cytochromes (Enzmann et al., 2018; Stams and Plugge, 2009). All methanogens of *Methanosarcinales* are cytochrome-containing methanogens (Thauer et al., 2008). Cytochromes can function as electron carriers during methanogenesis from acetate, as they participate in the oxidation of this substrate during its disproportionation (Whitman et al., 2006). Methanogens belonging to the orders *Methanopyrales*, *Methanococcales*, *Methanobacteriales*, and *Methanomicrobiales* do not possess cytochromes (Enzmann et al., 2018; Thauer et al., 2008). Hydrogenotrophic methanogens without cytochromes (the ones that exclusively use H_2/CO_2 for MP) can consume hydrogen at very low concentrations making use of ferredoxin and coenzyme F_{420} as redox mediators, being the most important methanogens for the removal of hydrogen in syntrophic communities (Stams and Plugge, 2009). Methanogenic archaea without cytochromes possess methyl-H_4MPT:CoM methyltransferase (Mtr) that couples the methyl group transfer to an electrochemical sodium gradient over the membrane (Enzmann et al., 2018). This Na^+ gradient can be used for ATP synthesis (Enzmann et al., 2018). In addition, the reduction of CoM-S-S-CoB with H_2 is catalysed by a complex involving a (methyl viologen-reducing) hydrogenase and heterodisulfide reductase (Mvh-Hdr) (Enzmann et al., 2018). This also couples the reduction of oxidized ferredoxin (Fd_{ox}) via flavin-based electron bifurcation (Enzmann et al., 2018). Electron bifurcation involves the separation of two electrons from ubiquinol (Thauer et al., 2008). On the other hand, cytochrome-containing methanogens (e.g., *M. barkeri*, *M. mazei*) also generates a Na^+ gradient over the membrane using Mtr (complex MtrA-H that contains a corrinoid bounded to the MtrA subunit, coupling the translocation of two sodium ions), but the reduction of CoM-S-S-CoB is catalysed differently

(Enzmann et al., 2018; Thauer et al., 2008). For that, methanogens with cytochromes use a membrane-bound heterodisulfide reductase (HdrED complex is an iron-sulphur haemoprtein) and the electrons derived from reduced methanophenazine ($MPhH_2$) via cytochrome *b* subunit, generating a proton motive force (Enzmann et al., 2018). In hydrogenotrophic metabolism, hydrogen is oxidized by a membrane-bound (F_{420} non-reducing) hydrogenase (VhoACG complex, a nickel-iron-sulfur haemoprotein) and electrons are transferred via cytochrome *b* to the oxidized methanophenazine (MPh), which creates a proton motive force again (Enzmann et al., 2018). The endergonic reduction of Fd_{ox} with H_2 can be coupled by another membranous energy-converting [NiFe] hydrogenase (complex EchA-F, a nickel-iron-sulfur protein) to the intrusion of H^+ (i.e., by using the proton motive force) (Enzmann et al., 2018). In these methanogens, methanogenesis is coupled with the generation of H^+ and Na^+ gradients (Enzmann et al., 2018). In some cases, Vh0 and Ech are absent, and an Rnf complex is thought to establish the Na^+ gradient over the membrane by transferring electrons from Fd_{red} to MPh (Enzmann et al., 2018). Then, a H^+ gradient will be generated as a result of the subsequent electron transport from $MPhH_2$ to HdrED (Enzmann et al., 2018). Another difference is that methanogens without cytochromes do not contain methanophenazine (which is an analogue for functional menaquinone), while cytochromes-containing methanogens do (Thauer et al., 2008).

In methanogenic environments like anaerobic digesters, cytochrome-containing methanogens, like *Methanosarcina*, cannot compete with methanogens without cytochromes for hydrogen (Enzmann et al., 2018). For instance, *M. barkeri* can use a variety of substrates, like acetate and H_2/CO_2 to produce methane, but methanogens without cytochromes would prevail when H_2/CO_2 is the available substrate (Thauer et al., 2008).

In summary, obligate syntrophic communities involving acetogenic bacteria and methanogenic archaea can only degrade VFA by cooperating with each other, where intermicrobial distances will affect the biodegradation rates and the specific growth rates of the microorganisms involved (Stams et al., 2012). So, the process is favoured by self-aggregation of syntrophic partners in aggregates, and the metabolism of one microorganism will be directly affected by the other members of the community (Stams et al., 2012; Stams and Plugge, 2009).

2.2. EFFECT OF (NANO)MATERIALS ON METHANE PRODUCTION

The metabolism of syntrophic partners can be enhanced in the presence of conductive (nano)materials, like Mag (10 $mmol \cdot L^{-1}$) (Liu et al., 2015) and GAC (0.05 $mmol \cdot L^{-1}$) (Rotaru et al., 2014a), where CIET was proved to occur. Several other studies were performed with the aim to enhance AD process and to

improve the efficiency of MP by applying different types of materials. The effects promoted in the presence of (nano)materials were positive in most studies, but the explanations behind these effects are generally not satisfactory, as they result mostly in speculations based on indirect proves. For instance, the shift of IET mechanisms from HIT/HFT to CIET is the main explanation based only on the observation of the improvement of AD performance and/or on the enrichment of electroactive microorganisms during biodegradation. The fact that IET does not occur in methanogenic pure cultures and methanogens alone can also be stimulated by CM rises even more doubts regarding the common justification for the improvements caused by CM. In the following subsections an overview of the studies showing the main effects caused by the presence of different (nano)materials towards the methanogenic activity in systems with different complexity, i.e., in pure cultures of methanogens and syntrophic cocultures, in microbial enrichments and in other complex microbial communities, will be presented.

2.2.1. Effect of CM on methanogenic pure cultures and on syntrophic cocultures

Little is known about the mechanisms behind the improvements towards the methanogenic activity of pure cultures of methanogens and syntrophic cocultures in the presence of (nano)materials, especially when *Geobacter* spp. are not the syntrophic partner. Table 2.3 presents a summary of studies showing the effects of materials on the activity of methanogenic pure cultures. The direct impact of materials was evaluated towards some acetoclastic species, such as *M. barkeri* (Fu et al., 2019; Xiao et al., 2020), *M. mazei* (Salvador et al., 2017; H. Wang et al., 2020; Xiao et al., 2020) and *M. concilii* (Salvador et al., 2017), and some hydrogenotrophic pure cultures like *M. formicicum* (Salvador et al., 2017), *M. hungatei* (Salvador et al., 2017), *M. maripaludis* (Fu et al., 2018; W. Zhang et al., 2018), and *Methanocella conradii* (Fu et al., 2018; Xia et al., 2019). More recently, Zheng *et al.* (2020) investigated the activity of *Methanobacterium* sp. strain YSL growing with formate as electron donor in the presence of CM (Zheng et al., 2020). The diversity of materials is huge but only the impact of CNT (Fu et al., 2019; Salvador et al., 2017; Xia et al., 2019; Xiao et al., 2020; W. Zhang et al., 2018), GAC (Zheng et al., 2020), Mag (Fu et al., 2019, 2018; H. Wang et al., 2020; Xia et al., 2019), nano-graphite (Fu et al., 2019) and reduced graphene oxide (rGO) (W. Zhang et al., 2018) was investigated. It seems that the effect of CM varies according to the microbial species. For example, the presence of 5 $g \cdot L^{-1}$ CNT enhanced the methane production rate (MPR) up to 17 times by *M. formicicum* (Salvador et al., 2017), and up to 4 times the MPR by *M. mazei* and *M. barkeri* with 0.2 $g \cdot L^{-1}$ CNT (Xiao et al., 2020), but 5 $g \cdot L^{-1}$ CNT inhibited the hydrogenotrophic activity of *M. maripaludis* (W. Zhang et al., 2018). The presence of GAC (25 $g \cdot L^{-1}$) was reported to inhibit the growth of the *Methanobacterium* sp. strain YSL (Zheng et al., 2020). Besides, Fu

et al. (2018) studied the effect of Mag (4.64 mmol·L^{-1} in Fe) towards *Syntrophomonas erecta* subsp. *sporosyntropha growing* in pure culture with crotonate, and no effects were observed in the presence of the material (Fu et al., 2018). Regarding the positive impacts, the presence of CNT contributed to significantly reduce the lag phases preceding MP by approximately 75 % in *M. formicicum* (Salvador et al., 2017), 100 % in *M. hungatei* (Salvador et al., 2017), and 12.5 % in *M. mazei* (Salvador et al., 2017) pure cultures, while Mag reduced up to 50 % the lag phase of *M. mazei* in pure cultures (H. Wang et al., 2020).

The presence of CM also caused an impact towards MPR and lag phases duration on syntrophic cocultures (Table 2.4). CNT (5 g·L^{-1}) accelerated the MRP (around 1.5 times) in syntrophic cocultures of *S. wolfei* with *M. hungatei* (Salvador et al., 2017). In addition, butyrate degradation by the syntrophic coculture *S. wolfei* with *M. maripaludis* was stimulated by CNT (2 g·L^{-1}) and rGO (0.1 g·L^{-1}), but not in the presence of kaolinite which is a clay mineral (considered a non-conductive material (non-CM)) (W. Zhang et al., 2018). The syntrophic ethanol degradation was also enhanced in the presence of GAC (25 g·L^{-1}) (Zheng et al., 2020).

The main explanations suggested for the improvements observed in pure cultures, in the presence of CM, were related with the microbial adhesion to the surface of CM serving as a support for microbial growth or the substrate adsorption to CM (Salvador et al., 2017). On the other hand, it was found that CM directly favoured MP from acetate (Xiao et al., 2020), and the explanation proposed for the improvement of acetoclastic methanogenesis was based on the redox cycling of Fe(II) and Fe(III) in Mag composition (H. Wang et al., 2020). In syntrophic cocultures, the main explanation suggested was the occurrence of CIET (W. Zhang et al., 2018; Zheng et al., 2020).

Table 2.3. Summary of studies with pure cultures of methanogens and the effects of materials on methanogenic activity. The main impacts highlighted were regarding the decrease (↓) of lag phase time (given in percentage, comparing the control condition with the best concentration of CM applied (best concentration in **bold** type)) and the number of times that MPR increases (+) or decreases relatively to the control

Pure culture	Substrate	CM	Effects on MP		References
			↓Lag phase	MPR	
Methanobacterium formicicum (DSM 1535T)	H_2/CO_2 (80:20, v/v; 1.7 × 10^5 Pa)	CNT (0.1, 0.5, 1 and **5** g·L^{-1})	75 %	(+) 16.6×	(Salvador et al., 2017)
Methanospirillum hungatei (DSM 864T)	H_2/CO_2 (80:20, v/v; 1.7 × 10^5 Pa)	CNT (0.1, 0.5, 1 and **5** g·L^{-1})	~ 100 %	(+) 5.5×	(Salvador et al., 2017)
Methanococcus maripaludis (DSM 14266)	H_2/CO_2 (80:20, v/v; 1.7 × 10^5 Pa)	rGO (0.02, 0.1, 0.2 g·L^{-1})	(no effect)	(no effect)	(W. Zhang et al., 2018)
Methanococcus maripaludis (DSM 14266)	H_2/CO_2 (80:20, v/v; 1.7 × 10^5 Pa)	CNT (0.2, 1, 2 and 5 g·L^{-1})	(no effect)	(-) negative effect	(W. Zhang et al., 2018)
Methanococcus maripaludis (DSM 14266)	H_2/CO_2 (80:20, v/v; 1.7 × 10^5 Pa)	Mag (4.64 mmol·L^{-1} in Fe)	(no effect)	(no effect)	(Fu et al., 2018)
Methanocella conradii (HZ254T)	H_2/CO_2 (80:20, v/v; 1.7 × 10^5 Pa)	Mag (10 mmol·L^{-1} in Fe)	(no effect)	(-) negative effect	(Xia et al., 2019)
Methanocella conradii (HZ254T)	H_2/CO_2 (80:20, v/v; 1.7 × 10^5 Pa)	CNT (5 g·L^{-1})	(-) negative effect	(no effect)	(Xia et al., 2019)
Methanocella conradii (DSM 24694)	H_2/CO_2 (80:20, v/v; 1.7 × 10^5 Pa)	Mag (4.64 mmol·L^{-1} in Fe)	(no effect)	(no effect)	(Fu et al., 2018)
Methanobacterium strain YSL (isolated)	formate (40 mmol·L^{-1})	GAC (25 g·L^{-1})	(Inhibition)	(Inhibition)	(Zheng et al., 2020)
Methanosaeta concilii (DSM 3671T)	acetate (10 mmol·L^{-1})	CNT (0.1, 0.5, **1** and 5 g·L^{-1})	(no effect)	(+) 1.2×	(Salvador et al., 2017)
Methanosarcina mazei (DSM 2053T)	acetate (20 mmol·L^{-1})	CNT (0.1, **0.5**, 1 and 5 g·L^{-1})	12.5 %	(+) 2.0×	(Salvador et al., 2017)

Table 2.3. Continued. Summary of studies with pure cultures of methanogens and the effects of materials on methanogenic activity. The main impacts highlighted were regarding the decrease (↓) of lag phase time (given in percentage, comparing the control condition with the best concentration of CM applied (best concentration in **bold** type)) and the number of times that MPR increases (+) or decreases (-) relatively to the control

Pure culture	**Substrate**	**CM**	**Effects on MP**		**References**
			↓Lag phase	MPR	
Methanosarcina mazei	acetate (20 mmol·L^{-1})	CNT (~0.2 g·L^{-1})	(no effect)	(+) ~ 4.1×	(Xiao et al., 2020)
Methanosarcina mazei zm-15 (isolated)	acetate (10 mmol·L^{-1})	Mag (7.5 mmol·L^{-1} in Fe)	51 %	(+) ~ 2.0×	(H. Wang et al., 2020)
Methanosarcina barkeri (DSM800)	acetate (10 mmol·L^{-1})	Mag (4.64 mmol·L^{-1} in Fe)	(no effect)	(+) ~ 2.0×	(Fu et al., 2019)
Methanosarcina barkeri (DSM800)	acetate (10 mmol·L^{-1})	Nano-graphite (Unknown concentration)	(no effect)	(-) ~ 0.7×	(Fu et al., 2019)
Methanosarcina barkeri (DSM800)	acetate (10 mmol·L^{-1})	CNT (Unknown concentration)	(no effect)	(no effect)	(Fu et al., 2019)
Methanosarcina barkeri	acetate (20 mmol·L^{-1})	CNT (~0.2 g·L^{-1})	(no effect)	(+) ~ 2.6×	(Xiao et al., 2020)
Syntrophomonas erecta subsp. *Sporosyntropha* (DSM 16215)	crotonate (20 mmol·L^{-1})	Mag (4.64 mmol·L^{-1} in Fe)	(no effect)	(no effect)	(Fu et al., 2018)

Table 2.4. Summary of studies showing the effect of the addition of materials on methanogenic activity of syntrophic cocultures by the number of times that MPR increases (+) relatively to the control, and the degree of decrease (↓) in lag phase time (in percentage), comparing the control without material with the assay with materials

Syntrophic coculture	Substrate	Materials	Effects on MP		References
			↓Lag phase	MPR	
Syntrophomonas wolfei (DSM 102351T) and *Methanospirillum hungatei* (DSM 864T)	butyrate (20 mmol·L^{-1})	CNT (5 g·L^{-1})	(no effect)	(+) 1.5×	(Salvador et al., 2017)
Syntrophomonas wolfei (DSM 102351) and *Methanococcus maripaludis* (DSM 14266)	butyrate (10 mmol·L^{-1})	CNT (2 g·L^{-1})	100 %	(+) ~ 1.5×	(W. Zhang et al., 2018)
Syntrophomonas wolfei (DSM 102351) and *Methanococcus maripaludis* (DSM14266)	butyrate (10 mmol·L^{-1})	rGO (0.1 g·L^{-1})	(no effect)	(+) ~ 1.5×	(W. Zhang et al., 2018)
Syntrophomonas wolfei (DSM 102351) and *Methanococcus maripaludis* (DSM 14266)	butyrate (10 mmol·L^{-1})	Kaolinite (2 g·L^{-1})	(no effect)	(no effect)	(W. Zhang et al., 2018)
Geobacter metallireducens strain GS-15 (ATCC 53774) and *Methanobacterium* strain YSL	ethanol (10 mmol·L^{-1})	GAC (25 g·L^{-1})	85 %	(no effect)	(Zheng et al., 2020)
PilA-deficient *Geobacter metallireducens* (mutant strain) and *Methanobacterium* strain YSL	ethanol (10 mmol·L^{-1})	GAC (25 g·L^{-1})	70 %	(+) ~ 2.9	(Zheng et al., 2020)

2.2.2. Effect of CM on microbial enrichments from natural sediments

The development of microbial enrichment cultures, under controlled laboratory conditions, is an approach to investigate the effect of different environmental conditions towards the microbial composition and activity (Vanwonterghem et al., 2014). This approach has been used to investigate the impact of (nano)materials when they are in contact with anaerobic communities for extended periods. In this subsection, a review on enrichment studies is presented in Table 2.5. In general, the presence of CM decreased the lag phases preceding MP, increased the MPR, and altered the relative abundances of microorganisms in the final communities. For instance, MPR from butyrate was improved in lake sediment microbiomes in the presence of CNT (5 $g \cdot L^{-1}$), whose incubations were transferred over time, and it was followed by changes in the microbial community composition, with the enrichment of typical fatty-acid degrading bacteria (*Syntrophomonas* spp.) (W. Zhang et al., 2018). However, different sediments led to different enrichment cultures (under the same conditions), with *Syntrophomonas* as the major group of the bacterial populations in both enrichments, but the dominant methanogens comprised *Methanosarcina* and *Methanospirillum* in one enrichment (from Weiming Lake) and *Methanoregula* and *Methanospirillum* in another (from Erhai Lake) (W. Zhang et al., 2018).

Under controlled conditions, as in anaerobic bioreactors, the addition of CM can be used as a strategy to boost MP, for recovering the biomethane which can be used as a sustainable energy (Castilho et al., 2022; Prussi et al., 2021). But at the same time, knowing that methanogenesis has a central role in the global carbon cycle in nature (Stams and Plugge, 2009), the increase of MP in the presence of CM is also a problem. Conductive minerals (e.g., iron oxide minerals) or black carbon are present in natural environments (e.g., lake and/or river sediments) as a result of incomplete burning of plant biomass (Amelia-Elena et al., 2018). Experimental studies have been demonstrated the acceleration of MP by enrichment cultures in the presence of CM, like Mag (Fu et al., 2019, 2018; Kato et al., 2012; Li et al., 2015; H. Wang et al., 2020; Xia et al., 2019; Zhang and Lu, 2016; W. Zhang et al., 2018), CNT (Fu et al., 2018; Xia et al., 2019; Zhang and Lu, 2016; W. Zhang et al., 2018), biochar (Yuan et al., 2018), and GAC (Amelia-Elena et al., 2018), using as inoculum anaerobic microbial communities from samples of different natural sediments. The anthropogenic activity can increase the input of CM in sediments via runoff from forestry industry or other industrial activities (Amelia-Elena et al., 2018), which can contribute to increase the methane fluxes to the atmosphere, where methane is a strong greenhouse gas (Stams et al., 2012; Stams and Plugge, 2009). Although natural sediments have been used as inoculum to study the impact of CM towards MP (Amelia-Elena et al., 2018; Fu et al., 2019, 2018; Kato et al., 2012; Li et

al., 2015; H. Wang et al., 2020; Xia et al., 2019; Yuan et al., 2018; Zhang and Lu, 2016; W. Zhang et al., 2018) (Table 2.5), less attention has been paid to enrichment studies using anaerobic sludge as inoculum.

CIET is commonly proposed as the cause for the improvements towards MP in enriched communities (Fu et al., 2018; Kato et al., 2012; Li et al., 2015; Xia et al., 2019; Zhang and Lu, 2016; W. Zhang et al., 2018), but not disregarding that IHT/IFT may occur at the same time (Fu et al., 2018; Xia et al., 2019; W. Zhang et al., 2018). The support for this hypothesis is usually the composition of the enriched microbial communities in the presence of materials. Some microbial enrichment studies with CM showed that electroactive bacteria like *Geobacter* spp. were enriched in the presence of biochar (growing on ethanol) (Yuan et al., 2018), GAC (growing on acetate) (Amelia-Elena et al., 2018), Mag (growing on butyrate) (Li et al., 2015), and Mag (growing on ethanol or acetate) (Kato et al., 2012), suggesting the hypothesis that CM stimulated CIET mechanism between *Geobacter* and methanogens. However, in other studies applying Mag or CNT for the degradation of VFA (e.g., acetate, propionate, butyrate), *Geobacter* was not enriched (Fu et al., 2019, 2018; H. Wang et al., 2020; Xia et al., 2019; Zhang and Lu, 2016; W. Zhang et al., 2018). Then, it was hypothesized that other species would be capable of participating in CIET. For instance, some reports raised the hypothesis that *Syntrophomonas* spp. would switch from IHT/IFT for CIET in the presence of CM, based on the improvement of methanogenic activity and the null impact of CM towards pure cultures of methanogens (Fu et al., 2018; W. Zhang et al., 2018).

Table 2.5. Summary of studies using CM to develop enrichment cultures, highlighting the main impacts promoted by the presence of materials in terms of lag phase reduction (↓) and MPR improvement for each transfer ("n" represents the number of transfers performed), and the main bacteria and methanogens enriched in the final microbial communities

Inoculum	Substrate	CM	n	Effects on MP		Bacteria enriched	Methanogens enriched	References
				↓Lag phase	MPR			
Wetland sediment	acetate (10 mmol·L^{-1})	Mag (4.6 mmol·L^{-1} in Fe)	1	52 %	(+) 1.5×	-	-	(H. Wang et al., 2020)
			2	79 %	(+) 1.3×	-	-	
			3	(no effect)	(+) 1.3×	-	-	
			4	100 %	(+) 1.4×	-	-	
		Mag (7.5 mmol·L^{-1} in Fe)	5	67 %	(+) 1.3×	*Syntrophomonas* spp. *Sporobacter termitidis* *Desulfovibrio magneticus*	*Methanosarcina mazei*	
Lake sediment	propionate (5 mmol·L^{-1})	Mag (10 mmol·L^{-1} in Fe)	1	(no effect)	(+) ~ 1.7×	-	-	(Xia et al., 2019)
			2	25 %	(+) ~ 1.7×	-	-	
			3	27 %	(+) ~ 1.7×	-	-	
			4	40 %	(+) ~ 1.4×	-	-	
			5	70 %	(+) 2.1×	*Smithella* (1st dominant) *Syntrophomonas* (2nd dominant) *Desulfovibrio* *Desulfobulbus* *Propionicimonas*	*Methanosaeta* (dominant) *Methanosarcina* *Methanoregula*	
		MWCNT (5 g·L-1)	1	(no effect)	(+) ~ 1.8×	-	-	
			2	25 %	(+) ~ 1.1×	-	-	
			3	27 %	(+) ~ 1.4×	-	-	
			4	50 %	(no effect)	-	-	
			5	70 %	(+) 1.7×	-	-	

Table 2.5. Continued. Summary of studies using CM to develop enrichment cultures, highlighting the main impacts promoted by the presence of materials in terms of lag phase reduction (↓) and MPR improvement for each transfer ("n" represents the number of transfers performed), and the main bacteria and methanogens enriched in the final microbial communities

Inoculum	Substrate	CM	n	Effects on MP		Bacteria enriched	Methanogens enriched	References
				↓Lag phase	MPR			
Wetland sediment	acetate (5 mmol·L^{-1})	Mag (4.6 mmol·L^{-1} in Fe)	1	(no effect)	(+) ~ 1.4×	-	-	(Fu et al., 2019)
	acetate (10 mmol·L^{-1})		4	100 %	(+) ~ 1.1×	-	-	
			7	100 %	(+) ~ 1.1×	-	-	
			10	100 %	(+) ~ 2.3×	-	-	
			14	83 %	(+) ~ 2.5×	*Azonexus* *Cytophaga* *Firmicutes* *Veillonellaceae* *Desulfovibrionaceae* *Anaerovorax* *Syntrophomonas* *Saccharofermentans acetigenes*	*Methanosarcina* (*M. barkeri* as the closest pure culture relative)	
Wetland sediment	butyrate (5 mmol·L^{-1})	Mag (4.6 mmol·L^{-1} in Fe)	1 and 2	(no effect)	(no effect)	-	-	(Fu et al., 2018)
			3	83 %	(+) no MP on control	-	-	
	butyrate (10 mmol·L^{-1})		4	100 %	(+) ~ 1.1×	-	-	
			5	100 %	(+) ~ 1.6×	-	-	
			6	100 %	(+) ~ 2.0×	-	-	
			7	100 %	(+) ~ 1.1×	-	-	
			8	100 %	(+) ~ 1.4×	-	-	
			13	57 %	(+) ~ 1.1×	*Syntrophomonas* (*S. wolfei* as the closest relative)	*Methanobacteria* *Methanocella*	

Table 2.5. Continued. Summary of studies using CM to develop enrichment cultures, highlighting the main impacts promoted by the presence of materials in terms of lag phase reduction (↓) and MPR improvement for each transfer ("n" represents the number of transfers performed), and the main bacteria and methanogens enriched in the final microbial communities

Inoculum	Substrate	CM	n	Effects on MP		Bacteria enriched	Methanogens enriched	References
				↓Lag phase	MPR			
Paddy soil sediment	ethanol (30 mmol·L^{-1})	Biochar from rice straw (~20 g·L^{-1})	1	33 %	(+) 10.7×	*Lysinibacillus* *Bacillus* *Thermincola* *Geobacter* (0.13 %)	*Methanosarcina* (dominant) *Methanobacterium*	(Yuan et al., 2018)
		Biochar from wood chips (~20 g·L^{-1})		(no effect)	(-) negative effect	*Thermincola* *Bacillus* *Geobacter*	*Methanosarcina* (dominant) *Methanobacterium*	
		Biochar from manure (~20 g·L^{-1})		67 %	(+) 12.3×	*Clostridium* *Geobacter*	*Methanobacterium* (dominant) *Methanosarcina* *Methanomassiliicoccus*	
Lake sediment (Weiming lake - WM)	Butyrate (10 mmol·L^{-1})	CNT (5 g·L^{-1})	1	71 %	(+) ~ 1.7×	-	-	
			2	33 %	(+) ~ 1.2×	-	-	
			3	(no effect)	(+) ~ 1.5×	-	-	
			4	(no effect)	(+) ~ 1.5×	*Syntrophomonas* (73 %) *Desulfovibrio* (27 %)	*Methanosarcina* (78 %) *Methanospirillum* (22 %)	
Lake sediment (Erhai lake - EH)	butyrate (10 mmol·L^{-1})	CNT (5 g·L^{-1})	1	(no effect)	(+) ~ 1.7×	-	-	(W. Zhang et al., 2018)
			2	(no effect)	(+) ~ 1.4×	-	-	
			3	(no effect)	(+) ~ 1.4×	-	-	
			4	(no effect)	(+) ~ 1.8×	*Syntrophomonas* (55 %) *Gracilibacter* Unclassified *Rhodospirillaceae* *Azospira* *Sulfurospirillum* *Desulfovibrio*	*Methanoregula* (64 %) *Methanospirillum* *Methanosarcina* *Methanosaeta*	

Table 2.5. Continued. Summary of studies using CM to develop enrichment cultures, highlighting the main impacts promoted by the presence of materials in terms of lag phase reduction (↓) and MPR improvement for each transfer ("n" represents the number of transfers performed), and the main bacteria and methanogens enriched in the final microbial communities

Inoculum	Substrate	CM	n	Effects on MP		Bacteria enriched	Methanogens enriched	References
				↓Lag phase	MPR			
Coastal sediments	acetate (10 mmol·L^{-1})	GAC (10 g·L^{-1})	6	80 %	(+) ~ 10.9×	*Geobacter* *Desulfuromonas*	*Methanosarcina*	(Amelia-Elena et al., 2018)
Lake sediment (Weiming Lake – WML)	butyrate (10 mmol·L^{-1})	Mag (10 mmol·L^{-1} in Fe)	1	63 %	(+) ~ 1.3×	-	-	(Zhang and Lu, 2016)
			2	(no effect)	(+) ~ 2.0×	-	-	
			3	(no effect)	(+) ~ 2.1×	-	-	
			4	(no effect)	(+) ~ 1.4×	*Syntrophomonas* (96 %) *Desulfovibrio*	*Methanosarcina* (84 %) *Methanomicrobia*	
Lake sediment (Erhai Lake – EHL)		Mag (10 mmol·L^{-1} in Fe)	1	(no effect)	(+) ~ 1.5×	-	-	
			2	18 %	(no effect)	-	-	
			3	(no effect)	(+) ~ 1.3×	-	-	
			4	(no effect)	(+) ~ 1.3×	*Syntrophomonas* (40 %) *Sulfurospirillum* *Paenibacillus* *Treponema* unclassified *Rikenellaceae*	*Methanoregula* (57 %) *Methanosarcina* (26 %) *Methanospirillum* (10 %) *Methanosaeta* (3 %) *Methanobacterium* (3 %)	
Rice paddy soil	propionate (10 mmol·L^{-1})	Mag (20 mmol·L^{-1} in Fe)	1	32 %	(no effect)	-	-	(Yang et al., 2016)
			2	49 %	(+) ~ 1.9×	-	-	
			3	42 %	(+) ~ 1.6×	-	-	
			4	34 %	(+) ~ 2.4×	-	-	
			5	56 %	(+) ~ 1.8×	*Thauera* (60 %) *Diaphorobacter* *Treponema*	*Methanobacterium* (dominant) *Methanospirillum* *Methanosaeta* *Methanosarcina*	

Table 2.5. Continued. Summary of studies using CM to develop enrichment cultures, highlighting the main impacts promoted by the presence of materials in terms of lag phase reduction (↓) and MPR improvement for each transfer ("n" represents the number of transfers performed), and the main bacteria and methanogens enriched in the final microbial communities

Inoculum	Substrate	CM	n	Effects on MP		Bacteria enriched	Methanogens enriched	References
				↓Lag phase	MPR			
Paddy soil	butyrate (10 mmol·L^{-1})	Mag (6.4 mmol·L^{-1} Fe ion)	1	(no effect)	(+) ~ 1.2×	-	-	(Li et al., 2015)
			2	(no effect)	(+) ~ 1.8×	-	-	
			3	33 %	(+) ~ 3.0×	-	-	
3rd transfer incubation (continuous transfers)		Mag (6.4 mmol·L^{-1} in Fe)	9	80 %	(+) ~ 1.6×	*Syntrophomonadaceae* *Geobacteraceae*	*Methanobacteriales* *Methanosarcinaceae* *Methanocellales*	
Rice paddy soil	ethanol (20 mmol·L^{-1})	Haematite (semi-conductive) (20 mmol·L^{-1} in Fe)	1	(no effect)	(+) ~ 1.4×	*Deltaproteobacteria* (*Geobacter*) *Firmicutes* (*Clostridium* and *Syntrophomonas*)	*Euryarchaeota* (*Methanosarcina*)	(Kato et al., 2012)
			2	(no effect)	(+) ~ 1.3×			
		Mag (conductive) (20 mmol·L^{-1} in Fe)	1	(no effect)	(+) ~ 1.4×	*Deltaproteobacteria* (*Geobacter*) *Firmicutes* (*Clostridium* and *Syntrophomonas*)	*Euryarchaeota* (*Methanosarcina*)	
			2	(no effect)	(+) ~ 1.3×			
		Ferrihydrite (insulative) (20 mmol·L^{-1} in Fe)	1	(no effect)	(-) ~0.8×	*Firmicutes* (*Clostridium* and *Syntrophomonas*) *Deltaproteobacteria* (*Geobacter*)	*Euryarchaeota* (*Methanobacterium*)	
			2	(no effect)	(-) ~0.5×			
	acetate (20 mmol·L^{-1})	Haematite (semi-conductive) (20 mmol·L^{-1} in Fe)	1	30 %	(+) ~ 1.6×	*Deltaproteobacteria* (*Geobacter*)	*Euryarchaeota* (*Methanosarcina*)	
			2	43 %	(+) ~ 1.2×			
		Mag (conductive) (20 mmol·L^{-1} in Fe)	1	30 %	(+) ~ 1.5×	*Deltaproteobacteria* (*Geobacter*) *Firmicutes* (*Clostridium* and *Syntrophomonas*)	*Euryarchaeota* (*Methanosarcina*)	
			2	43 %	(+) ~ 1.2×			
		Ferrihydrite (insulative) (20 mmol·L^{-1} in Fe)	1	(-) negative effect	(no effect)	*Deltaproteobacteria* (*Geobacter*) *Firmicutes* (*Clostridium* and *Syntrophomonas*)	*Euryarchaeota* (*Methanosarcina*)	
			2	(-) negative effect	(+) ~ 1.3×			

(-) The analysis of microbial composition was not carried out.

2.2.3. Effect of (nano)materials on anaerobic sludge, sediments, and other complex microbial communities

During the last years, researchers have been testing (nano)materials in anaerobic communities with the purpose of improving AD efficiency. Table 2.6 summarizes the initial effects of AC/GAC, Mag and Zeo on different types of microbial communities, such as anaerobic sludge and sediments degrading different substrates (e.g., sludge, synthetic and real wastewater, acetate, ethanol, butyrate). In the presence of AC/GAC and Mag, the duration of lag phases preceding MP tends to decrease and the MPR tends to be enhanced. On the other hand, the presence of Zeo seems to affect more the MPR than the duration of lag phase. Thus, the main observations are similar regarding the decrease of lag phases and the improvement of MPR, but depending on the type of material, the main impact observed may vary (Yiwei Liu et al., 2021; Martins et al., 2018). Some materials seem to mainly affect the decrease of lag phases, others affect more the MPR, or even the methane or biogas yields (Chen et al., 2022). For instance, GAC (50 $g \cdot L^{-1}$) impacted greatly the duration of lag phase during the degradation of dog food by anaerobic sludge, by decreasing it from 170 d (control without GAC) to 4 d (Dang et al., 2017). On the other hand, in other studies, no impact of materials like Mag or Zeo were observed in the duration of lag phases preceding MP (Fu et al., 2019, 2018; Li et al., 2022; Milán et al., 2001; Xu et al., 2018).

Taking into consideration diverse literature reviews (Abbas et al., 2021; Baniamerian et al., 2019; Castilho et al., 2022; H. Liu et al., 2021; Yiwei Liu et al., 2021; Martins et al., 2018; J. H. Park et al., 2018; Roopnarain et al., 2021; Wu et al., 2020; J. Zhang et al., 2018), the presence of materials in many anaerobic environments accelerates MP, which is highly relevant from an applied point of view since it increases the rate of AD process, making it even more competitive. In continuous anaerobic digesters, CM have been reported not only to accelerate the MP, but also to contribute for a more stable operation (Martins et al., 2018; J. H. Park et al., 2018). These results are very relevant since AD may be a slow process, with lower MP efficiencies (Yiwei Liu et al., 2021). The microorganisms involved in AD have different growth rates and specific activities, and particularly, methanogens have a slow growth rate, which could affect hydrogen removal of the system (Yiwei Liu et al., 2021; Stams et al., 2012). This could result in several problems: low efficient degradation of key intermediates (e.g., propionate and butyrate), consequently resulting in VFA accumulation; instability of the process by dropping the pH; and then the failure of the system (Yiwei Liu et al., 2021). The presence of (nano)materials seems to avoid this worst scenario.

Despite the beneficial effect of most (nano)materials, some studies have been reporting the toxic effect of certain CM towards microorganisms' activity (e.g., carbon black nanoparticles) (Martins et al., 2018; J. H. Park et al., 2018; Wu et al., 2020). Some materials may promote direct inhibition by the presence of Fe(III), substrate competition or toxic effects to microorganisms (e.g., by particle size) (Wu et al., 2020). Cellular oxidative stress and cell apoptosis are examples of toxicity to cell promoted by certain (nano)materials (Barua and Dhar, 2017; Wu et al., 2020). Also, iron-based materials, such as magnesium oxide, silver nanoparticles and ferrihydrite, were shown as inhibitors for methanogenic activity (Martins et al., 2018; Wu et al., 2020). This way, since the effects are not always positive, the evaluation of different (nano)materials is needed before their application in AD systems in order not to compromise the process.

Table 2.6. Summary of studies reporting the effect of AC, GAC, Mag and Zeo (and the concentration of material applied – C) on anaerobic sludge, sediments, and other complex microbial communities. The presence of (nano)materials affected the lag phase duration (by reducing (↓), or increasing (values < 0) it) and the MPR (i.e., MPR > 1, increased; MPR < 1, decreased), when comparing with the control condition without materials

Type of inoculum	Substrate	Materials		Lag phase			MPR	References
		Type	C/ ($g \cdot L^{-1}$)	Control/ d	Material/ d	↓Lag phase/ %		
Anaerobic sludge	butyrate	AC	0.5	1.3	1.3	5.3	1.0	In this study
Anaerobic sludge	kitchen waste	AC	10.0	0.0	0.0	0.0	4.0	(Hu et al., 2022)
Anaerobic sludge	activated sludge	AC	8.0	4.8	0.2	96.6	0.9	(Liu et al., 2020)
Anaerobic sludge	acetate c1	GAC	0.5	1.0	0.8	20.0	11.1	(Xu et al., 2018)
Anaerobic sludge	acetate c1	GAC	5.0	1.0	0.8	20.0	11.1	(Xu et al., 2018)
Anaerobic sludge	acetate c1	GAC	25.0	1.0	0.2	80.0	10.0	(Xu et al., 2018)
Anaerobic sludge	propionate c1	GAC	0.5	0.5	0.6	-20.0	0.9	(Xu et al., 2018)
Anaerobic sludge	propionate c1	GAC	5.0	0.5	0.6	-20.0	1.0	(Xu et al., 2018)
Anaerobic sludge	propionate c1	GAC	25.0	0.5	0.6	-20.0	0.8	(Xu et al., 2018)
Anaerobic sludge	butyrate c1	GAC	0.5	1.0	0.8	20.0	1.0	(Xu et al., 2018)
Anaerobic sludge	butyrate c1	GAC	5.0	1.0	0.5	50.0	1.1	(Xu et al., 2018)
Anaerobic sludge	butyrate c1	GAC	25.0	1.0	1.0	0.0	0.9	(Xu et al., 2018)
Anaerobic sludge	acetate c2	GAC	0.5	0.3	0.3	0.0	1.0	(Xu et al., 2018)
Anaerobic sludge	acetate c2	GAC	5.0	0.3	0.4	-33.3	1.1	(Xu et al., 2018)
Anaerobic sludge	acetate c2	GAC	25.0	0.3	0.4	-33.3	1.1	(Xu et al., 2018)
Coastal sediments	acetate	GAC	10.0	35.0	7.0	80.0	10.9	(Amelia-Elena et al., 2018)
Anaerobic sludge	commercial dog food	GAC	50.0	170.0	4.0	97.6	50.0	(Dang et al., 2017)
Anaerobic sludge	acetate	GAC	11.1	7.6	6.4	15.5	1.1	(Lee et al., 2020)
Anaerobic sludge	food waste	GAC	25.0	19.0	13.0	31.6	1.6	(Ryue et al., 2019)
Anaerobic granular sludge	oleate	GAC	2.0	23.5	7.7	67.2	0.1	(Tan and Lens, 2021)
Anaerobic granular sludge	oleate	GAC	2.0	23.5	14.6	37.9	0.2	(Tan and Lens, 2021)
Anaerobic granular sludge crushed	oleate	GAC	0.5	16.6	16.3	1.8	1.3	(Tan et al., 2021)

Table 2.6. Continued. Summary of studies reporting the effect of AC, GAC, Mag and Zeo (and the concentration of material applied – C) on anaerobic sludge, sediments, and other complex microbial communities. The presence of (nano)materials affected the lag phase duration (by reducing (↓), or increasing (values < 0) it) and the MPR (i.e., MPR > 1, increased; MPR < 1, decreased), when comparing with the control condition without materials

Type of inoculum	Substrate	Materials		Lag phase			MPR	References
		Type	C/ ($g \cdot L^{-1}$)	Control/ d	Material/ d	↓Lag phase/ %		
Anaerobic granular sludge crushed	oleate	GAC	1.0	16.6	15.5	6.6	1.4	(Tan et al., 2021)
Anaerobic granular sludge crushed	oleate	GAC	2.0	16.6	13.2	20.5	2.2	(Tan et al., 2021)
Anaerobic granular sludge crushed	oleate	GAC	4.0	16.6	12.0	27.7	3.0	(Tan et al., 2021)
Anaerobic granular sludge crushed	oleate	GAC	8.0	16.6	9.5	42.8	1.2	(Tan et al., 2021)
Anaerobic granular sludge crushed	oleate	GAC	16.0	16.6	2.6	84.3	0.8	(Tan et al., 2021)
Anaerobic granular sludge crushed	oleate	GAC	25.0	16.6	1.6	90.4	0.5	(Tan et al., 2021)
Anaerobic granular sludge crushed	oleate	GAC	33.0	16.6	1.6	90.4	0.6	(Tan et al., 2021)
Anaerobic granular sludge crushed	oleate	GAC	2.0	17.1	14.2	17.0	1.3	(Tan et al., 2021)
Anaerobic granular sludge	oleate	GAC	2.0	18.3	15.8	13.7	1.6	(Tan et al., 2021)
Anaerobic granular sludge crushed	oleate	GAC	2.0	16.4	12.6	23.2	1.1	(Tan et al., 2021)
Anaerobic granular sludge crushed	real butter wastewater	GAC	2.0	17.0	16.6	2.4	1.2	(Tan et al., 2021)
Anaerobic granular sludge crushed	real dairy wastewater	GAC	2.0	12.2	6.5	46.7	1.2	(Tan et al., 2021)
Anaerobic sludge	propionate c2	GAC	0.5	4.3	3.5	18.6	1.5	(Xu et al., 2018)
Anaerobic sludge	propionate c2	GAC	5.0	4.3	1.1	74.4	7.5	(Xu et al., 2018)
Anaerobic sludge	propionate c2	GAC	25.0	4.3	1.0	76.7	7.0	(Xu et al., 2018)
Anaerobic sludge	butyrate c2	GAC	0.5	13.0	11.0	15.4	1.6	(Xu et al., 2018)
Anaerobic sludge	butyrate c2	GAC	5.0	13.0	5.0	61.5	8.0	(Xu et al., 2018)

Table 2.6. Continued. Summary of studies reporting the effect of AC, GAC, Mag and Zeo (and the concentration of material applied – C) on anaerobic sludge, sediments, and other complex microbial communities. The presence of (nano)materials affected the lag phase duration (by reducing (↓), or increasing (values < 0) it) and the MPR (i.e., MPR > 1, increased; MPR < 1, decreased), when comparing with the control condition without materials

Type of inoculum	Substrate	Materials		Lag phase			MPR	References
		Type	C/ ($g \cdot L^{-1}$)	Control/ d	Material/ d	↓Lag phase/ %		
Anaerobic sludge	butyrate c2	GAC	25.0	13.0	7.0	46.2	8.8	(Xu et al., 2018)
Anaerobic sludge	acetate	GAC	6.0	6.6	6.5	1.5	1.7	(J.-H. Park et al., 2018)
Anaerobic sludge	acetate	GAC	12.0	6.6	6.4	3.0	1.7	(J.-H. Park et al., 2018)
Anaerobic sludge	ethanol	GAC	6.0	6.7	6.2	7.5	1.3	(J.-H. Park et al., 2018)
Anaerobic sludge	ethanol	GAC	12.0	6.7	6.6	1.5	1.7	(J.-H. Park et al., 2018)
Anaerobic sludge	fat, oil and grease + waste activated sludge	GAC	10.0	1.5	1.0	33.3	1.0	(He et al., 2021)
Anaerobic sludge	fat, oil and grease + waste activated sludge	GAC	5.0	1.5	0.5	66.7	1.0	(He et al., 2021)
Anaerobic sludge	fat, oil and grease + waste activated sludge	GAC	15.0	1.5	0.2	86.7	0.8	(He et al., 2021)
Anaerobic sludge	dewatered wasted activated sludge	GAC	3.3	0.0	0.0	0.0	1.2	(Yang et al., 2017)
Anaerobic sludge	dewatered wasted activated sludge	GAC	6.7	0.0	0.0	0.0	1.3	(Yang et al., 2017)
Anaerobic sludge	dewatered wasted activated sludge	GAC	13.3	0.0	0.0	0.0	1.4	(Yang et al., 2017)
Anaerobic sludge	dewatered wasted activated sludge	GAC	33.3	0.0	0.0	0.0	1.5	(Yang et al., 2017)
Anaerobic sludge	food waste	GAC	25.0	10.0	7.0	30.0	1.3	(Ryue et al., 2019)

Table 2.6. Continued. Summary of studies reporting the effect of AC, GAC, Mag and Zeo (and the concentration of material applied – C) on anaerobic sludge, sediments, and other complex microbial communities. The presence of (nano)materials affected the lag phase duration (by reducing (↓), or increasing (values < 0) it) and the MPR (i.e., MPR > 1, increased; MPR < 1, decreased), when comparing with the control condition without materials

Type of inoculum	Substrate	Materials		Lag phase			MPR	References
		Type	C/ ($g \cdot L^{-1}$)	Control/ d	Material/ d	↓Lag phase/ %		
Anaerobic sludge	acetate	GAC	30.3	6.0	3.0	50.0	1.8	(Zhang et al., 2017)
Wetland sediment	butyrate	Mag	0.4	1.0	1.0	0.0	1.0	(Fu et al., 2018)
Wetland sediment	acetate	Mag	0.4	1.0	1.0	0.0	1.4	(Fu et al., 2019)
Anaerobic sludge	sludge	Mag	9.7	0.0	0.0	0.0	1.5	(Li et al., 2022)
Anaerobic sludge	butyrate	Mag	0.5	1.3	1.3	3.8	0.9	In this study
Anaerobic granular sludge	glucose	Mag	0.3	-	-	nc	4.0	(Barrena et al., 2023)
Flocculent sludge	glucose	Mag	0.1	-	-	nc	0.7	(Barrena et al., 2023)
Flocculent sludge	glucose	Mag	0.3	-	-	nc	5.3	(Barrena et al., 2023)
Flocculent sludge	glucose	Mag	0.5	-	-	nc	6.7	(Barrena et al., 2023)
Flocculent sludge	glucose	Mag	1.0	-	-	nc	8.0	(Barrena et al., 2023)
Rice paddy soil	ethanol	Mag	1.5	10.0	10.0	0.0	1.4	(Kato et al., 2012)
Rice paddy soil	acetate	Mag	1.5	10.0	7.0	30.0	1.5	(Kato et al., 2012)
Anaerobic sludge	acetate	Mag	11.1	7.6	4.9	35.8	1.3	(Lee et al., 2020)
Paddy soil sediment	butyrate	Mag	0.5	8.0	8.0	0.0	1.2	(Li et al., 2015)
Rice paddy soil	propionate	Mag	1.5	17.1	11.7	31.9	0.9	(Yang et al., 2016)
Lake sediment	butyrate	Mag	0.8	72.0	27.0	62.5	1.3	(Zhang and Lu, 2016)
Anaerobic sludge	acetate	Mag	6.0	6.6	6.7	-1.5	1.4	(J.-H. Park et al., 2018)
Anaerobic sludge	ethanol	Mag	6.0	6.7	6.5	3.0	1.2	(J.-H. Park et al., 2018)

Table 2.6. Continued. Summary of studies reporting the effect of AC, GAC, Mag and Zeo (and the concentration of material applied – C) on anaerobic sludge, sediments, and other complex microbial communities. The presence of (nano)materials affected the lag phase duration (by reducing (↓), or increasing (values < 0) it) and the MPR (i.e., MPR > 1, increased; MPR < 1, decreased), when comparing with the control condition without materials

Type of inoculum	Substrate	Materials		Lag phase			MPR	References
		Type	C/ ($g \cdot L^{-1}$)	Control/ d	Material/ d	↓Lag phase/ %		
Lake sediment	butyrate	Mag	0.8	9.0	9.0	0.0	1.5	(Zhang and Lu, 2016)
Wetland sediment	acetate	Mag	0.4	5.2	2.5	52.0	1.5	(H. Wang et al., 2020)
Lake sediment	propionate	Mag	0.8	12.0	12.0	0.0	1.7	(Xia et al., 2019)
Anaerobic sludge	waste activated sludge	Mag	0.8	3.8	5.3	-38.5	2.6	(Yan et al., 2020)
Anaerobic sludge	wheat straw	Mag (-)	0.1	1.0	0.0	100.0	1.5	(Yang Liu et al., 2021)
Anaerobic sludge	wheat straw	Mag (+)	0.1	1.0	0.0	100.0	1.2	(Yang Liu et al., 2021)
Anaerobic sludge	wheat straw	Mag (neutral)	0.1	1.0	0.0	100.0	1.3	(Yang Liu et al., 2021)
Anaerobic granular sludge	oleate	PAC	2.0	23.5	3.4	85.5	0.2	(Tan and Lens, 2021)
Anaerobic sludge	acetate	PAC	6.0	6.6	6.4	3.0	1.4	(J.-H. Park et al., 2018)
Anaerobic sludge	ethanol	PAC	6.0	6.7	6.7	0.0	1.1	(J.-H. Park et al., 2018)
Anaerobic sludge	fruit and vegetable waste + layer chicken manure	PAC	10.0	5.0	0.0	100.0	1.3	(de Quadros et al., 2022)
Digestate	ethanol	PAC	20.0	1.7	2.1	-25.0	1.0	(König et al., 2022)
Anaerobic sludge	waste activated sludge	PAC	0.5	3.8	4.3	-12.8	2.7	(Yan et al., 2020)
Piggery waste manure	acetate	Zeo (natural)	0.4	0.0	0.0	0.0	1.0	(Milán et al., 2001)

Table 2.6. Continued. Summary of studies reporting the effect of AC, GAC, Mag and Zeo (and the concentration of material applied – C) on anaerobic sludge, sediments, and other complex microbial communities. The presence of (nano)materials affected the lag phase duration (by reducing (↓), or increasing (values < 0) it) and the MPR (i.e., MPR > 1, increased; MPR < 1, decreased), when comparing with the control condition without materials

Type of inoculum	Substrate	Materials		Lag phase			MPR	References
		Type	C/ ($g \cdot L^{-1}$)	Control/ d	Material/ d	↓Lag phase/ %		
Piggery waste manure	methanol	Zeo (natural)	0.4	0.0	0.0	0.0	1.1	(Milán et al., 2001)
Anaerobic sludge	butyrate	Zeo (type-13X)	0.5	1.9	1.9	-1.6	0.9	In this study
Piggery waste manure	swine wastes	Zeo	10.0	30.0	17.0	43.3	692.3	(Zheng et al., 2015)
Piggery waste manure	swine wastes	Zeo	10.0	30.0	30.0	0.0	3.0	(Zheng et al., 2015)
Piggery waste manure	swine wastes	Zeo	10.0	30.0	5.0	83.3	1620.0	(Zheng et al., 2015)
Municipal sludge	municipal activated sludge	Zeo	4.0	0.0	0.0	0.0	1.3	(Amen et al., 2017)
Anaerobic sludge	food waste (+ 4 $g \cdot L^{-1}$ NH_4^+)	Zeo	15.0	8.9	5.3	40.4	1.1	(Cardona et al., 2021)
Pig waste manure	pig waste	Zeo (natural)	4.0	2.0	2.0	0.0	1.0	(Kotsopoulos et al., 2008)
Pig waste manure	pig waste	Zeo (natural)	8.0	2.0	2.0	0.0	1.6	(Kotsopoulos et al., 2008)
Pig waste manure	pig waste	Zeo (natural)	12.0	2.0	2.0	0.0	1.7	(Kotsopoulos et al., 2008)
Pig waste manure	pig waste	Zeo (natural)	4.0	2.0	2.0	0.0	1.3	(Kotsopoulos et al., 2008)
Pig waste manure	pig waste	Zeo (natural)	8.0	2.0	2.0	0.0	1.7	(Kotsopoulos et al., 2008)
Pig waste manure	pig waste	Zeo (natural)	12.0	2.0	2.0	0.0	1.5	(Kotsopoulos et al., 2008)

Table 2.6. Continued. Summary of studies reporting the effect of AC, GAC, Mag and Zeo (and the concentration of material applied – C) on anaerobic sludge, sediments, and other complex microbial communities. The presence of (nano)materials affected the lag phase duration (by reducing (↓), or increasing (values < 0) it) and the MPR (i.e., MPR > 1, increased; MPR < 1, decreased), when comparing with the control condition without materials

Type of inoculum	Substrate	Materials		Lag phase			MPR	References
		Type	C/ ($g \cdot L^{-1}$)	**Control/** d	**Material/** d	↓Lag phase/ %		
Anaerobic sludge	slaughterhouse waste + industrial and food waste + stearic acid + palmitic acid	Zeo (natural)	5.0	10.0	0.0	100.0	1.3	(Nordell et al., 2013)
Anaerobic sludge	acetate	Zeo (natural)	30.3	6.0	6.0	0.0	1.8	(Zhang et al., 2017)
Anaerobic sludge	food waste	Zeo	15.0	6.5	6.9	-6.2	0.9	(Cardona et al., 2021)
Anaerobic sludge	fruit and vegetable waste + layer chicken manure	Zeo (natural)	10.0	5.0	5.0	0.0	1.1	(de Quadros et al., 2022)
Anaerobic sludge	fruit and vegetable waste + layer chicken manure	Zeo (faujasite)	10.0	5.0	0.0	100.0	1.3	(de Quadros et al., 2022)
Piggery waste manure	piggery waste + sewage	Zeo (natural)	2.0	0.0	0.0	0.0	1.0	(Montalvo et al., 2005)
Piggery waste manure	piggery waste + sewage	Zeo (natural)	4.0	0.0	0.0	0.0	1.3	(Montalvo et al., 2005)
Piggery waste manure	piggery waste + sewage	Zeo (natural)	6.0	0.0	0.0	0.0	1.3	(Montalvo et al., 2005)
Piggery waste manure	piggery waste + sewage	Zeo (natural)	8.0	0.0	0.0	0.0	1.3	(Montalvo et al., 2005)
Piggery waste manure	piggery waste + sewage	Zeo (natural)	10.0	0.0	0.0	0.0	1.3	(Montalvo et al., 2005)
Piggery waste manure	piggery waste + sewage	Zeo (natural)	12.0	0.0	0.0	0.0	1.3	(Montalvo et al., 2005)

Table 2.6. Continued. Summary of studies reporting the effect of AC, GAC, Mag and Zeo (and the concentration of material applied – C) on anaerobic sludge, sediments, and other complex microbial communities. The presence of (nano)materials affected the lag phase duration (by reducing (↓), or increasing (values < 0) it) and the MPR (i.e., MPR > 1, increased; MPR < 1, decreased), when comparing with the control condition without materials

Type of inoculum	Substrate	Materials		Lag phase			MPR	References
		Type	C/ ($g \cdot L^{-1}$)	Control/ d	Material/ d	↓Lag phase/ %		
Piggery waste manure	piggery waste + sewage	Zeo (natural)	16.0	0.0	0.0	0.0	1.0	(Montalvo et al., 2005)
Anaerobic sludge	slaughterhouse waste + industrial and food waste	Zeo (natural)	5.0	0.0	0.0	0.0	1.6	(Nordell et al., 2013)
Anaerobic sludge	pulp and paper sludge	Zeo (natural)	0.2	5.6	5.8	-3.7	1.0	(Huiliñir et al., 2014)
Anaerobic sludge	pulp and paper sludge	Zeo (natural)	0.5	5.6	6.9	-22.4	0.8	(Huiliñir et al., 2014)
Anaerobic sludge	pulp and paper sludge	Zeo (natural)	1.0	5.6	7.1	-27.0	0.9	(Huiliñir et al., 2014)
Anaerobic sludge	pulp and paper sludge	Zeo (natural)	20.0	-	-	nc	nc	(Huiliñir et al., 2014)
Digestate	ethanol	Zeo	10.0	2.7	2.5	9.2	0.9	(König et al., 2022)
Anaerobic sludge	VFA (acetic, propionic, butyric acids)	Zeo (natural)	1.4	10.0	10.0	0.0	0.7	(Milán et al., 2010)
Anaerobic sludge	food waste	Zeo (heated at 400 °C)	15.0	6.5	5.8	10.8	0.9	(Cardona et al., 2021)
Anaerobic sludge	food waste (+ 4 $g \cdot L^{-1}$ NH_4^+)	Zeo (heated at 400 °C)	15.0	8.9	7.1	20.2	1.1	(Cardona et al., 2021)
Anaerobic sludge	food waste	Zeo (soluble ions removed)	15.0	6.5	6.8	-4.6	1.0	(Cardona et al., 2021)

Table 2.6. Continued. Summary of studies reporting the effect of AC, GAC, Mag and Zeo (and the concentration of material applied – C) on anaerobic sludge, sediments, and other complex microbial communities. The presence of (nano)materials affected the lag phase duration (by reducing (↓), or increasing (values < 0) it) and the MPR (i.e., MPR > 1, increased; MPR < 1, decreased), when comparing with the control condition without materials

Type of inoculum	Substrate	Materials		Lag phase			MPR	References
		Type	C/ ($g \cdot L^{-1}$)	**Control**/ d	**Material**/ d	↓Lag phase/ %		
Anaerobic sludge	food waste (+ 4 $g \cdot L^{-1}$ NH_4^+)	Zeo (soluble ions removed)	15.0	8.9	9.0	-1.1	1.1	(Cardona et al., 2021)

* **c1** and **c2** represent increasing concentrations of substrates.

* nc – not calculated; in these studies, no MP was observed in the control condition but the material improved the substrate conversion to methane.

* Different types of Zeo differ in their chemical and mineralogical composition (e.g., natural Zeo are different regarding the composition in clinoptilolite), and particle sizes.

2.3. CHARACTERISTICS OF (NANO)MATERIALS AND THEIR ROLE ON MP

High surface area and porous structures, sorption capacity and catalytic characteristics are some of the properties that makes carbon-based materials so attractive to be applied in biological treatments (Barua and Dhar, 2017; A. R. Silva et al., 2021a). On the other hand, iron-based materials have magnetic properties that makes the recovery of the material easier with a magnetic field, and, their small size and high catalytic activity, make this kind of materials very attractive as well (A. R. Silva et al., 2021a; Song et al., 2019). Also, overall CM possess high electrical conductivity and high chemical stability which are also attractive properties (Abbas et al., 2021). Besides carbon- and iron-based materials, other materials like zeolites are less studied in syntrophic degradation of anaerobic compounds or methanogenic metabolites (i.e., acetate and H_2/CO_2). Zeolites are aluminosilicates with a three-dimensional interconnecting of alumina tetrahedra (AlO_4) and silica (SiO_4) (Montalvo et al., 2012). This material has a porous structure and a large surface area, with excellent sorbent capacity, which makes it an attractive material for diverse applications (e.g., air purification by water or CO_2 removal), including to improve AD processes (Montalvo et al., 2012).

The presence of materials, besides the above effects presented regarding MP, also helps the system to resist to inhibitory effects caused by several compounds, like high ammonia concentrations, VFA accumulation or heavy metals (Castilho et al., 2022; Kutlar et al., 2022). For instance, AD process can failure due to ammonia inhibition during the anaerobic treatment of nitrogen-rich organic matter once free ammonia (NH_3) can diffuse through cell membranes, interfering with the balance of proton and metabolic enzymes (Liu et al., 2020; C. Wang et al., 2022; Zheng et al., 2015). It was reported that in the presence of materials, such as Mag (C. Wang et al., 2022; Yan et al., 2020) and Zeo (Zheng et al., 2015), the methanogenic activity keeps occurring under ammonia inhibition conditions. Yet, it is not clear how and which properties of (nano)materials mainly affect methanogenesis. In this subsection, the characteristics and the possible roles of (nano)materials on MP will be highlighted.

2.3.1. Carbon-based materials

Carbon-based materials are characterized as presenting high electrical conductivity, large surface area, and chemical and mechanical stability (Barua and Dhar, 2017; W. Zhang et al., 2018). IET in defined syntrophic cocultures was observed to be mediated by carbon-based materials (Wu et al., 2023), like carbon cloth (Chen et al., 2014b), biochar (Chen et al., 2014a), and GAC (Liu et al., 2012), thanks to the electrical conductivity of these materials. In addition, in the studies with these carbon-based materials,

cells grew attached on their surface (as these materials are bigger than cells in size), so microbial partners did not have to connect physically by biological structures (like *e*-pili) required in DIET associations, being enough the connection provided by the CM (Lovley, 2017b). Particularly, the adhesion effect by immobilizing the microorganisms on the surface of materials and shortening the physical distances can also enhance the exchange of substances in syntrophic interactions (Xiao et al., 2022).

Besides the high electrical conductivity, GAC presents a high surface area and porosity, being reported to enhance MP in other AD systems (Wu et al., 2023; Xiao et al., 2022). This type of materials has been applied at concentrations from 0.5 to 50.0 $g \cdot L^{-1}$ in different anaerobic systems (Table 2.6). GAC or powdered activated carbon (PAC) are cheap materials with low biological toxicity, being initially used to adsorb toxic compounds with potential to inhibit the methanogenic activity (Castilho et al., 2022; M. Liu et al., 2021). For instance, the adsorption properties of GAC allowed to relieve problems caused by LCFA (which are intermediates during the conversion of fat, oil and grease to methane), such as the LCFA adsorption to the biomass that can cause sludge flotation, biomass washout and inhibitory effects on microorganisms like methanogens (He et al., 2021; Tan et al., 2021; Tan and Lens, 2021).

The different physicochemical characteristics of materials may also interfere with the results. For instance, Yuan *et al.* (2018) studied the application of biochars obtained from different feedstocks (rice straw, wood chips and manure) in methanogenic enrichment cultures of a paddy soil (Yuan et al., 2018). The results showed that biochars from rice straw and manure accelerated MP comparing with the control without biochar (MPR 11 and 12-folds higher, respectively), while biochar from wood chips had little effect on MP (Yuan et al., 2018). The authors mentioned that the differences on redox-active properties and in the functional groups (e.g., quinones) when present on the biochar surface may have a role in facilitating methanogenesis, which could explain the differences in the obtained results (Yuan et al., 2018).

The addition of multiwalled CNT in AD systems also contributed for enhancing MP (Salvador et al., 2017; W. Zhang et al., 2018). CNT is an expensive commercial material characterized as a cylindrical carbon nanostructure forming a hexagonal lattice, and presenting high electrical conductivity, thermal conductivity and mechanical strength (Castilho et al., 2022; J. H. Park et al., 2018). The presence of CNT was shown to alter the parameters of the growth medium, for instance, by decreasing redox potential (ORP) that can contribute to favour methanogenesis (Kutlar et al., 2022; Salvador et al., 2017). Besides the positive effects promoted by CNT (Table 2.4 and Table 2.5), the use of nanomaterials in AD should be performed with caution since the physical contact between CNT and microbial cells can damage the membranes resulting in cell disruption caused by the small size of nanomaterials (Castilho et al., 2022).

But the effect may be different regarding the shape and the size of the species in contact with the nanomaterial (Castilho et al., 2022).

2.3.2. Iron-based materials

Mag (Fe_3O_4), hematite (Fe_2O_3) and stainless steel, are examples of iron-based CM used in some studies (Martins et al., 2018). Mag and hematite are abundant in nature (e.g., soils and sediments), where their presence can facilitate EET by iron-reducing microorganisms (e.g., *Geobacter* species) (Barua and Dhar, 2017). Although Mag and hematite present different chemical compositions and electrical conductivities (Mag has 10^6-fold higher conductivity than hematite), both materials contributed for the reduction of the lag phases and for the acceleration of the MPR (J. H. Park et al., 2018). The role of materials like Mag has to be different from the roles of carbon-based materials in methanogenesis, because Mag is usually used in the form of nano-sized material (Wu et al., 2023). Mag is the most common iron oxide used in AD systems, mostly used in concentrations from 0.1 to 11.1 $g \cdot L^{-1}$ (Table 2.6), being Mag particles smaller than microbial cells. It was reported that Mag can replace cellular structures in syntrophic cocultures performing DIET as they can attach to individual cells substituting the function of *c*-type cytochromes (Liu et al., 2015; Lovley, 2017b), function as an electron conduit.

Other reports have shown that acetoclastic methanogens are capable of performing the reduction of Fe(III) (redox cycle of Fe(III)/Fe(II) in Mag), resulting in the acceleration of acetoclastic methanogenesis (Fu et al., 2019; H. Wang et al., 2020; Wu et al., 2020). For instance, the presence of Mag promoted an enrichment of *Methanosarcina* species closely related to a *M. barkeri* strain, and the MPR by pure cultures of *M. barkeri* was 2 times higher in the presence of Mag than in the control without Mag (Table 2.3) (Fu et al., 2019). Iron is also a micronutrient, which can be released from Mag and used as a trace element by methanogens as Fe can serve, for example, as a cofactor for enzymes (e.g., formyl-MF-dehydrogenase, hydrogenase, CO dehydrogenase) (Wu et al., 2023).

The presence of Mag can also help AD systems to resist to VFA inhibitory effects. For example, in the study carried out by Barrena *et al.* (2023), the presence of Mag helped to reverse the inhibitory effect of VFA and enabled the microbial consortia to recover from an induced acidification (addition of an inhibitory concentration of glucose for methanogenic activity). The control assay was inhibited under those conditions, but the presence of Mag allowed the community to recover methanogenic activity, thus improving the methane yield (Barrena et al., 2023).

2.3.3. Zeolites

Zeo can be natural or synthetic silicoaluminates (Busca, 2014). The most abundant natural Zeo is in the form of clinoptilolite, which is widely used as adsorbent in wastewater purification (e.g., to remove ammonium, heavy metal, organics) since it is a cheaper material (Busca, 2014). Zeo possess a microporous crystal structure, which can present different dimensions of the pore apertures (i.e., channels with different pore diameters: small-, medium-, large- and extra-large pores) (Busca, 2014). Zeo can also present different structures, like faujasite structure which can also differ in types X and Y (Busca, 2014). Thus, major differences can also be found regarding the structure and chemical composition (Si/Al ratio) (Busca, 2014), which can difficult the comparison of results obtained with different types of Zeo. The Si/Al ratio is an indicator of the content in silica and aluminium, i.e., high silica zeolites present Si/Al ratios > 10, intermediate silica zeolites shows Si/Al ratios between 1.5 and 10, and then low-silica zeolites have Si/Al ratios close to 1 (Busca, 2014). Faujasites type-X are reported to present Si/Al ratios between 1 and 1.5, while faujasites type-Y possess values above 1.5 (Busca, 2014). These differences in Si/Al ratios imply also differences in the Zeo' properties, such as particle size, morphology, and different distribution of framework aluminium (Busca, 2014).

The improvement of AD processes by Zeo (applied in concentrations from 0.4 to 30.3 $g \cdot L^{-1}$, Table 2.6) is many times attributed to the adsorption capacity of inhibitory substances, to its ion-exchange property, and to the physical support for microbial growth. For example, the application of Zeo (5 $g \cdot L^{-1}$) in AD systems demonstrated potential to decrease the inhibitory effects of LCFA by adsorption of LCFA on Zeo particles (Nordell et al., 2013). The application of Zeo in AD also seems to be favourable to overcome ammonia stress conditions (Cardona et al., 2021). For instance, Zeo can be used to remove ammonium during the treatment of wastewaters with high concentrations of nitrogen compounds, whose accumulation could harm the performance of the AD treatment (Montalvo et al., 2012). This is possible thanks to their ion-exchange property since they have cations in their crystalline structure that can be exchanged without significantly changing their structure (Montalvo et al., 2012). The porous structure of Zeo can accommodate a wide variety of cations, such as Na^{+}, K^{+}, Ca^{2+}, and Mg^{2+} (Montalvo et al., 2020). Some studies have been highlighting the importance of this property to explain the enhancement observed in AD systems in the presence of Zeo (Amen et al., 2017; Li et al., 2019). Zeo can also be modified to increase their ionic exchange capacity or to supply micronutrients, like Ni, Co, Mg (Romero-Güiza et al., 2016). Trace elements are important for anaerobic microorganisms, for instance, Co is a cofactor of vitamin B12 (methyltransferase), and Ni is essential for the synthesis of coenzyme F_{420} in methanogens (Wu et al., 2023). For example, the increase of biogas production by using 6.25 % in total solids (TS) of

Zeo during anaerobic degradation of deer manure was attributed to the trace elements provided by Zeo structure (such as Ca, K, Na) (Wang et al., 2019). In addition, Zeo can be simply used as a support for microbial adhesion (Montalvo et al., 2012). For instance, the presence of Zeo (15 $g \cdot L^{-1}$) improved food waste conversion to methane, under low ammonia stress by anaerobic sludge and one of the mechanisms suggested was the use of Zeo as a support for microbial growth (Cardona et al., 2021). The presence of this material resulted in a more balanced presence of VFA-producers and VFA-degraders, with the improvement of syntrophic degradation of propionate and butyrate (Cardona et al., 2021). The same mechanism was suggested for enhancing biomethane yield during anaerobic degradation of pulp and paper sludge in the presence of Zeo (from 0.2 to 1 $g \cdot L^{-1}$) (Huiliñir et al., 2014). Zeo can also be used as a microbial support in AD systems (fixed and fluidized reactors) for the treatment of different types of wastewater (Romero-Güiza et al., 2016). In other cases, both ammonia adsorption and microbial immobilization by Zeo (10 $g \cdot L^{-1}$) might contribute to enhance the AD treatment of swine wastes, as suggested by Zheng *et al.* (2015). Other studies with the addition of Zeo in AD processes were reviewed by Paritosh *et al.* (2020).

2.4. METHODOLOGIES TO EVALUATE THE EFFECT OF (NANO)MATERIALS ON METHANOGENIC CULTURES

To deep the knowledge about the mechanisms behind the enhancement of AD process in the presence of (nano)materials, methods like 16S rRNA gene sequencing and meta-omics approaches combined with microscopy analysis or with voltammetry could help to understand the IET occurring when (nano)materials are present (Van Steendam et al., 2019). Through this combination of methods, it is possible to identify microbial species, to evaluate gene expression in the presence of (nano)materials (helping to reconstruct the metabolic pathways), to investigate the morphological characteristics and spatial distribution of cells with (nano)materials, and even to investigate possible EET through the electrical properties of the systems (Van Steendam et al., 2019; Wu et al., 2023).

2.4.1. Taxonomic analysis

The 16S rRNA gene is present in all prokaryotic microorganisms, being a genetic marker that allows the identification of microorganisms and their relative abundance in microbial communities (Amann and Ludwig, 2000; Van Steendam et al., 2019). This methodology has been highly used in studies with (nano)materials and it has allowed to observe differences between the composition of microbial communities in the presence and in the absence of (nano)materials, as reviewed elsewhere (Martins et

al., 2018; Xu et al., 2022). For instance, Zhang *et al.* (2018) used this approach to perform the analysis of the microbial communities composition in enrichment cultures degrading butyrate with and without CNT (Table 2.5) (W. Zhang et al., 2018). Yet, the identification of microorganisms or changes in their relative abundance do not directly reveal which IET mechanism is taken place in a determined condition, but it could indicate possible syntrophic interactions. Thus, although some authors suggested the shift from IHT to CIET based on changes on microbial communities (Baek et al., 2017; Kato et al., 2012; Li et al., 2015; Jing Zhang et al., 2020; W. Zhang et al., 2018; Zhao et al., 2017b, 2016), this approach does not allow to reach this kind of conclusion.

2.4.2. Meta-omics analyses

Meta-omics approaches allow to detect functional genes, transcripts, or proteins, and to infer about the pathways that are taken place (Van Steendam et al., 2019). For instance, to investigate if DIET is occurring, the study would include the investigation of genes essential for this mechanism, such as *PilA* or *OmcS* genes (Van Steendam et al., 2019). In the case of IHT/IFT, other genes should be taken into consideration, like upregulation of HybA (uptake hydrogenase protein critical in IHT), and even observing the downregulation of *c*-type cytochrome proteins (e.g., OmcS) which are not common in typically syntrophic growth via IHT (Van Steendam et al., 2019). Supplementary tests, like targeted gene deletion studies, may also help to evaluate if cultures still has the ability to grow in the absence of that gene, determining if the gene under analysis is, or not, essential for a certain proposed mechanism (Rotaru et al., 2021; Van Steendam et al., 2019). A metatranscriptomic approach can be used to determine the functional significance of specific microbial taxa in complex microbial communities (Hao et al., 2020). As transcriptomic response of individual taxa can be measured in response to a specific environmental stimuli, changes in gene expression in the presence of (nano)materials can also be evaluated by (meta)transcriptomic analysis (Hao et al., 2020; Wu et al., 2023). The genes, transcripts or proteins can also be linked to a mechanism by monitoring the up or down regulation or expression under certain conditions (Van Steendam et al., 2019). On the other hand, these approaches also present disadvantages, because some genes, transcripts and proteins may be involved in other cell functions (Van Steendam et al., 2019; Wu et al., 2023). Also, some genes, transcripts and proteins that are associated with specific pathways, like *e*-pili and *OmcS* for DIET, might not be detected, and it doesn't prove that DIET is not occurring once different species may have different cellular machinery for EET (Van Steendam et al., 2019). But these approaches are relevant to deep the knowledge about IET. For instance, the discovery that *Methanothrix* could perform DIET in syntrophy with *Geocacher* was made by the detection of

expression of CO_2 reduction genes in *Methanothrix* spp. (Rotaru et al., 2014b). The reduction of CO_2 to produce methane is performed by hydrogenotrophic methanogens, but *Methanothrix* spp. are acetoclastic methanogens, incapable of using hydrogen and formate as electron donors to reduce CO_2 (Rotaru et al., 2014b; Van Steendam et al., 2019). Thus, in defined cocultures with *G. metallireducens*, it was demonstrated through the transcription of CO_2 genes in *Methanothrix* that *Methanothrix harundinacea* could accept electrons via DIET (Rotaru et al., 2014b). This way, meta-omics approaches can be helpful to detect genes, transcripts and proteins associated with IET mechanisms, like IHT/IFT or DIET (via CO_2 reduction pathway), and to better understand the relationships between microorganisms in microbial communities, and the influence of the presence of (nano)materials.

2.4.3. Microscopy analyses

Microscopy analyses allow to visualize the cellular spatial arrangement when cells are in contact with (nano)materials (Van Steendam et al., 2019). Examples of microscopic analyses are scanning electron microscopy (SEM) to observe the interaction of cells with (nano)materials, and transmission electron microscopy (TEM) used to identify cell morphology (Van Steendam et al., 2019). For instance, in the work of Salvador *et al.* (2017), SEM images showed the arrangement of different methanogenic cultures in the presence of CNT and the arrangement of cells without the material (Salvador et al., 2017). In other work, SEM images showed the morphology of cell aggregates in different sediment enrichments with and without CNT, for example, revealing information about the shape of cells present in each type of enrichment (W. Zhang et al., 2018). On the other hand, TEM images were taken to explore the effect of the size of Mag particles on a sludge during propionate degradation, showing differences in the abundances of egg- and rod-shaped bacteria for different sizes of Mag (Yin et al., 2022). These strategies may also allow the identification of biological structures like pili and cytochromes (Van Steendam et al., 2019; Wu et al., 2023). SEM can also be coupled with energy dispersive X-ray analysis (SEM-EDS), which allows to investigate the elemental composition of specific details during SEM observations, ultimately helping to understand if the elements present in abiotic materials can be incorporated or not by cells (Van Steendam et al., 2019). In addition, fluorescence *in situ* hybridizing (FISH) can be used to identify syntrophic partners, once it involves oligonucleotide probes whose target are unique sequences in DNA or RNA molecules, determining the spatial distribution of syntrophic partners stained after hybridization by observing the fluorescence signal in a fluorescence microscope or confocal laser scanner (Van Steendam et al., 2019; Wu et al., 2023). This technique was also used by Zhang *et al.* (2018) to observe the spatial distribution of bacteria and methanogens in different sediment enrichments with and without

CNT, and also in syntrophic cocultures (W. Zhang et al., 2018). Based on the results obtained in SEM and FISH analyses, the authors conclude that methanogens and bacteria form cell-CNT aggregates (W. Zhang et al., 2018).

2.4.4. Cyclic voltammetry

Specifically, to investigate EET mechanisms, cyclic voltammetry (CV) can be a suitable method to detect electron exchange between microorganisms and (nano)materials (Van Steendam et al., 2019; Wu et al., 2023). For example, through CV may be possible to characterize electron exchange between microorganisms and (nano)materials by determining the standard extracellular electron transfer rate constant, or the type of redox reactions occurring through electron transfer (Van Steendam et al., 2019; Wu et al., 2023). For example, it is known that acetate oxidation peak occurs at -0.35 V, and CO_2 reduction peak occurs at -0.32 V (Van Steendam et al., 2019). Besides, detecting an increased electron transfer rate could be related with an increase of electro-active microorganisms and mechanisms involving EET, like DIET, could be considered for further investigation (Van Steendam et al., 2019). This approach has been applied in some studies, for instance, to explore the electrochemical activity of cultures in the presence of GAC impregnated with Mag (Song et al., 2019) or carbon fibers (Barua et al., 2018). The disadvantage of this method is that usually it is applied *ex situ* and a sample of biomass (from the anaerobic system under study) has to be transferred to an electrochemical system (like an electrochemical cell), and the biofilm formation on the electrode has to occur before performing the analysis (Van Steendam et al., 2019). However, the sample taken from the original system may not be enough to represent the community or the biofilm growth on the electrode may change in community structure due to changes in environmental factors, so it could not be representative of the original system as well (Van Steendam et al., 2019; Wu et al., 2023).

CHAPTER 3

3. THE INFLUENCE OF CONDUCTIVE AND NON-CONDUCTIVE MATERIALS ON THE METABOLISM OF THE HYDROGENOTROPH *METHANOBACTERIUM FORMICICUM*

ABSTRACT

Hydrogenotrophic metabolism has been shown to be enhanced in the presence of carbon nanotubes (CNT), which is relevant once hydrogenotrophs are crucial microorganisms for the conversion of organic wastes to methane. In this study, the effect of several conductive materials (CM) including carbon-based (activated carbon (AC), CNT, modified AC) and iron-based materials (magnetite (Mag), CM impregnated with Fe), non-conductive materials (sand and glass beads), and one type of a zeolite (Zeo, type-13X), on the hydrogenotrophic activity of *Methanobacterium formicicum* was investigated. The aim was to test materials with distinct physicochemical properties to identify which are the characteristics of materials that contribute most for the methanogenic activity improvement. For that purpose, the methanogen was incubated with different concentrations of materials (from 0.1 to 5 $g \cdot L^{-1}$) and with H_2/CO_2, and methane production (MP) was followed. The materials were characterized regarding textural properties (specific surface area, area of mesopores, volume of micropores), pH at zero point charge, conductivity, and elemental composition. Chemical oxidation treatments with HNO_3 (AC_HNO_3), H_2SO_4 (AC_H_2SO_4) or both (AC_HNO_3_H_2SO_4), and thermal treatments, were applied to obtain modified AC. Microscopy techniques were used to investigate the interaction of cells with materials. All materials, with exception of Mag, and AC_HNO_3_H_2SO_4, improved the methanogenic activity. Carbon-based materials significantly reduced the lag phases preceding MP (from approximately 5 d, in the control, to circa 1 d). Zeo, sand, and glass beads, also reduced the lag phases but less than carbon-based materials (i.e., from 5 d to 1.5, 2.7 and 3.5 d, respectively). Additionally, exponential MP rates were up to 1.5 times higher in the assays with Zeo, glass beads and sand than in the assays with the control condition. A direct relationship between the physicochemical properties evaluated and the enhancement of MP was not found. Yet, the element silicon, common in all materials composition, was found to stimulate, per se, the activity of this methanogen.

3.1. INTRODUCTION

Hydrogenotrophic methanogens reduce CO_2 using H_2 or formate as electron donors (Lyu et al., 2018; Whitman et al., 2006). The production of methane from CO_2 reduction is very important as it maintains the concentration of hydrogen and formate at low levels, allowing endergonic acetogenic reactions to become exergonic, and enabling the syntrophic communities to survive (Morris et al., 2013; Stams et al., 2012; Stams and Plugge, 2009; Whitman et al., 2006; Zabranska and Pokorna, 2018).

Conductive materials (CM), like activated carbon (AC), magnetite (Mag), and carbon nanotubes (CNT) have been reported as contributing to accelerate methane production (MP) in anaerobic controlled systems, and promoting methanogenesis, including methanogenesis from H_2/CO_2 (Castilho et al., 2022; Martins et al., 2018). Modified materials also showed to stimulate MP in anaerobic systems, which has been attributed to their enhanced electron (in the case of materials like GAC combined with Mag) or ionic exchange capacity (in materials like Zeo) (Barua et al., 2019; Romero-Güiza et al., 2016; Song et al., 2019). Despite the research advances in this topic, many questions about the application of CM remain unexplained, including the importance of certain properties of the materials on methanogenic metabolism. The materials may differ in many properties, such as surface area, porosity, size, pH at zero point charge (pH_{pzc}), electrical conductivity, and chemical composition (Hassanein et al., 2021; H. Liu et al., 2021; Yiwei Liu et al., 2021; Paritosh et al., 2020; A. R. Silva et al., 2021a; Wu et al., 2020). As conductive minerals are also naturally present in natural sediments, their impact directly on MP by individual microorganisms deserves to be further investigated. So far, CM such as CNT (Fu et al., 2019; Salvador et al., 2017; Xia et al., 2019; Xiao et al., 2020; W. Zhang et al., 2018), granular activated carbon (GAC) (Zheng et al., 2020), Mag (Fu et al., 2019, 2018; H. Wang et al., 2020; Xia et al., 2019), nano-graphite (Fu et al., 2019) and reduced graphene oxide (rGO) (W. Zhang et al., 2018) were investigated towards the methanogenic activity by pure cultures of methanogens. The effect was tested on acetoclastic pure cultures, like *Methanosarcina barkeri* (Fu et al., 2019; Xiao et al., 2020), *Methanosarcina mazei* (Salvador et al., 2017; H. Wang et al., 2020; Xiao et al., 2020) and *Methanosaeta concilii* (Salvador et al., 2017), and some hydrogenotrophic species such as *Methanobacterium formicicum* (Salvador et al., 2017), *Methanospirillum hungatei* (Salvador et al., 2017), *Methanococcus maripaludis* (Fu et al., 2018; W. Zhang et al., 2018), and *Methanocella conradii* (Fu et al., 2018; Xia et al., 2019). Acetoclastic methanogens are more favoured by the presence of CM than hydrogenotrophs. For instance, it was reported that CNT enhanced the acetoclastic activity of *M. mazei* and *M. barkeri* (Xiao et al., 2020), but inhibited the hydrogenotrophic activity of *M. maripaludis,* particularly at high concentrations (at 5 $g \cdot L^{-1}$

CNT) (W. Zhang et al., 2018). The inhibitory effect of carbon-based materials like GAC was also reported on a culture of *Methanobacterium* sp. strain YSL growing on formate (Zheng et al., 2020), and CNT, as well as Mag, had a negative or no effect towards the methanogenic activity of the hydrogenotroph *M. conradii* (Fu et al., 2018; Xia et al., 2019). The acceleration of methane production rates (MPR) by hydrogenotrophic methanogens in the presence of CM was only reported in the work developed by Salvador *et al.* (2017). The authors reported the improvement of MPR by the pure cultures *M. hungatei* and *M. formicicum* up to 6- and 17-fold in the presence of CNT in comparison with the controls without CNT, respectively (Salvador et al., 2017). This is very important once hydrogenotrophs are essential microorganisms during the conversion of organic wastes to methane, making this research area particularly relevant.

From all methanogens reported in the literature so far, the metabolism of the hydrogenotroph *M. formicicum* was the most stimulated in the presence of CM. In this work, *M. formicicum* was incubated with several types of materials (AC, CNT, Mag, zeolite (Zeo), sand, glass beads, modified AC/CNT) to evaluate the effects and the possible properties influencing its methanogenic activity. It was hypothesized that methanogenic activity could be affected in a different extent by different types and concentrations of materials. *M. formicicum* was incubated separately with AC, CNT, and Mag, in concentrations ranging from 0.1 $g \cdot L^{-1}$ to 5 $g \cdot L^{-1}$. Besides, experiments with modified carbon-based materials and with materials like Zeo type-13X, sand, and glass beads, were performed aiming to investigate the influence of materials with different physicochemical properties towards MPR. The interaction of microbial cells with the materials was investigated by microscopic techniques.

3.2. MATERIALS AND METHODS

3.2.1. Conductive and non-conductive materials

Commercial materials, namely Mag (nanopowder, particle size 50 – 100 nm, Iron (II, III) oxide, Fe_3O_4), Zeo (Molecular sieve, type 13X - beads, 4-8 mesh) and glass beads (acid washed, 212-300 μm, 50-70 U.S. sieve), were purchased from Sigma-Aldrich (USA). Commercial AC (Norit ROX 0.8 GAC, pellets with 0.8 mm of diameter and 5 mm of length) was supplied by Norit, and commercial multiwall CNT (NC3100™) from Nanocyl S.A. (Sambreville, Belgium). The original characteristics of Zeo and CNT were described elsewhere (Salvador et al., 2017; R. M. Silva et al., 2021). Sand sample was collected from Apúlia beach (Esposende, Portugal), which was washed with distilled water several times, and followed by organic contaminants removal at 550 °C, for 2 h. In the experiments, GAC, modified AC, and Zeo,

were used as powder by being crushed (increasing the external surface area) and sieved (particle size < 280 μm). The other materials (glass beads and sand) were also sieved to limit the range of particle size in the assays (i.e., all materials were used with a particle size < 280 μm).

The tests with different materials can be divided into three main experiments (Figure 3.1): Experiment I – test the effect of AC, CNT, and Mag at different concentrations (0.1, 0.5, 1, 2 and 5 $g \cdot L^{-1}$); Experiment II – test the effect of modified AC with different physicochemical characteristics; Experiment III - test the effect of Zeo, sand and glass beads, which are materials different from carbon-based materials in physicochemical properties, including electrical conductivity. As experiments were performed in different periods, three different commercial AC (with different physicochemical characteristics) were used in the experiments and will be referred in this chapter as: i) AC from batch 1 (AC_{b1}) – used in the assays of Experiment I (Figure 3.1); ii) AC from batch 2 (AC_{b2}) – used in the assays of Experiment II (Figure 3.1), where AC_{b2} is the control to compare with modified AC, in order to conclude if any modification was better than the original material as AC_{b2} was the starting material to prepare the AC with different modifications; and iii) AC from batch 3 (AC_{b3}) - tested in the same round of the experiments with AC_{b2} (Figure 3.1, Experiment II). Regarding the assays with AC_{b2} and AC_{b3}, the aim was to investigate if the same type of material (AC from same supplier) would present different physicochemical characteristics when acquired in different moments. The assumption is that if these physicochemical differences contribute to differently affect the methanogenic activity, then it is possible to obtain different results even when it is considered the same material.

Starting from commercial AC_{b2}, and CNT, different modifications were made aiming to obtain a broaden number of materials, and composites (i.e., materials impregnated with magnetic nanoparticles), differing in some physicochemical properties according to the treatment applied, but the type of material remaining the same. The preparation of modified materials and composites, as their physicochemical characterization, were performed by the research group from Catalysis and Materials Associate Laboratory, at Engineering Faculty of Oporto University. The following treatments were carried out to prepare the modified AC, with AC_{b2} as the starting material: liquid phase treatments with H_2SO_4, HNO_3, or both, with different concentrations and/or contact times. Heat treatments at different temperatures were also performed, which remove some of the functional groups. In addition, a set of materials was prepared from the modified AC_{b2}, by doping them with nitrogen. Chemical oxidation treatments and thermal treatments allow to obtain materials with different surface chemistry, conferring to them acid or basic character (A. R. Silva et al., 2021a). Composites of AC (AC@2%Fe) and of CNT (CNT@2%Fe) impregnated

with 2 % of iron (amount of Fe^{2+} or Fe^{3+} to be impregnated) were also prepared. The final modified materials and composites used in the assays are summarized in Table 3.1.

The procedures to perform these types of modification or composites' preparation are described elsewhere (Pereira et al., 2017, 2010; Restivo et al., 2014; Rocha et al., 2014; Silva et al., 2020). The characterization of materials included the following surface and textural properties: Brunauer-Emmett-Teller (BET) specific surface area (S_{BET}), mesopore surface area (S_{meso}), micropore volume (V_{micro}), total pore volume ($Vp_{P/P0=0.95}$), and pH_{pzc}, as described elsewhere (Pereira et al., 2010; A. R. Silva et al., 2021b). The chemical characterization of the surface (surface groups releasing CO, CO_2, CO/CO_2 by temperature programme dessorption) was done only for AC_{b1}, as described by Pereira *et al.* (2010), and elemental analyses were performed for AC_{b2}, modified AC, and AC_{b3}, as described by Silva *et al.* (A. R. Silva et al., 2021b). The morphology of materials, namely AC_{b1}, Mag, CNT, and CNT@2%Fe, was attained by scanning electron microscopy (SEM) and chemical elemental composition was carried out by SEM coupled with energy dispersive spectroscopy (EDS) (values given in percentage, w/w).

Electrical conductivity of Mag and Zeo was obtained after determining their electrical resistance through electrochemical impedance spectroscopy (EIS). The device used for impedance analysis required a firm sample, and as Mag and Zeo were used in powder, pellets of each sample (Mag and Zeo) were obtained by applying a high pressure using a lab manual press machine. Firm circular pellets were obtained, and their thickness was measured (0.994 mm and 0.388 mm were obtained for Mag and Zeo, respectively) with a Digimatic Micrometer IP54 (Mitutoyo). Due to the physical characteristics of powder AC and CNT, the impedance analysis was not carried out due to the impossibility in obtaining firm pellets necessary to proceed with analysis. For EIS measurements, it was used a support cell and two parallel Au disk electrodes (Figueira et al., 2014). The measurements were carried out in triplicate to check data reproducibility, at room temperature, using GAMRY analyzer (GAMRY Instruments, Reference 600+, Potentiostat/Galvanostat/ZRA, 39008). Data was analyzed using Gamry Echem Analyst software as described elsewhere (Figueira et al., 2014). The resistance value for Mag was obtained using this software. The model fitting with the Gamry Echem Analyst software was not adequate for Zeo results, so the resistance value for Zeo was determined using the tools (for data analysis) of Origin software. Considering the resistance values for each sample, the values of conductivity were calculated as described by Figueira *et al.* (2014).

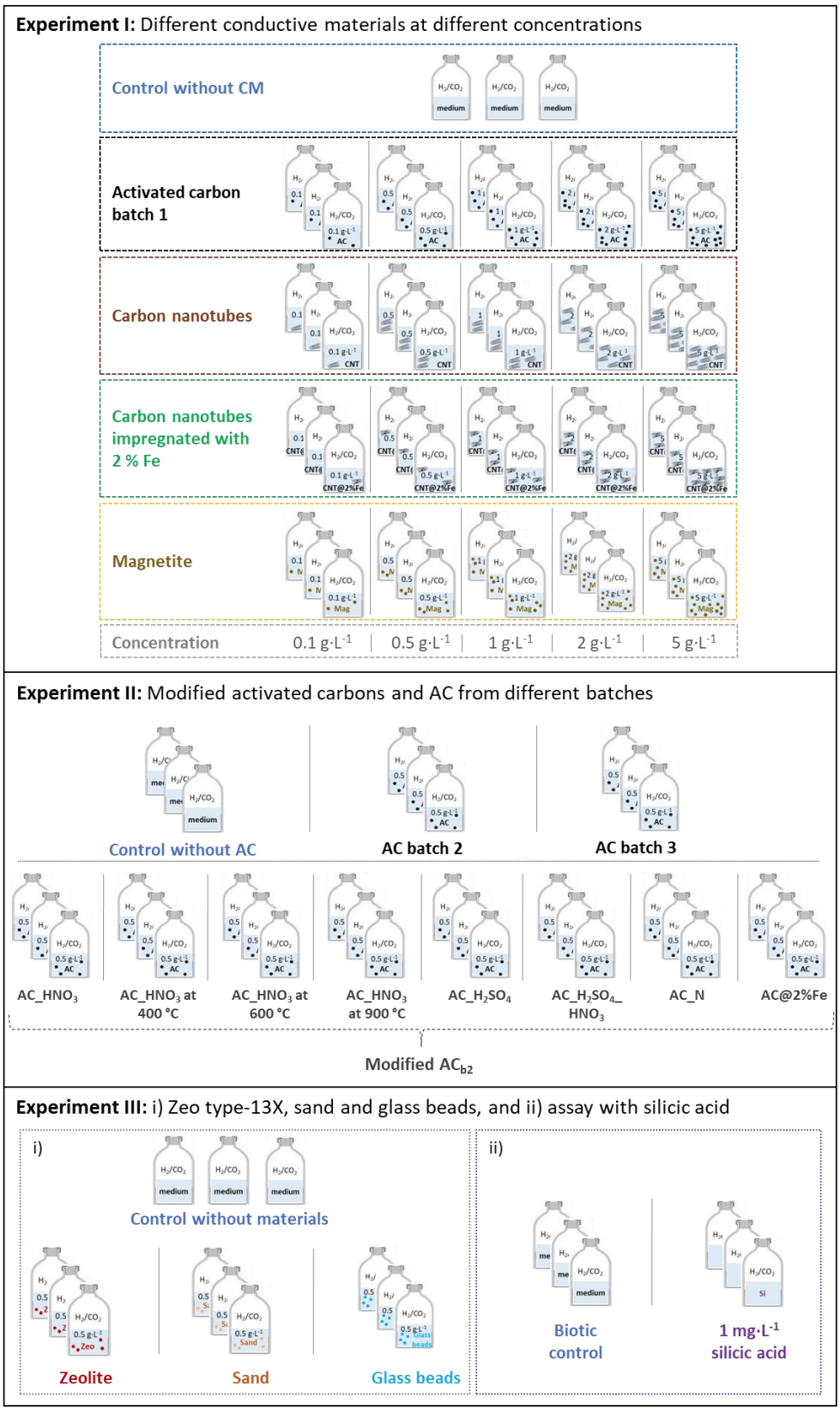

Figure 3.1. Illustrative scheme of the assays performed with the pure culture *M. formicicum*. The data obtained for control condition is the same for experiments II and III,i) (i.e., the control condition for the assays with modified AC, "Control without AC", and for the tests with Zeo, sand and glass beads, "Control without materials", is the same), once the assays were performed at the same time.

Table 3.1. Summary of the modified materials and composites used in the incubations

Modified materials/composites	Description
AC_HNO_3	AC treated with HNO_3
AC_HNO_3_400	AC treated with HNO_3 at 400 °C
AC_HNO_3_600	AC treated with HNO_3 at 600 °C
AC_HNO_3_900	AC treated with HNO_3 at 900 °C
AC_H_2SO_4	AC treated with H_2SO_4
AC_H_2SO_4_ HNO_3	AC treated with H_2SO_4 and HNO_3
AC_N	AC doped with nitrogen
AC@2%Fe	AC impregnated with 2 % of iron, calcinated and reduced at 400 °C
CNT@2%Fe	CNT impregnated with 2 % of iron, calcinated and reduced at 400 °C

3.2.2. Incubation conditions

The strain *M. formicicum* (DSM 1535^T) was obtained from DSMZ (Braunschweig, Germany) and maintained at the laboratory for many years under the conditions that will be described below.

Batch assays were performed in 120 mL serum bottles (50 mL of working volume), containing anaerobic medium prepared as described elsewhere (Salvador et al., 2017; Stams et al., 1993). The materials were added to the bottles, which were then sealed with butyl rubber stoppers and aluminium crimp caps. The headspace was flushed with H_2/CO_2 (80:20 % v/v; 1.7×10^5 Pa) and the bottles containing the medium growth and the materials were sterilized by autoclaving (120 °C, 20 min). Vitamins solution and sodium sulfide ($Na_2S{\cdot}9H_2O$, > 98 %, Acros Organics, Fisher Scientific, USA) were filter sterilized. Prior to inoculation, the anaerobic medium was reduced with $Na_2S{\cdot}9H_2O$ (0.8 mmol·L^{-1}), vitamins were supplemented, and acetate (acetic acid sodium salt, anhydrous, ≥ 99.0 %, Sigma-Aldrich, USA) added at 2 mmol·L^{-1} (sterilized by autoclaving). After inoculation (10 % v/v), the bottles were incubated at 37 °C, in the dark, and under agitation (120 min^{-1}), to improve the transfer of the substrate from the headspace to the liquid phase. All assays were performed in triplicate.

The biotic assays can be divided in three different experiments (schematic representation in Figure 3.1):

- In Experiment I, *M. formicicum* was incubated with AC, CNT, CNT@2%Fe, and Mag, in different concentrations (0, 0.1, 0.5, 1, 2 and 5 g·L^{-1}) to select the best material for accelerating methanogenic activity and the optimal concentration.
- The Experiment II was carried out with the various materials with distinct properties (AC_{b2}, AC_HNO_3, AC_HNO_3_400, AC_HNO_3_600, AC_HNO_3_900, AC_H_2SO_4, AC_H_2SO_4_ HNO_3, AC_N, AC@2%Fe, AC_{b3}), at 0.5 g·L^{-1}.

- In the last group of experiments, one set of assays were dedicated to exploring the effect of Zeo, glass beads, and sand, at 0.5 g·L^{-1} (Figure 3.1, Experiment III,i), and the other assay was performed to investigate the direct effect of 1 mg·L^{-1} of silicic acid (99.9 %, 20 µm, purified by refining, Sigma-Aldrich) in aqueous solution (sterilized by autoclaving) towards the methanogenic activity (Figure 3.1, Experiment III,ii).

Abiotic controls were performed in duplicate to assess the possible interaction of the gaseous substrate (H_2/CO_2, 80:20 %; 1.7 × 10^5 Pa) with the materials (possible adsorption effects). The conditions were the same described for the biotic assays (i.e., 37 °C, in the dark, under agitation) and the volume (10 % v/v) correspondent to the inoculation of the pure culture was replaced by anaerobic medium. The concentrations evaluated were 0.1 and 5 g·L^{-1} for abiotic assays with AC, CNT, CNT@2%Fe and Mag, and 0.5 g·L^{-1} for the abiotic assays with Zeo, glass beads and sand (assays carried out in different periods of time). Abiotic controls without materials were included. Parameters like pH, conductivity, and redox potential (ORP) of the anaerobic growth medium, with and without materials (in abiotic conditions), were measured in three moments during the time of the experiment, as described next.

3.2.3. Analytical methods

Hydrogen consumption and MP were monitored over time through the analysis of gas samples (0.5 mL) taken from the headspace of the bottles using a Pressure-Lock syringe (SGE Syringe, Trajan Scientific Australia Pty Ltd), under aseptic conditions. The gaseous samples were injected in a gas chromatograph (GC) BRUKER SCION 456 (Billerica, MA) in the same conditions described elsewhere (Salvador et al., 2017). The standard used was a mixture of a known gas containing 40 % of CH_4. Methane concentration from partial pressure in headspace was converted to mmol·L^{-1} in liquid medium according to Avogadro's Law.

Liquid samples (3 mL) were taken with a sterile syringe, in aseptic condition, to measure the ORP, pH and conductivity of the anaerobic growth media. ORP was evaluated with a portable meter C533 (Consort, Turnhout, Belgium) equipped with an ORP electrode D 223 (VWR, Radnor, PA). pH and conductivity were measured with a bench HI 207 pH meter (HANNA instruments, Ajman, UAE) and a digital conductivity meter CO 301 (VWR, Germany), respectively. These parameters were measured in three time points during Experiment I (beginning of the assay, middle of the exponential phase of MP, and at the end of the assay), and in two time points during Experiments II and III (24 h after the beginning of the assays and at the end of the assays). In abiotic assays, the measurements were performed at the beginning, at the middle and at the end of the experiments.

3.2.4. Scanning electron microscopy

Samples (1.5 mL) were collected from the liquid phase during the middle of the exponential phase of MP and fixed as described by Salvador *et al.* (2017). The images were acquired using a SEM FEI Nova 200 (FEG/SEM) (FEI, Hillsboro, OR, United States) at Materials Characterization Services of the University of Minho (SEMAT) (University of Minho, Guimarães, Portugal) and a SEM focused ion beam (Zeiss Auriga CrossBeam system) at Nanofabrication Laboratory at Universidade Nova de Lisboa (CENIMAT|i3N, FCT-UNL, Caparica, Portugal). SEM-EDS analyses were carried out to investigate the chemical elemental composition of abiotic (AC_{b1}, CNT, CNT@2%Fe, Mag) and biotic samples (values given in percentage, w/w), at SEMAT.

3.2.5. Transmission electron microscopy

TEM analyses for biotic control without materials and for some materials tested (namely AC, CNT, Mag, Zeo, sand and glass beads) were carried out by the Histology and Electron Microscopy (HEMS) team at i3S – *Instituto de Investigação e Inovação em Saúde da Universidade do Porto*. The thickness of cell wall was measured using the software image J and the scale of TEM images was used as reference. More than 30 measurements were performed for each condition and compared with the control without materials. Since this method is dependent of the user perspective to take the measurements, and in some TEM images it was difficult to distinguish the limits of the cell wall (e.g., in samples with sand), a statistical analysis was performed to compare the results.

3.2.6. Statistical analysis

The modified Gompertz model was formulated to describe bacterial growth curves (cell density versus time) in terms of exponential growth rate and lag phase duration. A modified Gompertz equation (Equation 3.1) was later adopted to evaluate the MP potential, assuming that the rate of MP is proportional to the microbial activity in anaerobic systems (Pan et al., 2016). The Equation 3.1 was used to obtain the values of kinetic parameters (e.g., lag phase time and exponential methane production rates (EMPR)):

$$M(t) = P \times exp\left[-exp\left[\frac{R_m \times e}{P}(\lambda - t) + 1\right]\right] \qquad \text{(Equation 3.1)}$$

where M (t) corresponds to the cumulative MP (in $mmol \cdot L^{-1}$) at time t, P refers to the maximum MP (in $mmol \cdot L^{-1}$), R_m is the EMPR (in $mmol \cdot L^{-1} \cdot d^{-1}$), e value is 2.7182818, and λ corresponds to the lag phase time (in d) (Sousa et al., 2013). The individual measurements carried out in triplicate for each assay were

used independently. The kinetic parameter values and R^2 values of the fitting were obtained by using Solver tool available in Excel. Standard errors for each kinetic parameter were calculated.

Statistical significance to evaluate the differences between conditions regarding the kinetic parameters was assessed by applying the single factor analysis of variances (ANOVA) using Excel tools. The statistical significance was set at the $p < 0.05$ level.

3.3. RESULTS

3.3.1. Characterization of (nano)materials

Images of the morphology of AC, CNT, CNT@2% and Mag in abiotic conditions can be observed in Figure 3.2. These materials presented very different forms and sizes. CNT can be described as hollow cylinders that form highly entangled networks (Abreu et al., 2022), while AC is a large material offering a high surface area (Rasapoor et al., 2020), and Mag, as a nanoparticle, has a reduced size (Barua and Dhar, 2017). CNT are also described as having high porosity, uniform pore size distribution, and surface-active sites that allow its interaction with different molecules (A. R. Silva et al., 2021a).

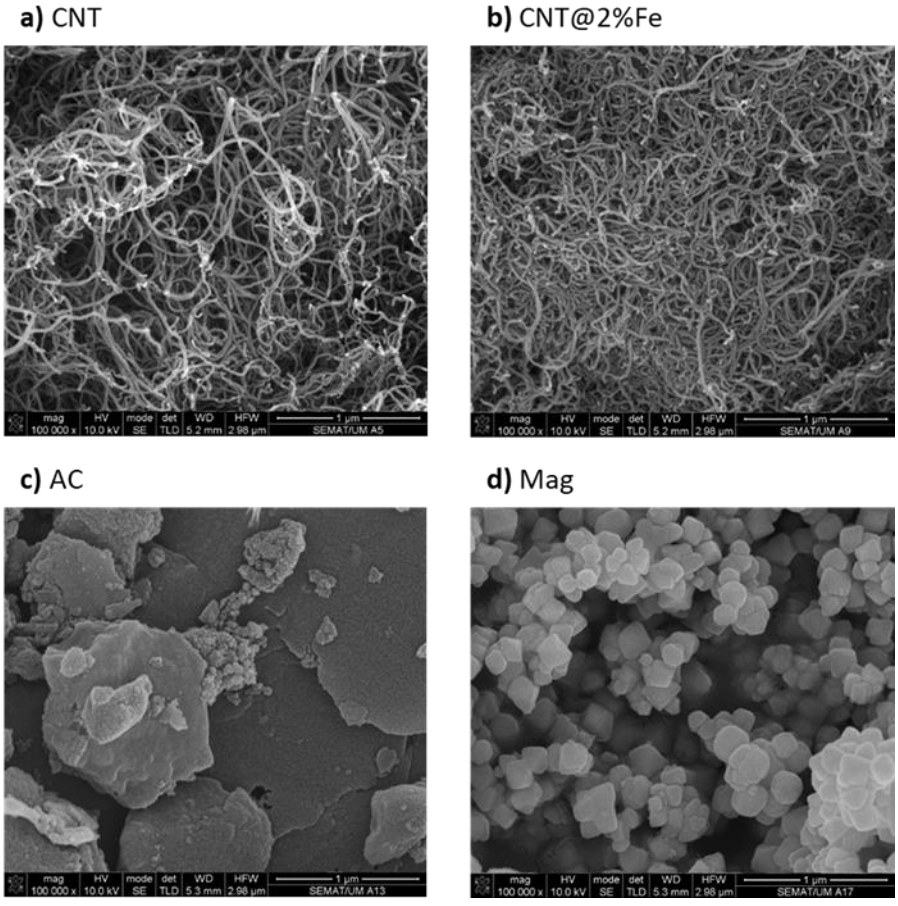

Figure 3.2. SEM images of a) CNT, b) CNT@2%Fe, c) AC_{b1}, and d) Mag, in abiotic conditions.

The surface and textural properties, pH_{pzc} values, conductivity values, elemental analysis and chemical elemental composition of the materials are specified in Table 3.2 and Table 3.3. The commercial AC used in this study purchased by the same supplier, but from different batches of GAC, showed some differences regarding surface and textural properties. For instance, AC_{b3} exhibits higher S_{BET} ((1291 ± 10) $m^2 \cdot g^{-1}$) than AC_{b2} ((1002 ± 10) $m^2 \cdot g^{-1}$), and both have higher S_{BET} than AC_{b1} ((824 ± 10) $m^2 \cdot g^{-1}$). Differences in the mesopore surface area and volume of micropores were observed too. Comparing AC-based materials with the other materials (Zeo, CNT, CNT@2%Fe and Mag), AC presented higher S_{BET} and micropore volumes, while Mag presented the lowest values for these properties. On the other hand, CNT exhibited higher mesopore surface areas.

The different treatments applied to AC_{b2} (starting material) allowed to obtain materials with distinct characteristics (Table 3.3). This is grounded by the fact that the S_{BET}, S_{meso}, and V_{micro} of AC can be altered by the incorporation or removal of functional groups according with treatments applied (A. R. Silva et al., 2021a). For example, nitric acid oxidation treatment will result in the incorporation mainly of carbonyl, carboxyl, anhydrides, lactone and phenol groups, on the surface of the material (A. R. Silva et al., 2021a). On the contrary, the thermal treatments at high temperatures allow the removal of the weakly bounded and highly active carbon atoms, such as carboxyl, sulfur compounds, nitrogen oxides and CO_2, prevailing only a few quinone groups on the surface of AC (A. R. Silva et al., 2021a). On the other hand, nitric acid treatment can promote a slight decrease of the S_{BET} and of the volume of micropores, once some of the micropore walls may collapse due to the severe conditions of the treatment, but also due to the incorporation of functional groups on the carbon structure (A. R. Silva et al., 2021a). The thermal treatment with nitrogen flow can cause the decrease of the mesoporous volume by the presence of N group on the surface of the modified material (A. R. Silva et al., 2021a). The surface chemistry also imparts an amphoteric character to the materials, which allows the surface charge of the material to be either positive or negative, depending on its isoelectric point (commonly represented by the pH_{pzc}) and the pH of the medium (A. R. Silva et al., 2021a). For example, high acidity of materials was promoted by the incorporation of acidic groups resulting in materials with lower pH_{pzc} values (Pereira et al., 2010), while materials with low oxygen-containing groups showed high basicity (i.e., high values of pH_{pzc}) (A. R. Silva et al., 2021a). The functional groups may influence positively or negatively the reactions under study (Soares et al., 2019).

Table 3.2. Physicochemical characterization of materials regarding S_{BET}, S_{meso}, V_{micro}, total pore volume (micropore and mesopore, $Vp_{P/Po=0.95}$), pH_{pzc}, conductivity, chemical analysis, and elemental composition assessed by SEM-EDS

Characterization	**AC_{b1}**	**CNT**	**CNT@2%Fe**	**Mag**	**Zeo**	**Sand**	**Glass beads**
S_{BET} (± 10)/ ($m^2 \cdot g^{-1}$)	824	273	266	8	488	-	-
S_{meso} (± 5)/ ($m^2 \cdot g^{-1}$)	126	273	266	-	43	-	-
V_{micro} (± 0.005)/ ($cm^3 \cdot g^{-1}$)	0.286	0	-	-	0.184	-	-
$Vp_{P/P0=0.95}$ (± 0.005)/ ($cm^3 \cdot g^{-1}$)	-	-	-	0.015	0.247	-	-
CO/ ($\mu mol \cdot g^{-1}$)	379 ± 20	200	-	-	-	-	-
CO_2/ ($\mu mol \cdot g^{-1}$)	173 ± 20	23	-	-	-	-	-
(CO/CO_2)/ ($\mu mol \cdot g^{-1}$)	2	9	-	-	-	-	-
pH_{pzc} (± 0.2)	-	6.6	6.5	4.6	11.6	9.5	8.8
Conductivity/ ($S \cdot cm^{-1}$)	> 1.68×10^{-4} *	10 to 100 *	-	$(2.1 \pm 0.7) \times 10^{-5}$	$(3.3 \pm 0.7) \times 10^{-6}$	-	-
Characterization by SEM-EDS	**AC_{b1}**	**CNT**	**CNT@2%Fe**	**Mag**	-	-	-
C/ (% wt)	88.77	87.75	90.32	4.50	-	-	-
O/ (% wt)	8.29	8.16	6.35	20.73	-	-	-
Na/ (% wt)	-	1.47	0.37	-	-	-	-
Al/ (% wt)	0.45	-	-	-	-	-	-
Si/ (% wt)	1.05	0.59	0.51	0.22	-	-	-
P/ (% wt)	-	-	0.85	0.84	-	-	-
S/ (% wt)	1.44	0.49	0.18	-	-	-	-
Cl/ (% wt)	-	1.54	-	-	-	-	-
Fe/ (% wt)	-	-	1.42	73.72	-	-	-

(-) values not determined.

* Values found in literature for conductivity of GAC and CNT: the range varied between (1.68×10^{-4}) $S \cdot cm^{-1}$ and (8.6×10^{-3}) $S \cdot cm^{-1}$ for GAC, and from 10 to 100 $S \cdot cm^{-1}$ for multiwalled CNT (Lee et al., 2020; Martins et al., 2018; Song et al., 2019).

Table 3.3. Characterization of AC_{b2} (starting material), modified AC, and AC_{b3}, in terms of S_{BET}, S_{meso}, V_{micro}, total pore volume ($Vp_{P/Po=0.95}$), pH_{pzc}, and elemental analysis

Characterization	AC_{b2}	AC_ HNO_3	AC_ HNO_3_400	AC_ HNO_3_600	AC_ HNO_3_900	AC_ H_2SO_4	AC_ HNO_3_ H_2SO_4	AC_N	AC@2%Fe	AC_{b3}
S_{BET} (± 10)/ ($m^2 \cdot g^{-1}$)	1002	852	880	908	1033	843	227	784	-	1291
S_{meso} (± 5)/ ($m^2 \cdot g^{-1}$)	165	131	129	129	154	145	45	117	-	127
V_{micro} (± 0.005)/ ($cm^3 \cdot g^{-1}$)	0.347	0.302	0.315	0.325	0.365	0.290	0.076	0.278	-	0.532
$Vp_{P/PO=0.95}$ (± 0.005)/ ($cm^3 \cdot g^{-1}$)	0.525	0.446	0.456	0.465	0.534	0.443	0.129	0.405	-	0.657
pH_{pzc} (± 0.2)	7.3	4.1	5.7	6.7	8.5	2.1	2.0	8.4	8.1	8.4
C_{EA}/ (% wt)	88.8	89.1	89.4	88.9	91.8	86.8	61.7	88.2	-	90.5
H_{EA}/ (% wt)	0.4	0.9	0.3	0.4	0.3	0.7	1.8	0.6	-	0.7
N_{EA}/ (% wt)	0.0	1.3	0.0	0.0	0.0	0.0	0.8	6.5	-	0.0
S_{EA}/ (% wt)	0.6	0.8	0.5	0.5	0.5	1.4	0.3	0.5	-	0.7

EA – determined by elemental analysis.

(-) values not determined.

So, the application of different treatments allowed to obtain AC with distinct characteristics. In summary, in this work, the AC samples treated with HNO_3 presented a lower specific surface area, lower mesopore surface area, and a slight decrease on micropore volume than the starting AC_{b2} (Table 3.3). These parameters in general slightly increased during heat treatment at increasing temperatures (400 °C, 600 °C and 900 °C). What also increased with HNO_3 treatment was mainly the content in nitrogen, followed a slight increase in hydrogen and sulfur. The combination of HNO_3 with heat treatment did not cause almost any impact on the H, N and S content in comparison with AC_{b2}. On the other hand, the treatment with H_2SO_4 allowed an increase in sulfur amount with a consequently decrease on specific surface area (more functional groups are spread around all surface of the material) comparing with AC_{b2}. Combining HNO_3 and H_2SO_3 treatments caused the decrease in almost all parameters, namely specific surface area, mesopore surface area, micropore volume and a drastically alteration of the distribution of elements (loss of some carbon material, decrease of sulfur content, and increase of hydrogen and nitrogen contents), comparing with AC_{b2}. By doping AC with nitrogen (AC_N), the increase of N content on the material occurred with a consequent decrease on the specific surface area, as well as on the mesopore surface area, and micropore volumes.

Regarding the pH_{pzc}, these values are critical to determine the net charge (positive or negative) carried on the materials surface as a function of the pH of the solution (Pereira et al., 2010). The surface becomes positively charged at pH < pH_{pzc} and negatively charged at pH > pH_{pzc} (Pereira et al., 2010). Considering that the pH of the growth medium is around 7, the results showed that the following materials presented a neutral or slightly acidic character: AC_{b2}, AC_ HNO_3_600, CNT and CNT@2%Fe. The lower values of pH_{pzc} in the materials AC_ HNO_3_ H_2SO_4, AC_ H_2SO_4, AC_ HNO_3, Mag, AC_ HNO_3_400, revealed that they are acidic materials (negatively charged surface at pH 7), while the rest (AC@2%Fe, AC_{b3}, AC_N, AC_ HNO_3_900, Glass beads, sand, Zeo) presented a basic character (positively charged surface at pH 7).

The elemental analysis of materials allows to get more details about their composition. For instance, Tessonier *et al.* (2009) determined the percentage of impurities present on commercial CNT, being iron (Fe), cobalt, sulfur (S) and aluminum (Al) the main contaminants found (Tessonnier et al., 2009). In carbon-based materials (AC, CNT), used in this study, carbon (C) was the most abundant element detected, while Fe was the most abundant element found in Mag, as expected. However, other elements were commonly observed comparing the different materials, but in different amounts. These elements include the silicon (Si) which was at higher percentages in AC_{b1} than in CNT or Mag (Table 3.2), and it is expected to be the main element in the composition of glass beads, sand, and Zeo. Zeo type-13X is an aluminosilicate constituted by 1 Na_2O:1 Al_2O_3:2.8 ± 0.2 SiO_2:xH_2O, with a structures similar to faujasite

structure (R. M. Silva et al., 2021). Other elements, namely nitrogen (N) and S also varied in amount for each material under study (Table 3.2 and Table 3.3).

In terms of conductivity, Mag ((2.1 ± 0.7) × 10^{-5} S·cm^{-1}) is almost 10 times more conductive than Zeo ((3.3 ± 0.7) × 10^{-6} S·cm^{-1}), both with a semiconductor profile. Materials or conjugated polymers can be classified as insulators, semiconductors, and conductors, according with the values of electrical conductivity. For instance, quartz and diamond are considered insulators since their electrical conductivity are in the range between 10^{-16} S·m^{-1} and 10^{-10} S·m^{-1} (Spadafora, 2011). In the range of 10^{-10} S·m^{-1} to 10^{2} S·m^{-1} are the semiconductors like glass (in the transition zone insulator-semiconductor) and silicon, while conductors like copper, iron or silver are in the range between 10^{2} S·m^{-1} and 10^{8} S·m^{-1} (Spadafora, 2011). In the literature, the values of electrical conductivity of Mag were reported as correlated with the amount and particles size of Mag samples (Weidenfeller et al., 2002). So, different values of electrical conductivity might be found for Mag in different studies. For instance, Lee *et al.* (2020) used a Mag with an electrical conductivity of 3.8 × 10^{-5} S·cm^{-1}, which is a higher value than in the present study, although in the same order of magnitude (Lee et al., 2020). Regarding the type of Zeo, the conductivity can also vary. For example, it was reported values from ((4.24 ± 0.22) × 10^{-4}) S·m^{-1} to ((6.99 ± 4.26) × 10^{-4}) S·m^{-1} for the faujasite type-Y (Yimlamai et al., 2011), which are higher values than the ones obtained in this study. However, in this study it was used the commercial type-13X, also with the faujasite structure, but with lower Si/Al ratio (R. M. Silva et al., 2021) (in contrast with type-Y). The differences in Si/Al ratios imply also differences in the Zeo' properties, such as the particle size, the morphology, and the distribution of framework aluminium (Busca, 2014), and then it is possibly that it could interfere in the value of electrical conductivity as well. The conductivity of AC and CNT were not obtained in this study due to the physical properties of these materials that hindered the measurement, with the type of equipment used. However, according to the literature, the value of conductivity for GAC can be around (1.68 × 10^{-4}) S·cm^{-1} ((Lee et al., 2020), (3 × 10^{-3}) S·cm^{-1} (Martins et al., 2018; J. H. Park et al., 2018), or even approximately (8.6 × 10^{-3}) S·cm^{-1} (Song et al., 2019), and 0.14 S·cm^{-1} for powdered AC (König et al., 2022), while CNT can present conductivities from 10 to 100 S·cm^{-1} (Martins et al., 2018). These values suggested that both GAC and CNT possess a conductor profile, with CNT being the material with the highest electrical conductivity.

3.3.2. Abiotic assays: effects of (nano)materials on growth medium parameters and interaction with gaseous substrates

The results of abiotic assays showed that the concentrations of hydrogen in the presence and absence of materials were maintained and followed the same profile (Figure 3.3), excluding the possible adsorption effects of the substrate to the surface of materials.

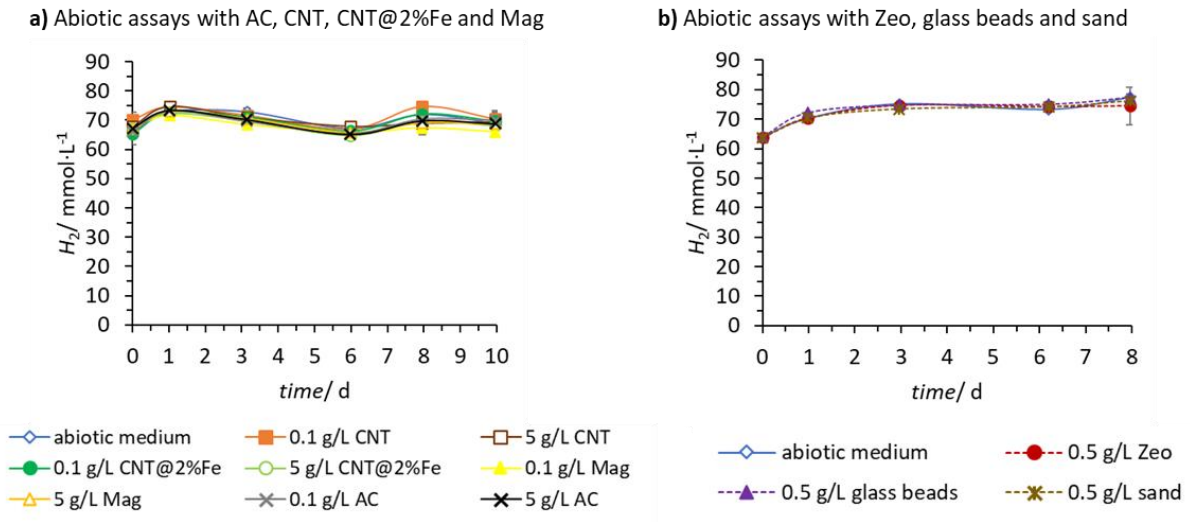

Figure 3.3. Monitoring of hydrogen concentration over time in the following abiotic conditions: a) with CNT, CNT@2%Fe, Mag and AC_{b1}, at 0.1 g·L^{-1} and 5 g·L^{-1}; and b) with Zeo, glass beads and sand, at 0.5 g·L^{-1}. The abiotic assays with the different set of materials were carried out in different periods. Each condition was evaluated in duplicate, and it is represented as the mean and the respective standard deviation.

The values for pH, ORP and conductivity in the abiotic anaerobic medium, with and without materials, are given in Table 3.4. The ORP and pH values exactly at the beginning of the assays differed slightly from the other sampling time points, maybe due to some reactions that were ongoing. Taken this into consideration, it was decided in further studies to measure these parameters after 24 h of the beginning of the assays to allow the stabilization of the reactions. For instance, the addition of sulfide solution results in products of sulfide oxidation which would be stabilized after 24 h (Whitman et al., 2006). Yet, initial differences were observed in the ORP values in the presence of carbon-based materials. At the highest concentration tested, the presence of AC and CNT decreased the values of ORP. During the time of the assay, the ORP values were decreasing during the time, excepting for the conditions with 5 g·L^{-1} of CNT@2%Fe and Mag. Indeed, the presence of Mag and CNT@2%Fe (mainly at 5 g·L^{-1}) contributed to the highest ORP values registered. Regarding pH and conductivity values, the presence of AC, CNT, CNT@2%Fe and Mag seems not to interfere with these parameters, as the values did not differ much

from those of the medium without materials. The presence of Zeo, sand and glass almost did not alter the values of ORP, pH and conductivity, although the values of pH of the medium tended to be higher with Zeo, which could be related with its basic character.

Table 3.4. Values of ORP, pH, and conductivity of the growth medium with H_2/CO_2, at the beginning (a), middle (b) and end (c) of abiotic assays in the presence of different concentrations (C) of materials

	C/ ($g \cdot L^{-1}$)	**ORP**/ (mV)			**pH**			**Conductivity**/ ($mS \cdot cm^{-1}$)		
		a	b	c	a	b	c	a	b	c
Abiotic medium	0	-179 ± 1	-263 ± 11	-351 ± 0	7.32 ± 0.03	7.30 ± 0.01	7.27 ± 0.01	-	5.84 ± 0.16	5.76 ± 0.06
CNT	0.1	-174 ± 15	-275 ± 1	-350 ± 8	7.35 ± 0.01	7.31 ± 0.06	7.27 ± 0.01	-	5.97 ± 0.21	5.86 ± 0.15
	5	-237 ± 75	-328 ± 8	-376 ± 18	7.42 ± 0.03	7.31 ± 0.02	7.28 ± 0.01	-	6.08 ± 0.09	5.98 ± 0.12
CNT@2%Fe	0.1	-158 ± 3	-306 ± 0	-373 ± 27	7.53 ± 0.03	7.37 ± 0.04	7.29 ± 0.04	-	5.95 ± 0.08	5.92 ± 0.06
	5	-183 ± 4	-241 ± 4	-222 ± 27	7.54 ± 0.07	7.40 ± 0.03	7.30 ± 0.01	-	6.01 ± 0.03	5.83 ± 0.02
AC_{b1}	0.1	-179 ± 2	-305 ± 1	-339 ± 3	7.43 ± 0.04	7.33 ± 0.01	7.28 ± 0.01	-	6.01 ± 0.06	5.93 ± 0.01
	5	-282 ± 51	-390 ± 10	-348 ± 2	7.44 ± 0.05	7.30 ± 0.06	7.27 ± 0.04	-	6.17 ± 0.33	6.18 ± 0.33
Mag	0.1	-187 ± 14	-308 ± 2	-337 ± 17	7.43 ± 0.01	7.35 ± 0.01	7.31 ± 0.07	-	5.93 ± 0.16	5.99 ± 0.11
	5	-184 ± 3	-210 ± 33	-212 ± 8	7.43 ± 0.01	7.36 ± 0.01	7.31 ± 0.01	-	6.05 ± 0.02	5.93 ± 0.01
Abiotic medium	0	-285 ± 5	-310 ± 19	-249 ± 28	7.16 ± 0.04	7.24 ± 0.04	7.28 ± 0.06	7.41 ± 0.17	7.45 ± 0.21	7.49 ± 0.21
Zeo	0.5	-291 ± 4	-333 ± 2	-297 ± 12	7.25 ± 0.01	7.35 ± 0.02	7.37 ± 0.00	7.71 ± 0.16	7.77 ± 0.12	7.79 ± 0.13
Glass beads	0.5	-295 ± 3	-341 ± 6	-311 ± 1	7.14 ± 0.01	7.26 ± 0.01	7.30 ± 0.01	7.73 ± 0.06	7.73 ± 0.08	7.77 ± 0.01
Sand	0.5	-307 ± 5	-339 ± 7	-290 ± 5	7.13 ± 0.01	7.24 ± 0.01	7.31 ± 0.01	7.68 ± 0.22	7.71 ± 0.23	7.70 ± 0.25

(-) equipment not available.

* The abiotic assays with AC, CNT, CNT@2%Fe and Mag were carried out in a different period of the abiotic assays with Zeo, glass beads and sand.

3.3.3. Biotic assays

3.3.3.1. Experiment I: Effect of different materials on MP

The presence of CM (i.e., CNT, CNT@2%Fe, AC and Mag) affected the methanogenic activity of *M. formicicum* (Figure 3.4). The main impact observed was the decrease of lag phases preceding MP in the presence of carbon-based materials and its increase in the presence of the iron-based material (i.e., Mag). Another observation was that increasing concentrations of carbon-based materials contributed to a higher

decrease of the lag phases duration. In the presence of the highest concentration of carbon-based materials tested, the lag phases were decreased from approximately 4 d (in the control condition) to less than 1 d (Table 3.5). For example, this impact corresponded to a decrease of 97.5 % of the lag phase in the presence of 5 $g \cdot L^{-1}$ of AC. On the other hand, the presence of Mag extended the lag phase duration up to 20 d, depending on the concentration tested. Therefore, this drastic decrease in the lag phases preceding MP in the presence of carbon-based materials led to an acceleration of the initial methane production rates (IMPR) during the first 3 d of incubation (Table 3.5). Consequently, the IMPR increased with increasing concentrations of CNT and CNT@2%Fe, up to the highest concentration evaluated, but only up to 0.5 $g \cdot L^{-1}$ with AC, and decreasing with 2 $g \cdot L^{-1}$ and 5 $g \cdot L^{-1}$ of AC (Table 3.5; Figure A. 1, Appendix). Evaluating the effects for each concentration tested, AC was always the best material in decreasing the lag phases and in increasing the IMPR, except for the concentration of 5 $g \cdot L^{-1}$, for which the stimulatory effect was more or less the same independently of the type of carbon-based material used (Figure 3.4).

Regarding the effects of CM towards the EMPR, the results showed that once the biotic control reached this phase of MP, its rate was by far faster than in the presence of any CM tested (Table 3.5). The complete MP profiles are presented in Figure A. 2 (Appendix). However, the effects of CM towards lag phase and IMPR cannot be ignored. For instance, considering the first 3 d of incubation, the presence of 0.5 $g \cdot L^{-1}$ of AC allowed the consumption of (41 ± 3) % of hydrogen, while almost no hydrogen consumption occurred ((2 ± 1) %) by the biotic control without CM, for the same period. Thus, the IMPR was around 15 times higher in comparison with the IMPR of the biotic control without CM (Table 3.6). Furthermore, the presence of 5 $g \cdot L^{-1}$ of CNT and CNT@2%Fe improved the IMPR up to 11 and 9 times, respectively. Another important remark was that the EMPR were less affected at lower concentrations of CM (Table 3.6), highlighting the importance of optimizing the concentration of materials.

Considering the effects of Mag, all concentrations caused a partial inhibition of the methanogenic activity by increasing the lag phases duration (Table 3.5). However, after some time the cultures eventually started to produce methane (**Erro! A origem da referência não foi encontrada.**, Appendix). The MP in the presence of Mag was different for each concentration tested and for each bottle, including replicates of the same concentration that evolved differently, showing big differences in their recovery, which is represented by the high standard deviations (Figure A. 2, Appendix; Table 3.5).

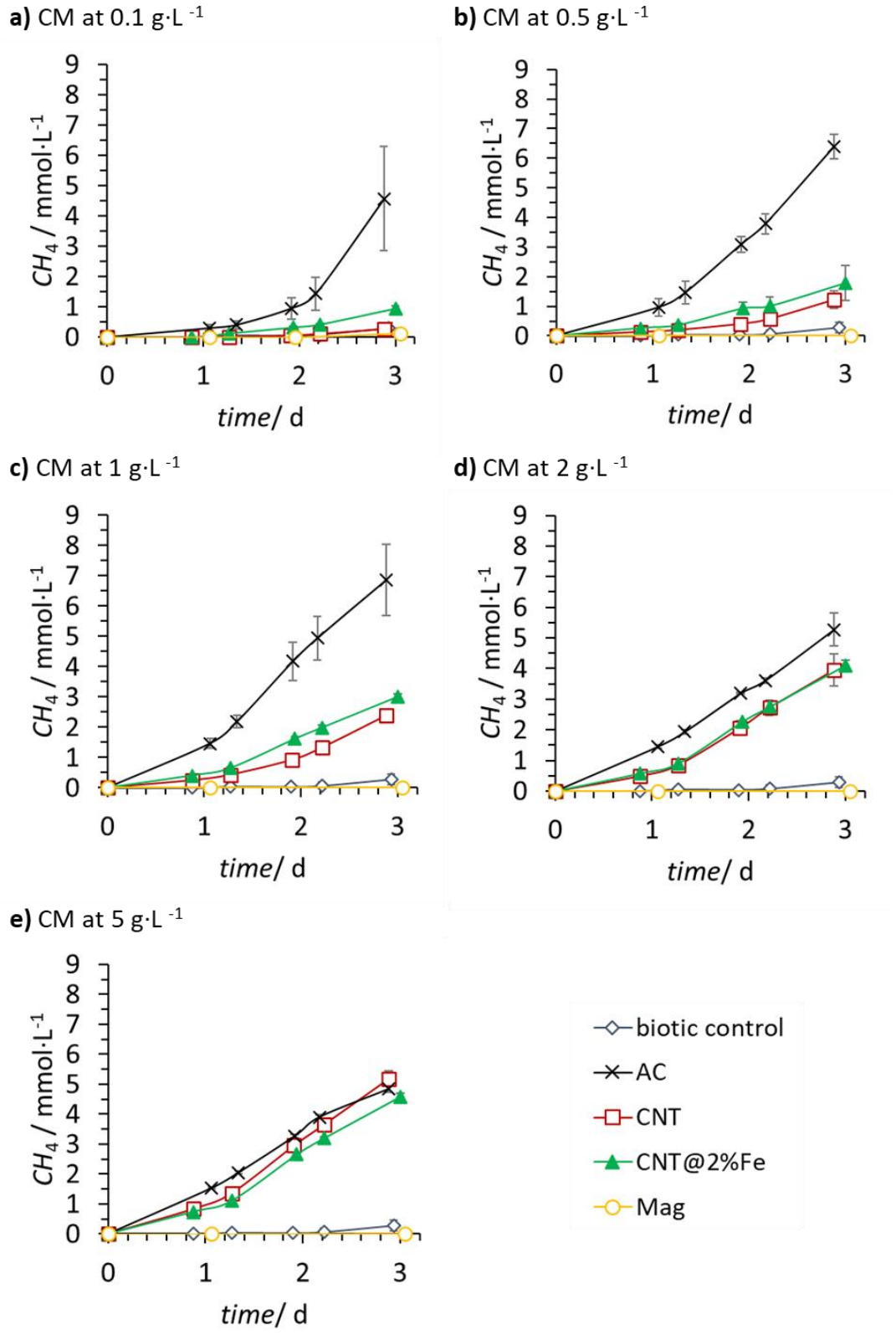

Figure 3.4. Cumulative methane production during the first days of incubation of *M. formicicum* with and without different CM, i.e., AC, CNT, CNT@2%Fe, and Mag, at concentrations varying between 0.1 g·L^{-1} and 5 g·L^{-1}. The results are the mean of triplicate assays with the respective standard deviation.

Table 3.5. Values of initial concentration of substrate (C_{H2}), lag phase duration, IMPR, EMPR, and incubation time (t) for the conversion of H_2/CO_2 to methane, for the assays with and without CM

Condition	CM/ g·L^{-1}	C_{H2}/ mmol·L^{-1}	Lag phase[a]/ d	IMPR [b]/ mmol·L^{-1}·d^{-1}	R^{2} [b]	EMPR [a]/ mmol·L^{-1}·d^{-1}	R^{2} [a]	t/ d
Biotic control	0	62.4 ± 0.7	3.9 ± 0.2	0.21 ± 0.10	0.80 ± 0.02	6.49 ± 0.42	1.00 ± 0.00	7
AC	0.1	62.9 ± 2.2	2.1 ± 0.4	2.25 ± 0.85	0.84 ± 0.01	5.84 ± 2.11	1.00 ± 0.00	8
	0.5	62.7 ± 0.6	1.2 ± 0.3	2.99 ± 0.35	0.99 ± 0.01	3.97 ± 0.82	0.99 ± 0.00	8
	1	62.4 ± 1.0	0.6 ± 0.3	3.02 ± 0.59	1.00 ± 0.00	3.04 ± 0.99	0.99 ± 0.01	9
	2	62.5 ± 1.9	0.5 ± 0.3	2.10 ± 0.30	0.99 ± 0.00	2.19 ± 0.51	0.99 ± 0.00	15
	5	61.3 ± 0.6	0.1 ± 0.1	1.87 ± 0.07	0.99 ± 0.01	1.71 ± 0.12	0.99 ± 0.00	24
CNT	0.1	61.4 ± 0.6	4.6 ± 0.6	0.17 ± 0.12	0.82 ± 0.16	3.43 ± 0.90	1.00 ± 0.00	13
	0.5	61.3 ± 0.6	2.8 ± 0.3	0.53 ± 0.16	0.88 ± 0.03	1.90 ± 0.27	1.00 ± 0.00	14
	1 (*)	65.0	1.8	1.05	0.94	1.86	1.00	14
	2	60.8 ± 0.2	0.9 ± 0.2	1.78 ± 0.23	0.99 ± 0.00	1.95 ± 0.49	0.99 ± 0.00	14
	5	61.8 ± 1.6	0.7 ± 0.1	2.22 ± 0.08	0.99 ± 0.00	2.24 ± 0.03	0.99 ± 0.00	14
CNT@2%Fe	0.1	61.9 ± 0.7	3.4 ± 0.3	0.43 ± 0.03	0.95 ± 0.02	6.18 ± 0.80	0.99 ± 0.00	8
	0.5	61.6 ± 0.1	2.0 ± 0.3	0.72 ± 0.25	0.97 ± 0.00	1.40 ± 0.21	1.00 ± 0.00	14
	1	62.2 ± 1.6	1.2 ± 0.1	1.27 ± 0.04	0.99 ± 0.00	1.68 ± 0.35	0.99 ± 0.00	14
	2	61.7 ± 0.3	0.9 ± 0.0	1.72 ± 0.07	0.99 ± 0.00	1.89 ± 0.03	0.99 ± 0.00	14
	5	61.8 ± 1.9	0.7 ± 0.0	1.89 ± 0.06	0.99 ± 0.00	1.94 ± 0.00	0.99 ± 0.00	14
Mag	0.1	61.7 ± 0.7	4.8 ± 0.4	-	-	4.27 ± 0.93	0.99 ± 0.00	9
	0.5	62.1 ± 0.6	13.1 ± 0.4	-	-	1.50 ± 0.24	0.99 ± 0.00	24
	1	60.6 ± 0.8	21.1 ± 2.5	-	-	1.84 ± 0.42	1.00 ± 0.00	> 29
	2	60.7 ± 1.0	16.7 ± 2.9	-	-	2.09 ± 0.69	0.93 ± 0.10	> 27
	5	61.2 ± 0.4	14.1 ± 1.2	-	-	1.81 ± 0.50	0.99 ± 0.00	24

(*) During the assays with 1 g·L^{-1} CNT, two bottles were lost, which means these values are only from one of the triplicates.

[a] kinetics parameters obtained by modified Gompertz model.

[b] IMPR was calculated for the early MP between days 1 and 3.

The complete conversion of H_2/CO_2 to methane was achieved almost in all conditions (**Erro! A origem da referência não foi encontrada.**, Appendix; Table 3.5). However, as Mag inhibited the activity of

M. formicicum and took longer times for converting the substrate to methane, the assays were given as finished before reaching the highest point of methane, being this one of the reasons why the values for MP in assays with Mag were lower comparing with the other conditions.

Table 3.6. Number of times that the IMPR and EMPR increases, or decreases (> 1 or < 1, respectively), relatively to the biotic control without CM

Concentration of CM/ g·L^{-1}	**AC**		**CNT**		**CNT@2%Fe**		**Mag**	
	IMPR	EMPR	IMPR	EMPR	IMPR	EMPR	IMPR	EMPR
0.1	11.0	0.9	0.8	0.5	2.1	1.0	#	0.7
0.5	14.6	0.6	2.6	0.3	3.5	0.2	#	0.2
1	14.7	0.5	5.1	0.3	6.2	0.3	#	0.3
2	10.2	0.3	8.7	0.3	8.4	0.3	#	0.3
5	9.1	0.3	10.8	0.3	9.2	0.3	#	0.3

#The number of times that IMPR was affected relatively to the control could not be calculated because there was no growth in *M. formicicum* assays with Mag for the period of analysis of the IMPR (i.e., the first 3 d of incubation).

Considering the results obtained, AC was selected as the best material to accelerate MP by *M. formicicum* pure cultures, and for this reason, the next experiments with modified materials had AC as the starting material. In experiments II and III (Figure 3.1), it was used the optimal concentration found for AC (0.5 g·L^{-1}).

3.3.3.1.1. Interaction of microbial cells with CM

The arrangement of cells with and without CM can be observed in Figure 3.5. In the presence of carbon-based materials, many cells were observed in direct contact with CNT (Figure 3.5ii), CNT@2%Fe (Figure 3.5iii), and AC (Figure 3.5i). Aggregates were formed between cells and carbon-based materials, and the cells seemed not to suffer any damage by the presence of CM. Particularly with AC, cells were attached to the surface of the material. On the other hand, lower abundance of cells was observed interacting with Mag, even the sample for SEM analysis had also been taken during the middle of the exponential of MP (Figure 3.5iv). These observations are aligned with the results of MP in the presence of these CM. In the absence of materials, the cells seemed to be aggregated to each other and linked by what seems to be extracellular substances (Figure 3.5v). The analysis by SEM-EDS of Z1 (in red at the image), showed that the elemental composition consisted in 0.49 % Al, 0.66 % Si, 0.85 % Cl, 43.37 % C, 12.43 % O, 1.54 % Ca, 10.43 % N, 2.93 % P, 3.07 % Fe, 1.22 % Na, 6.02 % S, 0.45 Mg, 9.47 % Au, 1.63 % Pd, and 5.45 % Zn (w/w).

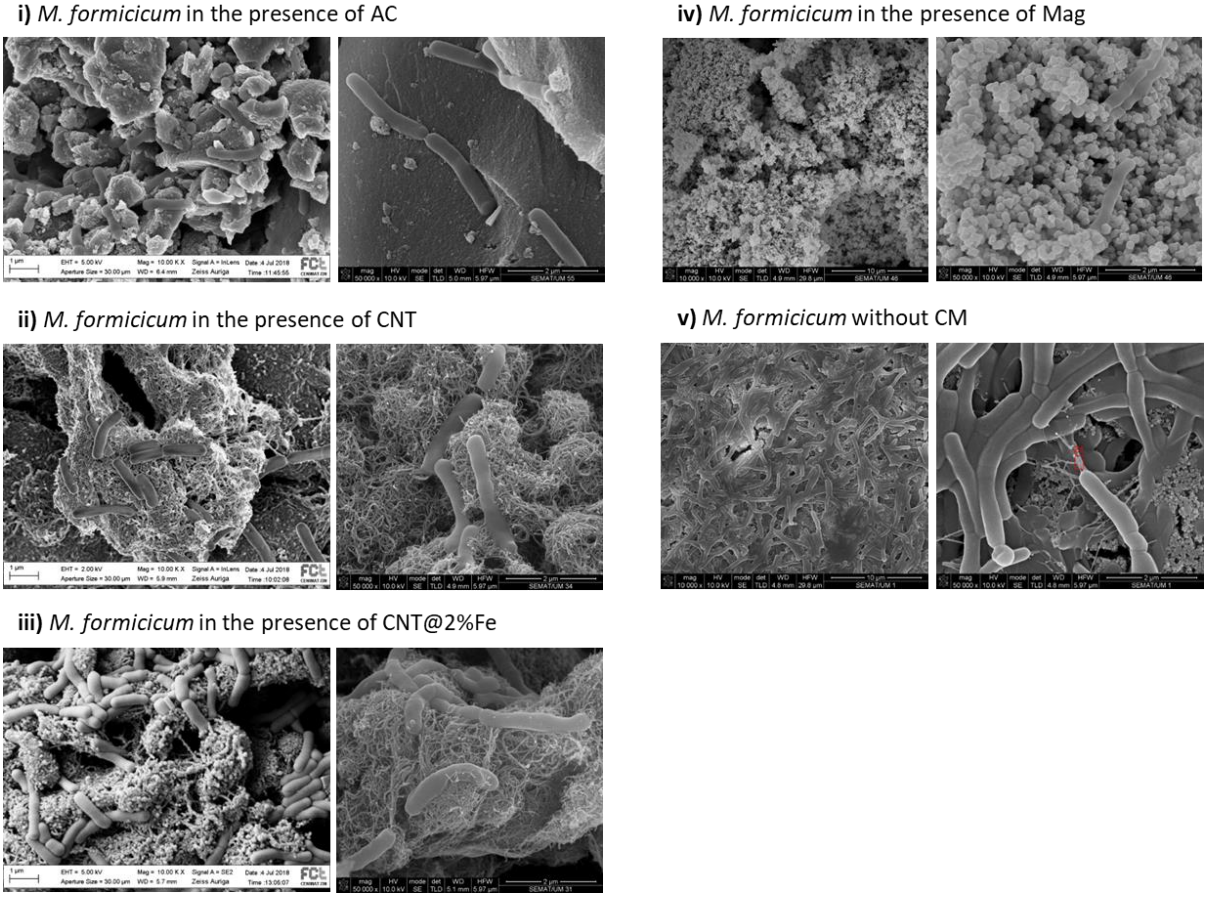

Figure 3.5. SEM images of *M. formicicum* incubated with i) AC), ii) CNT, iii) CNT@2%Fe, and iv) Mag, and v) without CM. In the control condition without CM, SEM-EDS analysis was performed at zone 1 (Z1) indicated at the image in red. The shape of cells are long or short rods (Whitman et al., 2006). The cell width of *M. formicicum* is typically between 0.4 µm to 0.8 µm, and cell length can vary from 2 µm to 15 µm (Whitman et al., 2006).

3.3.3.1.2. Effects of CM on growth medium parameters in biotic conditions

The presence of CM in biotic conditions did not significantly alter the values of pH and conductivity of the growth medium (Table 3.7). The values of these parameters varied during the incubation time, but without drastic differences among conditions. Regarding ORP values, the presence of carbon-based materials promoted the decrease of ORP (specially at 1 $g \cdot L^{-1}$ or 2 $g \cdot L^{-1}$) and higher ORP values were observed in the presence of Mag, and even in the presence of 5 $g \cdot L^{-1}$ CNT@2%Fe.

Table 3.7. Values of ORP, pH, and conductivity of the growth medium at (a) the beginning, (b) during exponential MP, and (c) at the end of incubations with *M. formicicum* pure cultures

Condition	C/ ($g \cdot L^{-1}$)	ORP/ (mV)			pH			Conductivity/ ($mS \cdot cm^{-1}$)		
		a	b	c	a	b	c	a	b	c
Biotic control	0	-308 ± 5	-348 ± 9	-352 ± 10	7.29 ± 0.02	7.51 ± 0.12	8.26 ± 0.23	5.78 ± 0.15	5.94 ± 0.13	5.78 ± 0.06
CNT	0.1	-318 ± 5	-380 ± 9	-367 ± 14	7.34 ± 0.11	7.98 ± 0.29	8.16 ± 0.09	6.18 ± 0.80	6.14 ± 0.50	6.80 ± 0.96
	0.5	-322 ± 26	-388 ± 21	-368 ± 10	7.30 ± 0.04	7.39 ± 0.05	8.07 ± 0.09	5.80 ± 0.21	5.76 ± 0.15	5.70 ± 0.17
	1	-338 ± 35	-380	-368	7.23 ± 0.06	7.43	8.24	5.80 ± 0.10	5.88	5.79
	2	-394 ± 7	-398 ± 4	-409 ± 2	7.15 ± 0.02	7.62 ± 0.09	8.02 ± 0.09	5.73 ± 0.09	5.79 ± 0.08	5.81 ± 0.09
	5	-329 ± 27	-371 ± 47	-397 ± 2	7.25 ± 0.03	7.40 ± 0.03	8.10 ± 0.05	5.85 ± 0.20	5.87 ± 0.21	5.78 ± 0.06
CNT@2%Fe	0.1	-323 ± 21	-353 ± 7	-355 ± 6	7.23 ± 0.03	7.59 ± 0.03	8.25 ± 0.04	5.77 ± 0.09	5.73 ± 0.02	5.70 ± 0.04
	0.5	-334 ± 22	-388 ± 15	-414 ± 1	7.23 ± 0.04	7.46 ± 0.03	8.22 ± 0.07	5.87 ± 0.21	5.81 ± 0.17	5.67 ± 0.39
	1	-341 ± 29	-417 ± 2	-396 ± 23	7.25 ± 0.02	7.41 ± 0.09	8.25 ± 0.03	5.85 ± 0.19	6.08 ± 0.27	5.75 ± 0.06
	2	-371 ± 14	-375 ± 28	-317 ± 45	7.26 ± 0.03	7.60 ± 0.02	8.21 ± 0.05	5.91 ± 0.05	5.92 ± 0.14	5.93 ± 0.15
	5	-342 ± 3	-215 ± 41	-216 ± 12	7.25 ± 0.04	7.38 ± 0.06	8.19 ± 0.08	5.73 ± 0.12	5.86 ± 0.03	5.71 ± 0.20
AC	0.1	-318 ± 4	-363 ± 5	-352 ± 2	7.27 ± 0.03	7.95 ± 0.22	8.24 ± 0.07	5.91 ± 0.10	5.89 ± 0.08	5.80 ± 0.13
	0.5	-365 ± 9	-379 ± 12	-355 ± 34	7.26 ± 0.03	8.11 ± 0.10	8.21 ± 0.04	5.92 ± 0.17	5.86 ± 0.11	5.81 ± 0.08
	1	-345 ± 8	-400 ± 7	-364 ± 25	7.29 ± 0.02	7.38 ± 0.04	8.29 ± 0.06	5.90 ± 0.12	5.91 ± 0.24	5.69 ± 0.09
	2	-331 ± 12	-374 ± 4	-383 ± 3	7.29 ± 0.07	7.74 ± 0.12	8.18 ± 0.01	5.97 ± 0.13	5.88 ± 0.10	5.82 ± 0.12
	5	-295 ± 48	-338 ± 11	-124 ± 71	7.27 ± 0.03	7.35 ± 0.01	8.20 ± 0.04	5.88 ± 0.14	5.76 ± 0.10	5.80 ± 0.09
Mag	0.1	-316 ± 3	-365 ± 4	-349 ± 11	7.28 ± 0.01	8.22 ± 0.11	8.19 ± 0.15	5.84 ± 0.11	5.74 ± 0.03	5.81 ± 0.03
	0.5	-321 ± 7	-310 ± 8	-310 ± 10	7.27 ± 0.03	8.05 ± 0.15	8.39 ± 0.47	6.01 ± 0.09	5.85 ± 0.20	5.87 ± 0.13
	1	-331 ± 21	-299 ± 34	-319 ± 27	7.20 ± 0.03	7.47 ± 0.06	7.99 ± 0.38	5.94 ± 0.07	6.21 ± 0.53	5.88 ± 0.16
	2	-311 ± 3	-299 ± 8	-353 ± 12	7.26 ± 0.01	7.87 ± 0.15	8.22 ± 0.11	5.86 ± 0.09	5.82 ± 0.11	5.77 ± 0.14
	5	-315 ± 7	-336 ± 18	-295 ± 43	7.26 ± 0.03	8.08 ± 0.14	8.31 ± 0.49	5.92 ± 0.09	5.82 ± 0.06	5.81 ± 0.10

(*) During the assays with 1 $g \cdot L^{-1}$ CNT, two bottles were lost, which means these values are only from one bottle (there are no replicates only for this condition).

3.3.3.2. Experiments II and III: Impact of modified AC, Zeo type-13X, glass beads, sand, and silicon on MP

The results of batch incubations of *M. formicicum* pure cultures with different modified AC are represented in Figure 3.6. The methanogenic activity of this pure culture, besides being improved in the presence of the starting AC (AC_{b2}), it was even better in the presence of modified AC, except for the one treated with both nitric and sulfuric acids ($AC\_H_2SO_4\_HNO_3$), which promoted an extension of lag phase, also resulting in longer incubation times for the complete conversion of H_2/CO_2 to methane (Figure 3.6b, Table 3.8). Within the group of AC treated with nitric acid, the faster MP was achieved with $AC\_HNO_3\_900$, by reducing 80 % the lag phase preceding MP, and accelerating the IMPR, which shortened in 37.5 % the time of incubation for the complete MP when compared with the biotic control (Figure 3.6a, Table 3.8). Regarding the effects of $AC\_H_2SO_4$, MP profiles similar to those of the starting AC_{b2} were obtained (Figure 3.6b, Table 3.8). Comparing the effects of AC_N and AC@2%Fe, the profiles of MP were slightly improved when compared with the starting material AC_{b2}, but all enhanced the MP of the pure culture (Figure 3.6c, Table 3.8). From all modified AC tested, the best material was the $AC\_HNO_3\_900$. Regarding the EMPR, the highest value achieved continued to be exhibited by the biotic control without materials, while the effect of AC on EMPR varied among the different materials (Table 3.8).

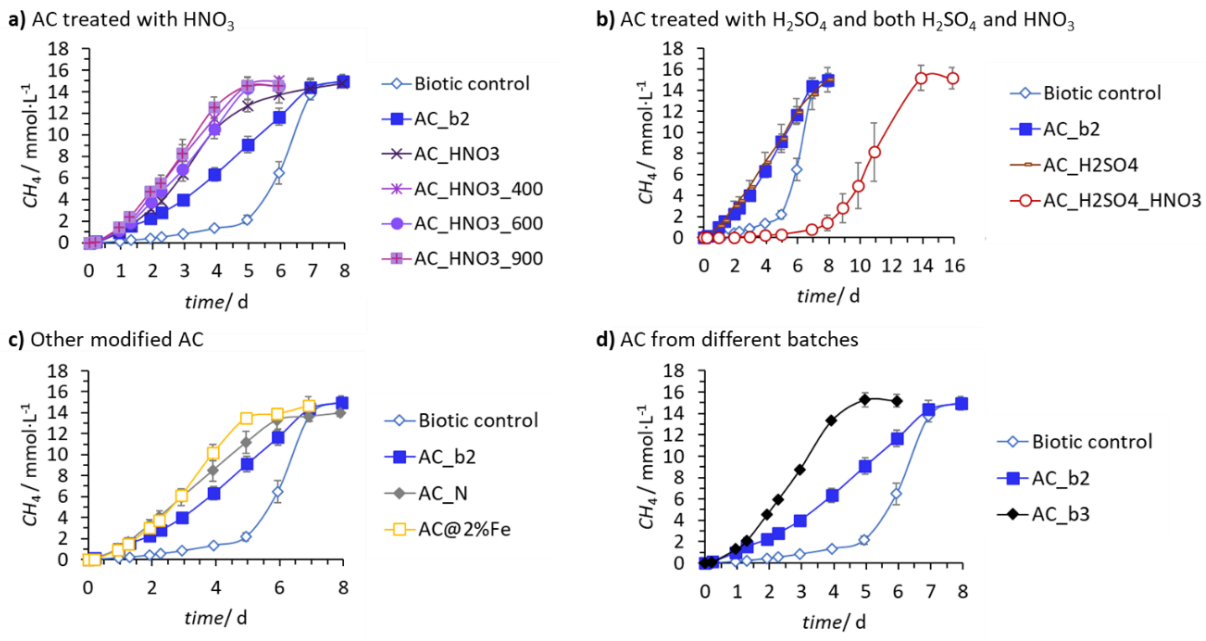

Figure 3.6. Cumulative methane production by pure cultures of *M. formicicum* incubated with 0.5 $g \cdot L^{-1}$ of different modified AC (a, b, c) and AC from different batches (d). The results are the mean with the respective standard deviation of triplicate assays.

Comparing the AC_{b2} and AC_{b3} from different batches (Figure 3.6d, Table 3.8), it was observed that AC_{b3} (IMPR of (3.26 ± 0.04) mmol·L^{-1}·d^{-1}) had a greater impact than AC_{b2} (IMPR of (1.43 ± 0.13) mmol·L^{-1}·d^{-1}) towards the IMPR of *M. formicicum* (control with IMPR of (0.30 ± 0.04) mmol·L^{-1}·d^{-1}) being as good as the best modified AC (IMPR of (3.07 ± 0.27) mmol·L^{-1}·d^{-1} with AC_HNO_3_900).

Table 3.8. Results of the incubations of *M. formicicum* with modified AC, AC from different batches, and with Zeo, glass beads and sand, regarding the initial concentration of substrate (C_{H2}), the duration of lag phase, the IMPR, the EMPR, and the time of incubation (t) required for the complete conversion of H_2/CO_2 to methane

Condition	C_{H2}/ mmol·L^{-1}	Lag phase[a]/ d	IMPR [b]/ mmol·L^{-1}·d^{-1}	R^2	EMPR [a]/ mmol·L^{-1}·d^{-1}	R^2	t/ d
Biotic control	64.1 ± 0.3	5.1 ± 0.4	0.30 ± 0.04	0.97 ± 0.01	7.64 ± 0.93	0.98 ± 0.00	8
AC_{b3}	65.2 ± 0.9	1.0 ± 0.1	3.26 ± 0.04	0.97 ± 0.01	4.85 ± 0.17	1.00 ± 0.00	5
AC_HNO_3_900	66.9 ± 0.3	1.0 ± 0.1	3.07 ± 0.27	0.98 ± 0.01	4.18 ± 0.15	0.99 ± 0.01	5
AC_HNO_3_400	64.3 ± 1.0	1.0 ± 0.1	2.99 ± 0.55	0.97 ± 0.00	4.32 ± 0.52	1.00 ± 0.00	6
AC_HNO_3_600	64.5 ± 1.2	1.0 ± 0.1	2.56 ± 0.26	0.98 ± 0.01	3.97 ± 0.38	0.99 ± 0.01	5
AC_HNO_3	63.8 ± 1.7	1.2 ± 0.0	2.31 ± 0.21	0.96 ± 0.01	3.97 ± 0.34	1.00 ± 0.00	8
AC@2%Fe	65.8 ± 0.9	1.2 ± 0.1	2.25 ± 0.20	0.96 ± 0.00	3.93 ± 0.14	1.00 ± 0.00	7
AC_N	65.3 ± 0.6	1.0 ± 0.1	2.22 ± 0.31	0.98 ± 0.00	3.11 ± 0.33	1.00 ± 0.00	8
AC_H_2SO_4	64.8 ± 0.3	1.0 ± 0.0	1.81 ± 0.19	0.99 ± 0.00	2.54 ± 0.32	1.00 ± 0.00	8
AC_{b2}	64.9 ± 1.6	1.3 ± 0.2	1.43 ± 0.13	0.99 ± 0.00	2.98 ± 0.60	0.99 ± 0.00	8
AC_H_2SO_4_HNO_3	64.7 ± 0.2	8.2 ± 0.7	0.03 ± 0.03	0.79 ± 0.00	3.14 ± 0.04	0.99 ± 0.00	14
Zeo	64.6 ± 1.1	1.5 ± 0.0	4.74 ± 0.14	0.86 ± 0.01	9.62 ± 0.82	1.00 ± 0.00	5
Sand	66.0 ± 0.7	2.6 ± 0.0	1.08 ± 0.06	0.78 ± 0.02	11.10 ± 0.63	0.99 ± 0.00	5
Glass beads	66.3 ± 0.3	3.5 ± 0.1	0.47 ± 0.02	0.93 ± 0.01	6.93 ± 0.22	0.98 ± 0.01	6

[a] kinetics parameters obtained by modified Gompertz model.

[b] IMPR was calculated for the early MP between days 0 and 3.

The evaluation of materials less conductive than AC, CNT and Mag, like Zeo, and the non-CM (i.e., glass beads and sand) showed surprising results regarding the enhancement of methanogenic activity by pure cultures of *M. formicicum* (Figure 3.7a). The presence of these materials resulted in a faster MP, by reducing the lag phases from 5 d (in the biotic control without materials) to 1.5 d with Zeo, 2.6 d with sand and 3.5 d with glass beads (which were not as low as the lag phases in the presence of carbon-based materials, i.e., around 1 d), as well as by decreasing the time of incubation (in a higher extension than the other materials) required to achieve a complete conversion of H_2/CO_2 to methane (Table 3.8). Contrarily to the effect of CM towards the EMPR (which delayed the rates during this phase of MP), the presence of Zeo and sand enhanced approximately 1.3 and 1.5 times the EMPR when compared with the biotic control without materials (Table 3.9).

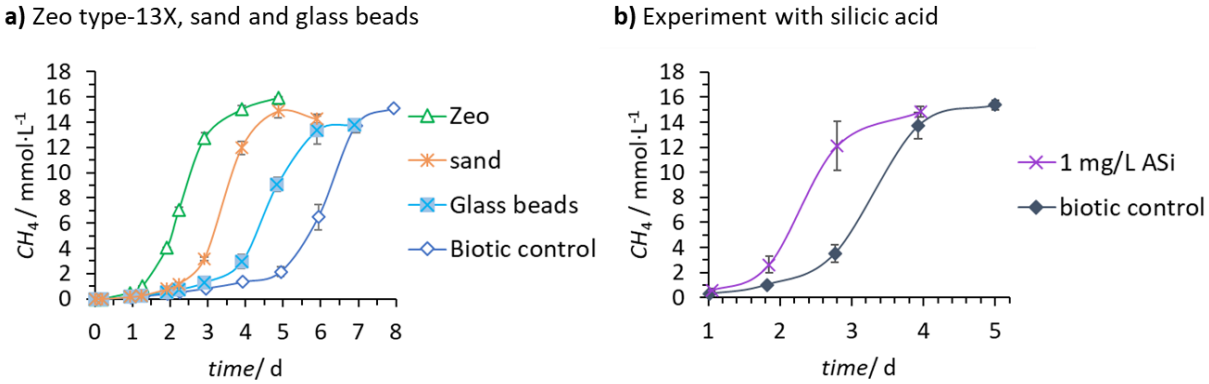

Figure 3.7. Cumulative methane production by pure cultures of *M. formicicum* in assays without and with a) Zeo type-13X, sand and glass beads, at 0.5 g·L^{-1}, and during b) the experiment with 1 mg·L^{-1} of silicic acid in aqueous solution (ASi). The results are the mean with the respective standard deviation of triplicate assays.

Table 3.9 presents the number of times that each material (CM and non-CM) affected the IMPR and EMPR, along with some of the differences in physicochemical properties of materials that could be related with the effects observed.

Table 3.9. Summary of the IMPR and EMPR improvements or decrease (> 1 or < 1, respectively), relatively to the biotic control without materials and some physicochemical properties of materials

IMPR	EMPR	Materials	S_{BET}/ ($m^2 \cdot g^{-1}$)	S_{meso}/ ($m^2 \cdot g^{-1}$)	V_{micro}/ ($cm^3 \cdot g^{-1}$)	$Vp_{P/Po=0.95}$/ ($cm^3 \cdot g^{-1}$)	Cell-materials interaction	N/ (%)	S/ (%)
15.6×	1.3×	Zeo	488	43	0.184	0.247	Attraction	-	-
10.7×	0.6×	AC_{b3}	1291	127	0.532	0.657	Attraction	0.0	0.7
10.1×	0.5×	AC_HNO_3_900	1033	154	0.365	0.534	Attraction	0.0	0.5
9.9×	0.6×	AC_HNO_3_400	880	129	0.315	0.456	Repulsion	0.0	0.5
8.4×	0.5×	AC_HNO_3_600	908	129	0.325	0.465	~Neutral	0.0	0.5
7.6×	0.5×	AC_HNO_3	852	131	0.302	0.446	Repulsion	**1.3**	0.8
7.4×	0.5×	AC@2%Fe	-	-	-	-	Attraction	-	-
7.3×	0.4×	AC_N	784	117	0.278	0.405	Attraction	**6.5**	0.5
5.9×	0.3×	AC_H_2SO_4	843	145	0.290	0.443	Repulsion	0.0	**1.4**
4.7×	0.4×	AC_{b2}	1002	165	0.347	0.525	~Neutral	0.0	0.6
1.7×	1.5×	Sand	-	-	-	-	Attraction	-	-
1.5×	0.9×	Glass beads	-	-	-	-	Attraction	-	-
0.1×	0.4×	AC_H_2SO_4_ HNO_3	227	45	0.076	0.129	Repulsion	0.8	0.3

Regarding the composition of all materials, a common element found was silicon, which is the main constituent of Zeo, glass beads, and sand, and was present in vestigial amounts on the composition of AC (element detected during SEM-EDS analysis, Table 3.2). To get further insights about the direct effect of this element towards the methanogenic activity, *M. formicicum* was incubated with silicic acid in

aqueous solution (Figure 3.7b). The results obtained confirmed that the presence of Si can stimulate the activity of *M. formicicum* in pure cultures. The lag phase preceding MP was (1.68 ± 0.05) d in the presence of Si, while it took (2.50 ± 0.02) d in the biotic control, representing a decrease of 32 % in the lag phase duration (results statistically different, $p < 0.05$ level). The EMPR were similar between these conditions, i.e., the EMPR was (12.62 ± 2.04) mmol·L^{-1}·d^{-1} for biotic control (R^2 = 0.996 ± 0.001) and (13.39 ± 3.07) mmol·L^{-1}·d^{-1} in the presence of Si (R^2 = 0.995 ± 0.005).

3.3.3.2.1. Effects of materials on growth medium parameters in biotic conditions

Considering the effect of incubation conditions (with and without materials) on growth medium parameters, the results still showed a significant decrease of ORP values in the presence of AC-based materials, but the other materials like Zeo, glass beads and sand, only slightly decreased the ORP of the medium (Table 3.10). Crossing ORP results with the improvements promoted by the presence of materials, the best material in enhancing MP was Zeo, but it was not the material that contributed the most for the decrease of ORP values. Regarding the pH of the growth medium, the values were not significantly altered by the presence of materials. The exceptions were the following: the incubations with AC_H_2SO_4_HNO_3 exhibited the lowest value of pH at the beginning (6.96 ± 0.00), and the incubations with Zeo showed the highest value of pH at the end (8.44 ± 0.05), which can be a direct influence of the acidity and basicity of each material, respectively. In terms of conductivity of the growth medium, the results showed that the value can be higher at the beginning when CM/non-CM are present, and slightly lower at the end of the assays when AC-based materials, glass beads, and sand, were present, in comparison with the biotic control without materials. The presence of Zeo does not seem to affect this parameter in the end of the assay.

Table 3.10. Effect of different modified AC, AC from different batches, and Zeo, glass beads, sand on the growth medium parameters (ORP, pH and conductivity) a) after 24 h the beginning and b) at the end of the incubations with the pure culture *M. formicicum*

Material	**ORP**/ mV		**pH**		**Conductivity**/ ($mS \cdot cm^{-1}$)	
	a	b	a	b	a	b
Biotic control	-284 ± 31	-337 ± 14	7.03 ± 0.02	8.13 ± 0.00	4.79 ± 0.46	5.71 ± 0.34
AC_{b2}	-363 ± 5	-385 ± 5	7.05 ± 0.02	8.09 ± 0.01	5.68 ± 0.12	5.44 ± 0.17
AC_HNO_3	-364 ± 2	-372 ± 11	7.04 ± 0.04	8.05 ± 0.18	5.65 ± 0.04	5.30 ± 0.14
$AC\_HNO_3\_400$	-374 ± 4	-381 ± 2	7.05 ± 0.02	8.08 ± 0.05	5.71 ± 0.06	5.40 ± 0.02
$AC\_HNO_3\_600$	-389 ± 2	-395 ± 4	7.05 ± 0.02	8.08 ± 0.05	5.63 ± 0.07	5.41 ± 0.19
$AC\_HNO_3\_900$	-391 ± 2	-397 ± 4	7.04 ± 0.00	7.91 ± 0.09	5.63 ± 0.18	5.45 ± 0.08
AC_N	-378 ± 4	-394 ± 15	7.05 ± 0.02	8.07 ± 0.05	5.62 ± 0.09	5.30 ± 0.19
AC@2%Fe	-385 ± 6	-354 ± 45	7.03 ± 0.03	8.07 ± 0.10	5.53 ± 0.12	5.33 ± 0.23
$AC\_H_2SO_4$	-390 ± 3	-390 ± 13	7.05 ± 0.02	8.06 ± 0.02	5.62 ± 0.11	5.30 ± 0.19
$AC\_H_2SO_4\_HNO_3$	-374 ± 8	-331 ± 30	6.96 ± 0.00	7.88 ± 0.04	5.41 ± 0.14	5.55 ± 0.11
AC_{b3}	-374 ± 2	-363 ± 10	7.05 ± 0.02	8.02 ± 0.10	5.54 ± 0.13	5.48 ± 0.07
Zeo	-324 ± 4	-321 ± 18	7.10 ± 0.03	8.44 ± 0.05	5.55 ± 0.05	5.71 ± 0.44
Glass beads	-334 ± 4	-358 ± 2	7.03 ± 0.02	8.11 ± 0.07	5.54 ± 0.12	5.40 ± 0.23
Sand	-342 ± 11	-349 ± 10	7.04 ± 0.00	8.12 ± 0.02	5.56 ± 0.19	5.43 ± 0.13

3.3.3.2.2. Impact of materials on cell wall thickness

Samples of the biotic control and samples with *M. formicicum* in contact with CNT, AC, Mag, Zeo, sand and glass beads were observed by TEM (Figure 3.8). The comparison among samples suggested that the thickness of the cell wall of *M. formicicum* was altered in the presence of certain materials. Cells in the presence of Mag showed thicker cell walls ((18 ± 4) nm) than cells without materials ((12 ± 3) nm) (results significantly different, $p < 0.05$ level). On the other hand, thinner cell walls were measured in samples with Zeo ((9 ± 2) nm) or glass beads ((9 ± 2) nm). No significant differences were observed in the thickness of cell walls in the presence of AC ((13 ± 5) nm), CNT ((15 ± 8) nm) and sand ((14 ± 6) nm). Considering the standard deviation associated to each set of measurements for each condition, the higher

differences were found in cells with Mag, being the values of thickness varying from 10 nm to 27 nm, while it varied only from 8 nm to 19 nm in the control without materials.

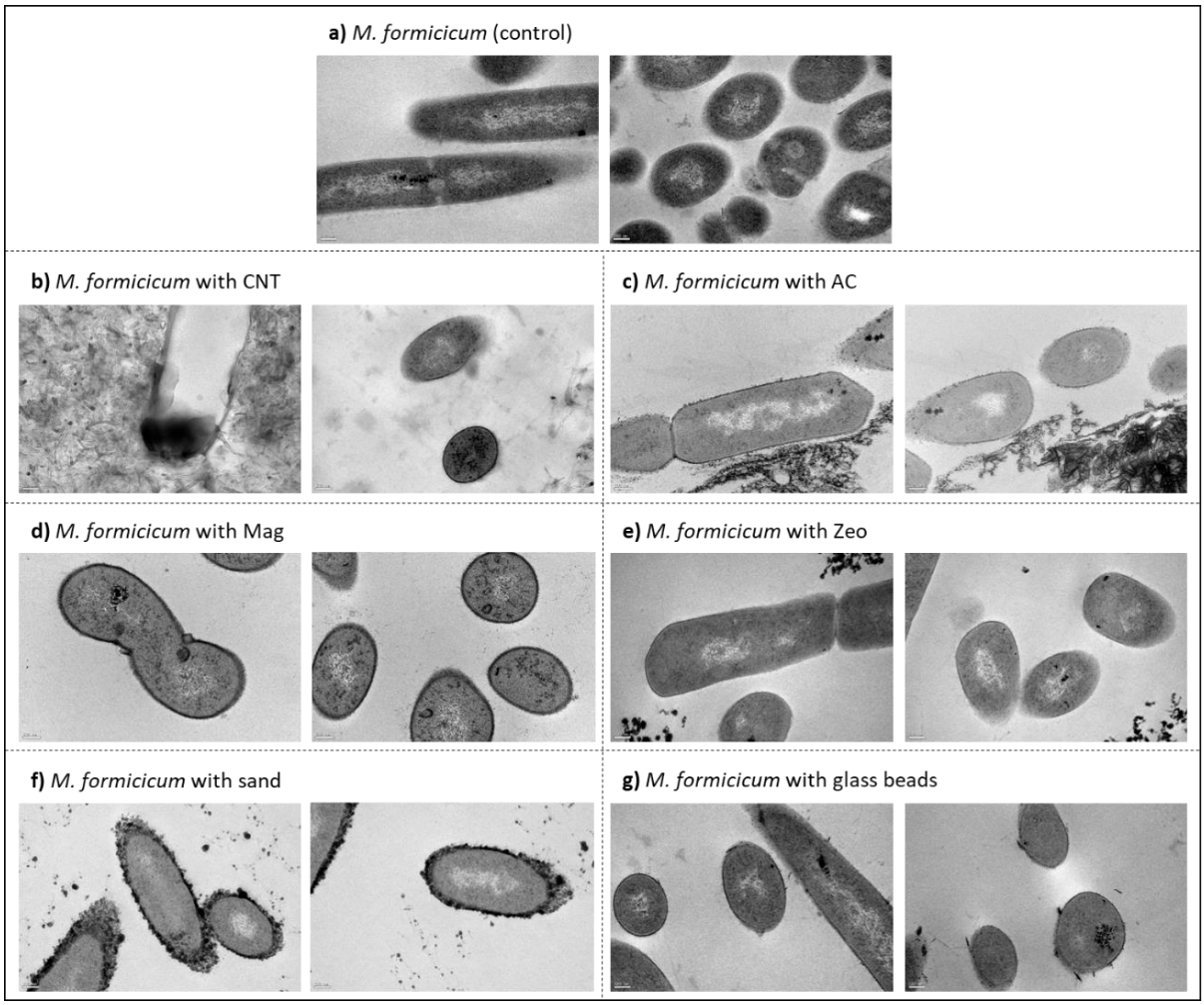

Figure 3.8. TEM micrographs of *M. formicicum* cells with and without materials. The images were acquired with a magnification of 100 000×, being the scale 100 nm.

3.4. Discussion

Different species and different physicochemical characteristics of materials can influence the effects on MP

This work showed that different types of materials, like CNT, increased the methanogenic activity of *M. formicicum*. This way, it is remarkable to observe that the same type of material can promote opposite effects for different species, once CNT negatively affected *M. maripaludis* and *M. conradii* (Xia et al., 2019; W. Zhang et al., 2018), but greatly stimulated *M. formicicum* activity. However, the present study also showed that the same type of material can promote different results depending on the batch that it

came from, even for the same supplier. This was observed in the incubations with AC from different batches (Table 3.3, Figure 3.6d), with AC_{b3} improving better the methanogenic activity than AC_{b2}. These results brought the attention to the importance of the physicochemical characterization of the materials as it can impact the results obtained. However, there is a lack of information about the characterization of materials in most of the studies, avoiding a clear comparison of results (e.g., values of electrical conductivity of CM) (Castilho et al., 2022; Martins et al., 2018). This study, and all the others published, show that results can be affected either by the different cultures or by materials with different characteristics (even when materials are considered to be of the same type).

Effects of different types of CM at different concentrations

In this study, *M. formicicum* was particularly stimulated in the presence of AC, at relatively low concentrations, when compared with CNT (Figure 3.4). From an applied point of view, the fact that AC can promote better results than CNT is something to be into account, because regardless the potential of CNT to improve the AD process, it can bring higher costs than AC, when applied in large scale (Abbas et al., 2021; Kumar et al., 2021). Furthermore, commercial AC can be replaced by bio-based carbons, being more economical and sustainable attractive, once AC can be obtained through different biomass wastes at lower costs (Abbas et al., 2021). The improvements observed by each material also varied with the concentration (Figure A. 1, Appendix). With CNT, the IMPR increased with increasing concentrations and the same effect was observed in other studies (Salvador et al., 2017). However, with AC, the best results were not obtained with the highest concentration tested (Figure A. 1, Appendix). In fact, concentrations higher than 1 $g \cdot L^{-1}$ impacted negatively the EMPR (Table 3.5 and Table 3.6). For instance, it was observed in other study that applying 5 or 25 $g \cdot L^{-1}$ of GAC would not promote significant differences in MP performance (Xu et al., 2018). Inhibitory effects have also been observed at high concentrations of other CM (Cavalcante et al., 2021; Yiwei Liu et al., 2021). Thus, this dose-effect impact become an important factor also to consider, as finding the optimal concentration will allow to achieve a cost-energy-effective treatment (Castilho et al., 2022; Xu et al., 2019).

Possible explanations behind the effects of carbon- and iron-based materials on MP

From a fundamental point of view, AC, CNT, and Mag caused different impacts towards the hydrogenotrophic activity of *M. formicicum*. The carbon-based materials contributed to decrease the lag phases preceding MP, and consequently increasing the IMPR, while Mag caused an extension of the lag phase preceding MP (Figure 3.4). The physicochemical characteristics of the materials may be relevant

for the results obtained. The analyses of many reports performed by Castilho *et al.* (2022) suggested that no apparent correlation existed between the enhancement of MP and the electrical conductivity of materials (Castilho et al., 2022). This is aligned with the results here presented, firstly because the conductivity of materials has been related with the mechanism of conductive material mediated interspecies electron transfer (CIET) (Martins et al., 2018) and there is no interspecies electron transfer in pure cultures and, secondly, CNT presents higher conductivity than AC (Table 3.2) and yet, AC resulted in the best results (Table 3.6). The particle size of material may also play a role, as large materials may support microbial growth (Castilho et al., 2022; Wu et al., 2020), and the results obtained showed the attachment of *M. formicicum* cells growing on the surface of AC (Figure 3.5i), which means it can serve as a support for cells growth. The substrate adsorption in the surface of materials could also contribute to influence the microbial activity. In this case, hydrogen adsorption to AC surface could bring closer *M. formicicum* and its substrate, but this phenomenon seemed not to be relevant here once hydrogen concentrations remained unchanged in abiotic conditions with or without CM (Figure 3.3). The effect of Mag towards *M. formicicum*, by causing a temporary MP inhibition, could be related with the sensitivity of *M. formicicum* to the Fe(III) present in the composition of Mag (H. Wang et al., 2020). In previous studies, it was shown the sensitivity of pure cultures of methanogens growing on H_2/CO_2 in the presence of Fe(III), which could be explained based on the possible inactivation of cofactors or proteins (e.g., factor F_{420}) by Fe(III), which are important in MP via hydrogenotrophic pathway (Van Bodegom et al., 2004). Other studies also reported the increase of lag phase duration up to 11.5 % when testing Mag, and one of the explanations proposed for the delay of methanogenesis was the requirement of higher time for the production of extracellular polymeric substances (EPS), as a defence mechanism against Mag as an exogenous substance (Zhong et al., 2022). In the study of Zhong *et al.* (2022), the highest EPS secretion was observed with the smallest Mag particles investigated, meaning that the size of Mag interfered with the result. In this study, it was not possible to conclude if this occurred, and further investigations would be needed to explore the influence of Mag (and the other materials) towards EPS secretion by *M. formicicum*. Yet, the analysis performed by SEM suggested that EPS secretion by *M. formicicum* would be lower in the presence of carbon-based materials (Figure 3.5i, 3.5ii, 3.5iii) comparing with the control without materials (Figure 3.5v, red zone Z1). In biotic conditions without materials (Figure 3.5v, Z1), the excretion of substances by *M. formicicum* seemed to be abundant. The impact of materials towards EPS production also seems to vary depending the study conditions, once CM are reported to increase EPS production in some studies with Mag, pyrite or CNT (Jiao et al., 2023; Xu et al., 2019; Yan et al., 2018), and reported to decrease it in assays with CNT in pure cultures of methanogens (Salvador et al., 2017).

The production of EPS is usually connected with the cluster formation by maintaining different microorganisms adhered to each other or to abiotic surfaces (Oh et al., 2018). For instance, the contribution of *M. formicicum* for EPS production in anaerobic granules was previously reported as being significant (Veiga et al., 1997). The polymer matrix of granules contributes to the adhesion between different species of methanogenic archaea and syntrophs, enhancing their stability (Veiga et al., 1997). At 37 °C (temperature of incubation in the present study), as expected, *M. formicicum* grew as clumps, as can be observed in SEM images (Figure 3.5v). Besides, the production of EPS by *M. formicicum* was also found to be reduced under lower nitrogen and phosphorous conditions (Veiga et al., 1997). Thus, the presence of carbon-based materials may contribute to decrease the EPS secretion by *M. formicicum* cells possibly: i) by acting as a support for cells adhesion maintaining cells close to each other and then there is no need of EPS for the formation of clumps; or ii) elements like sulfur, present in the composition of materials (Table 3.2 and Table 3.3), may function as a nutritional supplement, thus affecting the EPS secretion. The second hypothesis seems less likely, since species of *Methanobacterium* are usually known to use ammonium, sulfide, and elemental sulfur as nitrogen and sulfur sources (Whitman et al., 2006), and this element is present in the growth medium. Particularly, in the presence of Mag, EPS seemed not be produced in high amounts (Figure 3.5iv), but it is not a precise result since the amount of cells found near Mag was very reduced to reach any conclusion. However, it seemed clear that Mag represented toxicity for cells as methanogenic activity was negatively affected.

Observing the micrographs obtained during TEM analysis (Figure 3.8), differences in the thickness of cell walls, especially when cells were in contact with Mag (Figure 3.8d), seemed to be relevant. The cell envelope structure is diverse among methanogens, and the cell wall of the *Methanobacteriaceae* is composed of pseudomurein (Whitman et al., 2006). Pseudomurein confers shape to the rod cells. Depending on the mode of living, some methanogens were found to change their cell wall thickness (i.e., cell wall thickness was different for methanogens growing in syntrophic coculture than those growing in pure culture) (Nakamura et al., 2006). As cell wall represents an interface between the cells and the external environment, mechanisms may be activated to neutralize cell wall damage (e.g., reinforcing the cell wall integrity) and to adapt to new conditions, which may imply changes in the cell wall structure (Martínez et al., 2020). Considering the hypothesis of inhibition of cofactors and proteins by Fe(III), in hydrogenotrophs, and considering that the permeability of the cell wall is influenced by the thickness of pseudomurein (Nakamura et al., 2006), *M. formicicum* may have to activate mechanisms of defence in the presence of Mag, such as the increase of the cell wall thickness, as an adaptive mechanism to minimize the negative impact of Mag towards its metabolism.

Physicochemical characteristics of modified activated carbons and their effect on MP

Besides the impact of particle size, concentration, adsorption capacity, and electrical conductivity of materials towards MP, the results obtained may be due to the effect of other characteristics like surface area, ORP or pH_{pzc}(Castilho et al., 2022; Martins et al., 2018). Comparing the characterization of all materials tested by order of IMPR improvement (Table 3.9), it was not found a key property that could explain per se the improvements occurred in the presence of materials. The values of textural properties (e.g., S_{BET}, S_{meso}, V_{micro}) varied and, for example, neither the material with the highest value of S_{BET} (i.e., AC_{b3}) nor the material with the lowest value (i.e., AC_H_2SO_4_ HNO_3) corresponded to the one that promoted the best results (i.e, Zeo). So, it was not found a tendency between textural properties and improvements on MP promoted by materials. Considering the values of pH_{pzc} of the materials, it is possible to predict their net charge in the growth medium and therefore their interaction with cells (assuming that cells present a negative charge) (A. R. Silva et al., 2021a; Silva et al., 2020). This way, for positively charged materials an attractive interaction with cells would be expected, while for materials with a negatively charged surface a repulsive interaction would be expected. So, attractive interactions between cells and Zeo, AC_{b3}, AC_HNO_3_900, AC@2%Fe, AC_N, sand, and glass beads, and repulsive interactions with AC_HNO_3_400, AC_HNO_3, AC_H_2SO_4, AC_H_2SO_4_ HNO_3, may occur, while the rest of materials can be considered neutral. However, both acidic and alkaline materials improved the IMPR, as for example Zeo which improved up to 15.6 times (alkaline material) and AC_HNO_3_400 up to 9.9 (acidic material) the IMPR (Table 3.9). Thus, no evidence was found to support the explanation for MP improvements based on attractive interactions between cells and materials. The role of materials in providing nutrients, like N and S, for microbial growth was not considered important to explain the results here obtained as well (Table 3.9). Both N and S are considered macronutrients (Lamers et al., 2012), and they are essential nutrients for anaerobic microorganisms (Abbas et al., 2021). However, the materials with higher amounts of N (AC_HNO_3 and AC_N) or S (AC_H_2SO_4) were not responsible for the highest improvements, since the best materials to accelerate MP presented lower amounts of these elements in their composition (e.g., AC_HNO_3_900 from the group of modified AC).

The functionalization with iron could either offer Fe as a micronutrient (H. Liu et al., 2021; Paritosh et al., 2020) or it could be a strategy for materials recovery after the treatment, by the application of a simple magnetic field (Pereira et al., 2017). Within trace elements, iron is one of the micronutrient that can participate in the synthesis and activation of many enzymes involved in methanogenic metabolism, thereby affecting methanogenesis (H. Liu et al., 2021; Paritosh et al., 2020). On the other hand, magnetic nanoparticles combined with carbon-based materials would allow to apply a simple, low cost, quick and

efficient way of retain and recover the materials, which can be then re-use (Pereira et al., 2017). Although the presented results did not support that the presence of Fe would be important for the methanogenic activity of *M. formicicum*, the same results also showed that its presence in AC@2%Fe or CNT@2%Fe did not negatively affect the MP, so it can be used as a strategy for materials' recovery in specific applications.

Silicon effect on methanogenic activity

The acceleration of MP via hydrogenotrophic pathway in the presence of Zeo, glass beads and sand, was surprising. Interestingly, this group of materials even improved EMPR, which not occurred in the presence of carbon-based materials. The addition of Zeo in AD systems, or its application as a packing material column, has contributed to enhance AD performance (Cardona et al., 2021; Montalvo et al., 2012; Paritosh et al., 2020; Zheng et al., 2015). The effects are specially attributed to its capacity of immobilizing microorganisms and its ion-exchange property (attractive in ammonia stressful conditions by substituting cations like Na^{+}, Ca^{2+} and Mg^{2+} in its structure by NH_4^{+}, reducing ion ammonium in solution which can cause microbial activity inhibition) (Cardona et al., 2021; Montalvo et al., 2012; Paritosh et al., 2020; Zheng et al., 2015). Also, similar improvements were found with either Zeo or sand towards AD processes, suggesting their contribution for biomass immobilization to explain the higher performance observed comparing with the control (Montalvo et al., 2005). In another studies, the use of glass beads, or Zeo (as non-CM) did not improve methanogenesis (Amelia-Elena et al., 2018; König et al., 2022). These results show that conductivity of the material is not a requisite for improving the methanogenic activity of *M. formicicum*, as Zeo presented a lower conductivity than carbon-based materials, and sand and glass beads are considered non-CM (Amelia-Elena et al., 2018).

Giving the composition of each material (e.g., Zeo, sand, glass beads, AC), the main element found in common to all of them was Si. The most common component of Zeo, sand and glass, is silicon dioxide (SiO_2), also known as silica (Busca, 2014; Montalvo et al., 2005). During SEM-EDS analyses of the CM (Table 3.2), the presence of Si was also detected in low amounts in AC, CNT, CNT@2%Fe and Mag, being the highest percentage detected in AC samples. Silicon is an element that is not known as being essential for the activity of methanogens, like *M. formicicum*. The effect of silicon has been mainly studied in the growth of plants (Bist et al., 2020; Fauteux et al., 2005; Pavlovic et al., 2021), growth of fungi (Das and Das, 2010; Wainwright et al., 1997), and in the medical area (Jurkić et al., 2013). It was also reported that some zeolites can have the ortho-silicic acid-releasing property, which means these materials can release small but significant amounts of ortho-silicic acid (H_4SiO_4), which is the bioavailable form of silicon for microorganisms, plants, animals and humans (Jurkić et al., 2013). Thus, the availability of Si in the

growth medium may be a consequence of Si being released from Zeo or the other materials, and it can be the factor behind the enhancement of the *M. formicicum* metabolism. The impact of Zeo enhancing the growth of microorganisms like *Methanobacterium* was reported elsewhere (Cardona et al., 2021). Besides, the biogeochemistry of peatlands was also found to be influenced by Si availability (Reithmaier et al., 2017). The availability of Si was found to accelerate organic matter decomposition, increasing methane concentrations in these ecosystems, which confirmed the relevance of Si for the carbon cycle (Reithmaier et al., 2017). In the present study, preliminary assays showed the stimulatory effect of Si in MP by *M. formicicum*, using silicic acid (H_2SiO_3) in aqueous solution, which would result in the formation of H_4SiO_4 (Jurkić et al., 2013). However, these water soluble forms will be in reversible equilibrium reactions and be stable only in highly diluted aqueous solutions, or it can ended in its precipitation as hydrated silica (Jurkić et al., 2013). This way, 1 $mg \cdot L^{-1}$ was the concentration applied as the lowest concentration found as possible to be handle in laboratory conditions. The results suggested that Si can stimulate *M. formicicum* metabolism, but the exact biological roles of silicon towards methanogenic activity are unknown and this topic deserves to be further explored. Another strategy could be the incorporation of different amounts of Si on the materials, and to test its impact towards the microbial activity.

Changes on growth medium parameters in the presence of (nano)materials

In this study, it was not possible to observe a relation between the alterations on the growth medium parameters (like pH, ORP, and conductivity) in the presence of (nano)materials with the improvements on methanogenic activity. Regarding conductivity values of the growth medium, no big differences were detected among the different conditions. In the case of pH, the values varied from 7.0 to 7.3 at the start of incubations for all conditions, which is a range within the optimal pH for *M. formicicum* (between 6.6 and 7.8) (Whitman et al., 2006), and the pH increased up to 8.4 at the end of incubations. The increase of the final value of pH to around 8 could be related with the loss of buffer capacity in maintaining the pH at approximately 7, once bicarbonate buffer needs to be in equilibrium with CO_2 in the gas phase, but this CO_2 was consumed during MP. Nevertheless, the main change promoted by materials was observed for the ORP values of the growth medium. The main differences were in the presence of carbon-based materials that decreased the ORP values, while iron-based materials contributed to increase them. Methanogenesis is favoured at lower ORP values (between −200 mV to −400 mV), so it could be a possible explanation for MP improving in the presence of carbon-based materials (Salvador et al., 2017). Nonetheless, the results of this study did not fully support this explanation, once materials like Zeo did

not contribute as much as carbon-based materials to decrease ORP values and yet it was the best material to improve MP from all the materials tested. The increase of ORP values in the presence of iron-based materials has also been reported in other studies, and some attributed this to the inhibitory effects observed against methanogenesis once methanogens are sensitive to high ORP (Fu et al., 2019; Kato et al., 2012; Z. Wang et al., 2022; Wu et al., 2020). Yet, the inhibitory effect observed in these experiments did not seem to be caused by the increase of ORP by Mag, once the highest value reached was approximately -295 mV, which still is in the optimal range for methanogenesis. So, the results suggested that the improvements or inhibition effects were not related with changes in the growth medium parameters.

3.5. Conclusions

Several materials with different physicochemical properties were tested and all of them stimulated the methanogenic activity of *M. formicicum*, only with exception of Mag and AC_HNO_3_ H_2SO_4. The results do not show a direct influence of physicochemical properties of materials such as electrical conductivity, specific surface area, mesopores surface areas, micropores volumes, and pH_{pzc} on the improvements towards methanogenic activity. No evidence for the adsorption of gaseous substrate to the surface of materials facilitating the substrate access to microorganisms or even the extra nutrient supplementation provided by materials in their composition (with Fe, N or S) was found. The composition of all materials tested, i.e., AC, CNT, Mag, Zeo, sand and glass beads, had in common the element silicon. When silicic acid was supplemented, the results showed a stimulatory response by decreasing lag phases and the increasing MPR, which are similar effects as the ones observed in the presence of materials. The mechanisms behind the improvement of methanogenic activity of *M. formicicum* by materials or Si alone are still unknown. These results suggest that they can be related with the physicochemical characteristics of the materials (i.e., presence of silicon in their composition, but also possibly other properties).

Overall, having methanogenesis an important role in bioenergy production, the application of (nano)materials can be the key to boost the impact of AD process during the energetic transition. More studies are needed to evaluate the impact of sand and glass beads during the conversion of waste to methane, but if the effects were like the ones obtained during the conversion of H_2/CO_2 to methane, then they could be an alternative to replace the use of CM, as sand and glass beads are low-cost materials and with lower impact for natural environments than CM.

CHAPTER 4

4. METHANE PRODUCTION RATE BY PURE CULTURES OF METHANOGENS AND BY SYNTROPHIC COCULTURES IS REGULATED BY ACTIVATED CARBON, MAGNETITE AND ONE TYPE OF A ZEOLITE

ABSTRACT

Methane production rate (MPR) is enhanced by of conductive materials (CM), like activated carbon (AC), or magnetite (Mag), but the causes still require investigation. A screening of diverse CM (AC, Mag), and one zeolite (Zeo) (at 0.5 $g \cdot L^{-1}$) on the activity of four pure cultures of methanogens, and two syntrophic cocultures, is assessed and discussed taking into consideration the characteristics of the growth media (pH, redox potential (ORP), and conductivity) in the presence of the materials (AC, Mag, Zeo). The effect of materials on the different cultures was dissimilar. The hydrogenotrophic activity of *Methanobacterium formicicum* was the most affected, increasing significantly with AC and Zeo (MPR up to 20 times faster) and decreasing drastically with Mag (lag phases preceding methane production (MP) increased almost 3 times). Similarly, oleate degradation by the coculture of *Syntrophomonas zehnderi* with *M. formicicum* was also improved by AC, and severely inhibited by Mag. The effect of materials on the other microorganisms was not so impressive, although lag phases were generally reduced. The materials did not cause changes in the pH and conductivity of the growth medium, but altered the ORP, although there was no correlation between ORP variations and the impact on MP. The importance of physicochemical characteristics of the materials on MP was discussed. These results showed clearly that the MP by several species of methanogens is greatly improved by some materials, suggesting that their effect on complex microbial communities can be totally, or at least partially, attributed to this stimulatory effect towards methanogenic activity.

4.1. INTRODUCTION

The addition of conductive materials (CM) has been shown to improve methane production (MP) from several types of wastes (Martins et al., 2018), and it is also known that microbial interactions, including interspecies electron transfer (IET) (Rotaru et al., 2021), and the activity of pure cultures of methanogens are also affected (Fu et al., 2019, 2018; Salvador et al., 2017; H. Wang et al., 2020; Xia et al., 2019; Xiao et al., 2020; W. Zhang et al., 2018; Zheng et al., 2020). Nevertheless, different methanogens showed different responses to CM, particularly to those that are referenced in the literature as potential candidates to improve anaerobic digestion (AD), such as magnetite (Mag) and activated carbon (AC) (He et al., 2021; Lee et al., 2020; Peng et al., 2018; Jingxin Zhang et al., 2020; Zhao et al., 2017a). For example, Mag (an iron based-CM) accelerated the acetoclastic activity of *Methanosarcina barkeri* and *Methanosarcina mazei* (Fu et al., 2019; H. Wang et al., 2020), but inhibited the activity of *Methanocella conradii* (HZ254^T) (Xia et al., 2019), and had no effect towards the hydrogenotrophic activity of *Methanococcus maripaludis* and *M. conradii* (DSM 24694) (Fu et al., 2018) nor on the activity of *Syntrophomonas erecta* subsp. *sporosyntropha* (Fu et al., 2018). Furthermore, granular AC inhibited the growth of *Methanobacterium* sp. strain YSL (Zheng et al., 2020).

In this work, the effect of different types of materials on the activity of pure cultures of methanogens and syntrophic cocultures commonly found in anaerobic digesters, were investigated, namely AC, Mag and one type of a zeolite (Zeo), with distinct physicochemical characteristics, including different conductivities.

4.2. MATERIALS AND METHODS

4.2.1. Pure cultures and syntrophic cocultures

Two hydrogenotrophic methanogens (*Methanobacterium formicicum* (DSM 1535^T), *Methanospirillum hungatei* (DSMZ 864^T)), two acetoclastic methanogens (*Methanothrix harundinacea* (DSM 17206^T) and *Methanosarcina barkeri* (DSM 800^T)), and two syntrophic cocultures (*Syntrophomonas zehnderi* (DSM 1780^T) with *M. formicicum* (DSM 1535^T), and *Syntrophomonas wolfei* (DSM 102351^T) with *M. hungatei* (DSMZ 864^T)), were purchased from DSMZ (Braunschweig, Germany) and maintained in our laboratory. These cultures were incubated with AC, Mag and Zeo, at 0.5 g·L^{-1}. The exception was for the coculture of *S. zehnderi* with *M. formicicum*, where 0.1 g·L^{-1} AC was tested instead of 0.5 g·L^{-1} (the concentration of 0.1 g·L^{-1} was chosen based on preliminary assays in which this concentration increased the activity of *M. formicicum*), and the effect of Zeo on this coculture was not tested. The incubations were carried out in 120 mL serum bottles (working volume of 50 mL), containing the growth medium and prepared as

described in Chapter 3, subsection "3.2.2. Incubation conditions". The acetoclastic methanogens were grown under the conditions specified by DSMZ with the following modifications: trypticase peptone in *M. harundinacea* medium, and casitone in *M. barkeri* medium, were both replaced by tryptone enzymatic digested from casein (Sigma-Aldrich, USA), keeping the original concentrations. All solutions were previously sterilized by filtering or autoclaving (120 °C, 20 min) and added aseptically. Hydrogen-consuming methanogens (*M. formicicum*, *M. hungatei* and *M. barkeri*) were incubated in serum bottles with a mixture of H_2/CO_2 (80:20 %; 1.7 × 10^5 Pa) in the headspace, while acetoclastic methanogens (*M. barkeri* and *M. harundinacea*) were grown in bottles containing N_2/CO_2 (80:20 %; 1.7 × 10^5 Pa). In hydrogenotrophic incubations, acetate was added at 2 mmol·L^{-1}, while for growing *M. barkeri* and *M. harundinacea* under acetoclastic conditions, acetate was added at 20 mmol·L^{-1} and 10 mmol·L^{-1}, respectively. After inoculation (10 % v/v for hydrogenotrophic and 20 % v/v for acetoclastic cultures), the bottles were incubated at 37 °C, in the dark. Control assays without materials were also performed. All incubations were performed statically except the ones supplemented with hydrogen that were performed under agitation (120 min^{-1}). All assays were performed in triplicate.

For growing the syntrophic cocultures, first the methanogen was pre-grown as described above and the syntrophic cocultures were inoculated during the exponential growth phase, to guarantee a high methanogenic activity. Before the inoculation of the coculture, the bottles were opened, under aseptic conditions, to add the materials. The bottles were sealed immediately, the headspace filled with N_2/CO_2 (80:20 %; 1.7 × 10^5 Pa), and the medium was supplemented with extra reducing agent (3.6 mmol·L^{-1} Na_2S). The carbon and energy source, i.e., oleate (unsaturated C18:1, 99 %, Sigma-Aldrich, USA) (1 mmol·L^{-1}) for *S. zehnderi* and butyrate (butyric acid sodium salt, 98 %, Sigma-Aldrich, USA) (20 mmol·L^{-1}) for *S. wolfei*, was added and the syntrophic coculture was inoculated (10 %, v/v). The assays with the syntrophic cocultures were carried out in triplicate and were incubated statically, at 37 °C, in the dark. In addition, controls without the inoculation of the cocultures (i.e., containing only the pre-grown hydrogenotrophic culture) were performed, in which the headspace was flushed with H_2/CO_2 (80:20 %; 1.7 × 10^5 Pa) to support the growth of the methanogen. These biotic controls were also used to investigate the effect of materials when added to pre-grown cultures.

Abiotic controls were carried out in duplicate to investigate the interaction of liquid substrates (acetate, 10 mmol·L^{-1}; butyrate, 10 mmol·L^{-1}; oleate, 1 mmol·L^{-1}) with the materials (possible adsorption effects) in the same incubation conditions described for the biotic assays (i.e., 37 °C, in the dark, without agitation). The abiotic tests with H_2/CO_2 were presented in Chapter 3, subsection "3.3.2.Abiotic assays: effects of materials on growth medium parameters and interaction with gaseous substrates", Figure 3.3. Acetate

and butyrate interactions with AC, Mag and Zeo were investigated for 0.5 $g \cdot L^{-1}$ of each material. Oleate was tested with 0.1 $g \cdot L^{-1}$ and 1 $g \cdot L^{-1}$ of AC, and 0.1 $g \cdot L^{-1}$ and 0.5 $g \cdot L^{-1}$ of Mag.

4.2.2. Preparation and characterization of materials

The materials used in the assays (AC, Zeo and Mag) were the same described in Chapter 3, subsection "3.2.1. Conductive and non-conductive materials", and the characterization was presented in Table 3.2 and Table 3.3 (Chapter 3, subsection "3.3.1. Characterization of materials"). The two different batches of AC were used in these assays: AC batch 1 (AC_{b1}) – used in the assays with *M. formicicum* pure cultures and in the assay with the syntrophic coculture *S. zehnderi* with *M. formicicum*; AC batch 2 (AC_{b2}) – used in the other experiments.

4.2.3. Analytical methods

In incubations supplemented with H_2/CO_2, hydrogen consumption and MP were monitored over time as described in Chapter 3, subsection "3.2.3. Analytical methods". In incubations not supplemented with H_2/CO_2, MP was followed over time using a GC Chrompack 9000 (Shimadzu, Kyoto, Japan) with Carbowax 20 M (2 m × 2 mm, 80–120 mesh) column, using nitrogen (30 $mL \cdot min^{-1}$) as the carrier gas. The temperatures of column, injector, and flame ionization detector (FID) were set at 35 °C, 110 °C and 220 °C, respectively.

The measurements of the redox potential (ORP), pH and conductivity of the anaerobic growth media was carried out as explained in Chapter 3, subsection "Analytical methods". In *M. formicicum* pure cultures and *S. zehnderi* with *M. formicicum* syntrophic coculture experiments, pH and conductivity were measured with a bench HI 207 pH meter (HANNA instruments, Ajman, UAE) and a digital conductivity meter CO 301 (VWR, Germany), respectively. In the other experiments, pH and conductivity were evaluated with new devices Consort multi-parameter analyser C1020 and C3010, respectively. In pure cultures experiments, these parameters were measured in three time points: in the beginning of the assay, in the middle of the exponential phase of MP and at the end of the assay. In the other experiments, these parameters were evaluated in two sampling moments: 24 h after the beginning of the assays and at the end of the assays. Samples (1 mL) from liquid phase were also collected with a sterile syringe, centrifuged (10 min, 20 000 g), filtered through 0.22 µm filters and frozen until the moment of volatile fatty acid (VFA) analysis (i.e., formate, acetate and butyrate). VFA analysis was performed by high performance liquid chromatography (HPLC) (Jasco, Tokyo, Japan), using an Agilent Hi-Plex H column (300 mm x 7.7 mm). The oven temperature was maintained at 60 °C and the UV detection was set at

210 nm. The mobile phase (eluent) was sulfuric acid (5 mmol·L^{-1}) with a flow rate of 0.6 mL·min^{-1}. Crotonic acid (98%, Sigma-Aldrich, USA) (0.2 mmol·L^{-1}) was used as internal standard in all samples analysed. Oleate consumption was monitored by GC Varian 3800 equipped with FID. The extraction and quantification were conducted according to the method described elsewhere (Neves et al., 2009), which relies on quantification of free saturated and unsaturated long chain fatty acids (LCFA) from C12 to C18. Samples were prepared and analysed as described by Duarte *et al.* (Duarte et al., 2018).

4.2.4. Scanning electron microscopy

SEM analysis was performed as described in Chapter 3, subsection "3.2.4. Scanning electron microscopy".

4.2.5. Statistical analysis

Statistical analysis was carried out as mentioned in Chapter 3, subsection "3.2.6. Statistical analysis".

4.3. RESULTS

4.3.1. Effect of activated carbon, magnetite, and zeolite on methanogenic cultures

The presence of AC affected the methanogenic activity of all microbial cultures tested, mainly by decreasing the duration of the lag phases preceding MP, and consequently accelerating MP during the first days of incubation (Figure 4.1; Table A. 1, Appendix). The impact on methanogenic activity was different for the different species. For instance, cultures of *M. barkeri* and the coculture of *S. wolfei* and *M. hungatei* were only slightly affected, since the initial methane production rates (IMPR) and exponential methane production rates (EMPR) increased less than 1.8 times relatively to the control (Table 4.1). On the other hand, the IMPR from *M. hungatei* cultures increased 4.5 times, although the EMPR was lower in the assays with AC when compared with the control (Figure 4.1b, Table 4.1). This showed that AC had a high impact on the hydrogenotrophic activity during the first days of incubation, as MP started much earlier (after 0.9 d of incubation, while in the control, methane could only be detected after 1.4 d) (Figure 4.1b; Table A. 1, Appendix). This effect was even bigger with *M. formicicum*. Pure cultures of *M. formicicum* were very sensitive to the presence of AC, with lag phase duration decreasing by approximately 70 % (from more than 4.5 d to approximately 1.3 d) (Figure 4.1a; Table A. 1, Appendix). The IMPR in the presence of AC batch 1 was around 12 times higher in comparison with the control without materials (Table 4.1). In addition, circa 87 % of the H_2/CO_2 could be converted to methane in 5 d,

while in the incubations without AC, the equivalent MP was reached only after 7 d of incubation (Figure 4.1a).

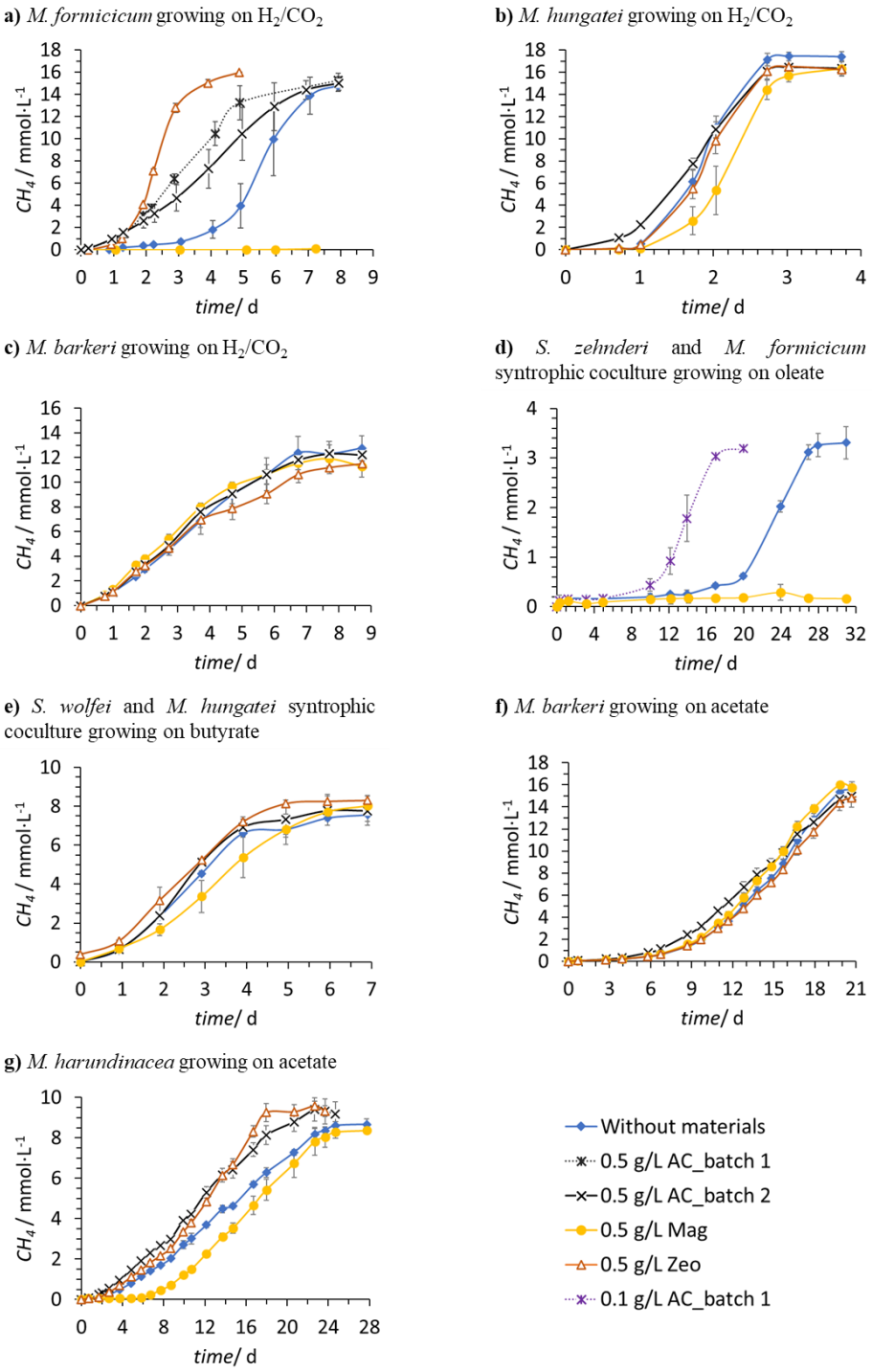

Figure 4.1. Cumulative MP profiles for the following assays with and without materials: a) *M. formicicum*, b) *M. hungatei*, and c) *M. barkeri,* in pure cultures growing on H_2/CO_2; d) *S. zehnderi* and *M. formicicum* in syntrophic coculture growing on oleate; e) *S. wolfei* and *M. hungatei* in syntrophic coculture growing on butyrate; f) *M. barkeri*, and g) *M. harundinacea* in pure cultures growing on acetate. The biotic control condition is represented as "without materials". The results are the mean and standard deviation of triplicate assays.

Table 4.1. Relation between the presence of AC, Mag or Zeo and the number of times the IMPR and EMPR increases, or decreases (> 1 or < 1, respectively), relatively to the control assays without materials

Microorganisms	AC batch 1		AC batch 2		Mag		Zeo	
	IMPR	EMPR	IMPR	EMPR	IMPR	EMPR	IMPR	EMPR
M. formicicum	12.4	0.6	6.8	0.4	#	0.2	19.6	1.4
S. zehnderi with *M. formicicum*	12.0	1.3	-	-	#	#	-	-
M. hungatei	-	-	4.5	0.6	0.2	0.9	0.9	0.9
S. wolfei with *M. hungatei*	-	-	#	1.1	#	0.8	#	1.0
M. barkeri in H_2/CO_2	-	-	#	1.0	#	1.1	#	0.9
M. barkeri in acetate	-	-	1.8	0.8	1.2	1.1	1.0	0.9
M. harundinacea	-	-	1.6	1.2	0.0	1.2	1.3	1.5

#The number of times that IMPR/EMPR was affected relatively to the control could not be determined because there was no growth (in *M. formicicum* pure cultures assays, and in *S. zehnderi* and *M. formicicum* coculture both with Mag) or there was no differences in lag phase duration occurred with or without materials (in *S. wolfei* and *M. hungatei*, and in *M. barkeri* growing in H_2/CO_2 assays) and consequently no initial MP occurred differently among conditions to be significantly compared with the control growing without materials.

The beneficial effects of AC (batch 1) were extended to the syntrophic coculture of *S. zehnderi* and *M.* formicicum (Figure 4.1d). The lag phases were significantly reduced from 18 to 10 d with 0.1 g·L-1 AC (Figure 4.1d; Table A. 1, Appendix). This meant a huge impact in the rate of conversion of oleate to methane. When the coculture incubated without AC started to produce methane (after 18 d of incubation), the coculture in the presence of AC had already converted all the substrate to methane, which could be only attained after 27 d by the coculture incubated without AC (Figure 4.1d). SEM images showed a close interaction between *M. formicicum* cells and AC when growing in pure culture (Figure 3.5i, Chapter 3), and also *S. zehnderi* and *M. formicicum* cells with AC (Figure 4.2b), as cells were attached to the surface of the material. Regarding the assays with the coculture, oleate also adsorbed on the surface of material. When oleate was added to the anaerobic medium without materials (abiotic assays), the medium turned highly turbid (Figure A. 3, Appendix), and adsorption of oleate to the bottle walls was visible (Figure A. 3b, Appendix) due to the poor oleate solubility. In the presence of increasing concentrations of the materials, the turbidity tended to decrease, suggesting adsorption of oleate onto the materials (Figure A. 3, Appendix). This affected the accuracy of oleate quantification in the abiotic assays (Figure A. 3a, Appendix).

a) *S. zehnderi* and *M. formicicum* syntrophic coculture incubated without materials

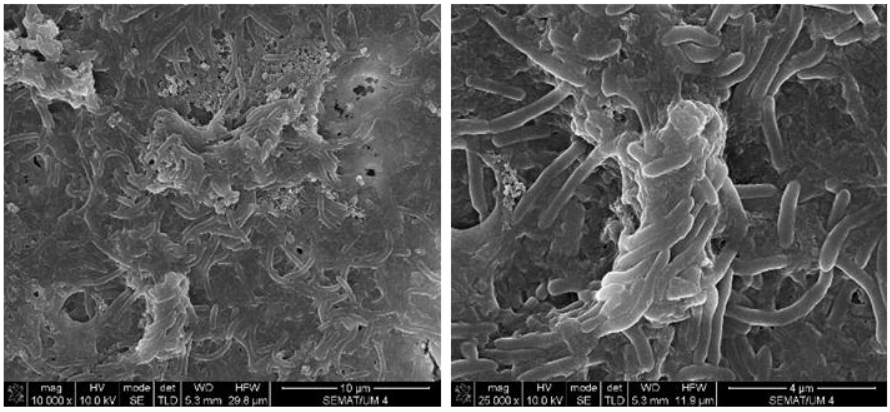

b) *S. zehnderi* and *M. formicicum* syntrophic coculture incubated with AC

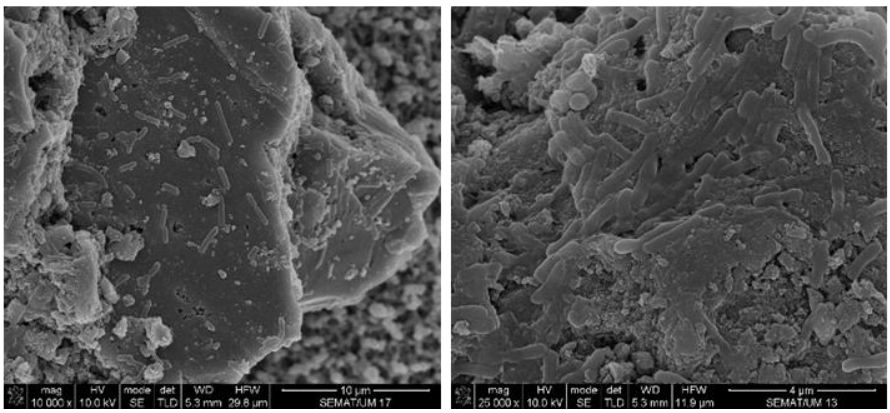

Figure 4.2. SEM images captured during the middle of exponential phase of MP in the assays with the syntrophic coculture *S. zehnderi* and *M. formicicum* a) without materials, and b) in the presence of AC batch 1. Slightly curved rods represent *S. zehnderi* cells, while *M. formicicum* cells are long rods.

Unlike the observations with AC, few *M. formicicum* cells could be observed in contact with Mag (Figure 3.5iv, Chapter 3). Indeed, the effect of this CM on the activity of *M. formicicum*, and *S. zehnderi* and *M. formicicum* cocultures was very adverse (Figure 4.1a, 4.1d). The methanogenic activity of *M. formicicum* was inhibited for 13 d (in pure culture assays), and the overall microbial activity of the coculture was completely inhibited for at least 60 d (Table A. 1, Appendix). Despite the high sensitivity of these microorganisms to Mag, the other species tested, i.e., *M. harundinacea*, *M. barkeri*, *M. hungatei*, and *S. wolfei* with *M. hungatei*, were less affected. The lag phase from *M. hungatei* was higher in the presence of Mag, showing an inhibition during the first days of incubation, but that was rapidly overcome (Figure 4.1b). The same trend was verified for the coculture of *S. wolfei* with *M. hungatei* (Figure 4.1e). None of the materials exerted a significant improvement on the activity of *M. barkeri* (Figure 4.1c, 4.1f). The acetate consumption over time can be observed in Figure A. 4a (Appendix). The lag phase of *M. barkeri* cultures (growing on acetate) was reduced from approximately 9 d (without materials) to around 7 d with

AC (Table A. 1, Appendix), and the acetate consumption was slightly faster in AC condition as well (Figure A. 4a, Appendix). However, these small improvements did not greatly impact the overall efficiency of MP, since the total time of incubation was similar for all conditions (Table A. 1, Appendix). So, although there were slight differences between incubations with and without materials, these differences were not significative (Figure 4.1c, 4.1f). On the other hand, the acetoclastic *M. harundinacea* was affected by all materials. Zeo and AC increased its methanogenic activity, with total acetate conversion to methane in 23 d, contrasting with the 25 d necessary for the culture growing without materials (Figure 4.1g; Table A. 1, Appendix). Mag affected the activity of *M. harundinacea* negatively, by increasing the lag phase, but it did not affect the total time necessary to convert acetate to methane, when compared to the control assay (Figure 4.1g). The consumption of acetate over time is shown in Figure A. 4b (Appendix). Zeo affected slightly the microorganisms (Figure 4.1b, 4.1c, 4.1e, 4.1f), with exception of *M. formicicum,* which was significantly stimulated by Zeo ($p < 0.05$ level). The presence of Zeo caused a reduction of the lag phase of approximately 67 % (from 4.5 to 1.5 d, Figure 4.1a; Table A. 1, Appendix), and the IMPR increased 19.6 times (Table 4.1).

No differences on hydrogen, acetate and butyrate quantification were detected among abiotic assays performed with and without materials, suggesting that no hydrogen, acetate or butyrate adsorption occurred on the surface of materials (Figure 3.3, Chapter 3; Figure A. 5, Figure A. 6, Appendix).

Furthermore, no stimulatory effect was observed when the materials were added to pre-grown cultures (Figure 4.3).

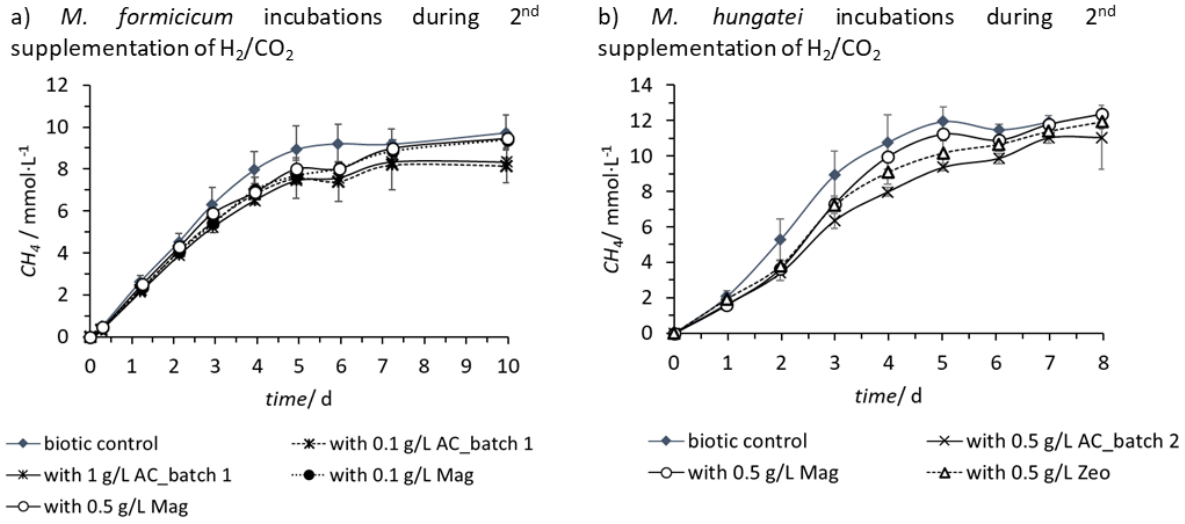

Figure 4.3. Cumulative MP in pre-grown pure cultures of a) *M. formicicum* and b) *M. hungatei*. The materials were only added after the cultures reached the exponential phase followed by a second supplementation with substrate (H_2/CO_2). The results are the mean and standard deviation of triplicate assays.

4.3.2. Effect of materials on ORP, pH and conductivity of the growth medium

The presence of materials in the growth medium affected mainly the values of ORP, either in biotic (Table A. **2**, Appendix) or abiotic assays (Table 3.4, Chapter 3; Table A. 3, Table A. 4, Table A. 5, Appendix). In general, the presence of AC contributed to decrease the ORP values of the growth medium of pure cultures (e.g., in *M. formicicum* assays, ORP decreased from (-296 ± 24) mV in the control to (-365 ± 9) mV at the beginning of the incubations) and syntrophic cocultures incubations (e.g., in assays with syntrophic coculture *S. wolfei* with *M. hungatei*, ORP changed from (-308 ± 7) mV in the control to (-338 ± 6) mV). On the other hand, Mag had the opposite effect by increasing ORP values (e.g., in syntrophic coculture *S. zehnderi* with *M. formicicum* assays, ORP increased from (-264 ± 14) mV in the control to (-176 ± 20) mV) (Table A. 2, Appendix). Similarly to AC, Zeo also decreased the ORP values of the growth medium (e.g., in *M. formicicum* assays, ORP decreased from (-296 ± 24) mV in the control to (-324 ± 4) mV at the beginning of the incubations; Table A. 2, Appendix), but generally less than AC. The pH values (between 7.0 and 7.3 at the beginning of all incubations) or conductivity values (around 4.0 $mS \cdot cm^{-1}$ for syntrophic coculture incubations of *S. zehnderi* with *M. formicicum*, and between 6 $mS \cdot cm^{-1}$ and 8 $mS \cdot cm^{-1}$ for the other incubations, at the beginning of the assays) were not considerably affected by the presence of materials (Table A. 2, Appendix).

The same trend was observed in the results of abiotic incubations with H_2/CO_2 (Table 3.4 in Chapter 3), acetate (Table A. 3, Appendix), butyrate (Table A. 4, Appendix), and oleate (Table A. 5, Appendix). In the presence of AC, ORP values were generally lower than the values obtained in abiotic assays without materials. These results were more evident in abiotic assays with AC and H_2/CO_2 (e.g., (-263 ± 11) mV in abiotic assay vs (-390 ± 10) mV with 5 $g \cdot L^{-1}$ of AC) (Table 3.4 in Chapter 3), or butyrate (e.g., (-343 ± 1) mV in abiotic assay vs (-378 ± 4) mV with 0.5 $g \cdot L^{-1}$ of AC) (Table A. 4, Appendix), mostly at the middle of incubation time. In addition, variations in the values of this parameter can also be observed over incubation time, as they were different between the beginning and the end of the assays (e.g., ORP values of abiotic assays with H_2/CO_2 were (-179 ± 1) mV at the beginning of incubation, (-263 ± 11) mV in the middle, and (-351 ± 0) mV at the end, Table 3.4 in Chapter 3). On the other hand, the presence of Mag increased the ORP values over the incubation time, being ORP values higher than the ones observed in the abiotic assay without materials (e.g., (-263 ± 11) mV in the abiotic assay vs (-210 ± 33) mV with 5 $g \cdot L^{-1}$ of Mag in the middle of time of the assay with H_2/CO_2, Table 3.4 in Chapter 3). Another observation was that the concentration of material also affected the ORP values. For instance, higher concentrations of AC contributed to decrease the ORP values in abiotic assays with H_2/CO_2 (for instance, (-263 ± 11) mV in abiotic assay vs (-305 ± 1) mV with 0.1 $g \cdot L^{-1}$ of AC vs (-390 ± 10) mV with 5 $g \cdot L^{-1}$ of

AC, in the middle of the assay), and higher concentrations of Mag increased the ORP values (for instance, (-263 ± 11) mV in abiotic assay vs (-308 ± 2) mV with 0.1 g·L^{-1} of Mag vs (-210 ± 33) mV with 5 g·L^{-1} of Mag, in the middle of the assay) (Table 3.4 in Chapter 3). In the case of abiotic assays with Zeo, in general, only a slight decrease of ORP values occurred, for instance, from (-285 ± 5) mV (abiotic assay) to (-291 ± 4) mV (with Zeo), at the beginning of incubations with H_2/CO_2 (Table 3.4 in Chapter 3). For the rest of the parameters (pH and conductivity), only slightly changes occurred among conditions, and these parameters were rather stable around pH 7.2 and 7.4, and conductivity around 4 mS·cm^{-1} for the abiotic assays with butyrate and oleate, and between 6 mS·cm^{-1} and 8 mS·cm^{-1} for the abiotic assays with H_2/CO_2, acetate, and butyrate (with and without Zeo).

4.4. Discussion

Motivated by the fact that some CM affect the activity of microbial communities and methanogenic microorganisms, this study aimed to understand how materials with different characteristics, and specifically different conductivities, affect a number of microorganisms typically found in anaerobic digesters and in anaerobic natural environments. The conductivity of the materials is usually linked to their function in serving as mediators for IET (Kato et al., 2012; Mostafa et al., 2020; Song et al., 2019; Wu et al., 2020; W. Zhang et al., 2018), but IET does not occur in pure cultures, so this cannot be the main explanation for the improvement of activity in all situations. In addition, besides the possible higher conductivity of AC in comparison with Zeo, the results of this study showed that Zeo can be even better than AC on accelerating MP, as it was observed for the assays of *M. formicicum* (Figure 4.1a). This is the first study showing the potential of Zeo to directly stimulate pure cultures of methanogens and syntrophic cocultures. However, previous studies showed that zeolites did not impact the biogas production of complex methanogenic communities (König et al., 2022). Apart from these studies, the potential of Zeo to improve AD processes has been explored mainly as an adsorbent for ammonium and heavy metals removal due to its unique property of ion exchange capacity, or used to adsorb organic micro pollutants (Cardona et al., 2021; Milán et al., 2010; Szerement et al., 2021). In other studies, great improvements towards MP with materials with different conductivities (e.g., carbon cloth vs GAC (Wu et al., 2020); Mag vs hematite (J. H. Park et al., 2018)) were also observed. For instance, the effect of Mag (0.038 mS·cm^{-1}) and GAC (0.168 mS·cm^{-1}) on microbial activity showed that Mag promoted a better methanogenic performance than GAC even with a lower conductivity value (Lee et al., 2020). In addition, biochars with similar values of conductivities (but originated from different feedstocks) did not have the same impact

on MPR by enrichment cultures of methanogenic microbial communities (Yuan et al., 2018). Thus, there is no correlation between conductivity and enhancement of microbial activity.

Other characteristics of the materials may also contribute to influence the microbial activity, such as the particle size, the adsorption capacity of the material, the pH_{pzc} values, the chemical composition, and the modifications that materials can exert in the growth medium, for instance by altering the ORP. Larger materials like AC (Bueno-López et al., 2020) and Zeo (Emami Moghaddam et al., 2018; Montalvo et al., 2020, 2012; Paritosh et al., 2020) may provide a support for cells growth and a closer interaction between different microorganisms (Paritosh et al., 2020; Wu et al., 2020). The attachment of *M. formicicum* and *S. zehnderi* onto AC surface was observed by SEM analysis highlighting the importance of AC as a support material (Figure 3.5i in Chapter 3, Figure 4.2b). The adsorption capacity of materials can also be important since it might bring microorganisms closer to their substrates. In the assays with the syntrophic coculture *S. zehnderi* and *M. formicicum* (Figure 4.1d), this phenomenon could have been especially relevant, with oleate becoming more bioavailable for the bacteria. Indeed, our results showed that oleate adsorption occurred during abiotic experiments (Figure A. 3a, Appendix), but the same was not observed for the other substrates (Figure 3.3, Chapter 3; Figure A. 5, Figure A. 6, Appendix). The pH_{pzc} values may also be important for the observations, since materials with pH_{pzc} values higher than the pH of the medium growth, which is the case of Zeo used in this study, tend to be positively charged (A. R. Silva et al., 2021a) and therefore attract the microbial cells (which are negatively charged (Lee et al., 2020; A. R. Silva et al., 2021a)). On the contrary, Mag had a pH_{pzc} lower than the pH of the growth medium, so cell repulsion is expected. Indeed, SEM images showed microbial cells growing on AC (neutral character or slightly positive charged in growth medium), but not on the Mag particles (Figure 3.5iv). Different elements present in the composition of different materials (Table 3.2 and Table 3.3, Chapter 3) might also influence the microbial activities, since some of them are important nutrients for the microorganisms. However, the growth medium used in our experiments was developed to guarantee the nutritional requirements and the important cofactors for methanogenic cultures. Nevertheless, one cannot rule out that extra elements provided by the materials (e.g., iron (Fe), sulfur (S), nitrogen (N), silicon (Si)) may be beneficial for cell growth (Jurkić et al., 2013; Lamers et al., 2012; Paritosh et al., 2020), however, this was not investigated in this work. On the other hand, although Fe could be used as a micronutrient by methanogens (Xiao et al., 2020), it is also known that Fe(III) (present in the composition of Mag (H. Wang et al., 2020)) can inhibit the hydrogenotrophic activity (Van Bodegom et al., 2004), as it was also observed in the assays with *M. formicicum* (Figure 4.1a). Additionally, the ORP of the growth medium is one of the physicochemical characteristics that have been shown to change in the presence of materials.

This was verified before by Salvador *et al.* (2017) with CNT (which caused a decrease on the values of ORP of the growth medium, favoring the methanogenic activity), and also in this work. It was verified that the ORP decreased with AC (which generally increased the methanogenic activity) but increased with Mag (which improved the activity of some cultures and inhibited others), and almost did not change with Zeo (which caused an increase of around 20 times on the activity of *M. formicicum*, Table 4.1) (Figure 4.1; Table A. 2, Appendix). Thus, ORP variations per se cannot explain the improvement of the microbial activity.

It seems clear that the microbial activity is not only influenced by the physicochemical properties of materials but is also dependent on the identity of the microorganisms. In this and in other studies, it is evident that the effect of materials is different depending on the microbial species. For instance, *M. formicicum* and *M. hungatei* were stimulated by AC and CNT (Salvador et al., 2017), but other hydrogenotrophic microorganisms were inhibited by CNT (e.g., *M. maripaludis* (W. Zhang et al., 2018)). The differences are also evident when these methanogens are cultivated in syntrophic cocultures. For instance, CNT stimulated the metabolism of *S. wolfei* with *M. maripaludis*, but the syntrophic coculture *S. wolfei* with *M. hungatei* was found to be only slightly stimulated by CNT (Salvador et al., 2017) and barely affected by AC (Figure 4.1e, Table 4.1), showing that depending on the syntrophic partner and type of material, the rate of butyrate conversion by cocultures with *S. wolfei* is different. On the other hand, AC stimulated the activity of the syntrophic coculture *S. zehnderi* with *M. formicicum*, as oleate degradation could be enhanced 12 times (Table 4.1) and lag phase was reduced from 18 d to 10 d (Figure 4.1d; Table A. 1, Appendix) in the presence of the material. These findings are extremely relevant from an applied point of view since anaerobic degradation of LCFA is a slow process that relies on the activity of syntrophic bacteria and hydrogenotrophs, such as *S. zehnderi* and *M. formicicum*. The fact that the coculture activity is significantly ($p < 0.05$ level) enhanced suggests that application of AC in AD is promising to boost MPR from LCFA especially for starting up phases of operation.

By the analysis of the results obtained in this and previous studies (Salvador et al., 2017; W. Zhang et al., 2018), it seems that generally, the materials have greater impact in slow growing cultures, for instance *M. formicicum* (Figure 4.1a; Table A. 1, Appendix) when compared to the other methanogens (Figure 4.1b and 4.1c in the present study, and Figure 7 in ref. (W. Zhang et al., 2018)) which grow faster. The same trend is verified with *S. zehnderi* which grows much slower in oleate than, for example, *S. wolfei* in butyrate (Figure 4.1d and 4.1e; Table A. 1, Appendix; Figure 1d in ref. (Salvador et al., 2017); Figure 6 in ref. (W. Zhang et al., 2018)). In addition, no improvement on methane production could be detected when the materials were added to pre-grown cultures (Figure 4.3). Also, most active inocula (as was the

case of cultures of *M. hungatei* and *M. barkeri*, as can be seen by the high activity of the cultures when growing without material (Figure 4.1b and 4.1c)), are generally less affected by the presence of materials. These observations indicate that the major impact of the materials is the lag phase reduction, i.e., accelerating the start-up of biodegradation and MP, which is particularly evident in less active slow growing microbial communities.

On the other hand, the enhancement of microbial activity in the presence of CM is usually attributed to the change in IET. In our study, we used *S. wolfei* and *S. zehnderi*, that are known to participate in interspecies hydrogen transfer (IHT), and are not reported to be capable of direct interspecies electron transfer (DIET) (Jessica R. Sieber et al., 2010; Sousa et al., 2007), so the hypothesis that the materials mediate IET doesn't seem plausible. The bacterium *S. wolfei* is a syntrophic bacteria which apparently lacks the genomic machinery required for extracellular electron transfer (Li et al., 2015). Indeed, traditional syntrophic fatty-acid degrading bacteria are probably not capable of DIET because they lack the genes for outer membrane *c*-type cytochromes and for pil*A*, which are reported as necessary for DIET (Sieber et al., 2014; Summers et al., 2010). Yet, the application of CM in AD has led to the enrichment of species assigned to *Syntrophomonas* and for that reason, the ability of this genus to transfer electrons via CM has been speculated (W. Zhang et al., 2018; Zhao et al., 2018). Many genera, including *Syntrophomonas,* contain genes coding for e-pili (Zhao et al., 2020), which means that the possibility of DIET by these microorganisms cannot be completely excluded. However, homologues for the *G. sulfurreducens* e-pili gene (Jessica R. Sieber et al., 2010), or for *c*-type cytochromes were not found in the genome of *S. wolfei* (by searching the UniProt database (data not shown)). Nevertheless, there is still much to discover about the genetic machinery and the microorganisms that might be able of donating and accepting electrons via DIET or via mediation with CM. For instance, the typical syntrophic bacterium *Syntrophus aciditrophicus*, known to perform IHT and interspecies formate transfer (IFT), was recently found to produce e-pili and to grow via DIET (Walker et al., 2020). This species was previously thought as unlikely to participate in DIET because it lacked a gene homologous to the pilin monomer that assembles e-pili in *Geobacter* (Walker et al., 2020). Thus, it cannot be ruled out that other typical syntrophic fatty-acids degrading bacteria, known to grow via IHT/IFT, might have the capacity to exchange electrons directly with other species with or without the mediation of CM (Walker et al., 2020; Yin et al., 2020; Zhao et al., 2020). Different electrical contacts, as well as the specific proteins that function as electrical contacts for DIET, have evolved and are different for different species (Zhao et al., 2020). Recognizing this, it is possible that the currently available metabolic model for *Geobacter* spp. may not be the same for other microbes that may be able to participate in DIET (Zhao et al., 2020). On the other

hand, studies with gene deletions showed that mutant strains lacking e-pili or key outer-surface *c*-type cytochromes were inhibited and incapable of DIET, but CM could mediate the extracellular electron transfer (Zhao et al., 2020). So, it could be also hypothesized that bacteria and methanogens that usually performed IHT/IFT, in the presence of CM could also use the materials to transfer electrons as a simple way of establishing the electrical connection (Zhao et al., 2020). Yet, it does not explain the impact of materials on the activity of pure cultures like hydrogenotrophs. Hydrogenotrophic methanogens are not known to participate in DIET, with the exception of *Methanobacterium* sp. strain YSL that was reported as being able to participate in DIET with *G. metallireducens* and in IET via GAC, but only growing in formate (Zheng et al., 2020). It was mentioned that strains of *Methanobacterium* growing with hydrogen cannot grow via DIET in coculture with *G. metallireducens* because they may have lost the features needed for DIET with the continuous transfers over the years (Zheng et al., 2020). Zheng *et al.* (2020) reinforced the idea that GAC would not be expected to improve IHT (Zheng et al., 2020), but other studies have reported the improvement of hydrogenotrophic activity in the presence of CNT (Salvador et al., 2017). In this work, the *M. formicicum* strain DSM1535 has been continuously transferred with hydrogen as electron donor and the results clearly show that its hydrogenotrophic activity was significantly stimulated both with AC and Zeo. But the reason behind this enhancement remains unclear.

4.5. Conclusions

In summary, the results obtained in our study highlight the different impacts of distinct materials, like AC, Zeo, and Mag, on different methanogens and syntrophic cocultures. The research developed suggests that different materials may improve or inhibit methanogenic activity, which seemed to be dependent on the microbial species, rather than on the type of metabolism, i.e., acetoclastic or hydrogenotrophic. In addition, this work clearly showed that the activity of several species of methanogens, catalyzing the last step of AD, can be largely improved in the presence of materials. The presence of materials mainly changed the values of ORP of the growth medium, but no correlation between ORP variations and the impact on MP was observed. The physicochemical properties of materials may have a role on their effect towards MP, but further research is still necessary to clarify which characteristics of materials are more important to affect the microbial activity, and to reveal the mechanisms behind the enhancement of MP in the presence of different materials.

CHAPTER 5

5. THE ACTIVITY OF MICROBIAL COMMUNITIES DICTATES THE EFFECT OF ACTIVATED CARBON, MAGNETITE, AND ZEOLITE, ON METHANE PRODUCTION

ABSTRACT

Conductive materials (CM) affect the efficiency of methanogenic processes by accelerating methane production (MP). Factors such as the conductivity of the materials, the presence of electroactive microorganisms that might exchange electrons directly via CM, the role as a support material for microbial growth, among others, have been pointed out as possible explanations for MP improvement. In this work, we incubated anaerobic communities with different microbial activities, in batch and in continuous bioreactors, treating butyrate and other volatile fatty acids, and ethanol. Incubations were performed with and without activated carbon (AC), magnetite (Mag), and zeolite (Zeo), which present different physicochemical characteristics. The results obtained showed that the application of those materials to active microbial communities did not improve MP, but highly affected the performance of MP by less active cultures. For example, the production of methane by a slow growing culture was enhanced by AC, once the presence of this material reduced the lag phase preceding MP in approximately 40 % when comparing with the slow growing culture without materials, allowing methane to be produced at an early stage of incubation. Extensive revision of the literature supports this conclusion. Based on this, from an applied point of view, the cost benefit analysis of applying materials should take into consideration the activity of sludge used in the anaerobic treatment.

5.1. INTRODUCTION

There are several studies reporting the effect of granular activated carbon (GAC), carbon nanotubes, biochar, magnetite (Mag), or carbon cloth on MP, either from complex waste (e.g., food waste) or from simpler substrates (such as acetate and H_2/CO_2) (Martins et al., 2018). This is a research topic that has been extensively studied and is very well reviewed (Castilho et al., 2022; Chen et al., 2022; H. Liu et al., 2021; M. Liu et al., 2021; Martins et al., 2018; Roopnarain et al., 2021). The main observations are that conductive materials (CM) accelerate waste conversion to methane, although its effect is not always the same. In the majority of the studies, the impact relies in the decrease of lag phases preceding methane production (MP), in others CM affect mostly the methane production rates (MPR), or the methane/biogas yields (Chen et al., 2022). For example, the presence of GAC allowed the degradation of dog food by anaerobic sludge with a lag phase of approximately 4 d, while in the condition without GAC no significant MP occurred during the time of incubation (170 d), in batch conditions (Dang et al., 2017). In another study, the presence of GAC barely affected the lag phase duration, but for example, the MPR increased up to 1.5 times, also in batch conditions, improving the sludge decomposition (Yang et al., 2017). In semi-continuous bioreactors the addition of GAC increased the methane yield by 130 % (Song et al., 2019), and in batch reactors approximately by 30 % (J.-H. Park et al., 2018). In addition, the substrate concentration seemed to influence the GAC effect. For example, depending on propionate, butyrate and acetate concentrations, GAC could either increase significantly the MPR (up to 11 times) or having no impact at all (Xu et al., 2018).

Another factor that might influence the effect of CM on anaerobic digestion (AD) process is the microbial communities' composition and their methanogenic activities. For instance, no positive impact of materials, like Mag or zeolite (Zeo), was found when an high active inoculum was used during anaerobic conversions to methane (Fu et al., 2019, 2018; Li et al., 2022; Milán et al., 2001; Xu et al., 2018). On the other hand, lag phases preceding MP were significantly reduced when using less active inocula, up to 97.6 % (Amelia-Elena et al., 2018; Dang et al., 2017; Lee et al., 2020; J.-H. Park et al., 2018; Ryue et al., 2019; Tan et al., 2021; Tan and Lens, 2021; Xu et al., 2018). For example, the presence of Mag decrease the lag phase from 72 d (in the control) to 27 d, reducing the time of incubation needed for butyrate degradation by a lake sediment from 120 d (in the control) to 60 d (in the presence of Mag) (Zhang and Lu, 2016). These results suggest that not only the CM, and the substrate, dictate the results obtained, but also the microbial community. To which extent the activity of microbial communities influences the effects of CM on waste conversion to methane has not yet been investigated.

In the study presented in this chapter, it was investigated the effect of different (nano)materials, namely activated carbon (AC), Mag and Zeo on volatile fatty acids (VFA) conversion to methane by anaerobic sludge with different activities, in batch and in continuous bioreactors, to evaluate the importance of the initial microbial activity on MP with and without materials. The effect of microbial activity in other studies involving the application of CM, was also extensively reviewed and discussed.

5.2. MATERIALS AND METHODS

5.2.1. Activated carbon, magnetite and zeolite

The commercial materials used in these assays are well described in the section "3.2. Materials and Methods" of Chapter 3 (subsection "3.2.1. Conductive and non-conductive materials"), and their characterization is present in Table 3.2 and Table 3.3 of the same chapter. These materials were used to perform all the anaerobic assays, both in batch and in continuous bioreactors. Regarding AC, the AC_{b2} (Table 3.3, chapter 3) was used in batch assays, and the AC_{b3} (Table 3.3, chapter 3) was used in the continuous bioreactors, due to the availability of each of these materials at the time of the respective test.

5.2.2. Incubation of anaerobic sludge with butyrate and materials

Two different batch experiments were performed to study the effect of the materials on the activity of an anaerobic sludge collected from a brewery wastewater treatment plant (Super Bock, Porto, Portugal). In the first batch experiment, the effect of AC and Mag was evaluated, and the incubation bottles were designated by B-AC and B-Mag, respectively. Incubations without addition of materials were conducted as well and designated by B-without-AC-Mag (Table 5.1). The effect of Zeo was tested in the second batch experiment (incubation bottles were designated by B-Zeo), which was performed with the same inoculum sludge but staggered in time (resulting in a different microbial activity). Similarly, incubations without Zeo were performed for comparative purposes and designated by B-without-Zeo. All assays were carried out in duplicate.

Table 5.1. Summary of the butyrate-degrading enrichment cultures used in batch incubations and the designation adopted

Designation of butyrate-degrading enrichment cultures	Cultures enriched with the following material	Number of incubations under the previous conditions before the experiment	Butyrate conversion to methane
More active cultures			
B-without-AC-Mag-1	Without material	0	Complete
B-without-AC-Mag-2	Without material	1	Complete
MoreAct-B-without-AC-Mag-3	Without material	9	Complete
B-AC-1	AC	0	Complete
B-AC-2	AC	1	Complete
MoreAct-B-AC-3	AC	9	Incomplete
B-Mag-1	Mag	0	Complete
B-Mag-2	Mag	1	Complete
MoreAct-B-Mag-3	Mag	8	Incomplete
B-without-Zeo-1	Without material	0	Complete
B-without-Zeo-2	Without material	1	Complete
B-Zeo-1	Zeo	0	Complete
B-Zeo-2	Zeo	1	Complete
MoreAct-B-Zeo-3	Zeo	6	Complete
Less active cultures			
LessAct-B-without-AC-Mag-1a	Without material	2	Complete
LessAct-B-without-AC-Mag-2a	Without material	3	Complete
LessAct-B-without-AC-Mag-1b	Without material	2	Complete
LessAct-B-without-AC-Mag-2b	Without material	3	Complete
LessAct-B-AC-1a	AC	2	Complete
LessAct-B-AC-2a	AC	3	Complete
LessAct-B-AC-1b	AC	2	Complete
LessAct-B-AC-2b	AC	3	Complete
LessAct-B-Mag-1a	Mag	2	Complete
LessAct-B-Mag-2a	Mag	3	Complete
LessAct-B-Mag-1b	Mag	2	Complete
LessAct-B-Mag-2b	Mag	3	Complete
LessAct-B-without-Zeo-1b	Without materials	4	Complete
LessAct-B-Zeo-1a	Zeo	4	Complete

* The anaerobic sludge used in the first incubation is represented as B-without-AC-Mag, B-AC, B-Mag, B-without-Zeo and B-Zeo. During successive transfers, cultures presented less activity (LessAct) or more activity (MoreAct) as they were becoming less or more adapted to each condition, respectively. The enrichments started with two bottles per condition (bottle **a**; bottle **b**) which were considered independent lines, constituting two enrichment lines per condition (aiming to select the most adapted culture for each condition, for further studies).

The sludge used as inoculum (0.083 g biomass per g volatile solids (VS), w/w, Table 5.2) was not previously adapted to butyrate degradation. The specific methanogenic activity (SMA) in acetate and hydrogen was evaluated through the pressure transducer technique as described elsewhere (Alves et al., 2001; Colleran et al., 1992). Before starting the incubations, the anaerobic granular sludge was incubated overnight (statically, at 37 °C) with sodium bicarbonate (3 $g \cdot L^{-1}$; 99.5 – 100.5 %, Sigma-Aldrich, USA) buffered medium (pH 7) containing resazurine (0.001 $g \cdot L^{-1}$; Sigma-Aldrich, USA), under an atmosphere of N_2/CO_2 (80:20 % v/v, (1.1×10^5) Pa), to allow the consumption of the residual substrate. Then, the

sludge was drained and disrupted to allow a higher contact between the microorganisms and the materials. The sludge (3 $g \cdot L^{-1}$ of VS) was distributed into serum bottles of 120 mL (50 mL of working volume) containing saline bicarbonate-buffered mineral salt medium (Stams et al., 1993), supplemented with a cocktail of vitamins and sodium sulfide (0.8 $mmol \cdot L^{-1}$; $Na_2S \cdot 9H_2O$, > 98 %, Acros Organics, Fisher Scientific, USA) as reducing agent. The materials, i.e., AC, Mag and Zeo, were added at a concentration of 0.5 $g \cdot L^{-1}$. The bottles were sealed with rubber stoppers and aluminum caps, and the headspace was flushed with N_2/CO_2 (80:20 % v/v; (1.7×10^5) Pa), to maintain the anaerobic conditions. Butyrate (butyric acid sodium salt, 98.0 %, Sigma-Aldrich, USA) was used as the sole carbon and energy source at a final concentration of 10 $mmol \cdot L^{-1}$. The anaerobic medium and the butyrate stock solution were sterilized by autoclaving, whereas vitamins solution and sodium sulfide were filter sterilized. The incubations were performed statically, at 37 °C, and protected from light.

5.2.3. Development of butyrate-degrading enrichment cultures

Enrichment cultures degrading butyrate were developed with and without AC, Mag or Zeo. The inoculum was the anaerobic sludge described in the previous section, i.e., it started with the incubations B-without-AC-Mag-1, B-AC-1, B-Mag-1, B-without-Zeo-1 and B-Zeo-1 (Table 5.1). Parallel enrichment lines (meaning two bottles, a and b, per condition) were developed, i.e., two lines for the enrichment with AC (B-AC-1a and B-AC-1b), for the enrichment with Mag (B-Mag-1a and B-Mag-1b), and for the enrichment without AC or Mag (B-without-AC-Mag-1a and B-without-AC-Mag-1b), and also for the enrichment with Zeo (B-Zeo-1a and B-Zeo-1b), and for the enrichment without Zeo (B-without-Zeo-1a and B-without-Zeo-1b). Methane production from butyrate was followed over time. Once butyrate degradation was nearly complete, cultures were successively transferred (10 % v/v) to fresh medium containing butyrate and at the same conditions of the original culture (i.e., enrichment cultures developed with AC were again incubated with AC, cultures developed without materials were again incubated without materials, and so on). For instance, the two bottles of B-AC-1 (in Table 5.1 are not represented as B-AC-1a and B-AC-1b, because the incubations started with the same anaerobic sludge and the results of the two bottles for MP were presented by the mean and standard deviation, being considered duplicates) were transferred to new bottles originating the cultures B-AC-2 (B-AC-2a and B-AC-2b, results of MP also considered duplicates at this point), and then, the next transfer would correspond to the cultures LessAct-B-AC-1a and LessAct-B-AC-1b (which became less active with the increase of the number of transfers, and from this point each bottle evolved differently and they were not considered duplicates anymore, Table 5.1), and so on, until obtain at least one enrichment culture line well-adapted in butyrate degradation in the presence of AC.

So, this procedure aimed to enrich microbial communities specialized in complete butyrate conversion to methane, according to the different conditions of the assays.

In order to enrich for cultures specialized on the syntrophic conversion of butyrate to methane and acetate, i.e., butyrate degradation coupled to hydrogen scavenging by hydrogenotrophic methanogens, different enrichment series were set up, under the same conditions described above (only for the conditions of the first batch experiment), with the difference that the cultures were transferred once the total methane produced exclusively from the hydrogenotrophic pathway was reached (approximately 5 mmol·L^{-1}). The inocula for these enrichment series were the enrichment cultures with AC and Mag involved in the complete conversion of butyrate to methane after 3 transfers, and after 4 transfers in the case of the condition without materials. In Table 5.1, these cultures are classified as incomplete for butyrate conversion to methane. In the cultures MoreAct-B-AC-3 and MoreAct-B-Mag-3, the confirmation that MP occurred via hydrogenotrophic pathway was obtained by the detection of acetate accumulation in the stoichiometric amounts expected from butyrate degradation (i.e., 10 mmol·L^{-1} of butyrate degradation would yield 20 mmol·L^{-1} of hydrogen and 20 mmol·L^{-1} of acetate, and then 20 mmol·L^{-1} of hydrogen would yield 5 mmol·L^{-1} of methane (Sousa et al., 2007)) (Table A. 6, Appendix).

Table 5.2. Summary of the values of VS for each sludge used as inoculum (Inoc.) in each type of incubation (in $g_{VS}·g_{biomass}^{-1}$ and $g_{VS}·L^{-1}$) and values of SMA in H_2/CO_2 (80/20, v/v) and acetate (30 mmol·L^{-1}). The pre-treatment applied to the sludge was also listed

Type of incubation	**Inoc.**	**VS/** (g·g^{-1})	**VS/** (g·L^{-1})	**SMA** (H_2/CO_2)/ $mL_{CH4@STP}·g_{VS}^{-1}·d^{-1}$	**SMA** (acetate)/ $mL_{CH4@STP}·g_{VS}^{-1}·d^{-1}$	**SMA** (acetate) */ gCH_4-COD·$gVSS^{-1}·d^{-1}$	**Pre-treatment**	**Notes**
Batch assays	AGS	0.083	3	738 ± 27 (in 1.25 d of incubation)	90 ± 1 (in 3.33 d of incubation)	~ 0.26	Sludge was incubated overnight for residual substrate consumption before starting the assays	Sludge was disrupted previously for batch assays
EGSB	AGS	0.108	15	662 ± 35 (in 1.25 d of incubation)	95 ± 8 (in 3.00 d of incubation)	~ 0.27	Sludge was previous acclimatized with 30 mmol·L^{-1} of ethanol	Sludge was not disrupted

* Calculated using the values of SMA in $mL_{CH4@STP}·g_{VS}^{-1}·d^{-1}$ and considering 1 gCOD = 350 mL CH_4.
AGS - Anaerobic granular sludge; VSS – Volatile suspended solids.

5.2.4. Incubation of active AC-, Mag- and Zeo- enrichment cultures in different conditions

The developed butyrate-degrading enrichment cultures were incubated with different materials, and in their absence, to evaluate whether the change of condition, would result in a beneficial or adverse effect on the activity of the original culture.

For that purpose, the most active enrichment line cultures obtained for each of the conditions were selected, i.e., butyrate enrichment cultures MoreAct-B-without-AC-Mag-3 (developed without materials, with complete butyrate conversion to methane), MoreAct-B-Zeo-3 (developed with Zeo, with complete butyrate conversion to methane), MoreAct-B-AC-3 (developed with AC, with butyrate conversion to methane and acetate), MoreAct-B-Mag-3 (developed with Mag, with butyrate conversion to methane and acetate) (Table 5.1). All assays were performed in triplicate. The culture without previous contact with materials (MoreAct-B-without-AC-Mag-3) was incubated separately in the following conditions: without materials, with AC, AC impregnated with 2 % of iron (AC@2%Fe), Mag, a mixture of AC and Mag, and Zeo (Figure 5.1a). The concentration of materials tested was 0.5 $g \cdot L^{-1}$ and in the mixture of AC and Mag was used 0.5 $g \cdot L^{-1}$ of each material. The material-adapted enrichment cultures were incubated without the material, and with the same material they were adapted to, i.e., MoreAct-B-Zeo-3 was incubated with and without Zeo (Figure 5.1b), MoreAct-B-AC-3, with and without AC (Figure 5.1c), MoreAct-B-Mag-3, with and without Mag (Figure 5.1d).

Butyrate consumption and acetate production were followed during the incubation time by high performance liquid chromatography (HPLC), while MP was measured by gas chromatography (GC). Conductivity, redox potential (ORP) and pH of the growth medium were measured at the beginning and at the end of the incubations.

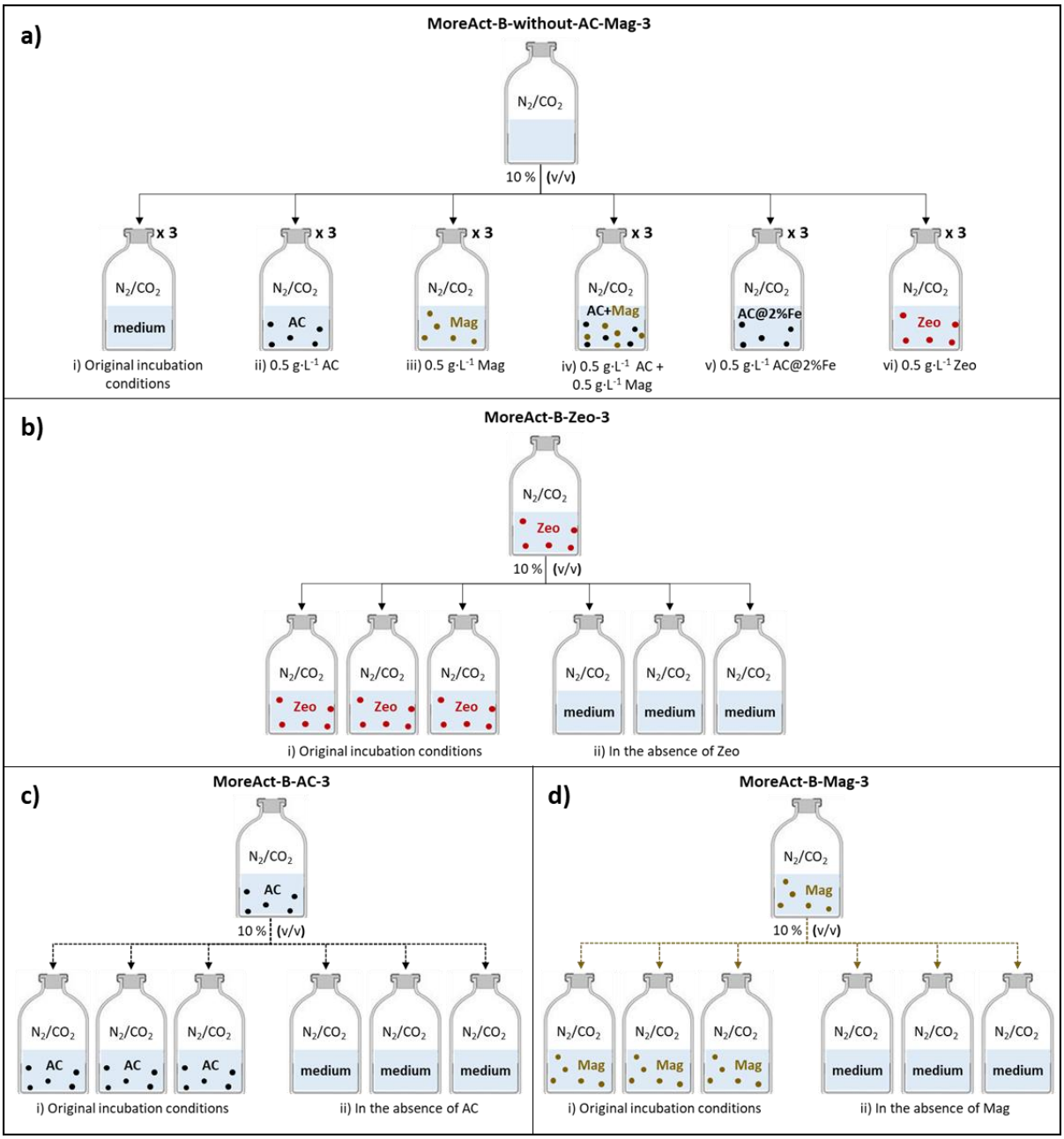

Figure 5.1. Schematic representation of the assays carried out with the most well-adapted and active cultures: a) MoreAct-B-without-AC-Mag-3 (developed without materials), b) MoreAct-B-Zeo-3 (developed with Zeo), c) MoreAct-B-AC-3 (developed with AC), and d) MoreAct-B-Mag-3 (developed with Mag). All cultures were characterized in triplicate (original incubation conditions) in terms of MP and extra testing conditions were included, such as incubating the cultures without previous contact with materials with different types of materials or incubating the material-adapted cultures in medium without the material to which the cultures were previously adapted to.

5.2.5. Continuous bioreactors

An expanded granular sludge bed (EGSB) reactor (in acrylic glass) with a working volume of 180 mL (and total volume of 200 mL) was used to evaluate the effect of GAC on MP under continuous mode. The

bioreactor was modified by adding a nylon membrane (pore size ≥ 125 μm) fixed in an acrylic circle (with similar internal diameter of the reactor), which was attached to the lid of reactor, in order to keep the GAC inside the reactor and avoid losses by washout. A schematic representation of the EGSB experimental set-up is shown in Figure 5.2a, and real photographs of the bioreactor, and of the nylon membrane, in Figure 5.2b. As the membrane was moveable/adjustable, it was possible to place the membrane below the liquid recycle's exit port, to keep GAC inside the bioreactor and in contact with anaerobic sludge. The bioreactor was inoculated with an anaerobic granular sludge (15 $g \cdot L^{-1}$ in VS) collected from an anaerobic digester treating wastewater from a cellulose industry. The VS were determined in the beginning (0.108 $g \cdot g^{-1}$, w/w) and at the end of the experiment according to the Standard Methods ("APHA/AWWA/WEF," 1998). The SMA in acetate and hydrogen was determined at the beginning of the experiment by using the procedures described elsewhere (Alves et al., 2001; Colleran et al., 1992). Table 5.2 contains information about the sludge used to inoculate the bioreactor. Before the inoculation of the reactor, the anaerobic granular sludge was previously acclimatized with 30 $mmol \cdot L^{-1}$ of ethanol (Ethanol, absolute, 99.8 % v/v, Fisher Chemical, Fisher Scientific, UK) in sodium bicarbonate buffered medium containing resazurine (0.001$g \cdot L^{-1}$), with an atmosphere of N_2/CO_2 (80:20 % v/v, (1.1×10^5) Pa). After the acclimatization, the medium was drained, and the sludge was used to inoculate the bioreactor. The feed composition was a mixture of acetate, propionate, butyrate and ethanol. Details on the feeding composition and preparation are given in the feed preparation subsection. The oxygen inside of the bioreactor was removed by flushing it with N_2. The bioreactor was maintained in batch mode overnight and then it was operated in continuous mode for 37 d. A gas counter was set at the top of the reactor to count the volume of biogas produced. Two peristaltic pumps were used, i.e., one for feeding and another for liquid recirculation (promoting the mixing and expansion of the sludge bed inside the bioreactor). The flow rate of feeding was approximately 0.45 $mL \cdot min^{-1}$ (corresponding to approximately 6 h of hydraulic retention time (HRT)) and the recycle around 69 $mL \cdot min^{-1}$. The operation was performed at mesophilic temperatures ((37 ± 1) °C).

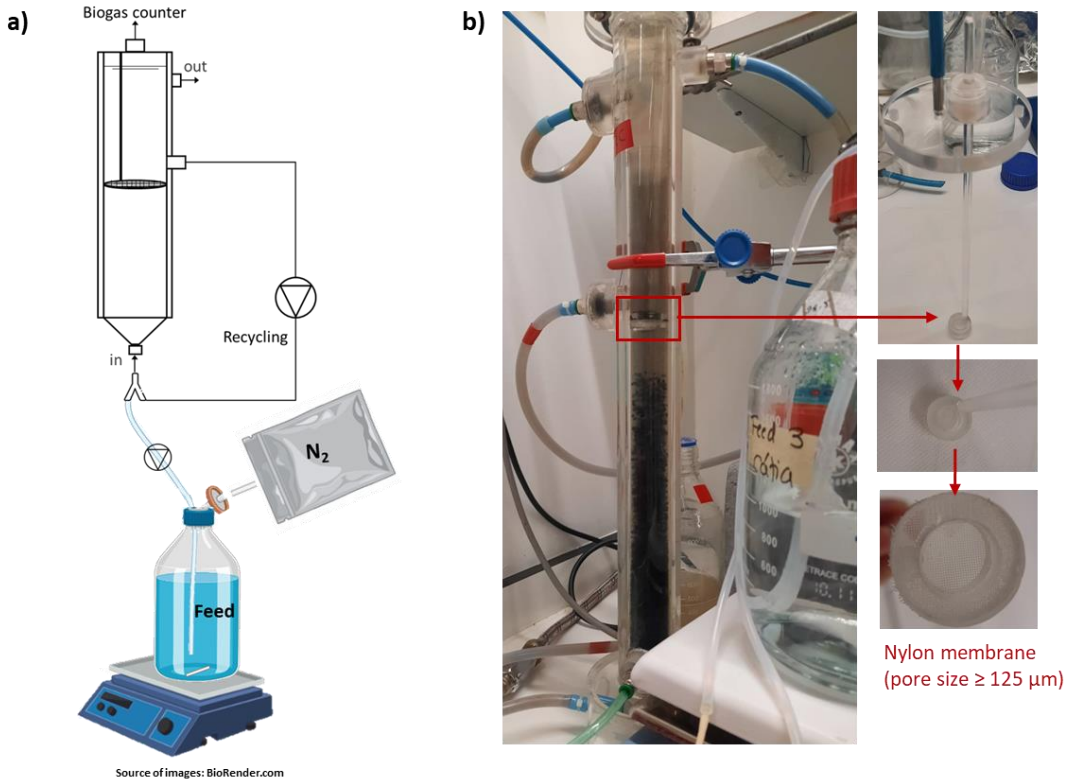

Figure 5.2. Schematic representation of the experimental set-up (a) and real photographs (b) of continuous bioreactor experiments.

5.2.5.1. Feed preparation

The synthetic feed consisted in a mixture of VFA, namely acetate (acetic acid sodium salt, anhydrous, ≥ 99.0 %, Sigma-Aldrich, USA), propionate (propionic acid sodium salt, ≥ 99.0 %, Fluka, Sigma-Aldrich, USA) and butyrate, and ethanol. Initially, the reactor was fed with 5 $g \cdot L^{-1}$ chemical oxygen demand (COD) of VFA and ethanol at 1:10:10:10 COD ratio of acetate, propionate, butyrate and ethanol, respectively. It was supplemented with macronutrients (0.6 mL per g of COD fed) and micronutrients (1 $mL \cdot L^{-1}$) as described elsewhere (Alves et al., 2001). Stock solutions of VFA and ethanol were sterilized by autoclaving (at 120 °C, for 20 min) and added under aseptic conditions to a bottle previously autoclaved containing distilled water, and the macronutrients and micronutrients. The feed was maintained with agitation during all time of operation. The feed bottle contained a gas bag filled with N_2 gas (to avoid oxygen diffusion inside the bioreactor, Figure 5.2a). As the pH_{in} varied between 6.7 and 6.4, and pH_{out} oscillated between 7.8 and 8.5 during all time of operation, sodium bicarbonate was not added.

5.2.5.2. Operation mode

The operation of the bioreactor was divided in four different periods. Until day 15 of the operation (Period I), the bioreactor was fed with 5 $g \cdot L^{-1}$ in COD, and without GAC; during Period II, between days 15 and 23, the bioreactor was operated with 0.5 $g \cdot L^{-1}$ GAC which was added at the end of Period I, and the COD fed was maintained; in Period III, between days 23 and 31, GAC was maintained and the COD was increased to 10 $g \cdot L^{-1}$; in Period IV (days between 31 and 37) additional 0.5 $g \cdot L^{-1}$ GAC was added, resulting in a final concentration of 1 $g \cdot L^{-1}$ GAC. In this experiment, GAC (Norit ROX 0.8 granular activated carbon) was used in pellets (particle size ≥ 500 µm) to minimize the losses by washout. During the last two days of each period (before changing the operational conditions), the performance of the reactor was evaluated by taking liquid samples (3 samples per day) of the in and out flows (to measure pH, COD, and VFA and ethanol concentrations) and gas samples (to determine the content of CH_4 in the biogas produced). The reactor feed was prepared in a daily base during the Periods I and II, and at each 2 days during Periods III and IV, always under sterile conditions.

5.2.6. Analytical methods

To follow MP during batch incubations, gas samples (0.5 mL) were taken from the headspace of the bottles with a Pressure-Lock syringe (SGE Syringe, Trajan Scientific Australia Pty Ltd) (in aseptic conditions) and analysed in a gas chromatograph GC-FID Chrompack 9000 (Shimadzu, Kyoto, Japan). The column was a Carbowax 20 M (2 m × 2 mm, 80–120 mesh) and the method conditions were the same described elsewhere (Salvador et al., 2019).

In bioreactor experiments, a Ritter MilliGascounter (Dr.-Ing. Ritter Apparatebau GmbH, Bochum, Germany) was used to measure the biogas production. The percentage of CH_4 in the biogas was determined in a GC BRUKER SCION 456 (Billerica, MA) with the method conditions described elsewhere (Salvador et al., 2019). Gas samples (0.5 mL) were taken using a graduated gas tight syringe (1750SL, HAMILTON® GASTIGHT® syringe, Reno, Nevada, USA) and analysed in triplicate.

Samples for VFA and ethanol analyses were collected, centrifuged (15 min, 20 000 g), filtered through 0.22 µm syringe filters and frozen until the moment of analysis. The analyses were carried out in a HPLC (SHIMADZU - LC2060C), using an BioRad Aminex HPX – 87H column (300 mm x 7.8 mm). HPLC was equipped with DAD (VFA analysis at 210 nm) and RI detectors (ethanol analysis). The temperature of the oven was set at 60 °C. The samples were prepared with an internal standard, which was crotonic acid (98%, Sigma-Aldrich, USA) (0.2 $mmol \cdot L^{-1}$). The eluent used (mobile phase) was sulfuric acid (5 $mmol \cdot L^{-1}$)

at 0.6 mL·min^{-1} of flow rate, and the total time of run to acquire data was 30 min per chromatogram/sample.

COD was determined in samples previously centrifuged (15 min, 20 000 g), using cuvette test kits (Hach Lange, Düsseldorf, Germany) and a DR 2800 spectrophotometer (Hach-Lange GmbH).

Electrical conductivity and pH of the growth medium were measured with a Consort multi-parameter analyser C3010 and C1020, respectively. ORP was measured with a portable metre C533 (Consort, Turnhout, Belgium) equipped with an ORP electrode D 223 (VWR, Radnor, PA).

5.2.7. Statistical analysis

In batch experiments, the kinetics parameters like lag phase and exponential methane production rate (EMPR) were obtained as explained in Chapter 3, subsection "3.2.6. Statistical analysis".

The statistical differences in the values obtained for kinetic parameters in batch experiments, and for methane yield during bioreactor operation, were evaluated using ANOVA also mentioned in the same subsection of Chapter 3.

5.3. RESULTS

5.3.1. Effect of materials on active microbial communities

5.3.1.1. Butyrate degradation in batch assays

The anaerobic sludge used in the batch assays was an active sludge, which was reflected by its SMA on acetate (0.26 gCH_4-COD·$gVSS^{-1}$·d^{-1}, Table 5.2), and the fast conversion of butyrate to methane (6 d and 9 d for complete conversion in B-without-AC-Mag-1 and in B-without-Zeo-1, respectively, Figure 5.3a). Indeed, to be considered an active sludge, the SMA on acetate should be around 0.3 gCH_4-COD·$gVSS^{-1}$·d^{-1} (Angelidaki et al., 2009), which was the value obtained for the anaerobic sludge used in these experiments (Table 5.2). The presence of AC, Mag or Zeo during butyrate degradation did not affect the conversion of butyrate to methane (Figure 5.3a), as MPR and the time needed for complete degradation was not significantly different between the assays performed with and without materials. The lag phases preceding MP had a duration of approximately 1.3 d in all conditions for the experiments of the first batch (with and without AC and Mag), and 1.9 d in the conditions for the experiments of the second batch (with and without Zeo). When the sludge was incubated a second time (by transferring 10 % v/v of the previous cultures, maintaining the original conditions), only slightly differences on the MP performance between conditions could be observed (Figure 5.3b). Lag phases preceding MP were similar for all conditions (with

or without materials), but the MP profile by B-AC-2 started to reveal a slightly improvement on the methanogenic activity comparing with the MP profile by B-without-AC-Mag-2. In the incubations with Zeo or Mag, no relevant differences were observed comparing with the incubations without materials (Figure 5.3b). From the first to the second incubations, it is important to note that the microbial communities lose some activity, as for example, the same amount of butyrate took more 9 d to be converted to methane in the assay B-without-AC-Mag-2 than B-without-AC-Mag-1. These results show that microbial communities with similar composition but different activities are differentially affected by the presence of materials. More active microbial communities are not affected by the addition of materials (Figure 5.3a), while differences on MP profiles started to be more evident in less active microbial communities (Figure 5.3b).

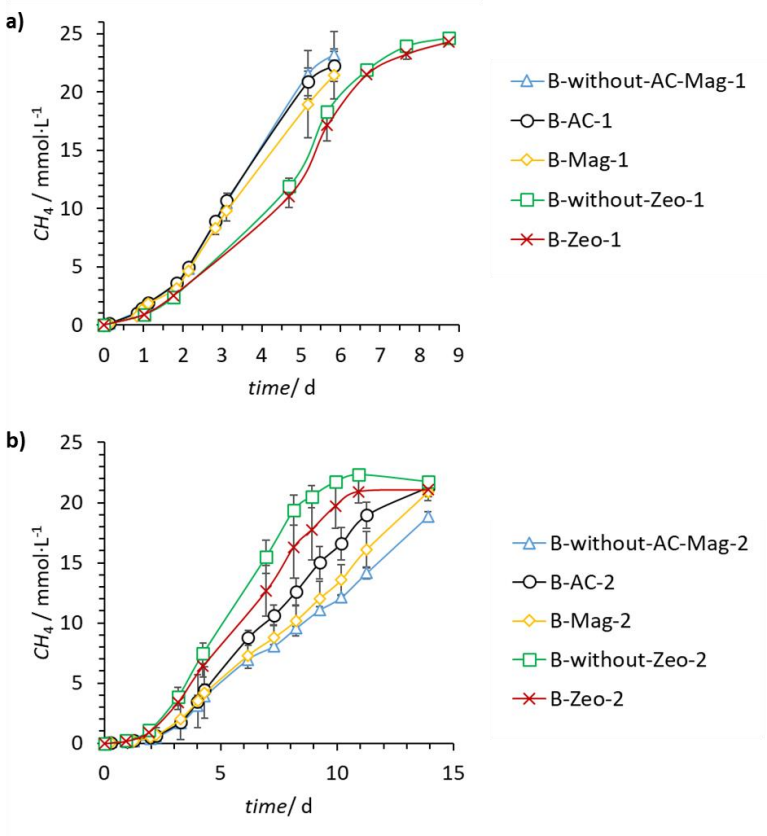

Figure 5.3. Cumulative methane production by a) active anaerobic sludge and b) butyrate-enrichment cultures. The results are the mean of two replicates with the respective standard deviation.

5.3.1.2. Fatty acids and ethanol degradation in a continuous bioreactor

The granular sludge used to inoculate the bioreactor was also an active sludge given its SMA in acetate (approximately 0.3 gCH_4-COD·$gVSS^{-1}$·d^{-1}, Table 5.2), and similarly to what was observed in the batch experiments, the addition of GAC did not improve the bioreactor performance in none of the operational periods (Figure 5.4). The bioreactor showed a good performance during Period I (when GAC was not

present), without accumulation of VFA (i.e., acetate, propionate, butyrate) or ethanol (Figure A. 7, Appendix), with complete removal of the 5 $gCOD \cdot L^{-1}$ fed, and with CH_4 content in the biogas of around 77.8 % (Figure 5.4a). The addition of GAC during Period II did not alter the bioreactor performance (Figure 5.4; Table A. 7, Appendix). At the end of Period II, the COD of the feed was increased to 10 $gCOD \cdot L^{-1}$, and the bioreactor performance was maintained. In order to evaluate whether the increase on GAC concentration would improve the bioreactor performance, GAC concentration was doubled (in Period IV) but neither methane recovery nor COD removal were altered (Figure 5.4; Table A. 7, Appendix). The methane yield, given in mL of methane produced per gram of COD removed, was (239 ± 12) $mL_{CH4} \cdot g_{CODrem}$ and (253 ± 11) $mL_{CH4} \cdot g_{CODrem}$ in Periods III and IV, respectively (Table A. 7, Appendix), and these results were not statistically different ($p > 0.05$). At the end of operation, the VS inside the bioreactor was (20 ± 2) $g \cdot L^{-1}$ (vs 15 $gVS \cdot L^{-1}$ at the beginning), showing the active growth of anaerobic microorganisms, although some biomass was washed out during all the operation.

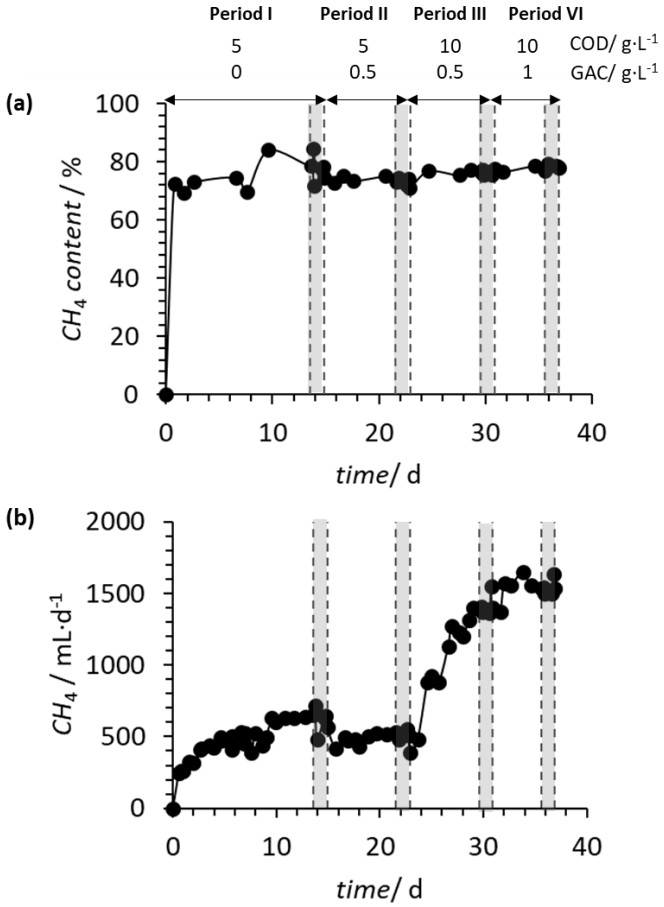

Figure 5.4. (a) Methane content and (b) methane production rate by anaerobic sludge in the EGSB. The area colored in grey corresponds to the characterization days, i.e., 2 d with 3 sampling points per day for each period of operation.

5.3.2. Effect of materials on active butyrate-degrading enrichment cultures developed with and without materials

The enrichment strategy applied resulted in several different cultures which convert butyrate to methane at different rates. The most efficient cultures include the ones designated by MoreAct-B-Zeo-3, MoreAct-B-AC-3, MoreAct-B-Mag-3 and MoreAct-B-without-AC-Mag-3, which were enriched with Zeo, AC, Mag and without materials, respectively (Table 5.1). Cultures MoreAct-B-without-AC-Mag-3 and MoreAct-B-Zeo-3 were specialized in the total conversion of butyrate to methane, which was achieved in approximately 12 d of incubation (Figure 5.5a, 5.5b). Cultures MoreAct-B-AC-3 and MoreAct-B-Mag-3 were specialized in the conversion of butyrate to methane and acetate which was achieved in 4 d and 6 d, respectively (Figure 5.5c, 5.5d). The addition of materials to the butyrate-degrading enrichment developed without materials (MoreAct-B-without-AC-Mag-3), didn't accelerate butyrate conversion to methane (Figure 5.5a). Excepting the assay with Zeo, in the assays with AC, Mag, mixture of AC and Mag, and AC@2%Fe, the MP was even delayed. For instance, the complete butyrate conversion to methane was achieved in 20 d in the presence of AC, whereas for the culture without materials only 14 d were required. Mag was the material which increased most the lag phase preceding MP, from 2 d (in the culture without materials) to 4 d, showing that the microbial enrichment in the presence of this material requires a longer adaptation time. Besides, the enrichment culture developed with Mag (MoreAct-B-Mag-3), was quite efficient on butyrate degradation, but when it was incubated without Mag, its activity was even higher, as the lag phase preceding MP was reduced in about 27 % (from 2.6 d in the incubation with Mag to 1.9 d in the incubation without Mag, Table 5.3, Figure 5.5d). These results showed that even microbial communities pre-adapted to the presence of Mag, performed better when Mag was not present, suggesting that this material did not contribute to stimulate butyrate degradation. The enrichment culture pre-adapted to AC (MoreAct-B-AC-3) slightly lost methanogenic performance when incubated in the absence of AC (Figure 5.5c). The lag phase duration by the original culture was (1.5 ± 0.0) d, which was lower than in its absence (2.1 ± 0.2) d (results statistically different $p < 0.05$, Table 5.3). The initial methane production rates (IMPR) were better with AC, changing from an IMPR of (0.27 ± 0.01) $mmol \cdot L^{-1} \cdot d^{-1}$ in the original condition with AC to (0.13 ± 0.03) $mmol \cdot L^{-1} \cdot d^{-1}$ in its absence (results statistically different $p < 0.05$, Table 5.3). However, the complete butyrate conversion to methane was achieved at the same time for all incubation conditions (around 4 d). On the other hand, the enrichment culture pre-adapted to Zeo almost maintained the microbial activity when incubated without Zeo, as differences on the MP profiles, with and without material, were not significant (Figure 5.5b). The behavior of these microbial enrichments when exposed to other incubation conditions (with or without materials), different from those they were adapted

to, showed that the presence or absence of the materials doesn't interfere much in butyrate degradation, because the microbial communities are well adapted and active.

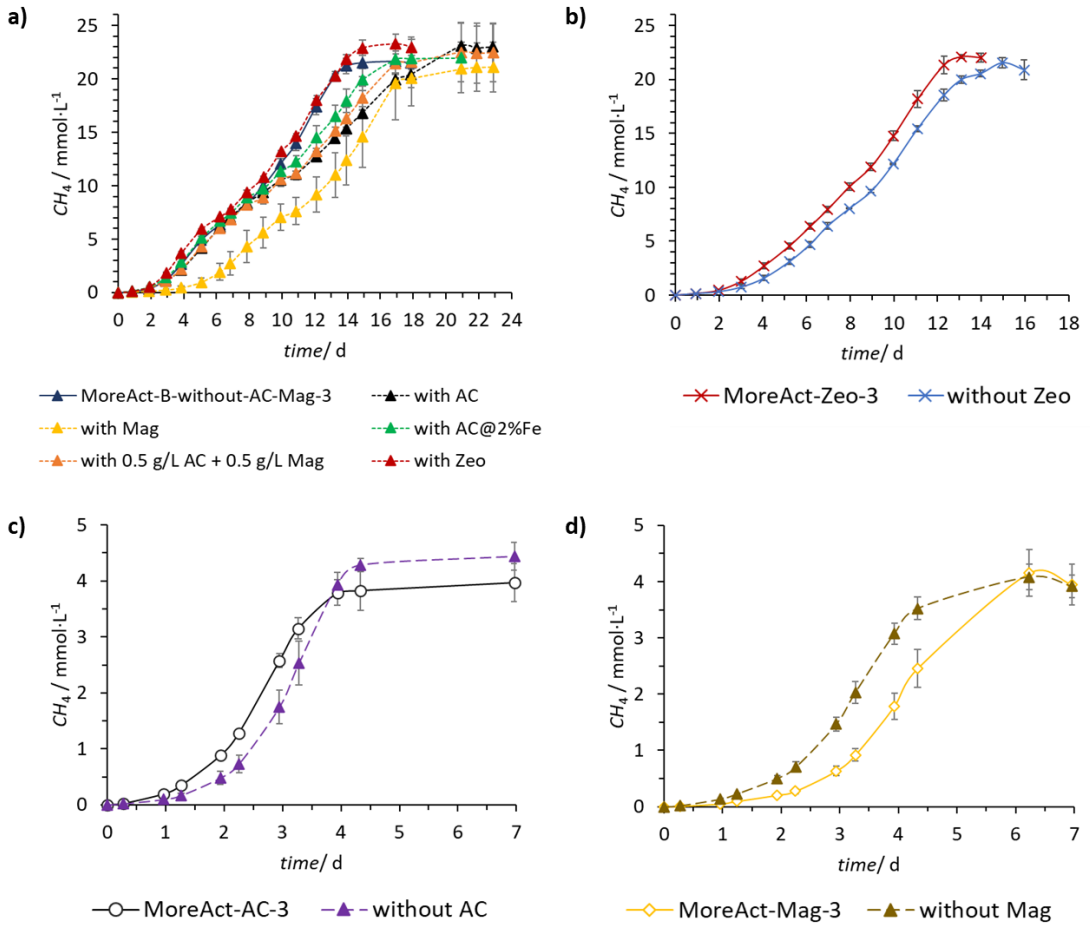

Figure 5.5. Cumulative MP profiles over time for the following active cultures experiments: a) adapted butyrate-degrading enrichment without AC or Mag (MoreAct-B-without-AC-Mag-3) incubated in the original conditions and with several different materials; b) Zeo-adapted butyrate-degrading enrichment (MoreAct-B-Zeo-3) incubated in the original conditions and without Zeo; c) AC-adapted enrichment (MoreAct-B-AC-3) incubated in the original conditions and without AC; and d) Mag-adapted enrichment (MoreAct-B-Mag-3) incubated in the original conditions and without Mag. The results are the mean with the standard deviation of three replicates.

The ORP of the growth medium changed with the presence of materials (Table A. 8, Appendix). Particularly, the presence of Mag increased the ORP values mainly at the end of incubations, for example, as it occurred in the assay of culture MoreAct-B-without-AC-Mag-3 with Mag, where ORP value was (-175 ± 23) mV, contrasting with (-333 ± 6) mV in the condition without materials. As methanogenesis is favoured at lower ORP (between −200 mV to −400 mV (Salvador et al., 2017)), the increase of ORP could affect MP. Although the results suggested that this material does not contribute to stimulate butyrate

degradation, the explanation cannot only be based on ORP alterations since the values measured in the beginning of incubations in the presence of Mag are within the optimal range for methanogenic activity.

Table 5.3. Adapted butyrate-degrading enrichment cultures in different conditions and the impacts towards the IMPR, the EMPR, the duration of lag phase and the time of incubation for MP

Assay	**Lag phase** [a]/ d	**IMPR** [b]/ mmol·L^{-1}·d^{-1}	R^2	**EMPR** [a]/ mmol·L^{-1}·d^{-1}	R^2	**t**/ d
MoreAct-B-AC-3	1.5 ± 0.0	0.27 ± 0.01	0.95 ± 0.00	1.9 ± 0.1	0.994 ± 0.001	4
MoreAct-B-AC-3 without AC	2.1 ± 0.2	0.13 ± 0.03	0.96 ± 0.00	2.3 ± 0.1	0.988 ± 0.001	4
MoreAct-B-Mag-3	2.6 ± 0.0	0.12 ± 0.02	0.94 ± 0.00	1.4 ± 0.2	0.993 ± 0.002	6
MoreAct-B-Mag-3 without Mag	1.9 ± 0.1	0.31 ± 0.04	0.93 ± 0.01	1.5 ± 0.1	0.992 ± 0.001	6

[a] kinetics parameters obtained by modified Gompertz model.

[b] IMPR were calculated for the first 1.3 d of incubation in the assays with MoreAct-B-AC-3 and for the first 2.2 d of incubation in the assays with MoreAct-B-Mag-3.

5.3.3. Effect of materials on slow growing microbial cultures

As MP was followed in each incubation, the initial changes in the MP profiles in the different conditions (with and without materials) were detected together with the changes in the total time of incubation required for the complete conversion of butyrate to methane as well as changes in lag phase time and MPR in each transfer. The profiles of MP presented in Figure 6 show the phase of MP where the presence of materials started to impact significantly the conversion of butyrate to methane, highlighting that in the first incubation of the anaerobic sludge no effects were observed (Figure 5.3a). After three incubations, the cultures developed with AC (LessAct-B-AC-1, Figure 5.6a) showed lower lag phase duration (less than 4 d) and a faster methanogenic activity in an early stage of incubation (with a transient acetate accumulation point when 5 mmol·L^{-1} of CH_4 was reached; Table A. 9, Appendix), in comparison with the other incubations (LessAct-B-without-AC-Mag-1 and LessAct-B-Mag-1, Figure 5.6a). On the other hand, the cultures developed with Mag were partially inhibited, which was represented by longer lag phases preceding MP (higher than 10 d, Figure 5.6a). The cultures developed in the absence of materials showed a MP performance below the cultures developed with AC and above the ones developed with Mag, with lag phases approximately of 6 d (Figure 5.6a). During the following incubation, the cultures with AC still showed to be slightly faster in producing methane in an early stage of incubation (until around 5 mmol·L^{-1} CH_4), with lower lag phase duration (less than 4 d) in comparison with the other conditions (Figure 5.6b). However, despite of this stimulatory effect by AC at the beginning of incubations, the total conversion of

butyrate to methane was slowed down (Figure A. 8, Appendix). AC cultures required more than 46 d to reach the total MP from complete butyrate degradation. In cultures with Mag, it was observed a longer lag phase duration, which varied between bottles (approximately 8 d for LessAct-B-Mag-2a, and 4 d for LessAct-B-Mag-2b, Figure 5.6b). Then, the complete MP was achieved in approximately 35 d for LessAct-B-Mag-2a and 42 d for LessAct-B-Mag-2b (Figure A. 8, Appendix). A transiently acetate accumulation was observed in all conditions (Table A. 9, Appendix). Complete butyrate conversion to methane was faster in cultures without materials (LessAct-B-without-AC-Mag-2a and LessAct-B-without-AC-Mag-2b, Figure 5.6a), which occurred approximately in 25 d. On the other hand, the cultures from the experiments of batch 2 only revealed differences between the two types of incubation (with and without Zeo) after 5 incubations (Figure 5.6c). LessAct-B-Zeo-1a showed to become quite faster in butyrate conversion to methane in comparison with LessAct-B-without-Zeo-1b (Figure 5.6c). Butyrate was converted to methane in almost 30 d with Zeo, while it took approximately 45 d in the culture without Zeo. Regarding the positive or negative impacts of the presence of materials, these results showed how the performance of slow growing cultures can be highly affected in the presence of different materials.

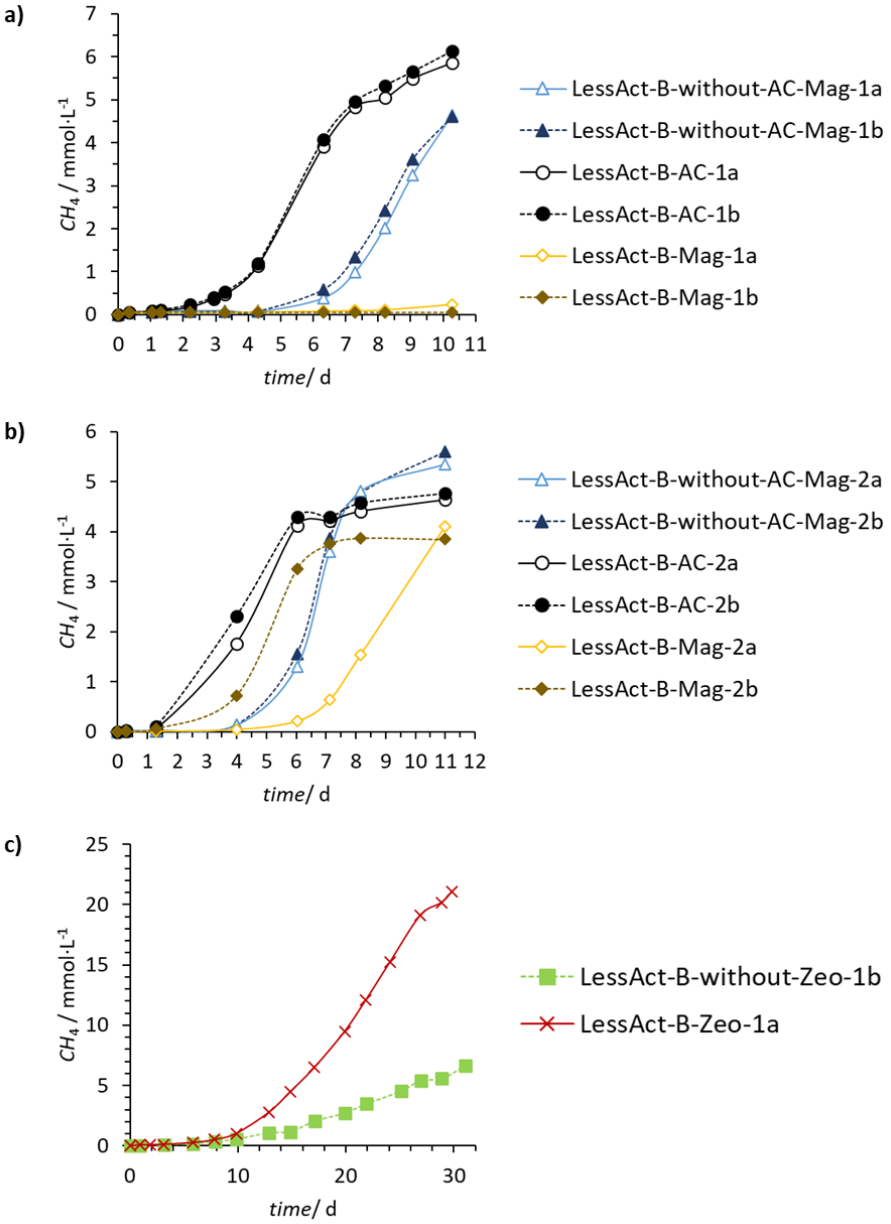

Figure 5.6. Cumulative MP profiles of the two lines of butyrate-degrading enrichment cultures, developed with and without AC, Mag and Zeo.

5.4. Discussion

There are several studies reporting the beneficial effect of CM on MP from diverse carbon sources. In this work, it is shown that the initial activity of the microbial community is a determining factor which dictates the effect of CM on MP efficiency. It was clear that the presence of materials in less active microbial communities reflects a major impact on MP profiles (Figure 5.6), while more active microbial communities are not much affected by the presence of materials (Figure 5.3, Figure 5.4, Figure 5.5). From an applied viewpoint, this finding suggests that the strategy of adding CM to AD processes is worth to be considered,

as it can accelerate waste conversion to methane, but only in the cases in which microbial communities are less active or poorly adapted. These observations were made for the case of butyrate degradation in batch cultures, and for the conversion of VFA and ethanol to methane in continuous bioreactors. By inspection of the studies in the literature, one can notice that our results can be generalized for a high number of cases (Table 2.6, Chapter 2). The effect of several materials (AC, Mag and Zeo) was studied during the AD of simpler to more complex wastes (e.g., acetate, butyrate, ethanol, food waste, swine wastes) and with microbial communities from different origins (e.g., anaerobic sludge, sediments), and the results are summarized in Table 2.6, Chapter 2.

The results obtained in this study showed that in less active cultures the presence of AC contributed to a lag phase reduction up to 50 % (Figure 5.6a). In the literature, there are reports on improvements up to 97.6 % in lag phase reduction in the presence of GAC (Table 2.6, Chapter 2). Similarly to what was observed in these experiments, the activity of microbial communities used in those studies was rather low, as the controls presented extended lag phases preceding MP. For example, 170 d of lag phase for an anaerobic sludge degrading dog food which decreased to 4 d with GAC (Dang et al., 2017) and 13 d for another anaerobic sludge degrading butyrate that decreased 61.5 % in the presence of GAC (Xu et al., 2018) (Table 2.6, Chapter 2). Other studies showed the reduction of lag phases preceding MP when GAC or powdered activated carbon (PAC) were present as well (Amelia-Elena et al., 2018; Lee et al., 2020; J.-H. Park et al., 2018; Ryue et al., 2019; Tan et al., 2021; Tan and Lens, 2021) (Table 2.6, Chapter 2). In the control conditions, no MP occurred during the time of incubation or low biogas/methane yields were achieved. Then, MP started sooner in the presence of GAC/PAC, which in some cases resulted also in an improvement of the MPR up to 50× (Amelia-Elena et al., 2018; Dang et al., 2017; J.-H. Park et al., 2018; Ryue et al., 2019; Tan et al., 2021; Xu et al., 2018). Besides, some studies showed the potential of this material mainly to improve the methane or biogas yield (Dang et al., 2017; Ryue et al., 2019). However, the observation that more active cultures did not benefit from the presence of materials like AC/GAC either in batch incubations (Figure 5.3) or during bioreactor operation (Figure 5.4), as no significant changes on methanogenic activity could be observed between batch incubations and bioreactors containing or not these materials, was verified in other studies, as well. In other studies, for example, the presence of GAC barely affected the conversion of acetate, propionate and butyrate to methane by an anaerobic sludge, as no differences in lag phase duration, MPR or time of incubation were observed comparing the incubations with and without GAC (Xu et al., 2018) (Table 2.6, Chapter 2).

Regarding MP, the application of modified materials was found to be advantageous in most of the cases (Al Hasani et al., 2022; Amen et al., 2017; Barrena et al., 2023; Barua et al., 2019; de Quadros et al.,

2022; Liu et al., 2020; Milán et al., 2010, 2001; Peng et al., 2018; Song et al., 2019). For instance, AC combined with zero-valent iron (ZVI) improved activated sludge degradation by an anaerobic sludge through the decrease of the lag phase preceding MP up to 70 % in the presence of these combined materials (Liu et al., 2020). In this study, the addition of modified AC, like AC@2%Fe, or the mixture of AC and Mag, did not cause any improvement of performance for the enrichment culture MoreAct-B-without-AC-Mag-3 (Figure 5.5a). This result of no enhancement of methanogenic performance in the presence of those materials was attributed to the fact that the experiment was performed towards an enrichment culture highly adapted and active in butyrate degradation.

In the case of Zeo, it has been applied in AD processes as a support for microbial immobilization, or used to remove nitrogen compounds like ammonium that could inhibit the AD process (Montalvo et al., 2012). In addition, this type of material is also used as a non-conductive control in experiments testing CM, like graphene and GAC/PAC, assuming that Zeo, by having a lower conductivity than these carbon-based materials, would not affect the methanogenic reactions (König et al., 2022; Zhang et al., 2017). However, in this study, Zeo showed to highly improved the total conversion of butyrate to methane in the assays with the slow growing enrichment LessAct-B-Zeo-1a, by reducing the total time of incubation in around 33 % comparing with the LessAct-B-without-Zeo-1b (Figure 5.6c), and Zeo showed no effect when added to more active enrichments (MoreAct-B-without-AC-Mag-3 with Zeo, Figure 5.5a), suggesting that its impact also depends on the microbial activity.

There are many reports where the presence of Mag is very relevant by increasing the MPR or even to decrease the lag phases preceding MP (Barrena et al., 2023; Kato et al., 2012; Lee et al., 2020; J.-H. Park et al., 2018; Zhang and Lu, 2016), but there are also studies pointing the opposite effect (Yan et al., 2020; Zhong et al., 2022). In this study, the incubation of the active anaerobic sludge with Mag showed no improvements on MP performance (Figure 5.3a). In addition, incubating the active enrichment with Mag (Figure 5.5a) even caused an inhibition of butyrate conversion to methane at the beginning of the incubations. However, when the contact of the microbial community with Mag is extended by continuous transfers, the microbial community recovers activity as showed by the enrichment MoreAct-Mag-3 (Figure 5.5d). Moreover, when this enrichment well-adapted to the presence of Mag was incubated in its absence, the methanogenic performance was enhanced (Figure 5.5d). These results showed that Mag was not beneficial when added to the microbial communities converting butyrate to methane (Figure 5.3, Figure 5.5a), but different results can be obtained with other microbial communities and other substrates. For instance, MPR was improved up to 8 times in the presence of Mag during glucose degradation by a flocculent sludge, also enhancing the methane yield (Barrena et al., 2023).

In general, the application of (nano)materials seems particularly attractive when the inoculum presents low activity, specially in the cases where the anaerobic process is compromised. For instance, the addition of materials seems to be a good strategy to recover the system that suffered an overloading or to allow the operation of bioreactors at high OLR by improving the stability of the AD. In the study carried out by Barrena *et al.* (2023), the presence of Mag helped to reverse the inhibitory effect of VFA and enabled the microbial consortia to recover from an induced acidification of the batch reactors (by addition of an inhibitory concentration of glucose for methanogenic activity) (Barrena et al., 2023). The control condition was inhibited in those conditions, but the presence of Mag recovered the MP, improving the methane yield (Barrena et al., 2023). The problems related with the accumulation of LCFA (which are intermediates during the degradation of fat, oil and grease) that adsorb onto biomass causing sludge flotation, biomass washout, and inhibitory effects on key microorganism (like methanogens), can be relieved using carbon-based materials such as GAC (He et al., 2021; Tan et al., 2021; Tan and Lens, 2021), and other materials like Zeo (Nordell et al., 2013). The degradation of nitrogen-rich wastes can lead to the failure of AD process due to ammonia inhibition, mainly promoted by the diffusion through cell membranes of free ammonia (NH_3) (causing proton imbalance and interference with metabolic enzymes of the microorganisms) (Liu et al., 2020; C. Wang et al., 2022; Zheng et al., 2015). It was reported that the presence of materials like ZVI (Liu et al., 2020; Yan et al., 2020), the mixture of ZVI with AC (Liu et al., 2020), Mag (Yan et al., 2020), and Zeo (Zheng et al., 2015), can preserve MP under ammonia inhibition conditions, in batch reactors, and with Mag (C. Wang et al., 2022) and Zeo (Zheng et al., 2015) in anaerobic bioreactors at lab scale. However, the presence of PAC worsened the methanogenic performance upon ammonia stress (Yan et al., 2020).

5.5. Conclusions

The effect of (nano)materials towards methane production is dependent of the microbial activity. The use of materials may be useless in high active inocula, with high methanogenic performance. On the other hand, the lower the methanogenic activity of the inoculum, the more impact on the kinetic parameters (like lag phase duration) can be observed when materials are added. These findings are relevant to guide the decision on applying (nano)materials to anaerobic digesters. For instance, (nano)materials can be extremely important for recovering anaerobic processes, but irrelevant in bioreactors with high performance, with highly active microbial communities. Cost-benefits should be taken into account when deciding.

CHAPTER 6

6. CONDUCTIVE MATERIALS MODULATE MICROBIAL COMMUNITIES AND ACCELERATE METHANE PRODUCTION FROM BUTYRATE WITHOUT CHANGING INTERSPECIES ELECTRON TRANSFER MECHANISMS

ABSTRACT

Previous research has been shown that conductive materials (CM) like carbon nanotubes and magnetite (Mag) can accelerate the methane production (MP) by anaerobic enrichment cultures. The presence of CM was found to alter the microbial composition, and improvements on MP efficiency were attributed to changes in the interspecies electron transfer (IET) mechanisms, from the typical IET via soluble molecules, like hydrogen and formate, to the conductive material mediated interspecies electron transfer (CIET). In this study, different enrichment cultures with and without activated carbon (AC), Mag, and zeolite, at 0.5 $g \cdot L^{-1}$ were developed. Methane production from butyrate was followed during the enrichment process, the taxonomic composition of stable microbial enrichments was obtained by 16S rRNA gene sequencing, and gene expression was investigated by performing metatranscriptomics analysis.

The results showed differences in the efficiency of butyrate conversion to methane among the different enrichments developed. Lag phases preceding MP were lower in AC-enrichment cultures, while complete conversion of butyrate to methane was faster in Mag-enrichment cultures. Microbial communities developed with different materials evolved differently, mostly in terms of relative abundance for each taxon identified. Yet, bacteria assigned to the genus *Syntrophomonas* (representing up to 80 % of the total bacterial community) were dominant in all butyrate-degrading enrichments. Both hydrogenotrophic and acetoclastic methanogens were identified. Hydrogenotrophic methanogens were highly enriched in the presence of AC (*Methanomicrobiales* represented 78 % of the archaea community), while the enrichment with Mag showed a more diverse acetoclastic community, with microorganisms assigned to *Methanosarcina* and *Methanotrix* genera. Genes involved in the β-oxidation of butyrate and in methanogenesis were highly expressed by the microbial enrichment developed with AC. Microorganisms assigned to the *Syntrophomonadaceae* family were the most active regarding butyrate degradation, and no genes typically related to DIET were detected.

6.1. INTRODUCTION

Regarding the effects of conductive materials (CM) on microbial communities, there are still open questions which deserve to be answered. For instance, it is not known how microbial communities evolve when growing in the presence of materials for long periods of time. Knowing that most of the materials tested so far tend to improve microbial activities, it would be worth determining if microbial communities developed with different materials show similar taxonomic composition or not. Another question that still exists is whether or not changes in interspecies electron transfer (IET) mechanisms take place in microbial communities adapted to CM. In the literature, there are no reports comparing the composition of microbial communities incubated with different materials, because studies were performed with different inocula and/or different carbon sources, avoiding a direct comparison (Chapter 2, Table 2.5).

It has been suggested that the main mechanism responsible for the improvements on methane production (MP) by microbial communities is the conductive material mediated interspecies electron transfer (CIET) (Fu et al., 2018; Kato et al., 2012; Li et al., 2015; Xia et al., 2019; Zhang and Lu, 2016; W. Zhang et al., 2018), although some authors do not exclude the possibility that CIET may occur together with interspecies hydrogen transfer (IHT) and interspecies formate transfer (IFT) (Fu et al., 2018; Xia et al., 2019; W. Zhang et al., 2018). However, only few studies demonstrated that CIET occurred in the presence of activated carbon (AC), magnetite (Mag), biochar, or carbon cloth, with these materials replacing the biological structures required for direct interspecies electron transfer (DIET) (Chen et al., 2014b, 2014a; Liu et al., 2015, 2012; Lovley, 2017b), or facilitating the IET between bacteria and methanogens (Chen et al., 2014b, 2014a; Liu et al., 2012; Rotaru et al., 2014a).

In this work, several butyrate-enrichment cultures were developed in the presence of AC, Mag and zeolite (Zeo). Mag and AC have been previously reported as materials that can facilitate CIET (Martins et al., 2018), but not Zeo. Butyrate was chosen as a substrate for this study because it is typically converted to methane by syntrophic cultures, which exchange hydrogen or formate between butyrate-degrading bacteria and hydrogenotrophic methanogens (Schmidt et al., 2013; Stams and Plugge, 2009). Therefore, such enrichment cultures would be suitable to investigate how microbial communities and electron transfer mechanisms change when in contact with (nano)materials. The composition of the microbial communities adapted to the three materials was

compared, and genes expressed were identified to get further insights on the IET mechanisms taking place during butyrate conversion to methane in the presence of AC.

6.2. MATERIALS AND METHODS

6.2.1. Development of butyrate-degrading enriched communities

The inoculum to start the butyrate-degrading enrichments was the anaerobic granular sludge collected from a brewery wastewater treatment plant (Super Bock, Porto, Portugal) described in Chapter 5, subsection "5.2.2. Incubation of anaerobic sludge with butyrate and materials".

Butyrate-enrichment cultures were developed with and without AC, Mag and Zeo (Figure 6.1), as described in Chapter 5, subsection "5.2.3. Development of butyrate-degrading enrichment cultures". The materials used are described in Chapter 3, subsection "3.2.1. Conductive and non-conductive materials" and also characterized in Chapter 3, Table 3.2 and Table 3.3 (the AC used during the development of butyrate-degrading enrichments was the AC_{b2}).

From the first batch experiment were developed butyrate-degrading enrichment cultures without materials (Bty-b1), with 0.5 $g \cdot L^{-1}$ AC (AC-B1) and with 0.5 $g \cdot L^{-1}$ Mag (Mag-b1) (Figure 6.1). From the second batch experiment were developed microbial enrichments without materials (Bty-b2) and with 0.5 $g \cdot L^{-1}$ Zeo (Zeo-b2) (Figure 6.1).

After microbial community adaptation to each enrichment condition, stable enrichment cultures were characterized in terms of butyrate consumption, MP, and microbial composition. For that purpose, a pre-inoculum was prepared before conducting the characterization assays in triplicate (Figure 6.1). Butyrate consumption and acetate production were followed during the incubation by high performance liquid chromatography (HPLC), while MP was measured by gas chromatography (GC). Conductivity, redox potential (ORP) and pH of the growth medium were measured at the beginning and at the end of the incubations. The taxonomic composition of the microbial enrichments was determined in duplicate by 16S rRNA gene sequencing.

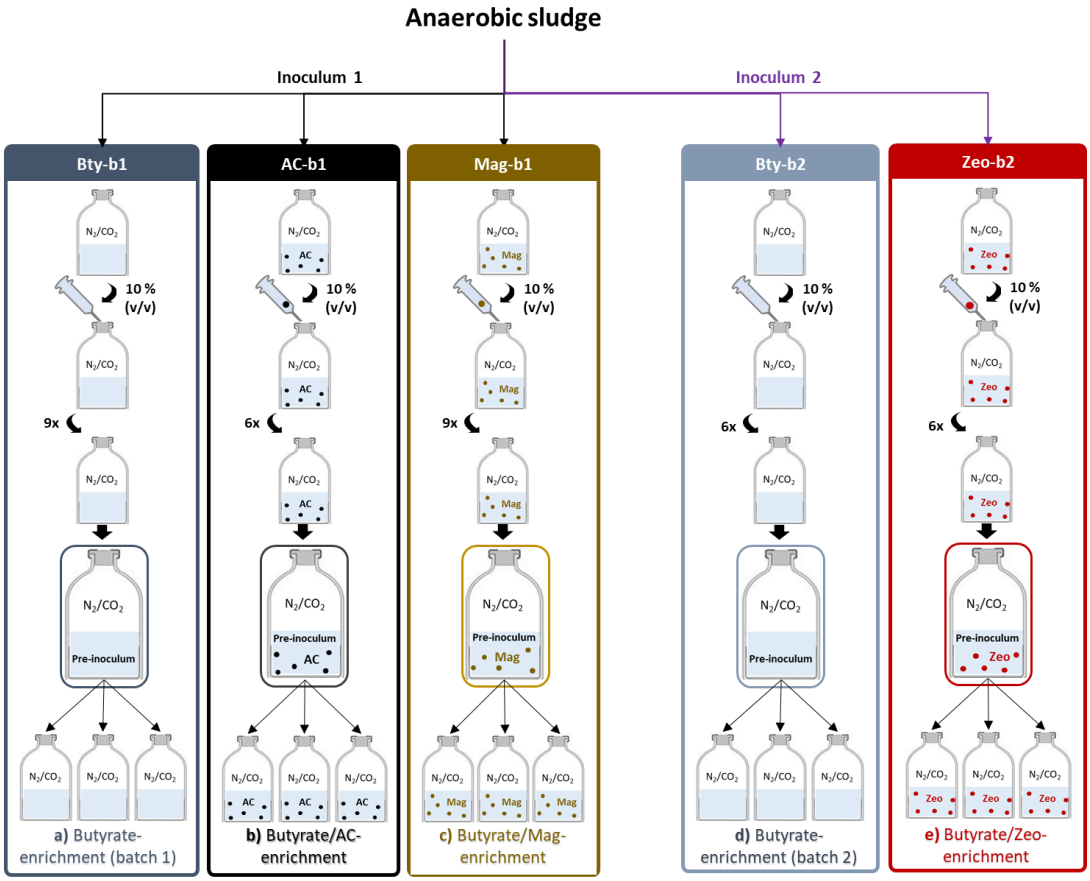

Figure 6.1. Schematic representation of continuous transfers to develop two different batch experiments. The enrichments were continuously transferred over time until reaching stable and well-adapted cultures. The total number (n) of transfers is indicated in the image with "nx". The characterization of each culture was carried out triplicate.

6.2.2. Analytical methods

Gas samples analysis from gaseous phase and measurements of ORP, pH and conductivity of liquid samples from liquid phase were carried out as described in Chapter 5, subsection "5.2.6. Analytical methods".

Samples to analyse the volatile fatty acids (i.e., formate, acetate and butyrate) were collected, centrifuged (15 min, 20 000 g), filtered through 0.22 µm filters and frozen until the moment of analysis. The analysis was performed by HPLC (Jasco, Tokyo, Japan), in the conditions described elsewhere (Duarte et al., 2020).

6.2.3. Phase contrast microscopy

The enrichment cultures were observed under contrast phase microscope (CX41 RF, Olympus) and the images were captured using an Olympus digital camera (high-resolution SC50) combined with the software OLYMPUS cellSens Entry.

6.2.4. Taxonomic characterization of microbial communities: RNA extraction and 16S rRNA gene sequencing

Aliquots of initial anaerobic sludge and adapted butyrate-degrading enrichment cultures were collected and centrifuged (15 min, 15 °C, 7000 g), followed by supernatant discharging and resuspension of the pellet with RNA later (Sigma-Aldrich). These samples were frozen at -20 °C until RNA extraction. RNA was extracted by using the FastRNA ProTM Soil-Direct Kit commercial kit (MP Biomedicals), following the manufacturer' instructions. The isolated RNA was treated with DNase I (Thermo Scientific), cDNA was synthetized by using a SuperScriptTM IV Reverse Transcriptase (InvitrogenTM, Thermo Fisher Scientific) and the prokaryotic universal reverse primer "1492rev" (Lane, 1991). cDNA was precipitated with ethanol and sent to the Research and Testing Laboratory (RTL, Texas), where cDNA amplification, Illumina libraries preparation, amplicon sequencing (Illumina MiSeq, Inc. SanDiego, California) and bioinformatics analysis was performed as described elsewhere (Salvador et al., 2019). The universal primer set 515F/806R (Caporaso et al., 2011), targeting the prokaryotic 16S rRNA gene was used in the amplification step.

6.2.5. Metatranscriptomics analysis

6.2.5.1. RNA isolation and RNA-Seq

AC-adapted enrichment (20 % v/v of inoculum) was incubated in the same conditions described above, but in bottles with a working volume of 300 mL and a headspace of 300 mL. Six biological replicates were performed. The content of each bottle was collected when approximately 3 $mmol \cdot L^{-1}$ of methane was achieved and centrifuged (15 min, 10 000 g, 10 °C) to collect the cells in the pellet, which were immediately immersed in RNA later (Sigma-Aldrich) and stored at -20 °C until RNA extraction. The RNA extraction was performed using the FastRNA ProTM Soil-Direct Kit commercial kit (MP Biomedicals) by following the manufacturer instructions. RNA samples were preserved at -80 °C and sent to the Centre Tecnològic de Catalunya (Eurecat) where cDNA

synthesis, libraries preparation and sequencing were performed as described by (Martins et al., 2021).

6.2.5.2. Bioinformatics analysis

Sequencing data was analysed using MOSCA pipeline (version 1.6.1) (Sequeira et al., 2018). Briefly, FASTQ files were submitted to preprocessing (with Trimmomatic for removal of adapters, low quality regions (average Phred score less than 20), reads and short reads (lower than 50 bp) and SortMeRNA for removal of rRNA reads, assembly (with Trinity (Celaj et al., 2014)), binning with MaxBin2 (Wu et al., 2016) (using the "40" markerset), gene calling with FragGeneScan (on the transcripts), and annotation with UPIMAPI (Sequeira et al., 2022) (using the entire UniProt database as reference), and reCOGnizer (Sequeira et al., 2022) (run with CDD, Protein Clusters, NCBIfam, TIGRFAM, Pfam, COG and SMART databases as references). Quantification of gene expression was obtained by aligning MT reads to the assembled transcripts with Bowtie2, and quantification values were normalized by dividing the read counts by the length of the contigs, and by using the EdgeR package (using the trimmed mean of M-values method).

Special attention was given to the enzymes involved in the following processes: degradation of fatty acids, electron transfer, and methanogenesis. The enzymes involved in each process were selected based on the literature review (Berghuis et al., 2019; Du et al., 2021; Enzmann et al., 2018; Fu et al., 2019; Kurth et al., 2020; Lie et al., 2012; Müller et al., 2010; Park et al., 2019; Schmidt et al., 2013; Sieber et al., 2015; Jessica R. Sieber et al., 2010; Sikora et al., 2018; G. Wang et al., 2020; Xiao et al., 2020; Ziels et al., 2019), and on the KEGG pathways information.

6.3. RESULTS

6.3.1. Characterization of stable butyrate-degrading enrichments

The continuous transfers of the cultures resulted in microbial enrichments with different performances regarding butyrate conversion to methane (Figure 6.2). Overall, the MP profiles of the cultures showed transiently acetate accumulation and consequently the division of MP profiles in two different slopes: the initial methane production rate (IMPR) was calculated in the first slope, which corresponded to the conversion of butyrate to methane and acetate, while a second methane production rate (MPR) was calculated in the second slope, which corresponded to the MP from acetate, as previously explained in Chapter 5 (subsection "5.2.3. Development of butyrate-

degrading enrichment cultures"). This transient accumulation of acetate was more evident in the enrichment cultures obtained from inoculum 1 (Figure 6.2a, 6.2b, 6.2c). Particularly, the kinetic parameters like lag phase duration, IMPR, and MPR were different regarding the enrichment conditions. The stable and well-adapted Bty-b1 enrichment (Figure 6.2a) showed a lag phase of approximately 2 d, while the other enrichments, AC-b1 and Mag-b1 (Figure 6.2b and 6.2c, respectively) started to produce methane after 1 d of incubation (Table 6.1). Thus, IMPR were faster in AC-b1 and Mag-b1 enrichments, comparing with IMPR in Bty-b1, and the highest IMPR was achieved by Mag-b1 enrichment (Table 6.1). Considering the stage of acetate conversion to methane, MPR was very slow (approximately 0.7 $mmol \cdot L^{-1} \cdot d^{-1}$) in AC-b1 enrichment, and faster in Mag-b2 enrichment (around 2.1 $mmol \cdot L^{-1} \cdot d^{-1}$) (Table 6.1). These differences in MPR contributed to the differences observed regarding the total time of incubation required for the complete conversion of butyrate to methane: 13 d for Mag-b1, 15 d for Bty-b1 and around 32 d for AC-b1 enrichment cultures. Regarding the enrichment cultures developed from inoculum 2 (Figure 6.2d and 6.2e), in the presence of Zeo, the lag phase was shorter and the IMPR and the MPR (Table 6.1) were faster than in the enrichment without Zeo, but it did not impact drastically the time of incubation since Zeo only reduced in 13 % the time required for butyrate degradation (Table 6.1).

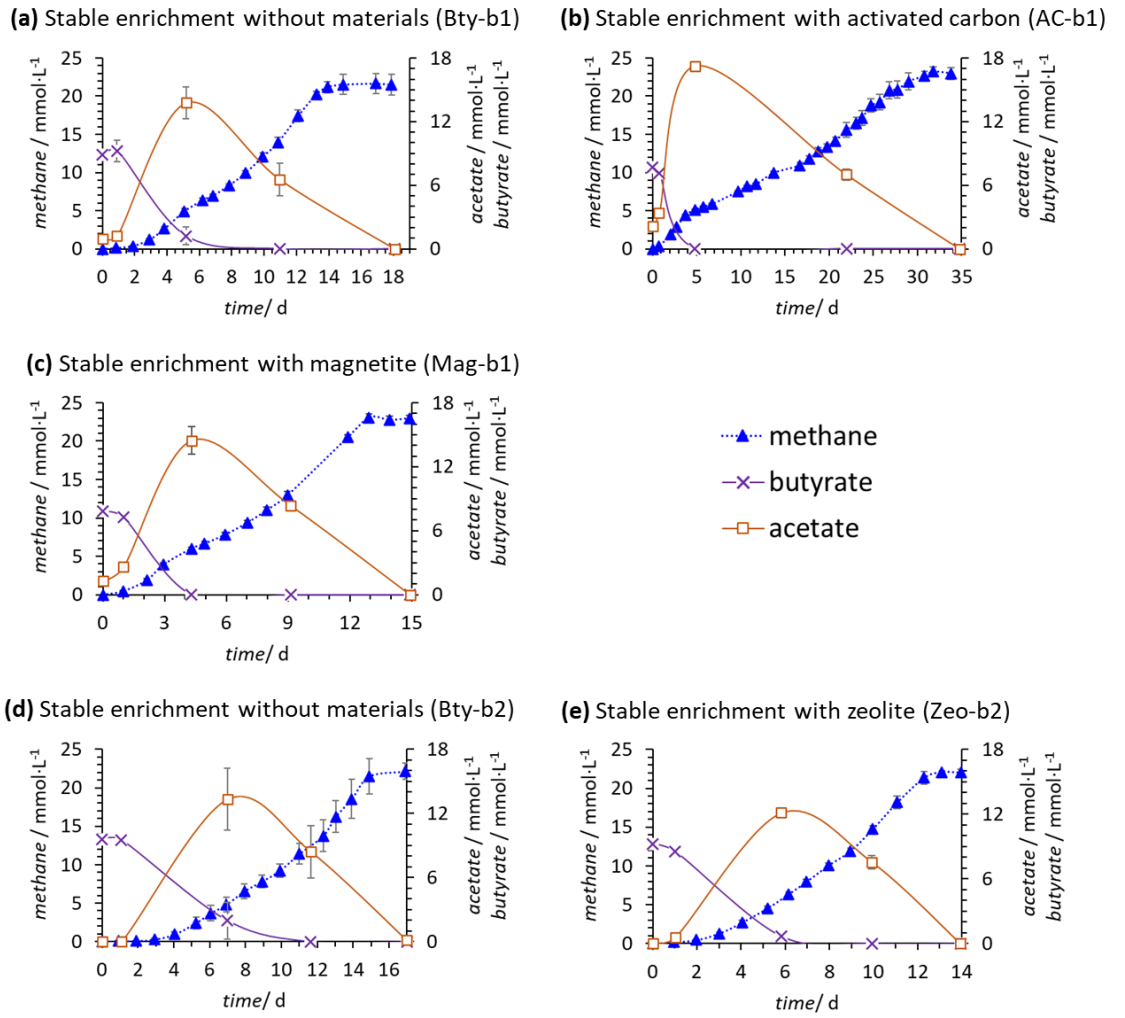

Figure 6.2. Cumulative MP, and butyrate and acetate consumption profiles, of well-adapted and stable butyrate-degrading enrichment cultures developed: a) without materials (Bty-b1), b) with AC (AC-b1), c) with Mag (Mag-b1), d) without materials (Bty-b2), and e) with Zeo (Zeo-b2). The results are the mean of three replicates with the respective standard deviation.

Microscopic observations performed during the development of the enrichment cultures also revealed potential differences regarding the microbial composition (Figure 6.3). Observations of abundant *Methanosaeta*-like cells (long filaments) were performed in all enrichments. In AC-enrichments, *Syntrophomonas*-like cells (slightly curved rods) and irregular cocci cells were also abundant (Figure 6.3b). On the other hand, *Methanosarcina*-like cells (cocci) were only detected in Mag-enrichments (Figure 6.3c).

Table 6.1. Characterization of butyrate-degrading enrichments without and with materials in terms of: number of transfers performed, lag phase duration, IMPR, MPR, and the time of incubation (t) required for the total conversion of butyrate to methane

Enrichment	**Number of transfers**	**Lag phase**/ d	**IMPR** [a]/ mmol·L^{-1}·d^{-1}	$R^{2\,a}$	**MPR** [b]/ mmol·L^{-1}·d^{-1}	$R^{2\,b}$	**t**/ d
Bty-b1	11	2	1.13 ± 0.11	0.91 ± 0.01	1.90 ± 0.18	0.98 ± 0.00	15
AC-b1	8	1	1.35 ± 0.03	0.99 ± 0.00	0.70 ± 0.05	0.97 ± 0.00	32
Mag-b1	11	1	1.72 ± 0.03	0.99 ± 0.00	2.12 ± 0.03	0.98 ± 0.00	13
Bty-b2	8	3	0.09 ± 0.04	0.90 ± 0.03	1.73 ± 0.18	0.98 ± 0.01	15
Zeo-b2	8	2	0.23 ± 0.04	0.99 ± 0.01	2.17 ± 0.07	0.98 ± 0.00	13

[a] IMPR was calculated for the first slope of MP: Bty-b1 between days 1 and 5; AC-b1 between days 1 and 4; Mag-b1 between days 1 and 4; Bty-b2 between days 0 and 3; Zeo-b2 between days 0 and 2.

[b] MPR was calculated for the second slope of MP: Bty-b1 between days 6 and 13; AC-b1 between days 5 and 29; Mag-b1 between days 5 and 13; Bty-b2 between days 4 and 14; Zeo-b2 between days 3 and 12.

In terms of growth media parameters, the presence of different materials altered the ORP values at the beginning of the assays, as Mag increased ORP values ((-254 ± 18) mV) compared with Bty-b1 enrichment ((-332 ± 6) mV), or Zeo that decreased the ORP values ((-336 ± 18) mV) in comparison with Bty-b2 incubation ((-273 ± 18) mV) (Table A. 10, Appendix). At the end of incubations, the ORP values were similar among different conditions, except for Mag incubations that presented higher ORP values. The values of pH were very close among conditions, between 7.3 and 7.4 either in the beginning or at the end of incubations (Table A. 10, Appendix). The exception was the medium growth with Zeo that reached a higher value of pH at the beginning and at the end of incubations (approximately 7.5). This was aligned with the fact that Zeo presented a basic character once its pH_{pzc} is around 11.6, and as a result the presence of Zeo may slightly increase the pH of the growth medium. On the other hand, the values of conductivity were not significantly different among the conditions for the enrichments developed from inoculum 1, except for the value of conductivity measured at the end of the growth medium in Mag-b1 incubation, which was the highest value registered ((7.35 ± 0.06) mS·cm^{-1}) (Table A. 10, Appendix). In the incubations obtained from inoculum 2, the values of conductivity of the growth medium were not significantly affected by the presence of Zeo.

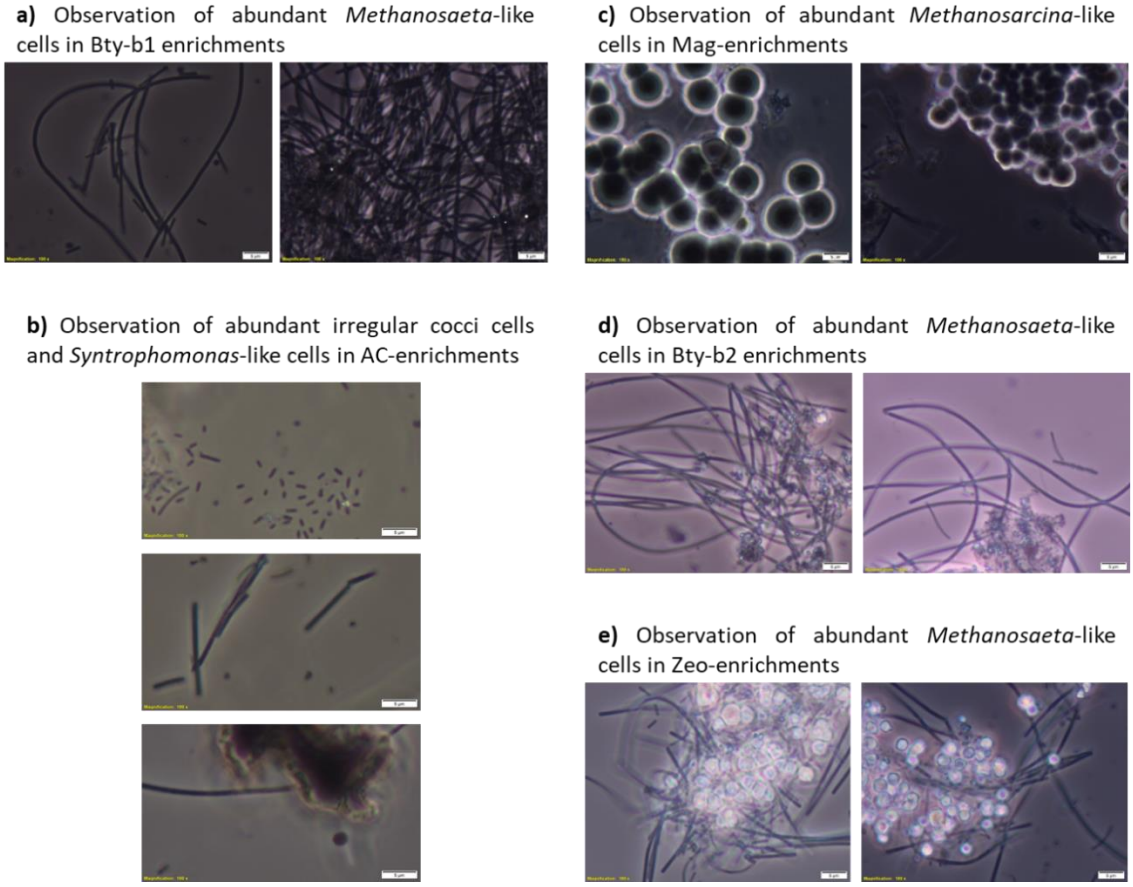

Figure 6.3. Microscopic observations during the development of the butyrate-degrading enrichments a) Bty-b1, b) AC-b1, c) Mag-b1, d) Bty-b2, and e) Zeo-b2. The images were captured with a magnification of 100×, which corresponds to a scale of 5 μm.

6.3.2. Microbial diversity of stable butyrate-degrading enrichments

Differences in the microbial composition between the initial inocula and butyrate-degrading enrichments were observed (Table 6.2; Table A. 11 presents the complete taxonomic characterization, Appendix). The major change during the enrichment process was the inversion in the relative abundances regarding methanogenic and bacterial groups of microorganisms. In the initial inoculum sludge, bacteria were highly abundant (i.e., around 61 % and 89 % in inocula 1 and 2, respectively) in the total microbial community. In the inoculum 2, the methanogenic archaea were even less abundant than in the inoculum 1. After successive transfers, the final communities were mainly enriched in microorganisms belonging to Archaea domain. Bty-b1 presented approximately 77 % of Archaea members and the other 23 % belonged to Bacteria; the community composition of AC-b1 was around 68 % of Archaea and 32 % of Bacteria; and in Mag-b1, approximately 79 % of relative abundance corresponded to Archaea members and 21 % to Bacteria.

In enrichments developed from inoculum 2, approximately 66 % and 75 % of microorganisms were assigned to Archaea in Bty-b2 and Zeo-b2, respectively, and the rest to Bacteria (34 % in Bty-b2 and 25 % in Zeo-b2). Within Archaea members, the relative abundances of the orders *Methanomicrobiales* (hydrogenotrophic methanogens) and *Methanosarcinales* (acetoclastic methanogens) varied as well among the different types of enrichments. In the enrichment cultures developed from inoculum 1, the Bty-b1 presented similar relative abundances of both orders, i.e., approximately 51 % of methanogens assigned to *Methanomicrobiales* and 49 % of methanogens belonging to *Methanosarcinales* order. In this enrichment, methanogens assigned to *Methanosaeta* genus were dominant (around 49 %), followed by *Methanospirillum* (approximately 34 %) and an unclassified genus within *Methanomicrobiaceae* (around 17 %), regarding the archaea community composition. In the presence of Mag, the enrichment in methanogens within *Methanomicrobiales* order (around 57 %) was a little bit higher, and the methanogens within *Methanosarcinales* order (approximately 43 %) was a little bit lower than in Bty-b1 enrichment. The presence of Mag also resulted in a more diverse archaea community composition, where it was detected genera like an unclassified genus within *Methanomicrobiaceae* (around 36 %), *Methanosaeta* (approximately 33 %), *Methanospirillum* (around 21 %), and *Methanosarcina* (approximately 10 %). On the other hand, in the presence of AC, the relative abundances of methanogens assigned to the orders *Methanomicrobiales* and *Methanosarcinales* were 78 % and 22 %, respectively. The relative abundance of *Methanosaeta* genus represented only approximately 22 % of the archaea community, while the unclassified genus within *Methanomicrobiaceae* represented around 43 %, and *Methanospirillum* genus about 35 %. Thus, during this first batch, the microorganisms belonging to *Methanomicrobiales* order were predominant. Conversely, during the second batch, the relative abundances of methanogens assigned to *Methanomicrobiales* order were 43 % and 38 %, while the methanogens assigned to *Methanosarcinales* order represented 57 % and 62 % in Bty-b2 and Zeo-b2 enrichment cultures, respectively. *Methanosaeta* genus was dominant in the archaea community in both enrichments (around 57 % in Bty-b2, and 61 % in Zeo-b2), followed by *Methanospirillum* (about 39 % in Bty-b2, and 28 % in Zeo-b2) and *Methanofollis* (approximately 4 % in Bty-b2, and 10 % in Zeo-b2) genera. The genera *Methanobacterium* and *Methanolinea* were found in the initial inocula sludge, but they were not enriched in the final enrichment cultures (Table 6.2).

Regarding bacterial community, relative abundance of most the bacteria identified in the enrichment cultures was ≤ 1.00 % (Table A. 11, Appendix). A slightly higher percentage was

observed only for bacteria assigned to *Anaerophaga* ((2.19 ± 0.14) %) in Bty-b1, ((3.16 ± 2.73) %) in AC-b1, ((1.36 ± 0.32) %) in Mag-b1 and ((1.55 ± 0.72) %) in Bty-b2; for some bacteria assigned to the phylum *Firmicutes* in Bty-b2 ((3.61 ± 3.93) %); and to *Desulfomicrobium* ((1.52 ± 1.09) %) in inoculum 2. On the other hand, bacteria assigned to the genera *Candidatus Cloacimonas* ((0.96 ± 0.74) %) and *Sulfuricurvum* ((1.21 ± 0.67) %) were found to be enriched only in Zeo-b2 when comparing with Bty-b2 ((0.14 ± 0.06) % and not detected, respectively). Bacteria assigned to *Levilinea* was in a relative abundance of ((0.57 ± 0.08) %) in Mag-b1, and lower abundance was detected in Bty-b1 or AC-b1 (Table A. 11, Appendix). This genus was also in a relative abundance of ((0.21 ± 0.14) %) in Bty-b2 and < 0.01 % in Zeo-b2. Other unclassified bacteria (some of them assigned to the phylum *Spirochaetes*, to the class *Clostridia*, and to the orders *Desulfuromonadales*, *Syntrophobacterales* and *Synergistales*) were detected with different relative abundances (up to 7 % of the total microbial community) regarding the microbial community under investigation (Table A. 11, Appendix). In all enrichments, *Syntrophomonas* species were the most abundant bacteria, representing over 11 % of the total microbial community and over 44 % of the bacterial community, although it was not detected in the inocula sludge. The high abundance of this genus was detected in AC-b1 enrichment ((26.18 ± 12.40) %, Table 6.2), representing around 82 % of the bacterial community, which is in accordance with the observations performed during microscopy observations (Figure 6.3b). On the other hand, although the genera *Geobacter* and *Syntrophobacter* were in relatively high abundances in the inocula sludge, these genera were not detected in the microbial enrichments after more than 6 successive transfers (Table 6.2).

Table 6.2. Taxonomic characterization presented at the Genus level (at relative abundance ≥ 2.00 %) of anaerobic inocula sludge and stable butyrate-degrading enrichment cultures, with and without (nano)materials, based on 16S rRNA gene amplicon sequencing. The relative abundance of each taxon (given in percentage) is the average and standard deviation for (at least) duplicate samples

Kingdom	Phylum	Class	Order	Family	Genus	Inoc-b1	Bty-b1	AC-b1	Mag-b1	Inoc-b2	Bty-b2	Zeo-b2
Archaea	*Euryarchaeota*	*Methanobacteria*	*Methanobacteriales*	*Methanobacteriaceae*	*Methanobacterium*	9.00 ± 3.26	nd	< 0.50	< 0.50	3.71 ± 2.31	< 0.50	nd
Archaea	*Euryarchaeota*	*Methanomicrobia*	*Methanomicrobiales*	*Methanomicrobiaceae*	*Methanofollis*	nd	< 0.50	< 0.50	< 0.50	nd	2.42 ± 1.36	7.82 ± 0.79
Archaea	*Euryarchaeota*	*Methanomicrobia*	*Methanomicrobiales*	*Methanomicrobiaceae*	Unclassified	nd	12.95 ± 2.82	29.22 ± 16.75	28.32 ± 2.57	nd	nd	nd
Archaea	*Euryarchaeota*	*Methanomicrobia*	*Methanomicrobiales*	*Methanoregulaceae*	*Methanolinea*	9.07 ± 0.63	< 0.50	< 0.50	nd	2.70 ± 2.18	< 0.50	nd
Archaea	*Euryarchaeota*	*Methanomicrobia*	*Methanomicrobiales*	*Methanospirillaceae*	*Methanospirillum*	< 0.50	25.88 ± 0.89	23.64 ± 2.77	16.53 ± 0.68	nd	25.47 ± 1.27	20.87 ± 0.03
Archaea	*Euryarchaeota*	*Methanomicrobia*	*Methanosarcinales*	*Methanosaetaceae*	*Methanothix*	20.00 ± 0.96	37.27 ± 2.01	14.88 ± 2.95	25.72 ± 0.51	4.13 ± 5.60	37.19± 16.64	46.21 ± 2.93
Archaea	*Euryarchaeota*	*Methanomicrobia*	*Methanosarcinales*	*Methanosarcinaceae*	*Methanosarcina*	nd	< 0.50	nd	8.21 ± 10	nd	< 0.50	nd
Bacteria	*Bacteroidetes*	*Bacteroidia*	*Bacteroidales*	*Marinilabiliaceae*	*Anaerophaga*	< 0.50	2.19 ± 0.14	3.16 ± 2.73	1.36 ± 0.32	< 0.50	.1.55 ± 0.72	< 0.50
Bacteria	*Firmicutes*	*Clostridia*	*Clostridiales*	*Syntrophomonadaceae*	*Syntrophomonas*	nd	15.62 ± 0.08	26.18 ± 12.40	12.43 ± 0.49	nd	15.43 ± 7.44	10.91 ± 1.84
Bacteria	*Firmicutes*	*Clostridia*	Unclassified	Unclassified	Unclassified	< 0.50	< 0.50	< 0.50	nd	0.61 ± 0.50	< 0.50	6.99 ± 2.27
Bacteria	*Firmicutes*	Unclassified	Unclassified	Unclassified	Unclassified	< 0.50	< 0.50	nd	< 0.50	< 0.50	3.61 ± 3.93	< 0.50
Bacteria	*Proteobacteria*	*Deltaproteobacteria*	*Desulfovibrionales*	*Desulfomicrobiaceae*	*Desulfomicrobium*	< 0.50	< 0.50	< 0.50	< 0.50	1.52 ± 1.09	< 0.50	< 0.50
Bacteria	*Proteobacteria*	*Deltaproteobacteria*	*Desulfuromonadales*	*Geobacteraceae*	*Geobacter*	14.42 ± 0.89	< 0.50	< 0.50	< 0.50	27.32 ± 1.59	< 0.50	nd
Bacteria	*Proteobacteria*	*Deltaproteobacteria*	*Desulfuromonadales*	Unclassified	Unclassified	< 0.50	nd	< 0.50	nd	6.49 ± 6.80	< 0.50	nd
Bacteria	*Proteobacteria*	*Deltaproteobacteria*	*Syntrophobacterales*	*Syntrophobacteraceae*	*Syntrophobacter*	15.87 ± 0.84	nd	nd	nd	26.32 ± 9.57	< 0.50	< 0.50

Table 6.2. Continued. Taxonomic characterization presented at the Genus level (at relative abundance ≥ 2.00 %) of anaerobic inocula sludge and stable butyrate-degrading enrichment cultures, with and without (nano)materials, based on 16S rRNA gene amplicon sequencing. The relative abundance of each taxon (given in percentage) is the average and standard deviation for (at least) duplicate samples

Kingdom	Phylum	Class	Order	Family	Genus	Inoc-b1	Bty-b1	AC-b1	Mag-b1	Inoc-b2	Bty-b2	Zeo-b2
Bacteria	*Proteobacteria*	*Deltaproteobacteria*	*Syntrophobacterales*	Unclassified	Unclassified	0.62 ± 0.09	nd	< 0.50	< 0.50	2.75 ± 0.74	< 0.50	nd
Bacteria	*Proteobacteria*	Unclassified	Unclassified	Unclassified	Unclassified	4.19 ± 0.75	< 0.50	< 0.50	nd	0.54 ± 0.34	< 0.50	nd
Bacteria	*Synergistetes*	*Synergistia*	*Synergistales*	Unclassified	Unclassified	< 0.50	< 0.50	.0.62 ± 0.11	< 0.50	< 0.50	0.72 ± 0.02	2.39 ± 0.40
Bacteria	Unclassified	Unclassified	Unclassified	Unclassified	Unclassified	18.64 ± 2.73	1.68 ± 0.43	< 0.50	4.65 ± 0.61	14.15 ± 3.05	11.10 ± 2.04	1.17 ± 0.60

nd – not detected.

Inoc-b1 – Inoculum for the first batch of experiments; Inoc-b2 – Inoculum for the second batch of experiments.

6.3.3. Metatranscriptomics analysis of stable butyrate-degrading AC-enrichment

Gene expression during butyrate degradation in the presence of AC was explored through metatranscriptomics analysis during the initial phase of MP using the AC-b1 enrichment culture. The results obtained revealed that 59 % of the genes were expressed by microorganisms belonging to Archaea, and 36 % by members of Bacteria (Figure 6.4a). Among methanogens, hydrogenotrophic microorganisms belonging to *Methanomicrobiales* represented over 55 % of gene expression, with *Methanofollis* (35 % of the total expression) and *Methanospirillum* (21 % of the total expression) as the most active methanogens, and acetoclasts assigned to *Methanosarcinales* represented 32 %, with *Methanothrix* as the most active methanogen converting acetate to methane (22 % of the total expression). Regarding the total expression by bacteria community, 56 % was assigned to *Firmicutes*. Around 94 % of the genes involved in β-oxidation were assigned to *Syntrophomonadaceae bacterium* (Figure 6.4b).

A schematic representation of the suggested syntrophic interactions occurring in the butyrate degrading enrichment developed with AC, based on the metatranscriptomics analysis, is given in Figure 6.5.

Abbreviations used in Figure 6.5: CoA - coenzyme A; EC number – enzyme commission numer; CoB - coenzyme B; CoM - coenzyme M; Fd - ferredoxin; Fd_{ox} - oxidized ferredoxin; Fd_{red} - reduced ferredoxin; ATPase - ATP synthase. Syntrophic butyrate metabolism: Act - acetyl-CoA acetyltransferase; Bcd - butyryl-CoA dehydrogenase; Ctr - crotonyl-CoA hydratase; HbdH - 3-hydroxybutyryl-CoA dehydrogenase; AtoB - acetyl-CoA C-acetyltransferase; Pta - phosphate acetyltransferase; Ak - acetate kinase; Hyd1 - electron confurcating hydrogenase; Hyd2 - membrane-bound [FeFe]-hydrogenase; Hyd3 - ferredoxin dependent hydrogenase; Fdh1, Fdh3 - formate dehydrogenases; Fdh2, Fdh4 - formate dehydrogenase (membrane bound, quinone reducing); Hdr - Heterodisulfide reductase; Fnt - formate transporter; MQ - menaquinone; EtfAB - Electron transfer flavoproteins A and B; FeS - complex membrane bound FeS-oxidoreductase; Fix complex - electron transfer flavoprotein:associated ferredoxin. Hydrogenotrophic metabolism: Mtr - tetrahydromethanopterin S-methyl-transferase; Mcr - methyl-coenzyme M reductase; Hdr - soluble heterodisulfide reductase; Fdh - formate dehydrogenase; Mvh - F_{420}-non-reducing hydrogenase; Frh - coenzyme F_{420}-reducing hydrogenase; Fwd - formyl-methanofuran dehydrogenase; Eha - energy-converting hydrogenase A; MFR - methanofuran; Ftr - Formyl-methanofurantetrahydromethanopterin formyl-transferase; H_4MPT – tetrahydromethanopterin; Mch - Methenyl-tetrahydromethanopterin cyclohydrolase; Hmd - H_2-dependent methylenetetrahydromethanopterin dehydrogenase; Mer - 5,10- methylenetetrahydromethanopterin reductase. Acetoclastic metabolism: Ack - Acetate kinase; At - phosphate acetyltransferase; Acs - acetyl-CoA decarbonylase/synthetase; Codh - carbon-monoxide dehydrogenase; Codh-Acs - carbon monoxide dehydrogenase/acetyl-CoA decarbonylase/synthase complex; MtrA-H - tetrahydromethanopterin S-methyltransferase; McrABG - methyl-coenzyme M reductase; HdrDE - membrane-bound heterodisulfide reductase; Ech - energy-converting hydrogenase; MPh – methanophenazine.

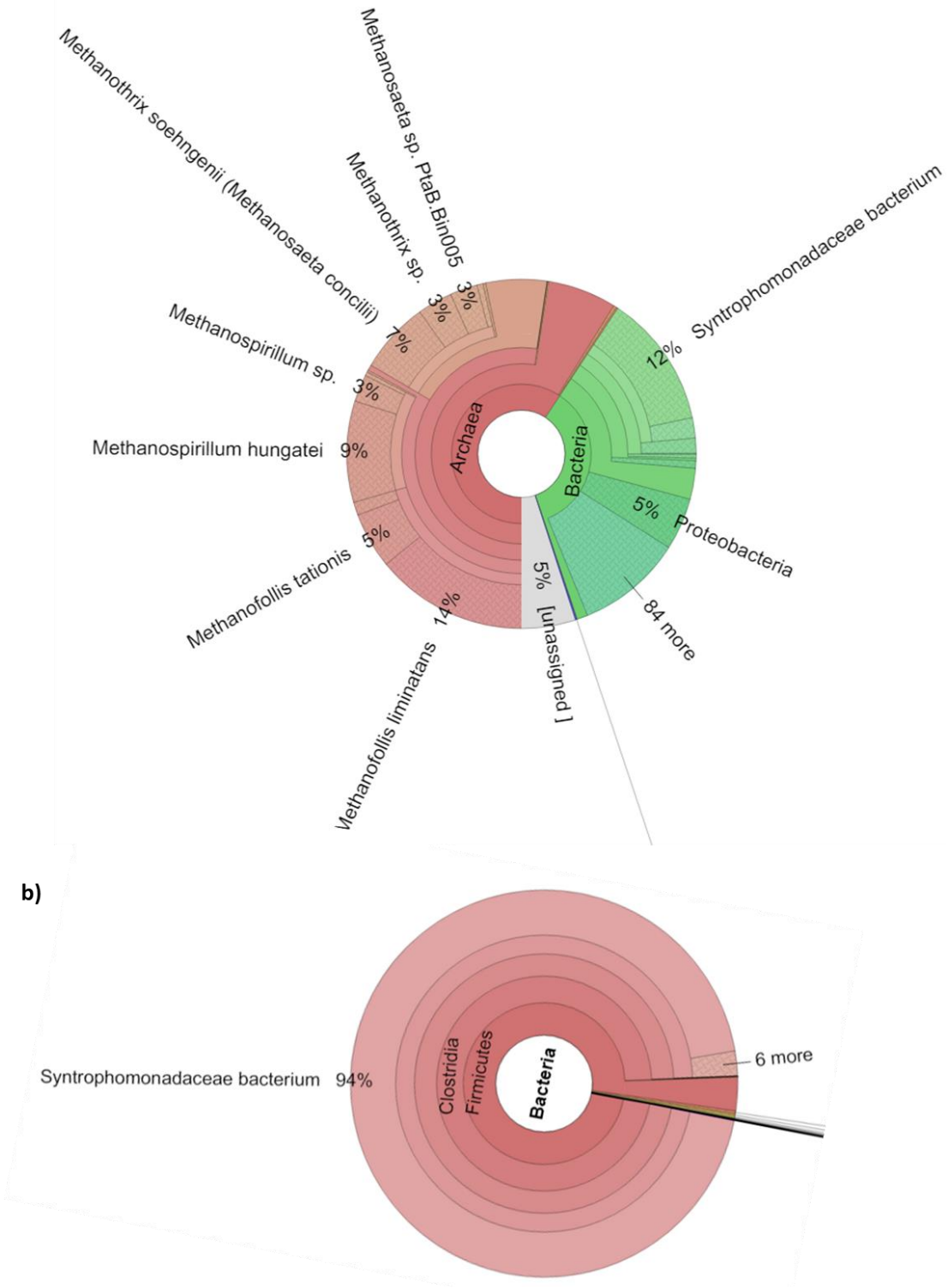

Figure 6.4. Krona plots showing the gene expression by microbial taxa during butyrate degradation in AC-enrichment cultures. (a) total gene expression by the microbial enrichment and (b) taxonomic assignment of genes involved in β-oxidation.

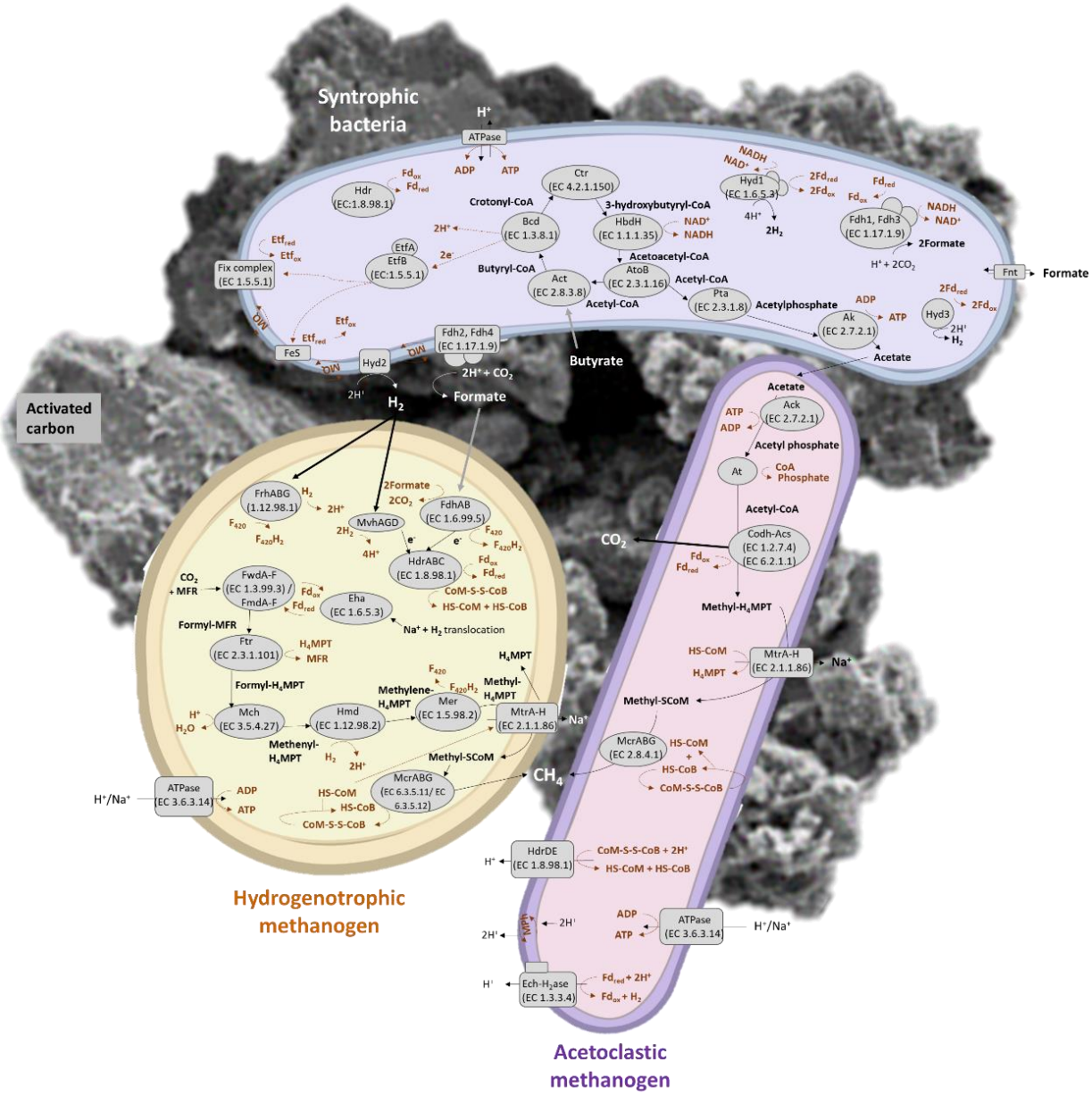

Figure 6.5. Scheme of the syntrophic butyrate degradation occurring in AC-enrichment, where most of the β-oxidation enzymes were assigned to *Syntrophomonadaceae spp.,* and genes involved in the MP via hydrogenotrophic pathway was mainly assigned to the genera *Methanofollis and Methanospirillum*, while MP via acetoclastic pathway was attributed to the activity of *Methanothrix.* Support references: (Enzmann et al., 2018; Kurth et al., 2020; Lie et al., 2012; Jessica R. Sieber et al., 2010; Stams et al., 2012; Stams and Plugge, 2009; Ziels et al., 2019).

6.4. Discussion

The differences found in the efficiency of butyrate conversion to methane by the enrichment cultures developed (with and without AC, Mag and Zeo) can be related with changes in microbial community

composition induced by each type of material. Bty-enrichments were efficient in butyrate conversion to methane (around 15 d of incubation time), but the cultures adapted to the materials (Mag or Zeo) were even more efficient (approximately 13 d of incubation time). On the other hand, the presence of AC affected the rate of acetate conversion to methane which caused the need of long incubation periods (approximately 32 d) for the complete butyrate degradation, although the conversion of butyrate to methane and acetate was fast (Table 6.1). Differences on the relative abundance of certain microorganisms in the enrichment culture (Table 6.2, Table A. 11, Appendix) may explain the distinct performances. In the presence of AC, hydrogenotrophic methanogens were highly enriched (assigned to *Methanomicrobiales*), while a lower abundance of acetoclastic methanogens was detected (within *Methanosarcinales*). These results were aligned with the slow acetate consumption observed in AC-b1 enrichment, resulting in the slowest EMPR and in the highest time of incubation for the total conversion of butyrate to methane (Table 6.1). The loss of acetoclastic methanogens and incomplete conversion of butyrate to methane was also previously reported in enrichment studies but in the presence of Mag (Fu et al., 2018). Thus, the results suggested that the presence of different materials impact the relative abundance of microorganisms, which could be related with higher or lower affinity of cells for each type of material. For instance, regarding specific enrichment taxa, it is interestingly that *Methanosarcina* was only enriched in Mag-b1 culture. This genus is known to perform the reduction of Fe(III) (present in Mag composition) as demonstrated previously in other studies (Fu et al., 2019; H. Wang et al., 2020). In fact, this could explain the longer periods preceding acetate consumption observed in the initial incubations of Mag-enrichments (data not shown), which could serve for cells to produce cellular structures (e.g., cytochromes) required for redox cycle of Fe(III)/Fe(II). After the adaptation of the cultures, it was observed that the overall efficiency was improved. The stimulation of acetoclastic activity in the presence of Mag was also previously reported in other studies (Fu et al., 2019; H. Wang et al., 2020; Wu et al., 2020).

In all enrichments, *Syntrophomonas* spp. were the most abundant bacteria, which was not surprisingly since this genus is known to be involved in butyrate degradation (J R Sieber et al., 2010; Stams et al., 2012; Stams and Plugge, 2009; Ziels et al., 2019). Although *Syntrophomonas* spp. is a well-known bacterium to exchange electrons with methanogenic archaea via IHT/IFT, some reports raised the hypothesis that IET via CM took place instead (Fu et al., 2018; W. Zhang et al., 2018). On the other hand, previous microbial enrichment studies with CM showed that electroactive bacteria like *Geobacter* spp. were enriched in the presence of biochar (growing on ethanol) (Yuan et al., 2018), GAC (growing on acetate) (Amelia-Elena et al., 2018), Mag (growing on butyrate) (Li et al., 2015), and Mag (growing on ethanol or acetate) (Kato et al., 2012), and suggested that CM stimulated CIET between *Geobacter* and

methanogens. In this study, *Geobacter* was found abundantly in both inocula (inoculum 1 and inoculum 2, Table 6.2), but it was not detected in the enrichment cultures, although the presence of CM and/or the presence of carbon sources (butyrate and acetate) which *Geobacter* species can utilize (Aklujkar et al., 2009; Lovley et al., 2011) could eventually stimulate their enrichment. Similarly, reports in the literature showed that *Geobacter* spp. were not enriched in other microbial enrichment in the presence of: Mag and acetate (Fu et al., 2019; H. Wang et al., 2020); Mag or CNT, and propionate (Xia et al., 2019); Mag or CNT, and butyrate (Fu et al., 2018; Zhang and Lu, 2016); CNT and butyrate (W. Zhang et al., 2018).

In this study, gene expression analysis allowed to conclude that butyrate was likely degraded by *Syntrophomonadaceae* spp. via β-oxidation, in syntrophic cooperation with hydrogenotrophs (mainly *Methanofollis* and *Methanospirillum*) via typical IHT/IFT, and *Methanothrix* as the acetoclastic methanogen (Figure 6.5). The families *Methanomicrobiaceae* and *Methanospirillaceae* are known to produce methane using as substrate H_2/CO_2 (Garcia et al., 2006), while *Methanosarcinales* order include the acetate consumers (Kendall and Boone, 2006). The results showed a higher expression of genes assigned to hydrogenotrophic methanogens, which makes sense since samples for metatranscriptomics analysis were taken during the first days of incubation, when MP resulted mainly from hydrogen consumption (highly consumed by methanogens within *Methanomicrobiaceae*). So, a lower contribution of acetoclastic activity was expected during this phase of butyrate degradation, as acetate was transiently accumulated and used to be degraded slower by this enrichment. According to the results of microbial composition, the most abundant methanogens (in relative abundance) belonged to an unclassified genus within *Methanomicrobiaceae* family, which probably correspond to the *Methanofollis* genus found as highly active by the metatranscriptomics analysis. In fact, during microscopy inspection in samples of AC-enrichment, many *Methanofollis*-like cells (Garcia et al., 2006) could be observed, which present a typical irregular cocci cell shape (Figure 6.3b). On the other hand, taxonomic analyses revealed the genus *Syntrophomonas* as the most abundant bacteria in the enrichment (around 26 % of relative abundance, Table 6.2), while the gene expression was attributed to *Syntrophomonadaceae* spp. Taking all these results into consideration, one can conclude that microorganisms assigned to *Syntrophomonas* are the ones responsible for butyrate degradation in this enrichment. Most of the genes coding for β-oxidation enzymes were assigned to *Syntrophomonadaceae bacterium*, but the taxonomic analysis identified *Syntrophomonas* genus as the most abundant within *Syntrophomonadaceae* family, and no *Syntrophomonadaceae bacterium* could be identified. This probably happened since the genes expressed were identified towards the genes present in public databases, which correspond to the genes from

microorganisms which genomes are sequenced, or environmental metagenomes. Few *Syntrophomonas* species are sequenced so far, and probably in this enrichment culture the *Syntrophomonas* species present does not have its genome sequenced. For this reason, the genes of this microorganism will be assigned to the genes of close relatives, in this case to *Syntrophomonas wolfei*, *Syntrophomonas zehnderi* and also *Syntrophomonadaceae bacterium*. According to the genes expression results, genes involved in syntrophic IHT were highly expressed (e.g., hydrogenases), while no genes related to DIET (e.g, *Omc*S, *Pil*A (Van Steendam et al., 2019)) could be detected. These results suggest that DIET or CIET did not take place in this enrichment culture.

6.5. CONCLUSIONS

Different specialized butyrate-degrading microbial enrichments were developed with and without AC, Mag and Zeo. The methanogenic performance of each enrichment culture was evolved over time and differences in methanogenic activity were observed regarding the type of material present. The best performance regarding the overall butyrate degradation was achieved by Mag-enrichment culture, but Zeo also demonstrated potential to enhance microbial activity. Thus, materials like Mag and Zeo are potential candidates to be used in anaerobic digestion for the treatment of organic wastes, increasing the overall rates of methanogenesis. The results also highlighted the potential of AC to accelerate IHT/IFT by favouring the enrichment in hydrogenotrophic methanogens. The metatranscriptomics results did not show evidence of changes in the traditional electron transfer mechanisms (IHT/IFT) used in syntrophic communities in the presence of AC.

CHAPTER 7

7. GENERAL CONCLUSIONS AND SUGGESTIONS FOR FUTURE WORK

7.1. GENERAL CONCLUSIONS

The work presented in this thesis contributed to raise the level of knowledge regarding the effects of different (nano)materials towards the methanogenic activity of simpler methanogenic cultures and more complex microbial communities. The main conclusions obtained were the following:

i. (nano)Materials such as activated carbon (AC), magnetite (Mag) and zeolite (zeo), despite their physicochemical differences, enhanced methanogenic activity, by decreasing the lag phases preceding methane production (MP) and increasing the methane production rates (Chapters 3, 4, 5).

ii. None of the following characteristics of the materials, per se, can explain the improvements on MP: specific surface area, area of mesopores, volume of micropores, electrical conductivity, material acidity/basicity, or impurities present on material composition (like sulfur and nitrogen) (Chapter 3).

iii. Silicon was an element common to all materials tested and, per se, was proved to stimulate the methanogenic activity by mechanisms yet unknown. Possibly, silicon has a role in nutritional or biological functions in some methanogens, but further investigation is needed to draw this conclusion (Chapter 3).

iv. Changes on redox potential, pH and conductivity of the growth medium were not directly correlated with the enhancement of MP (Chapters 3, 4, 5, 6).

v. Different concentrations of (nano)materials caused different impact on MP by pure cultures of methanogens, as it was observed in the incubations with *Methanobacterium formicicum* (Chapter 3).

vi. Different materials can affect differently the same methanogen. For example, *M. formicicum* was highly stimulated by AC and severely inhibited by Mag (Chapters 3 and 4).

vii. The same (nano)material does not affect different species in the same way. For instance, the presence of Mag drastically inhibited the methanogenic activity of *M. formicicum* but caused no effect on MP by *Methanosarcina barkeri* (both growing on H_2/CO_2). Also, the presence of Zeo enhanced methane production rates when incubated with *M. formicicum* and *Methanothrix harundinacea*, but Zeo had no effect on the methanogenic activity of *Methanospirillum hungatei* and *M. barkeri* (Chapter 4).

viii. The effect of materials in different pure cultures of methanogens does not seem to be related with acetoclastic or hydrogenotrophic metabolism, since the results suggested that individual species would be differently affected independently of the substrate used. For instance, the methanogenic activity of either *M. formicicum* growing on H_2/CO_2 or *M. harundinacea* growing on acetate was stimulated in the presence of AC and Zeo (Chapter 4).

ix. The effect of (nano)materials (like AC and Mag) also depends on the type of syntrophic coculture under study, as the metabolism of the syntrophic coculture *S. zehnderi* and *M. formicicum* can

be highly stimulated in the presence of AC, and drastically inhibited in the presence of Mag. Another coculture, composed by *S. wolfei* with *M. hungatei*, was not affected by (nano)materials (Chapter 4).

x. The effect of different (nano)materials varied according with the initial microbial activity, i.e., cultures with a high methanogenic activity do not benefit from the presence of materials, but less active cultures are greatly affected by materials, usually enhancing methanogenic activity. For instance, MP by *M. formicicum* was generally highly stimulated by AC but adding AC during the exponential growth phase had no effect as the culture was highly active (as showed by methanogenic activity performance of the biotic control without AC). This relation between the microbial activity and the effect of (nano)materials was also observed during the development of enrichment cultures with different (nano)materials, and during the operation of the anaerobic bioreactor with anaerobic sludge, degrading a mixture of volatile fatty acids (acetate, propionate, butyrate) and ethanol, in the presence and absence of granular AC (Chapters 4 and 5).

xi. The microbial composition of butyrate-degrading enrichment cultures differed depending on the material present (Chapter 6).

xii. The presence of different (nano)materials did not favour the enrichment in electroactive species (e.g., *Geobacter*), although this genus has been detected in the inoculum sludge used to start the enrichments (Chapter 6).

xiii. Gene expression, taxonomic and microscopic analyses indicated that microorganisms closed related to *Syntrophomonas* were responsible for butyrate conversion to acetate and hydrogen, in the enrichment cultures developed with and without (nano)materials, and no genes associated to DIET/CIET were detected (Chapter 6).

7.2. SUGGESTIONS FOR FUTURE WORK

Although a lot is known about the effect of (nano)materials in methanogenic processes, there are important questions which remain without answers. The increase of knowledge in this subject is fundamental for the application of nano(materials) in anaerobic digestion of waste and wastewater. Some approaches can be used to get more insights about the mechanisms behind MP improvement by (nano)materials, such as the following suggestions:

1) To investigate the influence of physical/chemical characteristics of (nano)materials and to try to correlate with the impact on microbial methanogenic activities. The modification of materials or the preparation of composites by impregnation of the surface with specific chemical elements could help to find the main property or factor behind the enhancement of MP. For instance, to explore the effect of silicon (present in the composition of (nano)materials), composite materials with different concentrations of silicon could be prepared and tested in batch assays. This could help to evaluate better if the presence of this element would contribute or not to stimulate the methanogenic activity, and at which extent according to the amount present in the material. Also, it can be considered to investigate other properties of materials like roughness (once it can influence the suitability for biofilm formation), by testing materials differing in this property (e.g., activated carbon, graphene, vitreous carbon, graphite, carbon nanotubes) or even to evaluate the effect of particle size on methanogenic activity.

2) To perform batch assays with different methanogenic pure cultures and syntrophic cocultures in the presence of different (nano)materials, including sand and glass beads. It could help to clarify the effect of these type of materials on MP for different species and on syntrophic interactions, also helping to understand the potential of these materials to accelerate MP in order to be applied in more complex communities, degrading more complex substrates.

3) To assess the potential of (nano)materials to treat real and complex organic waste, like sewage sludge, by operating lab scale bioreactors with and without (nano)materials in order to quantify the impact of the (nano)materials on biogas production (and MP efficiency).

4) To evaluate metabolic changes in pure cultures of methanogens, syntrophic cocultures and complex microbial communities in bioreactors with and without (nano)materials, additional (meta)genomics and (meta)transcriptomics analyses could be performed. Molecular methods based on 16S rRNA collected from RNA extracts in alternative to DNA extracts, and measurements of the enzyme's activities (genes expression profiles) revealed to be useful and could be applied in further studies, helping to draw more reliable conclusions and to link microbial identity to activity in incubations with and without (nano)materials. The combination of these approaches with microscopy techniques was also important

to observe the organization and interaction of cell-cell and cells-(nano)materials, thus these techniques could be also applied in future studies to understand better the effects of (nano)materials in contact with different anaerobic microorganisms. Materials can affect the proximity of cells, which favours biofilm formation, intercellular signalling, or quorum sensing, which could also contribute to improve the cell activity.

The results of the effects of (nano)materials in systems with different complexity towards MP, combined with results at gene expression level, would help to understand how (nano)materials modulates intra- and inter-species interactions and improves microbial activities, particularly the acceleration of methane production. Once revealed the mechanisms behind the improvements on methane production rates by (nano)materials, (nano)materials-catalyzed anaerobic digestion processes could be developed.

APPENDIX

APPENDIX - FIGURES

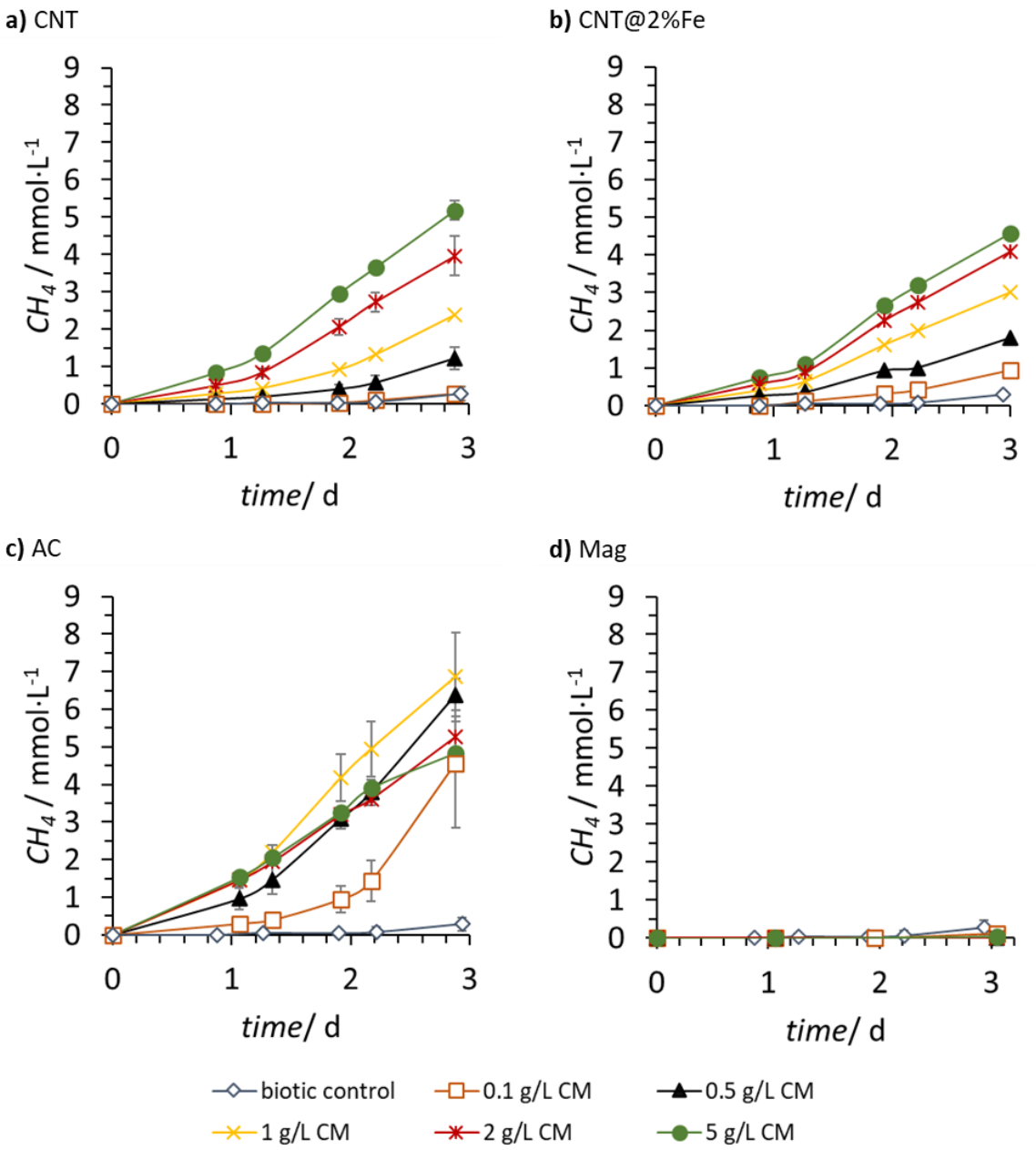

Figure A. 1. Profiles of cumulative methane production for increasing concentrations of conductive materials (CM) incubated with *M. formicicum* during the first 3 d of incubation.

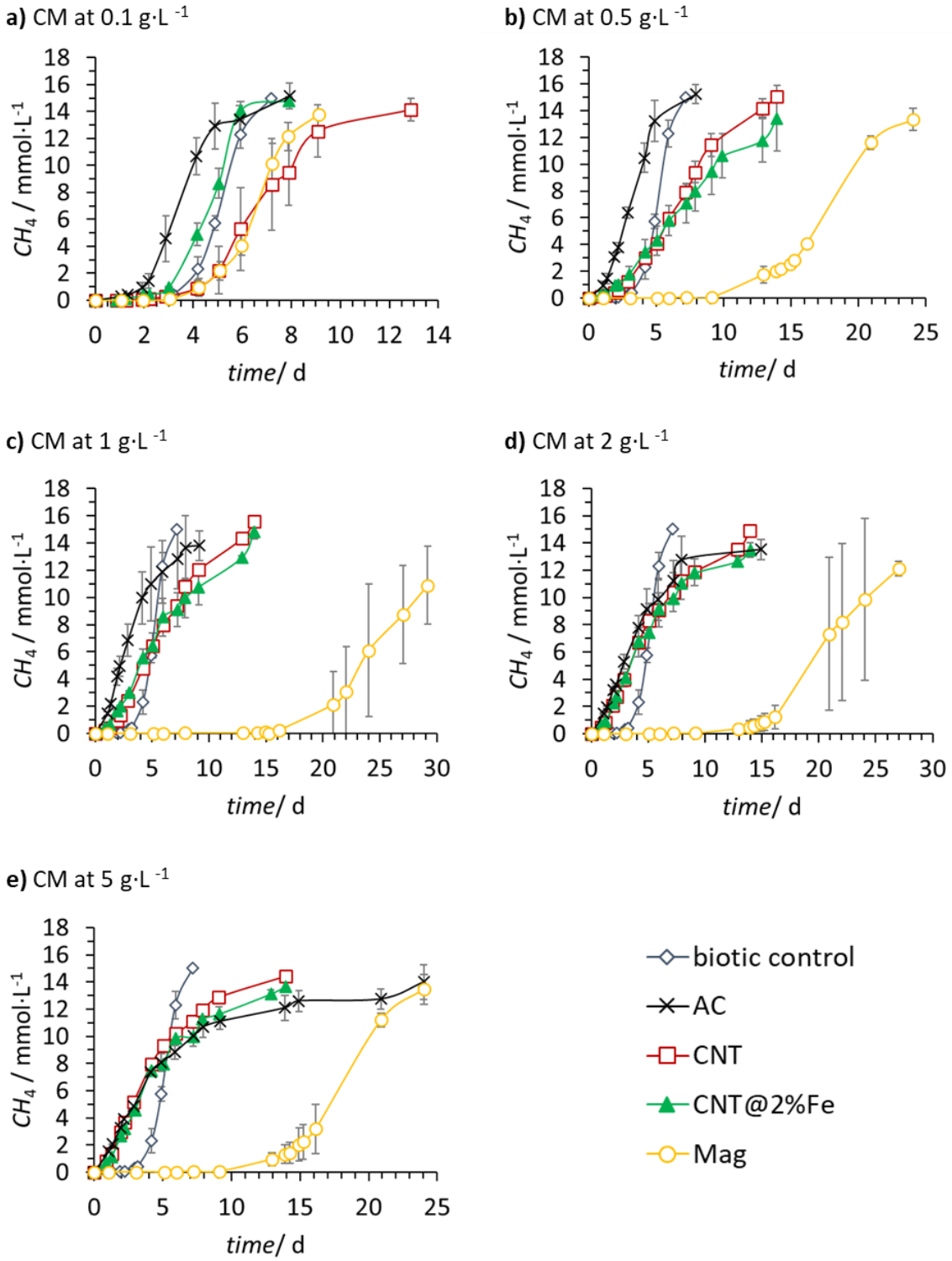

Figure A. 2. Complete profiles of cumulative methane production for the incubations of *M. formicicum* with different concentrations of conductive materials.

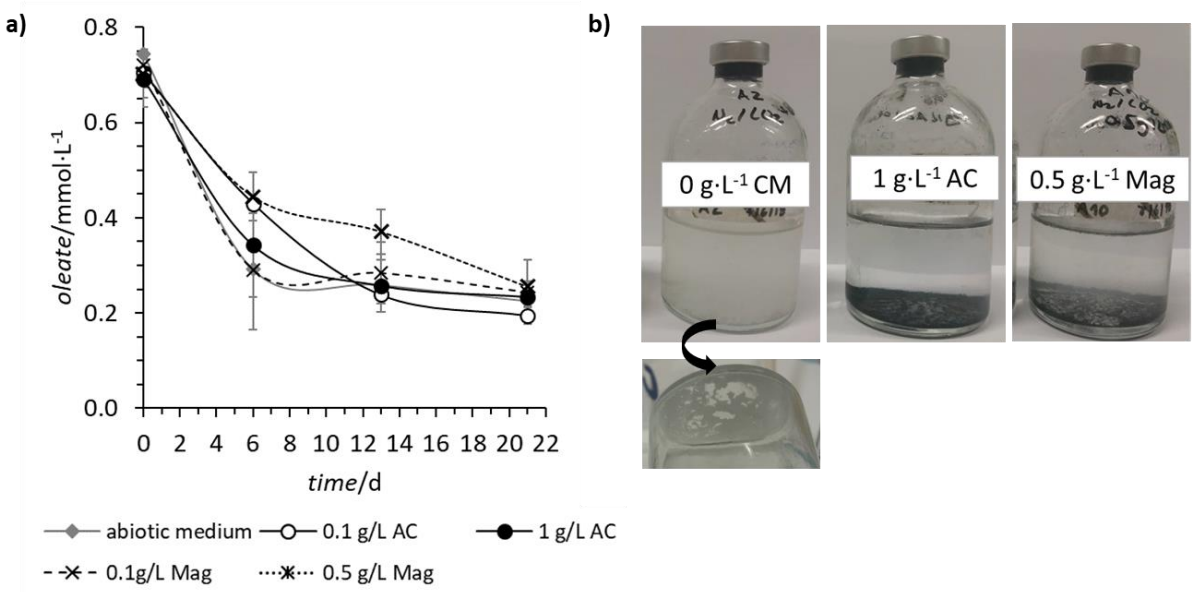

Figure A. 3. a) Variation of oleate concentration over time during abiotic experiments with and without activated carbon (AC, batch 1), and with magnetite (Mag), at different concentrations. Oleate quantification was affected by its poor solubility and tendency to be adsorbed in surfaces/materials. b) Images of the bottles in abiotic conditions with and without materials, and visual differences in the turbidity of the medium.

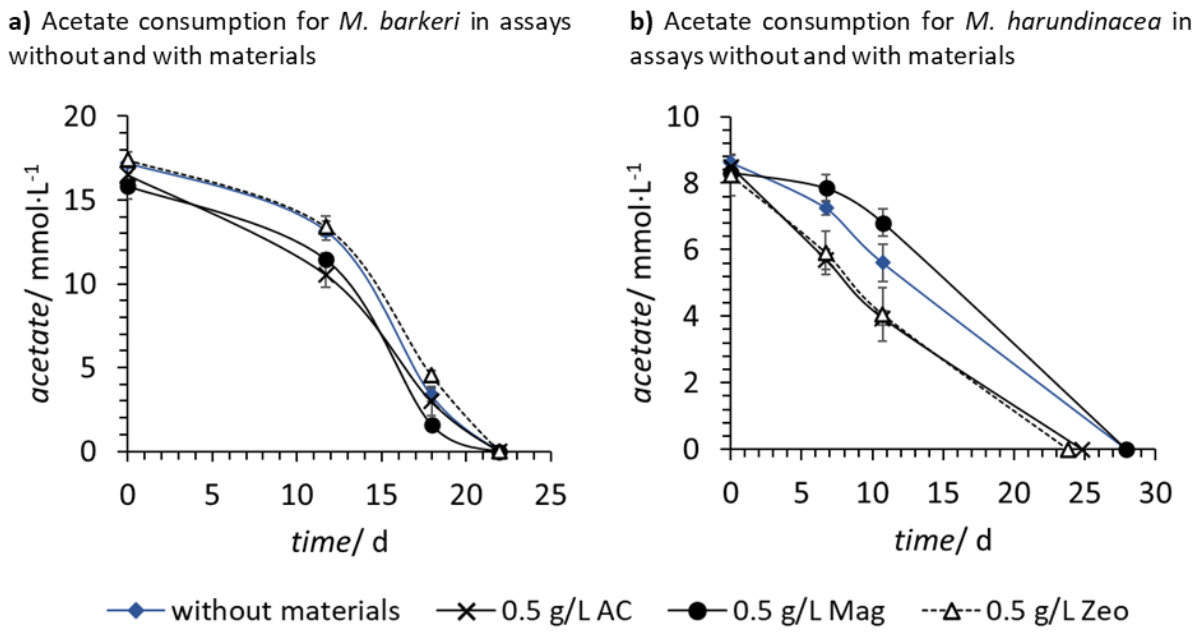

Figure A. 4. Acetate consumption over time for pure cultures of a) *M. barkeri* and b) *M. harundinacea*, growing without and with different materials (AC (batch 2), Mag, Zeo). The results are the mean and standard deviation of triplicate assays.

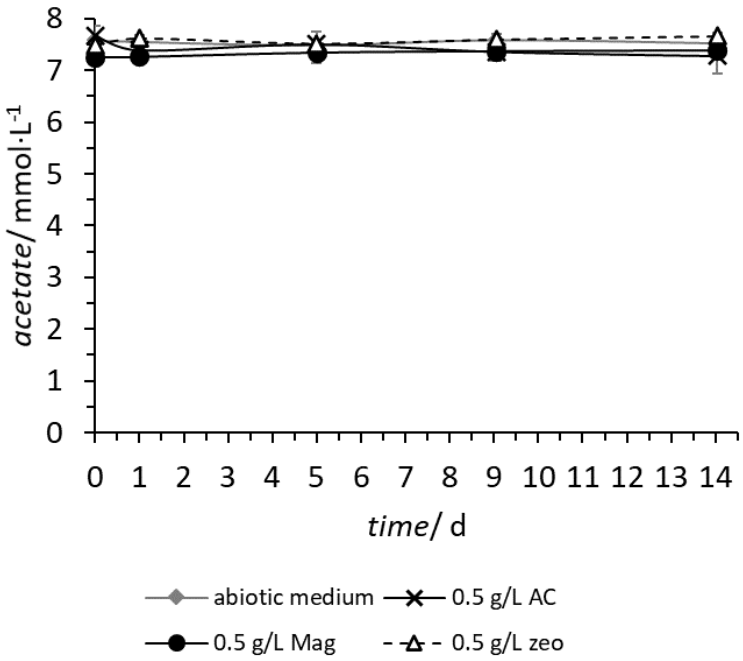

Figure A. 5. Acetate concentration over time in abiotic assays without materials and with 0.5 g·L^{-1} of AC (batch 2), Mag, and Zeo. Assays were performed in duplicates and the values represented the average and the respective standard deviation.

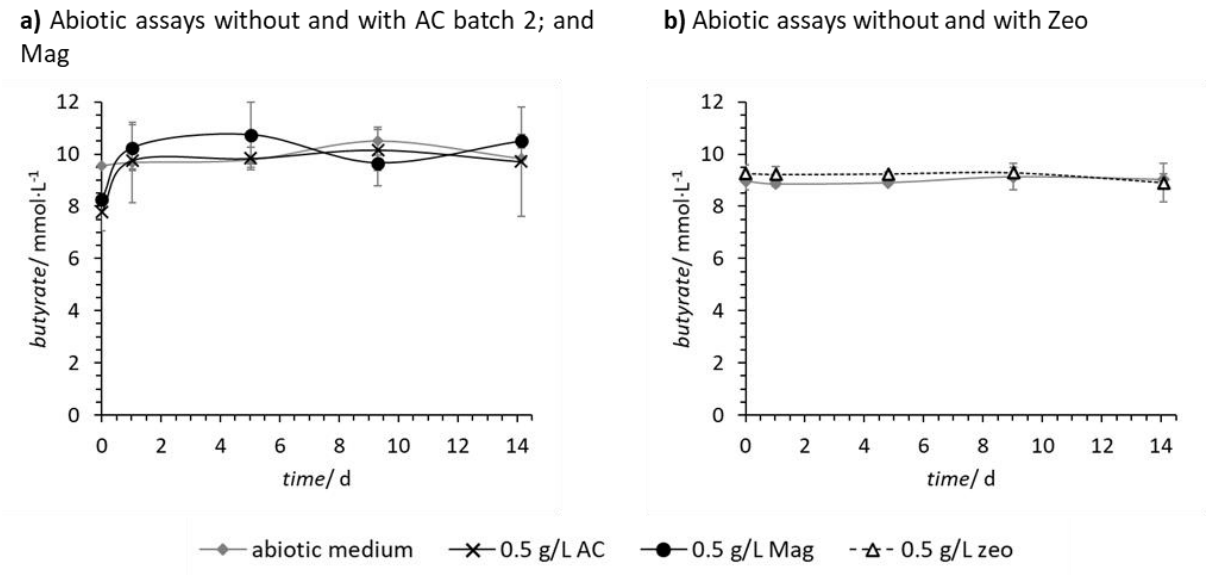

Figure A. 6. Butyrate concentration over time in abiotic assays with and without a) 0.5 g·L^{-1} of AC (batch 2) and Mag, and b) 0.5 g·L^{-1} of Zeo. The values are the average and the respective standard deviation of duplicate assays. Zeo tests were performed in a different period of AC and Mag experiments.

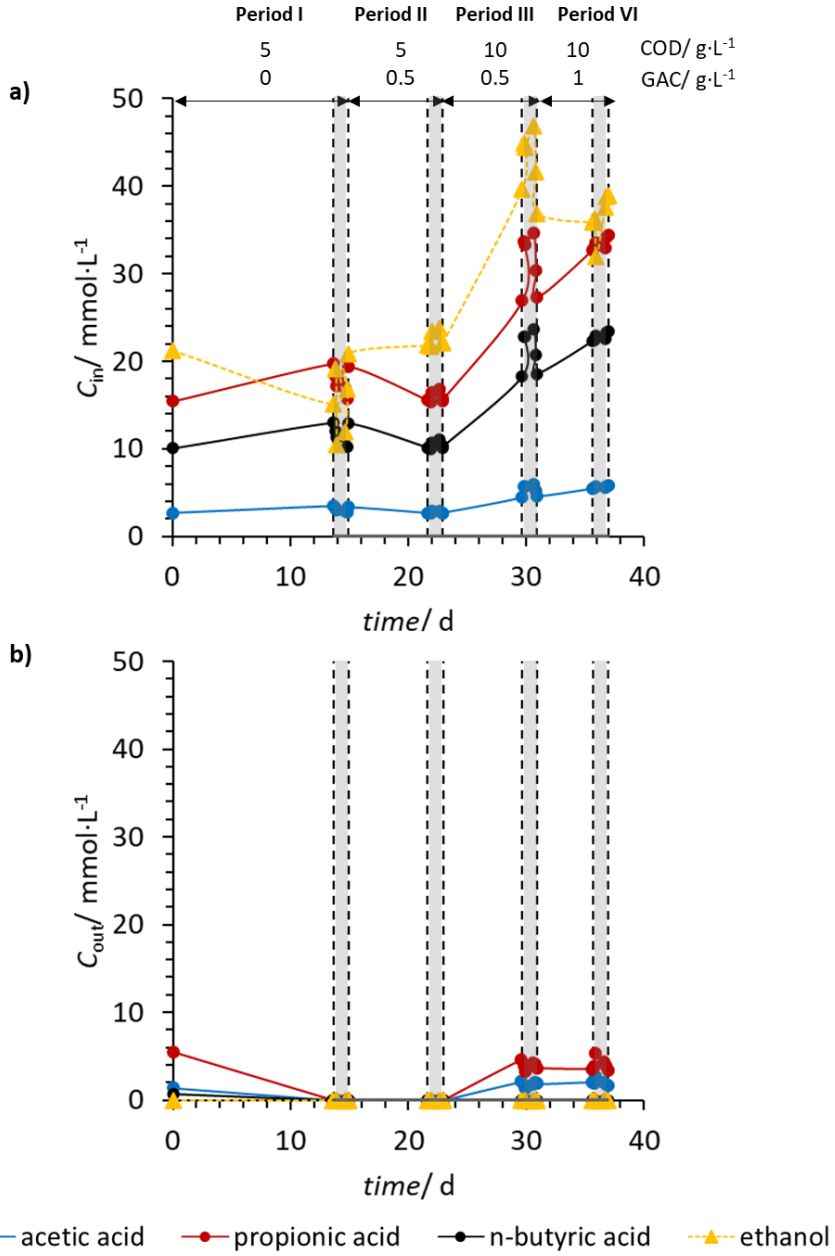

Figure A. 7. Concentrations over time of VFA (acetate, propionate, and butyrate) and ethanol in the influent (C_{in}) and effluent (C_{out}) during the continuous operation of the EGSB bioreactor. The operation occurred in four periods in which the variables were the COD of the feed and the presence or absence of GAC (and even its concentration inside the bioreactor).

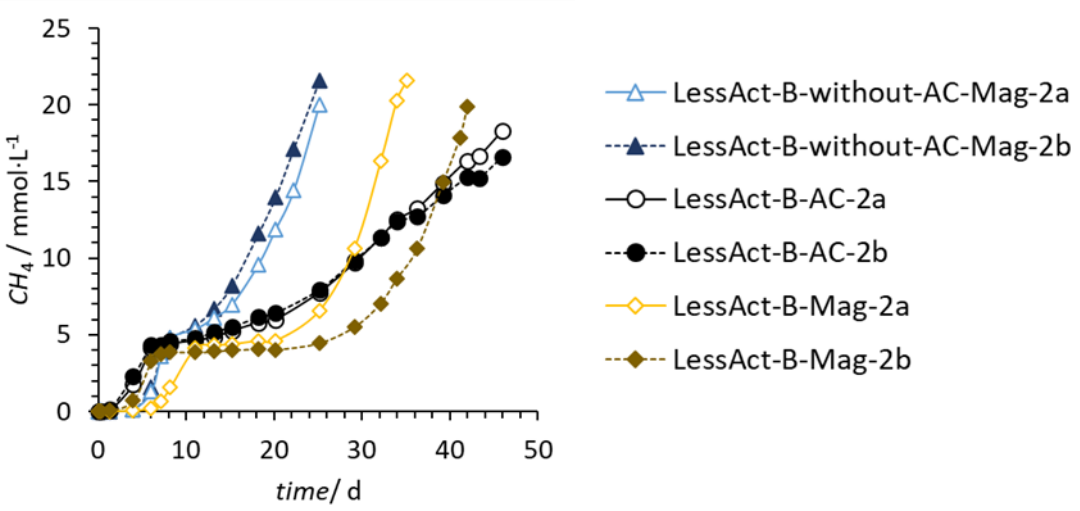

Figure A. 8. Complete cumulative MP profiles of the two lines of butyrate-degrading enrichment cultures, with and without conductive materials (AC, Mag).

APPENDIX - TABLES

Table A. 1. Values of initial concentration of substrates (C_i), lag phase duration, IMPR, EMPR, and the time of incubation (t) in each assay, with and without materials (namely, AC, Mag and Zeo)

Cultures	**Materials**	**C_i**/ mmol·L^{-1}	**Lag phase** [a]/ d	**IMPR** [b]/ mmol·L^{-1}·d^{-1}	R^{2} [b]	**EMPR** [a]/ mmol·L^{-1}·d^{-1}	R^{2} [a]	**t**/ d
M. formicicum in H_2/CO_2	Without material	63.2 ± 1.1	4.5 ± 0.7	0.24 ± 0.13	0.846 ± 0.188	7.07 ± 0.90	0.989 ± 0.009	8
	AC batch 1	62.7 ± 0.6	1.2 ± 0.3	2.99 ± 0.35	0.988 ± 0.009	3.97 ± 0.82	0.993 ± 0.002	8
	Mag	62.1 ± 0.6	13.1 ± 0.4	-	-	1.50 ± 0.24	0.993 ± 0.005	24
	AC batch 2	64.9 ± 1.6	1.3 ± 0.2	1.64 ± 0.36	0.986 ± 0.005	2.98 ± 0.60	0.995 ± 0.003	8
	Zeo	64.6 ± 1.1	1.5 ± 0.0	4.74 ± 0.14	0.864± 0.005	9.62 ± 0.82	0.997 ± 0.001	5
M. hungatei in H_2/CO_2	Without material	60.5 ± 1.4	1.4 ± 0.0	0.45 ± 0.13	0.701 ± 0.112	18.26 ± 1.60	0.998 ± 0.001	4
	AC batch 2	61.4 ± 1.2	0.9 ± 0.0	2.06 ± 0.16	0.929 ± 0.006	10.06 ± 0.49	0.992 ± 0.002	4
	Mag	61.3 ± 1.7	1.7 ± 0.2	0.09 ± 0.08	0.521 ± 0.000	15.71 ± 0.46	0.997 ± 0.001	4
	Zeo	59.8 ± 3.3	1.4 ± 0.0	0.40 ±0.12	0.791 ± 0.043	17.25 ± 1.38	0.997 ± 0.000	4
M. barkeri in H_2/CO_2	Without material	57.8 ± 0.4	0.9 ± 0.1	-	-	2.49 ± 0.31	0.998 ± 0.001	9
	AC batch 2	57.3 ± 0.5	0.8 ± 0.1	-	-	2.56 ± 0.28	0.998 ± 0.001	8
	Mag	55.4 ± 1.9	0.6 ± 0.1	-	-	2.76 ± 0.23	0.995 ± 0.005	8
	Zeo	52.7 ± 0.4	0.6 ± 0.1	-	-	2.14 ± 0.40	0.994 ± 0.000	9
S. zehnderi and *M. formicicum* in oleate	Without material	0.80 ± 0.03	18.4 ± 0.4	0.03 ± 0.00	0.952 ± 0.067	0.41 ± 0.05	0.982 ± 0.002	28
	AC batch 1	0.74 ± 0.04	10.3 ± 1.1	0.38 ± 0.02	0.969 ± 0.019	0.54 ± 0.07	0.985 ± 0.000	20
	Mag	0.71 ± 0.04	> 60	-	-	-	-	inhibited
S. wolfei and *M. hungatei* in butyrate	Without material	14.7 ± 0.6	1.0 ± 0.0	-	-	2.57 ± 0.04	0.991 ± 0.003	6
	AC batch 2	16.4 ± 3.9	1.0 ± 0.1	-	-	2.81 ± 0.14	0.998 ± 0.001	6
	Mag	15.2 ± 1.5	1.2 ± 0.1	-	-	2.07 ± 0.33	0.995 ± 0.001	6
	Zeo	16.7 ± 0.5	0.9 ± 0.2	-	-	2.57 ± 0.16	0.995 ± 0.005	6

Table A. 1. Continued. Values of initial concentration of substrates (C_i), lag phase duration, IMPR, EMPR, and the time of incubation (t) in each assay, with and without materials (namely, AC, Mag and Zeo)

Cultures	**Materials**	**C_i**/ mmol·L^{-1}	**Lag phase** [a]/ d	**IMPR** [b]/ mmol·L^{-1}·d^{-1}	R^{2} [b]	**EMPR** [a]/ mmol·L^{-1}·d^{-1}	R^{2} [a]	**t**/ d
M. barkeri in acetate	Without material	17.2 ± 0.3	9.3 ± 0.3	0.24 ± 0.01	0.912 ± 0.005	1.44 ± 0.07	0.996 ± 0.000	22
	AC batch 2	16.5 ± 0.8	7.2 ± 0.2	0.43 ± 0.04	0.933 ± 0.003	1.20 ± 0.05	0.998 ± 0.000	21
	Mag	15.8 ± 0.8	8.9 ± 0.2	0.28 ± 0.03	0.909 ± 0.007	1.54 ± 0.05	0.994 ± 0.001	21
	Zeo	17.4 ± 0.5	9.1 ± 0.2	0.25 ± 0.01	0.920 ± 0.001	1.31 ± 0.08	0.997 ± 0.000	22
M. harundinacea in acetate	Without material	8.6 ± 0.2	5.1 ± 0.8	0.26 ± 0.01	0.987 ± 0.002	0.48 ± 0.01	0.994 ± 0.007	25
	AC batch 2	8.5 ± 0.1	3.2 ± 0.1	0.41 ± 0.01	0.996 ± 0.001	0.59 ± 0.03	0.998 ± 0.000	23
	Mag	8.3 ± 0.2	8.6 ± 0.5	0.00 ± 0.01	0.259 ± 0.266	0.60 ± 0.10	0.998 ± 0.002	25
	Zeo	8.2 ± 0.6	4.8 ± 0.3	0.33 ± 0.01	0.995 ± 0.000	0.75 ± 0.09	0.987 ± 0.006	23

[a] kinetics parameters obtained by modified Gompertz model.

[b] IMPR was calculated for the early methane production during the following periods of time: between days 1 and 3 in *M. formicicum* experiments; between days 0 and 1 in *M. hungatei* assays; between days 10 and 17 in *S. zehnderi* and *M. formicicum* coculture assays; between days 4 and 9 in *M. barkeri* growing in acetate; and between days 2 and 6 for *M. harundinacea* experiments.

Table A. 2. Values of the growth medium parameters, i.e., ORP, pH, and conductivity, at the beginning (a), during exponential MP (b), and at the end (c) of incubations

Conditions	**ORP**/ mV			**pH**			**Conductivity**/ (mS·cm^{-1})		
	a	b	c	a	b	c	a	b	c
M. formicicum	-296 ± 24	-348 ± 9	-345 ± 13	7.16 ± 0.15	7.51 ± 0.12	8.20 ± 0.16	5.29 ± 0.62	5.94 ± 0.13	5.75 ± 0.22
M. formicicum + 0.5 g·L^{-1} AC batch 1	-365 ± 9	-379 ± 12	-355 ± 34	7.26 ± 0.03	8.11 ± 0.10	8.21 ± 0.04	5.92 ± 0.17	5.86 ± 0.11	5.81 ± 0.08
M. formicicum + 0.5 g·L^{-1} Mag	-321 ± 7	-310 ± 8	-310 ± 10	7.27 ± 0.03	8.05 ± 0.15	8.39 ± 0.47	6.01 ± 0.09	5.85 ± 0.20	5.87 ± 0.13
M. formicicum + 0.5 g·L^{-1} AC batch 2	-363 ± 5	-	-385 ± 5	7.05 ± 0.02	-	8.09 ± 0.01	5.68 ± 0.12	-	5.44 ± 0.17
M. formicicum + 0.5 g·L^{-1} Zeo	-324 ± 4	-	-321 ± 18	7.10 ± 0.03	-	8.44 ± 0.05	5.55 ± 0.05	-	5.71 ± 0.44
S. zehnderi and *M. formicicum* coculture	-	-264 ± 14	-	-	7.24 ± 0.06	-	-	4.32 ± 0.04	-
Coculture + 0.1 g·L^{-1} AC batch 1	-	-267 ± 16	-	-	7.27 ± 0.06	-	-	4.28 ± 0.12	-
Coculture + 0.5 g·L^{-1} Mag	-	-176 ± 20	-	-	7.40 ± 0.02	-	-	4.40 ± 0.03	-
M. hungatei	-294 ± 3	-293 ± 7	-268 ± 23	7.19 ± 0.02	7.46 ± 0.03	8.31 ± 0.00	6.71 ± 0.16	7.07 ± 0.12	6.98 ± 0.39
M. hungatei + 0.5 g·L^{-1} AC batch 2	-354 ± 7	-350 ± 1	-306 ± 8	7.23 ± 0.05	7.48 ± 0.03	8.18 ± 0.02	6.94 ± 0.04	7.05 ± 0.13	6.96 ± 0.19
M. hungatei + 0.5 g·L^{-1} Mag	-290 ± 2	-280 ± 3	-290 ± 3	7.18 ± 0.02	7.33 ± 0.05	8.27 ± 0.00	7.07 ± 0.15	7.15 ± 0.07	7.04 ± 0.09
M. hungatei + 0.5 g·L^{-1} Zeo	-300 ± 6	-300 ± 7	-314 ± 3	7.24 ± 0.04	7.52 ± 0.05	8.56 ± 0.04	7.19 ± 0.29	7.23 ± 0.14	7.06 ± 0.09
M. hungatei with *S. wolfei* coculture	-	-308 ± 7	-313 ± 6	-	7.09 ± 0.07	7.04 ± 0.04	-	7.94 ± 0.25	7.85 ± 0.33
Coculture + 0.5 g·L^{-1} AC batch 2	-	-338 ± 6	-340 ± 5	-	7.05 ± 0.07	6.99 ± 0.08	-	7.79 ± 0.10	7.83 ± 0.15
Coculture + 0.5 g·L^{-1} Mag	-	-307 ± 7	-278 ± 16	-	7.16 ± 0.08	7.00 ± 0.02	-	7.76 ± 0.09	7.70 ± 0.17
Coculture + 0.5 g·L^{-1} Zeo	-	-333 ± 3	-328 ± 7	-	7.06 ± 0.02	6.99 ± 0.04	-	7.80 ± 0.06	7.87 ± 0.14

Table A. 2. Continued. Values of the growth medium parameters, i.e., ORP, pH, and conductivity, at the beginning (a), during exponential MP (b), and at the end (c) of incubations

Conditions	**ORP**/ mV			**pH**			**Conductivity**/ (mS·cm^{-1})		
	a	b	c	a	b	c	a	b	c
M. barkeri in H_2/CO_2	-247 ± 23	-250 ± 33	-284 ± 37	7.08 ± 0.00	7.21 ± 0.08	7.61 ± 0.39	6.96 ± 0.14	7.00 ± 0.44	6.80 ± 0.19
M. barkeri + 0.5 g·L^{-1} AC batch 2	-316 ± 4	-294 ± 8	-359 ± 4	7.08 ± 0.00	7.29 ± 0.00	7.82 ± 0.02	6.88 ± 0.13	6.73 ± 0.11	6.83 ± 0.05
M. barkeri + 0.5 g·L^{-1} Mag	-270 ± 13	-268 ± 9	-332 ± 3	7.09 ± 0.02	7.34 ± 0.02	7.87 ± 0.00	6.87 ± 0.04	6.76 ± 0.05	6.70 ± 0.19
M. barkeri + 0.5 g·L^{-1} Zeo	-304 ± 14	-293 ± 4	-361 ± 2	7.12 ± 0.00	7.35 ± 0.05	7.97 ± 0.02	6.81 ± 0.05	6.69 ± 0.05	6.73 ± 0.10
M. barkeri in acetate	-301 ± 15	-268 ± 13	-290 ± 7	7.05 ± 0.04	7.26 ± 0.05	7.32 ± 0.02	8.79 ± 0.26	9.56 ± 0.31	9.13 ± 0.23
M. barkeri + 0.5 g·L^{-1} AC batch 2	-330 ± 3	-287 ± 4	-306 ± 11	7.05 ± 0.00	7.25 ± 0.00	7.29 ± 0.00	8.66 ± 0.18	9.33 ± 0.17	8.94 ± 0.15
M. barkeri + 0.5 g·L^{-1} Mag	-311 ± 3	-255 ± 5	-268 ± 4	7.05 ± 0.00	7.25 ± 0.00	7.32 ± 0.02	8.82 ± 0.07	9.38 ± 0.14	9.20 ± 0.11
M. barkeri + 0.5 g·L^{-1} Zeo	-322 ± 2	-291 ± 3	-304 ± 12	7.10 ± 0.02	7.28 ± 0.02	7.37 ± 0.00	8.74 ± 0.23	9.43 ± 0.13	9.02 ± 0.16
M. harundinacea	-279 ± 19	-259 ± 22	-304 ± 9	7.16 ± 0.00	7.22 ± 0.02	7.29 ± 0.01	7.10 ± 0.04	7.26 ± 0.15	7.80 ± 0.14
M. barkeri + 0.5 g·L^{-1} AC batch 2	-291 ± 20	-294 ± 13	-298 ± 13	7.14 ± 0.02	7.21 ± 0.00	7.22 ± 0.00	6.96 ± 0.32	7.20 ± 0.01	7.79 ± 0.21
M. harundinacea + 0.5 g·L^{-1} Mag	-277 ± 7	-266 ± 3	-272 ± 5	7.19 ± 0.02	7.21 ± 0.00	7.30 ± 0.00	7.12 ± 0.03	7.22 ± 0.07	7.88 ± 0.14
M. harundinacea + 0.5 g·L^{-1} Zeo	-293 ± 10	-285 ± 2	-275 ± 15	7.23 ± 0.03	7.26 ± 0.02	7.23 ± 012	7.14 ± 0.07	7.29 ± 0.10	7.85 ± 0.02

#Note: The variations on values of conductivity of the growth medium are due to the use of different equipment regarding the period in time in which the assay was performed.

Table A. 3. Effect of different materials (at 0.5 g·L^{-1}) on parameters (ORP, pH and conductivity) of abiotic medium with acetate (10 mmol·L^{-1}) at the beginning (a), after 24 h (b), in the middle (c) and at the end (d) of abiotic assays (same composition of *M. harundinacea* growth medium)

Conditions	**ORP**/ (mV)				**pH**				**Conductivity**/ (mS·cm^{-1})			
	a	b	c	d	a	b	c	d	a	b	c	d
Abiotic medium	-264 ± 16	-302 ± 30	-308 ± 11	-329 ± 92	7.08 ± 0.00	7.12 ± 0.00	7.17 ± 0.00	7.21 ± 0.00	7.29 ± 0.76	7.32 ± 0.42	6.91 ± 0.01	7.16 ± 0.33
AC batch 2	-265 ± 16	-316 ± 2	-263 ± 13	-281 ± 4	7.12 ± 0.00	7.12 ± 0.00	7.17 ± 0.00	7.25 ± 0.00	6.92 ± 0.10	7.13 ± 0.08	7.09 ± 0.08	7.04 ± 0.06
Mag	-297 ± 7	-279 ± 12	-247 ± 15	-189 ± 6	7.12 ± 0.00	7.15 ± 0.01	7.19 ± 0.03	7.25 ± 0.00	7.06 ± 0.02	7.15 ± 0.06	7.31 ± 0.18	7.16 ± 0.01
Zeo	-289 ± 3	-296 ± 8	-317 ± 7	-288 ± 2	7.16 ± 0.00	7.22 ± 0.03	7.25 ± 0.00	7.31 ± 0.03	7.20 ± 0.10	7.26 ± 0.14	7.26 ± 0.03	7.23 ± 0.03

Table A. 4. Effect of different materials (at 0.5 g·L^{-1}) on ORP, pH, and conductivity of anaerobic medium (a) at the beginning, (b) after 24 h, (c) in the middle and (d) at the end of the of abiotic tests with butyrate (10 mmol·L^{-1})

Conditions	**ORP**/ (mV)				**pH**				**Conductivity**/ (mS·cm^{-1})			
	a	b	c	d	a	b	c	d	a	b	c	d
Abiotic medium	-308 ± 0	-343 ± 1	-291 ± 1	-297 ± 21	7.22 ± 0.01	7.31 ± 0.01	7.33 ± 0.01	7.32 ± 0.02	3.85 ± 0.06	3.92 ± 0.02	3.98 ± 0.16	3.78 ± 0.01
AC batch 2	-359 ± 4	-378 ± 4	-335 ± 9	-335 ± 12	7.18 ± 0.07	7.27 ± 0.05	7.25 ± 0.07	7.25 ± 0.06	3.89 ± 0.06	3.95 ± 0.07	3.83 ± 0.02	3.74 ± 0.03
Mag	-330 ± 13	-328 ± 10	-262 ± 11	-273 ± 5	7.21 ± 0.02	7.30 ± 0.04	7.30 ± 0.01	7.29 ± 0.02	3.89 ± 0.08	3.97 ± 0.01	3.76 ± 0.05	3.70 ± 0.05
Abiotic medium	-331 ± 3	-348 ± 3	-292 ± 11	-299 ± 15	7.31 ± 0.06	7.37 ± 0.01	7.45 ± 0.01	7.55 ± 0.01	8.29 ± 0.18	8.35 ± 0.16	8.07 ± 0.16	8.08 ± 0.07
Zeo	-328 ± 3	-351 ± 1	-294 ± 4	-309 ± 1	7.38 ± 0.03	7.36 ± 0.04	7.45 ± 0.02	7.47 ± 0.06	8.56 ± 0.23	8.56 ± 0.32	8.28 ± 0.26	8.23 ± 0.28

* The abiotic assays with AC and Mag were carried out in a different period of the abiotic assays with Zeo.

Table A. 5. Values of ORP, pH and conductivity of anaerobic medium with oleate (1 mmol·L^{-1}) at the middle of the abiotic assays without materials and with different concentrations (C) of AC and Mag

Conditions	**C**/ (g·L^{-1})	**ORP**/ (mV)	**pH**	**Conductivity**/ (mS·cm^{-1})
Abiotic medium	0	-223 ± 11	7.16 ± 0.02	4.14 ± 0.08
AC batch 1	0.1	-235 ± 6	7.16 ± 0.01	4.27 ± 0.06
	1	-143 ± 10	7.23 ± 0.02	4.23 ± 0.11
Mag	0.1	-216 ± 1	7.20 ± 0.01	4.07 ± 0.03
	0.5	-160 ± 4	7.21 ± 0.01	4.29 ± 0.01

Table A. 6. Initial butyrate concentration and values of acetate accumulation in the assays with enrichment cultures specialized in MP only via hydrogenotrophic pathway: AC-adapted culture (MoreAct-B-AC-3) and Mag-adapted culture (MoreAct-B-Mag-3) in the original incubation conditions and in the absence of the material to which each the culture was adapted to

Assay	**Initial butyrate concentration**/ mmol·L^{-1}	**t**/ d	**Concentration of acetate accumulated**/ mmol·L^{-1}
MoreAct-B-AC-3	8.8 ± 0.6	7	21.0 ± 3.2
MoreAct-B-AC-3 without AC	11.5 ± 0.4	7	23.3 ± 0.4
MoreAct-B-Mag-3	9.1 ± 0.9	7	19.5 ± 2.5
MoreAct-B-Mag-3 without Mag	11.0 ± 1.2	7	20.4 ± 2.0

Table A. 7. Mean values of the COD fed, organic loading rate (OLR), methane produced as its COD equivalent (g COD-CH_4) and methane yield expressed as the volume of CH_4 produced per gram of COD removed (CODrem) obtained for each period

Period	**time**/ d	**COD fed**/ (g·L^{-1})	**OLR**/ (kg/m^3·d)	**CH_4-COD**/ (g)	mL CH_4/ g CODrem
I	13.7 to 14.9	4.48 ± 0.33	16.32 ± 1.19	2.18 ± 0.29	213 ± 33
II	21.6 to 22.9	5.13 ± 0.32	18.58 ± 1.18	2.51 ± 0.28	150 ± 20
III	29.6 to 30.9	9.93 ± 0.16	34.91 ± 0.64	5.11 ± 0.25	239 ± 12
IV	35.6 to 36.9	10.09 ± 0.41	36.13 ± 1.53	5.75 ± 0.19	253 ± 11

* The calculations involved in the conversion of methane produced to its COD equivalent (g COD-CH_4) and methane yields were performed as explained by Cavaleiro *et al.* (2009) in Supporting Information (Cavaleiro et al., 2009).

Table A. 8. Values for ORP, pH and conductivity measured after 24 h of the beginning and at the end of the incubation of adapted butyrate-degrading cultures developed with and without materials (in original conditions and when incubated in other conditions)

Enrichments	**ORP**/ (mV)		**pH**		**Conductivity**/ ($mS \cdot cm^{-1}$)	
	After 24 h	At the end	After 24 h	At the end	After 24 h	At the end
MoreAct-B-without-AC-Mag-3	-332 ± 6	-333 ± 6	7.35 ± 0.02	7.26 ± 0.02	6.86 ± 0.16	6.88 ± 0.15
MoreAct-B-without-AC-Mag-3 with Zeo	-341 ± 2	-328 ± 2	7.46 ± 0.05	7.29 ± 0.04	7.02 ± 0.12	7.05 ± 0.10
MoreAct-B-without-AC-Mag-3 with AC@2%Fe	-364 ± 1	-309 ± 9	7.39 ± 0.03	7.24 ± 0.05	6.87 ± 0.16	6.99 ± 0.23
MoreAct-B-without-AC-Mag-3 with (0.5 $g \cdot L^{-1}$ AC + 0.5 $g \cdot L^{-1}$ Mag)	-349 ± 5	-219 ± 10	7.38 ± 0.03	7.19 ± 0.02	7.00 ± 0.16	6.95 ± 0.21
MoreAct-B-without-AC-Mag-3 with AC	-361 ± 8	-278 ± 19	7.38 ± 0.03	7.21 ± 0.02	7.03 ± 0.08	7.07 ± 0.29
MoreAct-B-without-AC-Mag-3 with Mag	-331 ± 2	-175 ± 23	7.41 ± 0.11	7.20 ± 0.04	6.86 ± 0.12	7.05 ± 0.62
MoreAct-B-Zeo-3	-336 ± 18	-301 ± 4	7.42 ± 0.02	7.52 ± 0.03	8.68 ± 0.16	8.41 ± 0.17
MoreAct-B-Zeo-3 without Zeo	-346 ± 6	-306 ± 13	7.36 ± 0.05	7.40 ± 0.01	8.55 ± 0.15	8. 62 ± 0.15
MoreAct-B-AC-3	-373 ± 5	-352 ± 5	7.29 ± 0.04	7.16 ± 0.02	3.66 ± 0.06	3.86 ± 0.08
MoreAct-B-AC-3 without AC	-333 ± 15	-316 ± 4	7.28 ± 0.02	7.12 ± 0.02	3.59 ± 0.07	3.75 ± 0.06
MoreAct-B-Mag-3	-314 ± 5	-287 ± 4	7.25 ± 0.00	7.15 ± 0.02	3.58 ± 0.05	3.76 ± 0.05
MoreAct-B-Mag-3 without Mag	-321 ± 6	-319 ± 11	7.24 ± 0.02	7.14 ± 0.04	3.61 ± 0.04	3.78 ± 0.04

Table A. 9. Values of the substrate concentration and concentration of acetate after some time (t) of incubation for less active butyrate-degrading enrichment cultures

Enrichment cultures	**Initial butyrate concentration**/ mmol·L^{-1}	**t**/ d	**Concentration of acetate accumulated** (*)/ mmol·L^{-1}
LessAct-B-withou-AC-Mag-1a	12.0	14	16.2
LessAct-B- withou-AC-Mag-2a	8.0	8	23.5
LessAct-B- withou-AC-Mag-1b	11.0	14	15.4
LessAct-B- withou-AC-Mag-2b	11.7	8	26.7
LessAct-B-AC-1a	9.1	14	13.8
LessAct-B-AC-2a	10.7	8	20.8
LessAct-B-AC-1b	10.7	14	14.9
LessAct-B-AC-2b	9.9	8	23.4
LessAct-B-Mag-1a	8.3	14	7.3
LessAct-B-Mag-2a	9.4	11	18.6
LessAct-B-Mag-1b	8.0	21	15.6
LessAct-B-Mag-2b	13.3	8	26.6

(*) Acetate concentration can be higher than stoichiometrically expected, since some acetate can come with the pre-inoculum during transfers (around 1 or 2 mmol·L^{-1}) and some interferences could have occurred during HPLC analysis contributing with slight variances on the final concentration values.

Table A. 10. Values of ORP, pH and conductivity, measured after 24 h of the beginning and at the end of the incubation of stable and well-adapted butyrate-degrading enrichment cultures developed with and without (nano)materials

Enrichment cultures	**ORP**/ (mV)		**pH**		**Conductivity**/ (mS·cm^{-1})	
	After 24 h	At the end	After 24 h	At the end	After 24 h	At the end
Bty-b1	-332 ± 6	-333 ± 6	7.35 ± 0.02	7.26 ± 0.02	6.86 ± 0.16	6.88 ± 0.15
AC-b1	-307 ± 12	-338 ± 3	7.28 ± 0.03	7.30 ± 0.02	7.26 ± 0.12	7.13 ± 0.10
Mag-b1	-254 ± 18	-202 ± 33	7.31 ± 0.02	7.42 ± 0.04	7.21 ± 0.11	7.35 ± 0.06
Bty-b2	-273 ± 18	-304 ± 6	7.34 ± 0.08	7.29 ± 0.09	8.24 ± 0.29	8.45 ± 0.21
Zeo-b2	-336 ± 18	-301 ± 4	7.42 ± 0.02	7.52 ± 0.03	8.68 ± 0.16	8.41 ± 0.17

Table A. 11. Complete taxonomic characterization presented at the Genus level of inocula (anaerobic sludge) and microbial enrichment communities specialized in butyrate degradation, developed with and without (nano)materials, based on 16S rRNA gene amplicon sequencing. The average and standard deviation for (at least) duplicate samples is given (in percentage) for the relative abundance of each taxon. The double line in the table separates archaea members from bacteria

Phylum	Order	Genus	Inoc-b1	Bty-b1	AC-b1	Mag-b1	Inoc-b2	Bty-b2	Zeo-b2
Euryarchaeota	*Methanobacteriales*	*Methanobacterium*	9.0036 ± 3.2597	nd	0.0370 ± 0.0199	0.0024 ± 0.0034	3.7092 ± 2.3081	0.0145 ± 0.0130	nd
Euryarchaeota	*Methanobacteriales*	*Methanobrevibacter*	0.0034 ± 0.0048	nd	nd	nd	nd	nd	nd
Euryarchaeota	*Methanomicrobiales*	*Methanofollis*	nd	0.0159 ± 0.0077	0.0410 ± 0.0109	0.0398 ± 0.0461	nd	2.4166 ± 1.3566	7.8196 ± 0.7928
Euryarchaeota	*Methanomicrobiales*	Unclassified	nd	12.946 ± 2.8197	29.2177 ± 16.7515	28.3209 ± 2.5700	nd	nd	nd
Euryarchaeota	*Methanomicrobiales*	*Methanolinea*	9.0700 ± 0.6319	0.2349 ± 0.0066	0.3141 ± 0.4088	nd	2.7013 ± 2.1826	0.0340 ± 0.0119	nd
Euryarchaeota	*Methanomicrobiales*	*Methanospirillum*	0.0737 ± 0.0244	25.8783 ± 0.8869	23.638 ± 2.7684	16.5295 ± 0.6774	nd	25.4747 ± 1.2687	20.8663 ± 0.0322
Euryarchaeota	*Methanosarcinales*	*Methanosaeta*	19.9979 ± 0.9559	37.2721 ± 2.0107	14.8803 ± 2.9539	25.7180 ± 0.5081	4.1268 ± 5.6014	37.1893 ± 16.6354	46.213 ± 2.9313
Euryarchaeota	*Methanosarcinales*	*Methanomethylovorans*	0.0258 ± 0.0018	nd	0.0056 ± 0.0020	nd	0.0276 ± 0.0339	0.0100 ± 0.0141	nd
Euryarchaeota	*Methanosarcinales*	*Methanosarcina*	nd	0.0774 ± 0.0127	nd	8.2110 ± 0.0954	nd	0.1080 ± 0.0970	nd
Euryarchaeota	*Methanosarcinales*	Unclassified	0.0237 ± 0.0048	0.0011 ± 0.0015	0.0207 ± 0.0031	0.0012 ± 0.0017	nd	0.3643 ± 0.5152	0.3074 ± 0.4347
Euryarchaeota	*Thermoplasmatales*	Unclassified	nd	nd	nd	nd	0.0011 ± 0.0022	0.0046 ± 0.0066	nd
Euryarchaeota	Unclassified	Unclassified	0.0958 ± 0.0141	nd	nd	nd	0.0605 ± 0.0739	nd	nd
Crenarchaeota	Unclassified	Unclassified	0.0618 ± 0.0213	nd	nd	nd	0.0274 ± 0.0319	nd	nd
Unclassified	Unclassified	Unclassified	0.7651 ± 0.0726	0.2546 ± 0.0604	0.1021 ± 0.0295	0.2262 ± 0.0620	0.2007 ± 0.1442	0.0353 ± 0.0086	0.0028 ± 0.0003

Table A. 11. Continued. Complete taxonomic characterization presented at the Genus level of inocula (anaerobic sludge) and microbial enrichment communities specialized in butyrate degradation, developed with and without (nano)materials, based on 16S rRNA gene amplicon sequencing. The average and standard deviation for (at least) duplicate samples is given (in percentage) for the relative abundance of each taxon. The double line in the table separates archaea members from bacteria

Phylum	Order	Genus	Inoc-b1	Bty-b1	AC-b1	Mag-b1	Inoc-b2	Bty-b2	Zeo-b2
Acidobacteria	*Acidobacteriales*	Unclassified	0.0655 ± 0.0127	nd	nd	nd	0.1940 ± 0.2753	nd	nd
Actinobacteria	*Actinomycetales*	Unclassified	0.0034 ± 0.0048	nd	nd	nd	0.0103 ± 0.0206	nd	nd
Actinobacteria	*Corynebacteriales*	*Corynebacterium*	nd	nd	nd	nd	0.0034 ± 0.0069	nd	nd
Actinobacteria	*Corynebacteriales*	*Turicella*	nd	nd	nd	nd	0.5413 ± 0.9337	0.0066 ± 0.0094	nd
Actinobacteria	*Micrococcales*	*Brevibacterium*	nd	nd	nd	nd	0.0017 ± 0.0034	nd	nd
Actinobacteria	*Micrococcales*	*Actinotalea*	nd	nd	nd	nd	0.0025 ± 0.0050	nd	nd
Actinobacteria	*Micrococcales*	*Cellulomonas*	nd	nd	nd	nd	0.0015 ± 0.0030	nd	nd
Actinobacteria	*Micrococcales*	*Rothia*	nd	nd	nd	nd	0.0055 ± 0.0111	nd	nd
Actinobacteria	*Pseudonocardiales*	*Lentzea*	nd	nd	nd	nd	0.0053 ± 0.0106	nd	nd
Actinobacteria	Unclassified	Unclassified	0.0167 ± 0.0077	nd	nd	nd	0.0207 ± 0.0273	nd	nd
Actinobacteria	*Solirubrobacterales*	*Solirubrobacter*	0.0622 ± 0.0079	0.0026 ± 0.0037	nd	nd	0.2150 ± 0.0818	0.0729 ± 0.0585	nd
Actinobacteria	*Unclassified*	*Unclassified*	0.0034 ± 0.0048	nd	0.0035 ± 0.0049	nd	0.1425 ± 0.2850	nd	nd
Bacteroidetes	*Bacteroidales*	*Bacteroides*	0.5960 ± 0.0291	0.0093 ± 0.0020	0.0271 ± 0.0207	nd	0.8402 ± 0.3208	nd	0.0038 ± 0.0054
Bacteroidetes	*Bacteroidales*	*Anaerophaga*	0.0390 ± 0.0040	2.1947 ± 0.1362	3.1603 ± 2.7349	1.3604 ± 0.3211	0.0845 ± 0.1101	1.5475 ± 0.7151	0.3304 ± 0.2145

Table A. 11. Continued. Complete taxonomic characterization presented at the Genus level of inocula (anaerobic sludge) and microbial enrichment communities specialized in butyrate degradation, developed with and without (nano)materials, based on 16S rRNA gene amplicon sequencing. The average and standard deviation for (at least) duplicate samples is given (in percentage) for the relative abundance of each taxon. The double line in the table separates archaea members from bacteria

Phylum	Order	Genus	Inoc-b1	Bty-b1	AC-b1	Mag-b1	Inoc-b2	Bty-b2	Zeo-b2
Bacteroidetes	*Bacteroidales*	*Petrimonas*	nd	0.2224 ± 0.0001	nd	nd	nd	nd	0.0839 ± 0.0740
Bacteroidetes	*Bacteroidales*	*Prevotella*	nd	nd	nd	nd	0.0281 ± 0.0562	nd	nd
Bacteroidetes	*Cytophagales*	*Cytophaga*	0.1725 ± 0.0204	0.0456 ± 0.0202	nd	0.0517 ± 0.0254	0.1347 ± 0.0989	0.0580 ± 0.0626	nd
Bacteroidetes	*Flavobacteriales*	*Flavobacterium*	nd	nd	nd	nd	0.0488 ± 0.0482	nd	nd
Bacteroidetes	*Flavobacteriales*	*Sufflavibacter*	nd	nd	nd	nd	0.0100 ± 0.0199	nd	nd
Bacteroidetes	Unclassified	Unclassified	nd	nd	nd	nd	0.0011 ± 0.0023	nd	nd
Bacteroidetes	Unclassified	Unclassified	nd	nd	nd	nd	0.0040 ± 0.0080	nd	nd
candidate division NC10	Unclassified	Unclassified	0.0190 ± 0.0045	nd	nd	nd	0.0992 ± 0.1184	nd	nd
Candidatus Atribacteria	Unclassified	Unclassified	nd	nd	nd	nd	0.1071 ± 0.0771	0.0258 ± 0.0086	0.0053 ± 0.0074
Chlorobi	*Chlorobiales*	*Chlorobium*	0.0024 ± 0.0001	nd	nd	nd	nd	nd	nd
Chloroflexi	*Anaerolineales*	*Anaerolinea*	0.9190 ± 0.2111	nd	nd	nd	0.3928 ± 0.2660	nd	nd
Chloroflexi	*Anaerolineales*	*Bellilinea*	0.0290 ± 0.0132	nd	nd	nd	0.0110 ± 0.0118	nd	nd
Chloroflexi	*Anaerolineales*	*Flexilinea*	0.0174 ± 0.0073	nd	nd	nd	0.0029 ± 0.0057	nd	nd

Table A. 11. Continued. Complete taxonomic characterization presented at the Genus level of inocula (anaerobic sludge) and microbial enrichment communities specialized in butyrate degradation, developed with and without (nano)materials, based on 16S rRNA gene amplicon sequencing. The average and standard deviation for (at least) duplicate samples is given (in percentage) for the relative abundance of each taxon. The double line in the table separates archaea members from bacteria

Phylum	Order	Genus	Inoc-b1	Bty-b1	AC-b1	Mag-b1	Inoc-b2	Bty-b2	Zeo-b2
Chloroflexi	*Anaerolineales*	*Leptolinea*	0.0142 ± 0.0009	nd	nd	0.0013 ± 0.0019	0.0118 ± 0.0236	0.0112 ± 0.0008	nd
Chloroflexi	*Anaerolineales*	*Levilinea*	0.0397 ± 0.0109	0.2174 ± 0.0041	0.0539 ± 0.0320	0.5731 ± 0.0807	0.0146 ± 0.0169	0.2077 ± 0.1435	0.0069 ± 0.0097
Chloroflexi	*Anaerolineales*	*Longilinea*	0.3892 ± 0.0565	0.0084 ± 0.0029	nd	nd	0.5193 ± 0.4281	0.0177 ± 0.0251	nd
Chloroflexi	*Anaerolineales*	*Pelolinea*	0.0035 ± 0.0015	nd	0.0035 ± 0.0049	0.0039 ± 0.0021	nd	nd	nd
Chloroflexi	*Anaerolineales*	Unclassified	0.1286 ± 0.0289	0.0333 ± 0.0047	0.0126 ± 0.0149	0.0098 ± 0.0100	0.0625 ± 0.0655	0.3285 ± 0.2373	0.0641 ± 0.0089
Chloroflexi	*Caldilineales*	*Caldilinea*	0.0108 ± 0.0056	nd	nd	nd	nd	nd	nd
Chloroflexi	*Caldilineales*	Unclassified	0.0412 ± 0.0008	nd	nd	nd	0.1769 ± 0.1469	nd	nd
Chloroflexi	*Chloroflexales*	Unclassified	0.0270 ± 0.0034	nd	nd	nd	0.0011 ± 0.0023	nd	nd
Chloroflexi	*Dehalococcoidales*	*Dehalococcoides*	0.0167 ± 0.0077	nd	0.0021 ± 0.0029	nd	0.0414 ± 0.0368	0.0267 ± 0.0096	nd
Chloroflexi	Unclassified	*Dehalogenimonas*	0.0081 ± 0.0045	nd	nd	nd	0.0287 ± 0.0259	nd	nd
Chloroflexi	Unclassified	Unclassified	0.1968 ± 0.0315	0.1133 ± 0.0211	nd	nd	0.1865 ± 0.1502	0.0956 ± 0.0431	0.0042 ± 0.0016
Cloacimonetes	Unclassified	*Candidatus Cloacimonas*	nd	nd	nd	nd	nd	0.1438 ± 0.0558	0.9561 ± 0.7428
Deferribacteres	*Deferribacterales*	*Deferribacter*	0.0036 ± 0.0019	0.0021 ± 0.0030	0.0010 ± 0.0015	0.0135 ± 0.0116	nd	nd	nd

Table A. 11. Continued. Complete taxonomic characterization presented at the Genus level of inocula (anaerobic sludge) and microbial enrichment communities specialized in butyrate degradation, developed with and without (nano)materials, based on 16S rRNA gene amplicon sequencing. The average and standard deviation for (at least) duplicate samples is given (in percentage) for the relative abundance of each taxon. The double line in the table separates archaea members from bacteria

Phylum	**Order**	**Genus**	**Inoc-b1**	**Bty-b1**	**AC-b1**	**Mag-b1**	**Inoc-b2**	**Bty-b2**	**Zeo-b2**
Deferribacteres	Unclassified	Unclassified	0.0095 ± 0.0039	nd	nd	nd	nd	nd	nd
Firmicutes	*Bacillales*	*Planococcus*	nd	nd	nd	nd	0.0273 ± 0.0545	nd	nd
Firmicutes	*Bacillales*	*Dehalobacterium*	nd	nd	nd	nd	0.0394 ± 0.0570	nd	nd
Firmicutes	*Lactobacillales*	*Lactococcus*	nd	nd	nd	nd	0.0183 ± 0.0367	nd	nd
Firmicutes	*Bacillales*	*Staphylococcus*	nd	nd	nd	nd	0.0908 ± 0.1768	nd	nd
Firmicutes	*Lactobacillales*	*Streptococcus*	nd	nd	nd	nd	0.1136 ± 0.2168	nd	nd
Firmicutes	*Clostridiales*	*Christensenella*	0.0141 ± 0.0025	nd	nd	nd	0.0229 ± 0.0334	nd	nd
Firmicutes	*Clostridiales*	*Clostridium*	0.0224 ± 0.0003	nd	0.0459 ± 0.0237	0.0277 ± 0.0051	0.2757 ± 0.3840	nd	0.0633 ± 0.0598
Firmicutes	*Clostridiales*	*Anaerovorax*	nd	nd	nd	nd	0.0011 ± 0.0022	nd	nd
Firmicutes	*Clostridiales*	*Fusibacter*	nd	nd	nd	nd	0.0085 ± 0.0098	nd	nd
Firmicutes	*Clostridiales*	*Alkalibacter*	nd	0.0125 ± 0.0066	nd	nd	0.0328 ± 0.0640	nd	nd
Firmicutes	*Clostridiales*	*Eubacterium*	nd	nd	nd	nd	0.0023 ± 0.0046	nd	nd
Firmicutes	*Clostridiales*	*Tyzzerella*	nd	nd	nd	nd	0.0034 ± 0.0069	nd	nd

Table A. 11. Continued. Complete taxonomic characterization presented at the Genus level of inocula (anaerobic sludge) and microbial enrichment communities specialized in butyrate degradation, developed with and without (nano)materials, based on 16S rRNA gene amplicon sequencing. The average and standard deviation for (at least) duplicate samples is given (in percentage) for the relative abundance of each taxon. The double line in the table separates archaea members from bacteria

Phylum	Order	Genus	Inoc-b1	Bty-b1	AC-b1	Mag-b1	Inoc-b2	Bty-b2	Zeo-b2
Firmicutes	*Clostridiales*	Unclassified	0.0011 ± 0.0016	nd	nd	0.0027 ± 0.0038	nd	nd	nd
Firmicutes	*Clostridiales*	*Dehalobacter*	0.0057 ± 0.0046	nd	nd	nd	nd	nd	nd
Firmicutes	*Clostridiales*	*Papillibacter*	nd	nd	nd	nd	0.0858 ± 0.1716	nd	nd
Firmicutes	*Clostridiales*	*Saccharofermentans*	nd	nd	nd	nd	0.0222 ± 0.0292	nd	nd
Firmicutes	*Clostridiales*	*Syntrophomonas*	nd	15.6173 ± 0.0849	26.1796 ± 12.3991	12.4318 ± 0.4923	nd	15.4328 ± 7.4375	10.9072 ± 1.8444
Firmicutes	*Clostridiales*	Unclassified	nd	nd	nd	nd	0.0165 ± 0.0285	nd	nd
Firmicutes	*Thermoanaerobacterales*	*Thermoanaerobacter*	0.0190 ± 0.0045	0.0126 ± 0.0118	nd	0.0013 ± 0.0019	nd	nd	nd
Firmicutes	*Thermoanaerobacterales*	Unclassified	nd	nd	nd	nd	0.0157 ± 0.0227	nd	nd
Firmicutes	Unclassified	Unclassified	0.0595 ± 0.0181	0.0185 ± 0.0040	0.0021 ± 0.0029	nd	0.6070 ± 0.4966	0.0384 ± 0.0377	6.9907 ± 2.2660
Firmicutes	*Selenomonadales*	*Schwartzia*	nd	nd	nd	nd	0.0418 ± 0.0485	nd	nd
Firmicutes	*Selenomonadales*	Unclassified	0.0037 ± 0.0052	0.1181 ± 0.0218	0.0147 ± 0.0120	nd	nd	nd	nd
Firmicutes	*Selenomonadales*	*Centipeda*	0.0153 ± 0.0007	nd	nd	nd	0.0177 ± 0.0354	nd	nd
Firmicutes	*Tissierellales*	*Peptoniphilus*	nd	nd	nd	nd	0.0161 ± 0.0321	nd	nd

Table A. 11. Continued. Complete taxonomic characterization presented at the Genus level of inocula (anaerobic sludge) and microbial enrichment communities specialized in butyrate degradation, developed with and without (nano)materials, based on 16S rRNA gene amplicon sequencing. The average and standard deviation for (at least) duplicate samples is given (in percentage) for the relative abundance of each taxon. The double line in the table separates archaea members from bacteria

Phylum	Order	Genus	Inoc-b1	Bty-b1	AC-b1	Mag-b1	Inoc-b2	Bty-b2	Zeo-b2
Firmicutes	Unclassified	Unclassified	0.0745 ± 0.0095	0.3073 ± 0.0353	nd	0.2510 ± 0.0440	0.1411 ± 0.1045	3.6094 ± 3.9348	0.0038 ± 0.0054
Ignavibacteriae	*Ignavibacteriales*	*Ignavibacterium*	nd	0.0440 ± 0.0104	nd	nd	nd	nd	nd
Ignavibacteriae	*Ignavibacteriales*	Unclassified	0.0025 ± 0.0035	nd	0.0035 ± 0.0049	nd	nd	nd	nd
Nitrospirae	*Nitrospirales*	Unclassified	0.2631 ± 0.0175	nd	0.0046 ± 0.0066	nd	0.5092 ± 0.1622	nd	nd
Nitrospirae	*Nitrospirales*	Unclassified	nd	nd	nd	nd	0.0063 ± 0.0126	nd	nd
Planctomycetes	*Phycisphaerales*	Unclassified	nd	nd	nd	nd	0.0023 ± 0.0046	nd	nd
Planctomycetes	*Unclassified*	Unclassified	0.0034 ± 0.0048	nd	nd	nd	0.0684 ± 0.0830	nd	nd
Planctomycetes	*Planctomycetales*	Unclassified	0.0047 ± 0.0003	0.0263 ± 0.0113	nd	nd	0.0170 ± 0.0238	nd	0.0061 ± 0.0087
Planctomycetes	Unclassified	Unclassified	0.3810 ± 0.0246	0.0309 ± 0.0044	nd	nd	0.0996 ± 0.1394	0.0013 ± 0.0019	0.0042 ± 0.0016
Proteobacteria	*Caulobacterales*	*Phenylobacterium*	nd	nd	nd	nd	0.0092 ± 0.0184	nd	nd
Proteobacteria	*Pelagibacterales*	*Candidatus Pelagibacter*	nd	nd	nd	nd	0.0132 ± 0.0264	nd	nd
Proteobacteria	*Rhizobiales*	*Ochrobactrum*	0.0083 ± 0.0022	0.0034 ± 0.0012	0.0012 ± 0.0016	nd	nd	nd	nd
Proteobacteria	*Rhizobiales*	*Aliihoeflea*	nd	nd	nd	nd	0.0030 ± 0.0059	nd	nd

Table A. 11. Continued. Complete taxonomic characterization presented at the Genus level of inocula (anaerobic sludge) and microbial enrichment communities specialized in butyrate degradation, developed with and without (nano)materials, based on 16S rRNA gene amplicon sequencing. The average and standard deviation for (at least) duplicate samples is given (in percentage) for the relative abundance of each taxon. The double line in the table separates archaea members from bacteria

Phylum	Order	Genus	Inoc-b1	Bty-b1	AC-b1	Mag-b1	Inoc-b2	Bty-b2	Zeo-b2
Proteobacteria	*Rhizobiales*	*Bradyrhizobium*	nd	nd	nd	nd	0.0022 ± 0.0044	nd	nd
Proteobacteria	*Rhizobiales*	*Rhizobium*	0.0023 ± 0.0032	nd	nd	nd	nd	nd	nd
Proteobacteria	*Rhizobiales*	*Labrys*	nd	nd	nd	nd	0.5238 ± 1.0476	nd	nd
Proteobacteria	*Rhodobacterales*	*Amaricoccus*	nd	nd	nd	nd	0.0011 ± 0.0023	nd	nd
Proteobacteria	*Rhodobacterales*	*Paracoccus*	nd	nd	nd	nd	0.0244 ± 0.0459	nd	nd
Proteobacteria	*Burkholderiales*	*Pusillimonas*	nd	nd	nd	nd	0.0029 ± 0.0057	nd	nd
Proteobacteria	*Burkholderiales*	*Ralstonia*	0.0399 ± 0.0043	nd	nd	nd	0.0120 ± 0.0185	nd	nd
Proteobacteria	*Burkholderiales*	*Simplicispira*	nd	nd	nd	nd	0.0011 ± 0.0023	nd	nd
Proteobacteria	*Methylophilales*	*Methylobacillus*	0.0154 ± 0.0026	nd	nd	nd	nd	nd	nd
Proteobacteria	*Rhodocyclales*	*Propionivibrio*	0.0057 ± 0.0046	nd	nd	nd	0.0248 ± 0.0496	nd	nd
Proteobacteria	*Rhodocyclales*	*Thauera*	nd	nd	nd	nd	0.0086 ± 0.0172	nd	0.0365 ± 0.0219
Proteobacteria	*Desulfobacterales*	*Desulfobacter*	nd	nd	nd	nd	0.0011 ± 0.0022	nd	nd
Proteobacteria	*Desulfobacterales*	*Unclassified*	0.0805 ± 0.0148	nd	nd	nd	0.0863 ± 0.0609	nd	nd

Table A. 11. Continued. Complete taxonomic characterization presented at the Genus level of inocula (anaerobic sludge) and microbial enrichment communities specialized in butyrate degradation, developed with and without (nano)materials, based on 16S rRNA gene amplicon sequencing. The average and standard deviation for (at least) duplicate samples is given (in percentage) for the relative abundance of each taxon. The double line in the table separates archaea members from bacteria

Phylum	Order	Genus	Inoc-b1	Bty-b1	AC-b1	Mag-b1	Inoc-b2	Bty-b2	Zeo-b2
Proteobacteria	*Desulfovibrionales*	*Desulfomicrobium*	0.4694 ± 0.0517	0.0058 ± 0.0008	0.0023 ± 0.0033	0.0142 ± 0.0065	1.5245 ± 1.0929	0.0082 ± 0.0023	0.0023 ± 0.0032
Proteobacteria	*Desulfovibrionales*	*Desulfovibrio*	0.0324 ± 0.0203	0.1090 ± 0.0062	0.2083 ± 0.0236	0.0371 ± 0.0082	0.0278 ± 0.0265	0.2701 ± 0.1007	0.1514 ± 0.0543
Proteobacteria	*Desulfuromonadales*	*Desulfuromonas*	nd	nd	0.0093 ± 0.0131	nd	nd	nd	nd
Proteobacteria	*Desulfuromonadales*	*Geobacter*	14.4161 ± 0.8948	0.0013 ± 0.0019	0.0010 ± 0.0015	0.1430 ± 0.0215	27.3189 ± 1.5909	0.0465 ± 0.0601	nd
Proteobacteria	*Desulfuromonadales*	*Pelobacter*	0.0393 ± 0.0140	0.0026 ± 0.0037	nd	nd	0.0825 ± 0.0872	0.0030 ± 0.0042	nd
Proteobacteria	*Desulfuromonadales*	Unclassified	0.0023 ± 0.0032	nd	0.0012 ± 0.0016	nd	6.4929 ± 6.8006	0.0043 ± 0.0023	nd
Proteobacteria	*Myxococcales*	*Chondromyces*	0.0115 ± 0.0093	nd	nd	nd	0.0216 ± 0.0252	nd	nd
Proteobacteria	*Syntrophobacterales*	*Desulfomonile*	0.1328 ± 0.0070	nd	0.0182 ± 0.0169	0.0090 ± 0.0025	0.2755 ± 0.1848	0.2699 ± 0.2230	0.0139 ± 0.0085
Proteobacteria	*Syntrophobacterales*	*Smithella*	0.0910 ± 0.0105	nd	nd	0.0166 ± 0.0030	0.2226 ± 0.2856	0.0591 ± 0.0836	0.0031 ± 0.0043
Proteobacteria	*Syntrophobacterales*	*Syntrophus*	0.4453 ± 0.0698	nd	nd	nd	0.6372 ± 0.1173	0.0138 ± 0.0195	nd
Proteobacteria	*Syntrophobacterales*	Unclassified	0.0634 ± 0.0062	nd	nd	nd	0.0011 ± 0.0022	nd	nd
Proteobacteria	*Syntrophobacterales*	*Syntrophobacter*	15.8668 ± 0.8374	nd	nd	nd	26.3232 ± 9.5734	0.0172 ± 0.0036	0.0008 ± 0.0011
Proteobacteria	*Syntrophobacterales*	Unclassified	0.0035 ± 0.0015	nd	nd	nd	0.0090 ± 0.0109	nd	nd

Table A. 11. Continued. Complete taxonomic characterization presented at the Genus level of inocula (anaerobic sludge) and microbial enrichment communities specialized in butyrate degradation, developed with and without (nano)materials, based on 16S rRNA gene amplicon sequencing. The average and standard deviation for (at least) duplicate samples is given (in percentage) for the relative abundance of each taxon. The double line in the table separates archaea members from bacteria

Phylum	Order	Genus	Inoc-b1	Bty-b1	AC-b1	Mag-b1	Inoc-b2	Bty-b2	Zeo-b2
Proteobacteria	*Syntrophobacterales*	*Syntrophorhabdus*	0.1086 ± 0.0284	nd	nd	nd	0.1718 ± 0.2321	nd	nd
Proteobacteria	*Syntrophobacterales*	Unclassified	0.6200 ± 0.0943	nd	0.0054 ± 0.0011	0.0240 ± 0.0036	2.7470 ± 0.7435	0.0251 ± 0.0077	nd
Proteobacteria	Unclassified	Unclassified	0.2750 ± 0.0215	0.0153 ± 0.0005	nd	0.0040 ± 0.0057	0.2830 ± 0.2336	0.0109 ± 0.0071	0.0034 ± 0.0026
Proteobacteria	*Campylobacterales*	*Arcobacter*	0.0023 ± 0.0032	nd	nd	0.0027 ± 0.0038	0.0218 ± 0.0436	nd	nd
Proteobacteria	*Campylobacterales*	*Sulfurospirillum*	nd	nd	nd	nd	0.0033 ± 0.0066	nd	nd
Proteobacteria	*Campylobacterales*	*Sulfuricurvum*	0.0326 ± 0.0114	nd	nd	nd	0.0188 ± 0.0294	nd	1.2072 ± 0.6669
Proteobacteria	*Campylobacterales*	*Sulfurimonas*	nd	nd	nd	nd	0.1069 ± 0.0931	nd	nd
Proteobacteria	Unclassified	*Sulfurovum*	nd	nd	0.3591 ± 0.3812	nd	nd	nd	nd
Proteobacteria	*Cellvibrionales*	*Cellvibrio*	nd	nd	nd	nd	0.0017 ± 0.0034	nd	nd
Proteobacteria	*Methylococcales*	*Methylobacter*	0.0105 ± 0.0044	nd	nd	nd	nd	nd	nd
Proteobacteria	*Methylococcales*	Unclassified	0.0072 ± 0.0038	nd	nd	nd	0.0052 ± 0.0103	nd	nd
Proteobacteria	*Oceanospirillales*	*Hahella*	nd	nd	nd	nd	0.0023 ± 0.0046	nd	nd
Proteobacteria	*Pasteurellales*	*Haemophilus*	nd	nd	nd	nd	0.0037 ± 0.0074	0.0013 ± 0.0019	0.0046 ± 0.0065

Table A. 11. Continued. Complete taxonomic characterization presented at the Genus level of inocula (anaerobic sludge) and microbial enrichment communities specialized in butyrate degradation, developed with and without (nano)materials, based on 16S rRNA gene amplicon sequencing. The average and standard deviation for (at least) duplicate samples is given (in percentage) for the relative abundance of each taxon. The double line in the table separates archaea members from bacteria

Phylum	Order	Genus	Inoc-b1	Bty-b1	AC-b1	Mag-b1	Inoc-b2	Bty-b2	Zeo-b2
Proteobacteria	*Pseudomonadales*	*Acinetobacter*	nd	nd	nd	nd	0.0040 ± 0.0080	nd	nd
Proteobacteria	*Pseudomonadales*	*Pseudomonas*	nd	0.1379 ± 0.0196	0.0078 ± 0.0021	0.5644 ± 0.0172	0.0498 ± 0.0651	nd	nd
Proteobacteria	*Thiotrichales*	*Thioalkalimicrobium*	nd	nd	nd	nd	0.0007 ± 0.0015	nd	nd
Proteobacteria	*Thiotrichales*	*Thiomicrospira*	nd	nd	nd	nd	0.0292 ± 0.0339	nd	nd
Proteobacteria	*Thiotrichales*	*Thiothrix*	0.0012 ± 0.0017	nd	nd	nd	0.0022 ± 0.0044	nd	0.0008 ± 0.0011
Proteobacteria	*Xanthomonadales*	*Rhodanobacter*	nd	nd	nd	nd	0.0257 ± 0.0441	0.0033 ± 0.0047	0.0015 ± 0.0022
Proteobacteria	Unclassified	Unclassified	0.0252 ± 0.0165	nd	nd	nd	nd	nd	nd
Proteobacteria	Unclassified	Unclassified	4.1874 ± 0.7505	0.0013 ± 0.0019	0.0067 ± 0.0036	nd	0.5422 ± 0.3371	0.0007 ± 0.0009	nd
Spirochaetes	*Spirochaetales*	*Spirochaeta*	0.0447 ± 0.0006	0.0101 ± 0.0069	nd	0.0891 ± 0.0274	0.0185 ± 0.0312	0.0033 ± 0.0009	0.0173 ± 0.0059
Spirochaetes	*Spirochaetales*	*Treponema*	nd	nd	nd	nd	0.0023 ± 0.0046	nd	nd
Spirochaetes	*Spirochaetales*	Unclassified	0.0433 ± 0.0091	0.2709 ± 0.0464	0.1850 ± 0.1026	0.2540 ± 0.0352	0.0332 ± 0.0499	0.0349 ± 0.0175	0.0373 ± 0.0230
Spirochaetes	Unclassified	Unclassified	0.1359 ± 0.0218	0.0975 ± 0.0195	0.0246 ± 0.0112	0.0717 ± 0.0180	0.2784 ± 0.1672	0.0089 ± 0.0043	0.0013 ± 0.0019
Spirochaetes	Unclassified	Unclassified	0.5095 ± 0.0077	1.3135 ± 0.2480	nd	0.0064 ± 0.0023	0.0258 ± 0.0253	nd	0.1379 ± 0.0539

Table A. 11. Continued. Complete taxonomic characterization presented at the Genus level of inocula (anaerobic sludge) and microbial enrichment communities specialized in butyrate degradation, developed with and without (nano)materials, based on 16S rRNA gene amplicon sequencing. The average and standard deviation for (at least) duplicate samples is given (in percentage) for the relative abundance of each taxon. The double line in the table separates archaea members from bacteria

Phylum	Order	Genus	Inoc-b1	Bty-b1	AC-b1	Mag-b1	Inoc-b2	Bty-b2	Zeo-b2
Synergistetes	*Synergistales*	*Aminivibrio*	0.0739 ± 0.0311	0.0074 ± 0.0044	nd	0.0038 ± 0.0015	0.2179 ± 0.2195	0.0046 ± 0.0066	nd
Synergistetes	*Synergistales*	*Aminobacterium*	0.0034 ± 0.0048	0.0032 ± 0.0045	nd	nd	0.0017 ± 0.0034	nd	0.0127 ± 0.0006
Synergistetes	*Synergistales*	*Lactivibrio*	0.0011 ± 0.0016	nd	nd	nd	0.0029 ± 0.0057	nd	nd
Synergistetes	*Synergistales*	*Synergistes*	0.0455 ± 0.0122	0.1053 ± 0.0249	nd	0.0276 ± 0.0087	0.1801 ± 0.1207	0.0890 ± 0.0563	0.0357 ± 0.0058
Synergistetes	*Synergistales*	*Thermovirga*	nd	0.0071 ± 0.0010	nd	nd	nd	nd	nd
Synergistetes	*Synergistales*	Unclassified	0.0284 ± 0.0050	0.0224 ± 0.0165	0.0646 ± 0.0028	0.0101 ± 0.0028	0.0052 ± 0.0103	0.0328 ± 0.0325	0.0302 ± 0.0167
Synergistetes	*Synergistales*	Unclassified	0.1116 ± 0.0300	0.4382 ± 0.1388	0.6224 ± 0.1093	0.2967 ± 0.0101	0.1081 ± 0.0852	0.7152 ± 0.0218	2.3886 ± 0.4043
Synergistetes	Unclassified	Unclassified	0.0071 ± 0.0004	nd	nd	nd	0.1178 ± 0.0866	nd	nd
Thermotogae	*Kosmotogales*	*Mesotoga*	0.4921 ± 0.1944	0.0523 ± 0.0074	0.2640 ± 0.1319	nd	0.0141 ± 0.0163	nd	0.1027 ± 0.0301
Thermotogae	*Petrotogales*	*Geotoga*	nd	nd	nd	nd	0.0069 ± 0.0138	nd	nd
Thermotogae	*Thermotogales*	Unclassified	0.0037 ± 0.0052	nd	nd	nd	nd	nd	nd
Unclassified	Unclassified	*Caldithrix*	0.0047 ± 0.0003	nd	nd	nd	0.0264 ± 0.0368	nd	nd
Unclassified	Unclassified	Unclassified	18.6409 ± 2.7324	1.6783 ± 0.4313	0.4481 ± 0.2685	4.6482 ± 0.6089	14.1518 ± 3.0509	11.1024 ± 2.0375	1.1719 ± 0.6021

Table A. 11. Continued. Complete taxonomic characterization presented at the Genus level of inocula (anaerobic sludge) and microbial enrichment communities specialized in butyrate degradation, developed with and without (nano)materials, based on 16S rRNA gene amplicon sequencing. The average and standard deviation for (at least) duplicate samples is given (in percentage) for the relative abundance of each taxon. The double line in the table separates archaea members from bacteria

Phylum	**Order**	**Genus**	**Inoc-b1**	**Bty-b1**	**AC-b1**	**Mag-b1**	**Inoc-b2**	**Bty-b2**	**Zeo-b2**
Verrucomicrobia	*Verrucomicrobiales*	Unclassified	0.0268 ± 0.0100	nd	nd	nd	0.0306 ± 0.0612	nd	nd
Verrucomicrobia	*Verrucomicrobiales*	*Verrucomicrobium*	0.0069 ± 0.0062	nd	nd	nd	nd	nd	nd

nd – not detected.

Inoc-b1 – Inoculum for the first batch of experiments; Inoc-b2 – Inoculum for the second batch of experiments

REFERENCES

REFERENCES

Abbas, Y., Yun, S., Wang, Z., Zhang, Y., Zhang, X., Wang, K., 2021. Recent advances in bio-based carbon materials for anaerobic digestion: A review. Renew. Sustain. Energy Rev. 135, 110378. https://doi.org/https://doi.org/10.1016/j.rser.2020.110378

Abreu, B., Pires, A.S., Guimarães, A., Fernandes, R.M.F., Oliveira, I.S., Marques, E.F., 2022. Polymer/surfactant mixtures as dispersants and non-covalent functionalization agents of multiwalled carbon nanotubes: Synergism, morphological characterization and molecular picture. J. Mol. Liq. 347, 118338. https://doi.org/https://doi.org/10.1016/j.molliq.2021.118338

Aklujkar, M., Krushkal, J., DiBartolo, G., Lapidus, A., Land, M.L., Lovley, D.R., 2009. The genome sequence of *Geobacter metallireducens*: features of metabolism, physiology and regulation common and dissimilar to *Geobacter sulfurreducens*. BMC Microbiol. 9, 109. https://doi.org/10.1186/1471-2180-9-109

Al Hasani, Z., Kumar Nayak, J., Alhimali, H., Al-Mamun, A., 2022. Enhancing methane production of co-digested food waste with granular activated carbon coated with nano zero-valent iron in an anaerobic digester. Bioresour. Technol. 363, 127832. https://doi.org/https://doi.org/10.1016/j.biortech.2022.127832

Alberici, S., Grimme, W., Toop, G., 2022. Biomethane production potentials in the EU: Feasibility of REPowerEU 2030 targets, production potentials in the Member States and outlook to 2050. Netherlands.

Alves, M.M., Mota Vieira, J.A., Álvares Pereira, R.M., Pereira, M.A., Mota, M., 2001. Effect of lipids and oleic acid on biomass development in anaerobic fixed-bed reactors. Part I: Biofilm growth and activity. Water Res. 35, 255–263. https://doi.org/https://doi.org/10.1016/S0043-1354(00)00241-4

Amann, R., Ludwig, W., 2000. Ribosomal RNA-targeted nucleic acid probes for studies in microbial ecology. FEMS Microbiol. Rev. 24, 555–565. https://doi.org/10.1111/j.1574-6976.2000.tb00557.x

Amelia-Elena, R., Federica, C., Hryhoriy, S., Florin, M., Malla, S.P., Sophia, W.H., O, S.-W.O.L., J, H.P.O., H, R.H., Niculina, M., Bo, T., J, G.S., 2018. Conductive Particles Enable Syntrophic Acetate Oxidation between *Geobacter* and *Methanosarcina* from Coastal Sediments. Am. Soc. Microbiol. 9. https://doi.org/10.1128/mBio.00226-18

Amen, T.W.M., Eljamal, O., Khalil, A.M.E., Matsunaga, N., 2017. Biochemical methane potential enhancement of domestic sludge digestion by adding pristine iron nanoparticles and iron nanoparticles coated zeolite compositions. J. Environ. Chem. Eng. 5, 5002–5013. https://doi.org/https://doi.org/10.1016/j.jece.2017.09.030

Angelidaki, I., Alves, M., Bolzonella, D., Borzacconi, L., Campos, J.L., Guwy, A.J., Kalyuzhnyi, S., Jenicek, P., van Lier, J.B., 2009. Defining the biomethane potential (BMP) of solid organic wastes and energy crops: a proposed protocol for batch assays. Water Sci. Technol. 59, 927–934. https://doi.org/10.2166/wst.2009.040

APHA/AWWA/WEF, 1998. , in: Standard Methods for the Examination of Water and Wastewater. American Public Health Association/American Water Works Association/American Water Works Association and Water Environmental Federation, Washington DC, USA.

Baek, G., Jung, H., Kim, J., Lee, C., 2017. A long-term study on the effect of magnetite supplementation

in continuous anaerobic digestion of dairy effluent – Magnetic separation and recycling of magnetite. Bioresour. Technol. 241, 830–840. https://doi.org/10.1016/j.biortech.2017.06.018

Baniamerian, H., Ghofrani, P., Tsapekos, P., 2019. Application of nano-structured materials in anaerobic digestion: Current status and perspectives. Chemosphere 229, 188–199. https://doi.org/10.1016/j.chemosphere.2019.04.193

Barrena, R., del Carmen Vargas-García, M., Catacora-Padilla, P., Gea, T., Abo Markeb, A., Moral-Vico, J., Sánchez, A., Font, X., Aspray, T.J., 2023. Magnetite-based nanoparticles and nanocomposites for recovery of overloaded anaerobic digesters. Bioresour. Technol. 128632. https://doi.org/https://doi.org/10.1016/j.biortech.2023.128632

Barua, S., Dhar, B.R., 2017. Advances towards understanding and engineering direct interspecies electron transfer in anaerobic digestion. Bioresour. Technol. 244, 698–707. https://doi.org/10.1016/j.biortech.2017.08.023

Barua, S., Zakaria, B.S., Dhar, B.R., 2018. Enhanced methanogenic co-degradation of propionate and butyrate by anaerobic microbiome enriched on conductive carbon fibers. Bioresour. Technol. 266, 259–266. https://doi.org/https://doi.org/10.1016/j.biortech.2018.06.053

Barua, S., Zakaria, B.S., Lin, L., Dhar, B.R., 2019. Magnetite doped granular activated carbon as an additive for high-performance anaerobic digestion. Mater. Sci. Energy Technol. 2, 377–384. https://doi.org/https://doi.org/10.1016/j.mset.2019.04.002

Berghuis, B.A., Yu, F.B., Schulz, F., Blainey, P.C., Woyke, T., Quake, S.R., 2019. Hydrogenotrophic methanogenesis in archaeal phylum Verstraetearchaeota reveals the shared ancestry of all methanogens. Proc. Natl. Acad. Sci. 116, 5037–5044. https://doi.org/10.1073/pnas.1815631116

Bist, V., Niranjan, A., Ranjan, M., Lehri, A., Seem, K., Srivastava, S., 2020. Silicon-Solubilizing Media and Its Implication for Characterization of Bacteria to Mitigate Biotic Stress. Front. Plant Sci. 11, 28. https://doi.org/10.3389/fpls.2020.00028

Borja, R., De, I., Csic, G., 2011. 2.55 - Biogas Production. Compr. Biotechnol. 2, 785–798. https://doi.org/10.1016/B978-0-08-088504-9.00126-4

Bueno-López, J.I., Nguyen, C.H., Rangel-Mendez, J.R., Sierra-Alvarez, R., Field, J.A., Cervantes, F.J., 2020. Effects of graphene oxide and reduced graphene oxide on acetoclastic, hydrogenotrophic and methylotrophic methanogenesis. Biodegradation 31, 35–45. https://doi.org/10.1007/s10532-020-09892-0

Busca, G., 2014. Chapter 7 - Zeolites and Other Structurally Microporous Solids as Acid–Base Materials, in: Busca, G. (Ed.), Heterogeneous Catalytic Materials. Elsevier, Amsterdam, pp. 197–249. https://doi.org/https://doi.org/10.1016/B978-0-444-59524-9.00007-9

Caporaso, J.G., Lauber, C.L., Walters, W.A., Berg-Lyons, D., Lozupone, C.A., Turnbaugh, P.J., Fierer, N., Knight, R., 2011. Global patterns of 16S rRNA diversity at a depth of millions of sequences per sample. Proc. Natl. Acad. Sci. 108, 4516–4522. https://doi.org/10.1073/pnas.1000080107

Cardona, L., Mazéas, L., Chapleur, O., 2021. Zeolite favours propionate syntrophic degradation during anaerobic digestion of food waste under low ammonia stress. Chemosphere 262, 127932. https://doi.org/https://doi.org/10.1016/j.chemosphere.2020.127932

Castilho, T.G., Rodrigues, J.A.D., García, J., Subtil, E.L., 2022. Recent advances and perspectives in the use of conductive materials to improve anaerobic wastewater treatment: A systematic review approached. J. Water Process Eng. 50, 103193.

https://doi.org/https://doi.org/10.1016/j.jwpe.2022.103193

Cavalcante, W.A., Gehring, T.A., Zaiat, M., 2021. Stimulation and inhibition of direct interspecies electron transfer mechanisms within methanogenic reactors by adding magnetite and granular actived carbon. Chem. Eng. J. 415, 128882. https://doi.org/https://doi.org/10.1016/j.cej.2021.128882

Cavaleiro, A.J., Salvador, A.F., Alves, J.I., Alves, M., 2009. Continuous High Rate Anaerobic Treatment of Oleic Acid Based Wastewater is Possible after a Step Feeding Start-Up. Environ. Sci. Technol. 43, 2931–2936. https://doi.org/10.1021/es8031264

Celaj, A., Markle, J., Danska, J., Parkinson, J., 2014. Comparison of assembly algorithms for improving rate of metatranscriptomic functional annotation. Microbiome 2, 39. https://doi.org/10.1186/2049-2618-2-39

Chen, L., Fang, W., Chang, J., Liang, J., Zhang, P., Zhang, G., 2022. Improvement of Direct Interspecies Electron Transfer via Adding Conductive Materials in Anaerobic Digestion: Mechanisms, Performances, and Challenges. Front. Microbiol. 13, 860749. https://doi.org/10.3389/fmicb.2022.860749

Chen, S., Rotaru, A., Shrestha, P.M., Malvankar, N.S., Liu, F., Fan, W., Nevin, K.P., Lovley, D.R., 2014a. Promoting Interspecies Electron Transfer with Biochar. Sci. Rep. 4, 5019. https://doi.org/10.1038/srep05019

Chen, S., Rotaru, A.E., Liu, F., Philips, J., Woodard, T.L., Nevin, K.P., Lovley, D.R., 2014b. Carbon cloth stimulates direct interspecies electron transfer in syntrophic co-cultures. Bioresour. Technol. 173, 82–86. https://doi.org/10.1016/j.biortech.2014.09.009

Colleran, E., Concannon, F., Golden, T., Geoghegan, F., Crumlish, B., Killilea, E., Henry, M., Coates, J., 1992. Use of Methanogenic Activity Tests to Characterize Anaerobic Sludges, Screen for Anaerobic Biodegradability and Determine Toxicity Thresholds against Individual Anaerobic Trophic Groups and Species. Water Sci. Technol. 25, 31–40. https://doi.org/10.2166/wst.1992.0136

Comission, E., 2022a. Communication from the Comission to the European Parliament, the European Council, the Council, the European Economic and Social Committee and the Committee of the Regions [WWW Document]. Brussels. URL https://eur-lex.europa.eu/legal-content/EN/TXT/?uri=COM%3A2022%3A230%3AFIN&qid=1653033742483 (accessed 11.7.22).

Comission, E., 2022b. Commission staff working document: Implementing the REPower EU action plan: investiment needs, hydrogen accelerator and achieving the bio-methane targets [WWW Document]. Brussels. URL https://eur-lex.europa.eu/legal-content/EN/TXT/?uri=SWD%3A2022%3A230%3AFIN&qid=1653033922121 (accessed 11.7.22).

Dang, Y., Sun, D., Woodard, T.L., Wang, L.-Y., Nevin, K.P., Holmes, D.E., 2017. Stimulation of the anaerobic digestion of the dry organic fraction of municipal solid waste (OFMSW) with carbon-based conductive materials. Bioresour. Technol. 238, 30–38. https://doi.org/https://doi.org/10.1016/j.biortech.2017.04.021

Das, P., Das, S., 2010. A general classification of silicon utilizing organisms, in: AGU Fall Meeting Abstracts. pp. B51I-0466.

de Quadros, T.C.F., Mangerino Sicchieri, I., Fernandes, F., Kiyomi Kuroda, E., 2022. Selection of additive materials for anaerobic co-digestion of fruit and vegetable waste and layer chicken manure. Bioresour. Technol. 361, 127659. https://doi.org/https://doi.org/10.1016/j.biortech.2022.127659

Desmond-Le Quéméner, E., Moscoviz, R., Bernet, N., Marcus, A., 2021. Modeling of interspecies electron

transfer in anaerobic microbial communities. Curr. Opin. Biotechnol. 67, 49–57. https://doi.org/https://doi.org/10.1016/j.copbio.2020.12.019

Du, Q., Mu, Q., Wu, G., 2021. Metagenomic and bioanalytical insights into quorum sensing of methanogens in anaerobic digestion systems with or without the addition of conductive filter. Sci. Total Environ. 763, 144509. https://doi.org/https://doi.org/10.1016/j.scitotenv.2020.144509

Duarte, M.S., Salvador, A.F., Cavaleiro, A.J., Stams, A.J.M., Pereira, M.A., Alves, M.M., 2020. Multiple and flexible roles of facultative anaerobic bacteria in microaerophilic oleate degradation. Environ. Microbiol. 22, 3650–3659. https://doi.org/https://doi.org/10.1111/1462-2920.15124

Duarte, M.S., Silva, S.A., Salvador, A.F., Cavaleiro, A.J., Stams, A.J.M., Alves, M.M., Pereira, M.A., 2018. Insight into the Role of Facultative Bacteria Stimulated by Microaeration in Continuous Bioreactors Converting LCFA to Methane. Environ. Sci. Technol. 52, 6497–6507. https://doi.org/10.1021/acs.est.8b00894

Emami Moghaddam, S.A., Harun, R., Mokhtar, M.N., Zakaria, R., 2018. Potential of Zeolite and Algae in Biomass Immobilization. Biomed Res. Int. 2018, 6563196. https://doi.org/10.1155/2018/6563196

Enzmann, F., Mayer, F., Rother, M., Holtmann, D., 2018. Methanogens: biochemical background and biotechnological applications. AMB Express 1–22. https://doi.org/10.1186/s13568-017-0531-x

Fauteux, F., Rémus-Borel, W., Menzies, J.G., Bélanger, R.R., 2005. Silicon and plant disease resistance against pathogenic fungi. FEMS Microbiol. Lett. 249, 1–6. https://doi.org/10.1016/j.femsle.2005.06.034

Figueira, R.B., Silva, C.J.R., Pereira, E. V., Salta, M.M., 2014. Alcohol-Aminosilicate Hybrid Coatings for Corrosion Protection of Galvanized Steel in Mortar. J. Electrochem. Soc. 161, C349–C362. https://doi.org/10.1149/2.103406jes

Fu, L., Song, T., Zhang, W., Zhang, J., Lu, Y., 2018. Stimulatory effect of magnetite nanoparticles on a highly enriched butyrate-oxidizing consortium. Front. Microbiol. 9, 1–11. https://doi.org/10.3389/fimmu.2018.01480

Fu, L., Zhou, T., Wang, J., You, L., Lu, Y., Yu, L., Zhou, S., 2019. NanoFe3O4 as Solid Electron Shuttles to Accelerate Acetotrophic Methanogenesis by *Methanosarcina barkeri*. Front. Microbiol. 10, 1–13. https://doi.org/10.3389/fmicb.2019.00388

Garcia, J.-L., Ollivier, B., Whitman, W.B., 2006. The Order *Methanomicrobiales*, in: Dworkin, M., Falkow, S., Rosenberg, E., Schleifer, K.-H., Stackebrandt, E. (Eds.), Prokaryotes. Springer, pp. 208–230. https://doi.org/10.1007/0-387-30743-5_10

Hao, L., Michaelsen, T.Y., Singleton, C.M., Dottorini, G., Kirkegaard, R.H., Albertsen, M., Nielsen, P.H., Dueholm, M.S., 2020. Novel syntrophic bacteria in full-scale anaerobic digesters revealed by genome-centric metatranscriptomics. ISME J. 14, 906–918. https://doi.org/10.1038/s41396-019-0571-0

Harirchi, S., Wainaina, S., Sar, T., Nojoumi, S.A., Parchami, Milad, Parchami, Mohsen, Varjani, S., Khanal, S.K., Wong, J., Awasthi, M.K., Taherzadeh, M.J., 2022. Microbiological insights into anaerobic digestion for biogas, hydrogen or volatile fatty acids (VFAs): a review. Bioengineered 13, 6521–6557. https://doi.org/10.1080/21655979.2022.2035986

Hassanein, A., Naresh Kumar, A., Lansing, S., 2021. Impact of electro-conductive nanoparticles additives on anaerobic digestion performance - A review. Bioresour. Technol. 342, 126023. https://doi.org/https://doi.org/10.1016/j.biortech.2021.126023

He, X., Guo, Z., Lu, J., Zhang, P., 2021. Carbon-based conductive materials accelerated methane production in anaerobic digestion of waste fat, oil and grease. Bioresour. Technol. 329, 124871. https://doi.org/https://doi.org/10.1016/j.biortech.2021.124871

Holmes, D.E., Rotaru, A.-E., Ueki, T., Shrestha, P.M., Ferry, J.G., Lovley, D.R., 2018. Electron and Proton Flux for Carbon Dioxide Reduction in *Methanosarcina barkeri* During Direct Interspecies Electron Transfer. Front. Microbiol. 9. https://doi.org/10.3389/fmicb.2018.03109

Hu, F., Zhang, S., Wang, X., Wang, C., Wu, J., Xu, L., Xu, G., Hu, Y., 2022. Investigating the role of different materials supplementation in anaerobic digestion of kitchen waste: Performance and microbial community dynamics. Biochem. Eng. J. 184, 108490. https://doi.org/https://doi.org/10.1016/j.bej.2022.108490

Huiliñir, C., Quintriqueo, A., Antileo, C., Montalvo, S., 2014. Methane production from secondary paper and pulp sludge: Effect of natural zeolite and modeling. Chem. Eng. J. 257, 131–137. https://doi.org/https://doi.org/10.1016/j.cej.2014.07.058

Jiao, P., Zhang, X., Qiu, S., Zhou, X., Tian, Z., Liang, Y., Zhang, Y., Ma, L., 2023. Pyrite-enhanced sludge digestion via stimulation of direct interspecies electron transfer between syntrophic Propionate- and Sulfur-oxidizing bacteria and Methanogens: Genome-centric metagenomics evidence. Chem. Eng. J. 456, 141089. https://doi.org/https://doi.org/10.1016/j.cej.2022.141089

Jurkić, L.M., Cepanec, I., Pavelić, S.K., Pavelić, K., 2013. Biological and therapeutic effects of ortho-silicic acid and some ortho-silicic acid-releasing compounds: New perspectives for therapy. Nutr. Metab. (Lond). 10, 2. https://doi.org/10.1186/1743-7075-10-2

Kato, S., Hashimoto, K., Watanabe, K., 2012. Methanogenesis facilitated by electric syntrophy via (semi)conductive iron-oxide minerals. Environ. Microbiol. 14, 1646–1654. https://doi.org/10.1111/j.1462-2920.2011.02611.x

Kendall, M.M., Boone, D.R., 2006. The Order *Methanosarcinales*, in: Dworkin, M., Falkow, S., Rosenberg, E., Schleifer, K.-H., Stackebrandt, E. (Eds.), Porkaryotes. Springer, pp. 244–256. https://doi.org/10.1007/0-387-30743-5_12

König, R., Cuomo, M., Pianta, E., Buetti, A., Mauri, F., Tanadini, M., Principi, P., 2022. Addition of Conductive Materials to Support Syntrophic Microorganisms in Anaerobic Digestion. Fermentation 8, 354. https://doi.org/10.3390/fermentation8080354

Kotsopoulos, T.A., Karamanlis, X., Dotas, D., Martzopoulos, G.G., 2008. The impact of different natural zeolite concentrations on the methane production in thermophilic anaerobic digestion of pig waste. Biosyst. Eng. 99, 105–111. https://doi.org/https://doi.org/10.1016/j.biosystemseng.2007.09.018

Kumar, S.S., Ghosh, P., Kataria, N., Kumar, D., Thakur, S., Pathania, D., Kumar, V., Nasrullah, M., Singh, L., 2021. The role of conductive nanoparticles in anaerobic digestion: Mechanism, current status and future perspectives. Chemosphere 280, 130601. https://doi.org/https://doi.org/10.1016/j.chemosphere.2021.130601

Kurth, J.M., Op den Camp, H.J.M., Welte, C.U., 2020. Several ways one goal—methanogenesis from unconventional substrates. Appl. Microbiol. Biotechnol. 104, 6839–6854. https://doi.org/10.1007/s00253-020-10724-7

Kutlar, F.E., Tunca, B., Yilmazel, Y.D., 2022. Carbon-based conductive materials enhance biomethane recovery from organic wastes: A review of the impacts on anaerobic treatment. Chemosphere 290, 133247. https://doi.org/https://doi.org/10.1016/j.chemosphere.2021.133247

Lamers, L., Van Diggelen, J., Op Den Camp, H., Visser, E., Lucassen, E., Vile, M., Jetten, M., Smolders, A., Roelofs, J., 2012. Microbial Transformations of Nitrogen, Sulfur, and Iron Dictate Vegetation Composition in Wetlands: A Review. Front. Microbiol. 3, 156. https://doi.org/10.3389/fmicb.2012.00156

Lane, D.J., 1991. 16S/23S rRNA Sequencing, in: Stackebrandt, E. and Goodfellow, M., Eds., Nucleic Acid Techniques in Bacterial Systematic. John Wiley & Sons, New York, pp. 115–175.

Lee, S.-H., Kang, H.-J., Lim, T.-G., Park, H.-D., 2020. Magnetite and granular activated carbon improve methanogenesis via different metabolic routes. Fuel 281, 118768. https://doi.org/https://doi.org/10.1016/j.fuel.2020.118768

Li, H., Chang, J., Liu, P., Fu, L., Ding, D., Lu, Y., 2015. Direct interspecies electron transfer accelerates syntrophic oxidation of butyrate in paddy soil enrichments. Environ. Microbiol. 17, 1533–1547. https://doi.org/https://doi.org/10.1111/1462-2920.12576

Li, L., Liu, H., Chen, Y., Yang, D., Cai, C., Yuan, S., Dai, X., 2022. Effect of Magnet-Fe3O4 composite structure on methane production during anaerobic sludge digestion: Establishment of direct interspecies electron transfer. Renew. Energy 188, 52–60. https://doi.org/https://doi.org/10.1016/j.renene.2022.01.101

Li, R., Liu, D., Zhang, Yifeng, Zhou, J., Tsang, Y.F., Liu, Z., Duan, N., Zhang, Yuanhui, 2019. Improved methane production and energy recovery of post-hydrothermal liquefaction waste water via integration of zeolite adsorption and anaerobic digestion. Sci. Total Environ. 651, 61–69. https://doi.org/https://doi.org/10.1016/j.scitotenv.2018.09.175

Lie, T.J., Costa, K.C., Lupa, B., Korpole, S., Whitman, W.B., Leigh, J.A., 2012. Essential anaplerotic role for the energy-converting hydrogenase Eha in hydrogenotrophic methanogenesis. Proc. Natl. Acad. Sci. 109, 15473–15478. https://doi.org/10.1073/pnas.1208779109

Liu, F., Rotaru, A., Shrestha, P.M., Malvankar, N.S., Nevin, K.P., Lovley, D.R., 2012. Promoting direct interspecies electron transfer with activated carbon. Energy Environ. Sci. 5, 8982–8989. https://doi.org/10.1039/c2ee22459c

Liu, F., Rotaru, A.E., Shrestha, P.M., Malvankar, N.S., Nevin, K.P., Lovley, D.R., 2015. Magnetite compensates for the lack of a pilin-associated c-type cytochrome in extracellular electron exchange. Soc. Appl. Microbiol. John Wiley Sons Ltd 17, 648–655. https://doi.org/10.1111/1462-2920.12485

Liu, H., Xu, Y., Li, L., Dai, X., Dai, L., 2021. A review on application of single and composite conductive additives for anaerobic digestion: Advances, challenges and prospects. Resour. Conserv. Recycl. 174, 105844. https://doi.org/https://doi.org/10.1016/j.resconrec.2021.105844

Liu, J., Zheng, J., Niu, Y., Zuo, Z., Zhang, J., Wei, Y., 2020. Effect of zero-valent iron combined with carbon-based materials on the mitigation of ammonia inhibition during anaerobic digestion. Bioresour. Technol. 311, 123503. https://doi.org/https://doi.org/10.1016/j.biortech.2020.123503

Liu, M., Wei, Y., Leng, X., 2021. Improving biogas production using additives in anaerobic digestion: A review. J. Clean. Prod. 297, 126666. https://doi.org/https://doi.org/10.1016/j.jclepro.2021.126666

Liu, X., Zhuo, S., Rensing, C., Zhou, S., 2018. Syntrophic growth with direct interspecies electron transfer between pili-free *Geobacter* species. ISME J. 12, 2142–2151. https://doi.org/10.1038/s41396-018-0193-y

Liu, Yiwei, Li, X., Wu, S., Tan, Z., Yang, C., 2021. Enhancing anaerobic digestion process with addition of conductive materials. Chemosphere 278, 130449. https://doi.org/https://doi.org/10.1016/j.chemosphere.2021.130449

Liu, Yang, Xiao, Q., Ye, X., Wang, C., Jia, Z., Du, J., Kong, X., Xi, Y., 2021. Effect of different charged Fe3O4 nanoparticles on methane production for anaerobic digestion of wheat straw. J. Clean. Prod. 328, 129655. https://doi.org/https://doi.org/10.1016/j.jclepro.2021.129655

Lovley, D.R., 2017a. Happy together: microbial communities that hook up to swap electrons. ISME 11, 327–336. https://doi.org/10.1038/ismej.2016.136

Lovley, D.R., 2017b. Syntrophy Goes Electric : Direct Interspecies Electron Transfer. Annu. Rev. Microbiol. 643–657.

Lovley, D.R., Ueki, T., Zhang, T., Malvankar, N.S., Shrestha, P.M., Flanagan, K.A., Aklujkar, M., Butler, J.E., Giloteaux, L., Rotaru, A.-E., Holmes, D.E., Franks, A.E., Orellana, R., Risso, C., Nevin, K.P., 2011. *Geobacter*: the microbe electric's physiology, ecology, and practical applications, in: Poole, R.K. (Ed.), Advances in Microbial Physiology. Elsevier Ltd, Amsterdam: The Netherlands, pp. 1–100. https://doi.org/10.1016/B978-0-12-387661-4.00004-5

Lyu, Z., Shao, N., Akinyemi, T., Whitman, W.B., 2018. Methanogenesis. Curr. Biol. 28, R727–R732. https://doi.org/https://doi.org/10.1016/j.cub.2018.05.021

Martínez, B., Rodríguez, A., Kulakauskas, S., Chapot-Chartier, M.-P., 2020. Cell wall homeostasis in lactic acid bacteria: threats and defences. FEMS Microbiol. Rev. 44, 538–564. https://doi.org/10.1093/femsre/fuaa021

Martins, G., Salvador, A.F., Pereira, L., Alves, M.M., 2018. Methane Production and Conductive Materials: A Critical Review. Environ. Sci. Technol. 52, 10241–10253. https://doi.org/10.1021/acs.est.8b01913

Martins, V.R., Freitas, C.J.B., Castro, A.R., Silva, R.M., Gudiña, E.J., Sequeira, J.C., Salvador, A.F., Pereira, M.A., Cavaleiro, A.J., 2021. Corksorb Enhances Alkane Degradation by Hydrocarbonoclastic Bacteria. Front. Microbiol. 12, 618270. https://doi.org/10.3389/fmicb.2021.618270

Milán, Z., Montalvo, S., Ruiz-Tagle, N., Urrutia, R., Sánchez, E., Borja, R., 2010. Influence of heavy metal supplementation on specific methanogenic activity and microbial communities detected in batch anaerobic digesters. J. Environ. Sci. Heal. Part A 45, 1307–1314.

Milán, Z., Sánchez, E., Borja, R., Weiland, P., Cruz, M., 2001. Synergistic effects of natural and modified zeolites on the methanogenesis of acetate and methanol. Biotechnol. Lett. 23, 559–562. https://doi.org/10.1023/A:1010356708118

Montalvo, S., Díaz, F., Guerrero, L., Sánchez, E., Borja, R., 2005. Effect of particle size and doses of zeolite addition on anaerobic digestion processes of synthetic and piggery wastes. Process Biochem. 40, 1475–1481. https://doi.org/https://doi.org/10.1016/j.procbio.2004.06.032

Montalvo, S., Guerrero, L., Borja, R., Sánchez, E., Milán, Z., Cortés, I., Angeles de la la Rubia, M., 2012. Application of natural zeolites in anaerobic digestion processes: A review. Appl. Clay Sci. 58, 125–133. https://doi.org/https://doi.org/10.1016/j.clay.2012.01.013

Montalvo, S., Huiliñir, C., Borja, R., Sánchez, E., Herrmann, C., 2020. Application of zeolites for biological treatment processes of solid wastes and wastewaters – A review. Bioresour. Technol. 301, 122808. https://doi.org/https://doi.org/10.1016/j.biortech.2020.122808

Moraes, B.S., Zaiat, M., Bonomi, A., 2015. Anaerobic digestion of vinasse from sugarcane ethanol production in Brazil : Challenges and perspectives. Renew. Sustain. Energy Rev. 44, 888–903. https://doi.org/10.1016/j.rser.2015.01.023

Morris, B., Henneberger, R., Huber, H., Moissl-Eichinger, C., 2013. Microbial syntrophy: interaction for the common good. FEMS Microbiol. Rev. 37, 384–406. https://doi.org/10.1111/1574-6976.12019

Mostafa, A., Im, S., Song, Y.-C., Kang, S., Kim, D.-H., 2020. Enhanced Anaerobic Digestion of Long Chain Fatty Acid by Adding Magnetite and Carbon Nanotubes. Microorganisms 8, 333. https://doi.org/10.3390/microorganisms8030333

Müller, N., Worm, P., Schink, B., Stams, A.J.M., Plugge, C.M., 2010. Syntrophic butyrate and propionate oxidation processes: from genomes to reaction mechanisms. Environ. Microbiol. Rep. 2, 489–499. https://doi.org/https://doi.org/10.1111/j.1758-2229.2010.00147.x

Nakamura, K., Terada, T., Sekiguchi, Y., Shinzato, N., Meng, X.-Y., Enoki, M., Kamagata, Y., 2006. Application of Pseudomurein Endoisopeptidase to Fluorescence In Situ Hybridization of Methanogens within the Family *Methanobacteriaceae*. Appl. Environ. Microbiol. 72, 6907–6913. https://doi.org/10.1128/AEM.01499-06

Neves, L., Pereira, M.A., Mota, M., Alves, M.M., 2009. Detection and quantification of long chain fatty acids in liquid and solid samples and its relevance to understand anaerobic digestion of lipids. Bioresour. Technol. 100, 91–96. https://doi.org/10.1016/j.biortech.2008.06.018

Nordell, E., Hansson, A.B., Karlsson, M., 2013. Zeolites relieves inhibitory stress from high concentrations of long chain fatty acids. Waste Manag. 33, 2659–2663. https://doi.org/https://doi.org/10.1016/j.wasman.2013.08.009

Oh, J.K., Yegin, Y., Yang, F., Zhang, M., Li, J., Huang, S., Verkhoturov, S. V, Schweikert, E.A., Perez-Lewis, K., Scholar, E.A., Taylor, T.M., Castillo, A., Cisneros-Zevallos, L., Min, Y., Akbulut, M., 2018. The influence of surface chemistry on the kinetics and thermodynamics of bacterial adhesion. Sci. Rep. 8, 17247. https://doi.org/10.1038/s41598-018-35343-1

Pan, X., Angelidaki, I., Alvarado-Morales, M., Liu, H., Liu, Y., Huang, X., Zhu, G., 2016. Methane production from formate, acetate and H2/CO2; focusing on kinetics and microbial characterization. Bioresour. Technol. 218, 796–806. https://doi.org/https://doi.org/10.1016/j.biortech.2016.07.032

Paritosh, K., Yadav, M., Chawade, A., Sahoo, D., Kesharwani, N., Pareek, N., Vivekanand, V., 2020. Additives as a Support Structure for Specific Biochemical Activity Boosts in Anaerobic Digestion: A Review. Front. Energy Res. 8, 88. https://doi.org/10.3389/fenrg.2020.00088

Park, J.H., Kang, H.J., Park, K.H., Park, H.D., 2018. Direct interspecies electron transfer via conductive materials: A perspective for anaerobic digestion applications. Bioresour. Technol. 254, 300–311. https://doi.org/10.1016/j.biortech.2018.01.095

Park, J.-H., Park, Jong-Hun, Seong, H.J., Sul, W.J., Jin, K.-H., Park, H.-D., 2018. Metagenomic insight into methanogenic reactors promoting direct interspecies electron transfer via granular activated carbon. Bioresour. Technol. 259, 414–422. https://doi.org/10.1016/j.biortech.2018.03.050

Park, S.-G., Rhee, C., Shin, S.G., Shin, J., Mohamed, H.O., Choi, Y.-J., Chae, K.-J., 2019. Methanogenesis stimulation and inhibition for the production of different target electrobiofuels in microbial electrolysis cells through an on-demand control strategy using the coenzyme M and 2-bromoethanesulfonate. Environ. Int. 131, 105006.

https://doi.org/https://doi.org/10.1016/j.envint.2019.105006

Pavlovic, J., Kostic, L., Bosnic, P., Kirkby, E.A., Nikolic, M., 2021. Interactions of Silicon With Essential and Beneficial Elements in Plants. Front. Plant Sci. 12, 1224. https://doi.org/10.3389/fpls.2021.697592

Peng, H., Zhang, Y., Tan, D., Zhao, Z., Zhao, H., Quan, X., 2018. Roles of magnetite and granular activated carbon in improvement of anaerobic sludge digestion. Bioresour. Technol. 249, 666–672. https://doi.org/https://doi.org/10.1016/j.biortech.2017.10.047

Pereira, L., Dias, P., Soares, O.S.G.P., Ramalho, P.S.F., Pereira, M.F.R., Alves, M.M., 2017. Synthesis, characterization and application of magnetic carbon materials as electron shuttles for the biological and chemical reduction of the azo dye Acid Orange 10. Appl. Catal. B Environ. 212, 175–184. https://doi.org/10.1016/j.apcatb.2017.04.060

Pereira, L., Pereira, R., Pereira, M.F.R., van der Zee, F.P., Cervantes, F.J., Alves, M.M., 2010. Thermal modification of activated carbon surface chemistry improves its capacity as redox mediator for azo dye reduction. J. Hazard. Mater. 183, 931–939. https://doi.org/10.1016/j.jhazmat.2010.08.005

Prussi, M., Julea, A., Lonza, L., Thiel, C., 2021. Biomethane as alternative fuel for the EU road sector: analysis of existing and planned infrastructure. Energy Strateg. Rev. 33, 100612. https://doi.org/https://doi.org/10.1016/j.esr.2020.100612

Rasapoor, M., Young, B., Brar, R., Sarmah, A., Zhuang, W., Baroutian, S., 2020. Recognizing the challenges of anaerobic digestion: Critical steps toward improving biogas generation. Fuel 261, 1–12. https://doi.org/10.1016/j.fuel.2019.116497

Reithmaier, G.-M.S., Knorr, K.-H., Arnhold, S., Planer-Friedrich, B., Schaller, J., 2017. Enhanced silicon availability leads to increased methane production, nutrient and toxicant mobility in peatlands. Sci. Rep. 7, 8728. https://doi.org/10.1038/s41598-017-09130-3

Restivo, J., Rocha, R.P., Silva, A.M.T., Órfão, J.J.M., Pereira, M.F.R., Figueiredo, J.L., 2014. Catalytic performance of heteroatom-modified carbon nanotubes in advanced oxidation processes. Chinese J. Catal. 35, 896–905. https://doi.org/https://doi.org/10.1016/S1872-2067(14)60103-0

Rocha, R.P., Silva, A.M.T., Romero, S.M.M., Pereira, M.F.R., Figueiredo, J.L., 2014. The role of O- and S-containing surface groups on carbon nanotubes for the elimination of organic pollutants by catalytic wet air oxidation. Appl. Catal. B Environ. 147, 314–321. https://doi.org/https://doi.org/10.1016/j.apcatb.2013.09.009

Romero-Güiza, M.S., Vila, J., Mata-Alvarez, J., Chimenos, J.M., Astals, S., 2016. The role of additives on anaerobic digestion: A review. Renew. Sustain. Energy Rev. 58, 1486–1499. https://doi.org/https://doi.org/10.1016/j.rser.2015.12.094

Roopnarain, A., Rama, H., Ndaba, B., Bello-Akinosho, M., Bamuza-Pemu, E., Adeleke, R., 2021. Unravelling the anaerobic digestion 'black box': Biotechnological approaches for process optimization. Renew. Sustain. Energy Rev. 152, 111717. https://doi.org/https://doi.org/10.1016/j.rser.2021.111717

Rotaru, A.-E., Posth, N.R., Löscher, C.R., Miracle, M.R., Vicente, E., Cox, R.P., Thompson, J., Poulton, S.W., Thamdrup, B., 2018. Interspecies interactions mediated by conductive minerals in the sediments of the ferruginous Lake La Cruz, Spain. bioRxiv. https://doi.org/10.1101/366542

Rotaru, A.-E., Shrestha, P.M., Liu, F., Markovaite, B., Chen, S., Nevin, K.P., Lovley, D.R., 2014a. Direct interspecies electron transfer between *Geobacter metallireducens* and *Methanosarcina barkeri*. Appl. Environ. Microbiol. 80, 4599–4605. https://doi.org/10.1128/AEM.00895-14

Rotaru, A.-E., Shrestha, P.M., Liu, F., Shrestha, M., Shrestha, D., Embree, M., Zengler, K., Wardman, C., Nevin, K.P., Lovley, D.R., 2014b. A new model for electron flow during anaerobic digestion: direct interspecies electron transfer to *Methanosaeta* for the reduction of carbon dioxide to methane. Energy Environ. Sci. 7, 408–415. https://doi.org/10.1039/C3EE42189A

Rotaru, A.-E., Yee, M.O., Musat, F., 2021. Microbes trading electricity in consortia of environmental and biotechnological significance. Curr. Opin. Biotechnol. 67, 119–129. https://doi.org/https://doi.org/10.1016/j.copbio.2021.01.014

Ryue, J., Lin, L., Liu, Y., Lu, W., McCartney, D., Dhar, B.R., 2019. Comparative effects of GAC addition on methane productivity and microbial community in mesophilic and thermophilic anaerobic digestion of food waste. Biochem. Eng. J. 146, 79–87. https://doi.org/https://doi.org/10.1016/j.bej.2019.03.010

Salvador, A.F., Cavaleiro, A.J., Paulo, A.M.S., Silva, S.A., Guedes, A.P., Pereira, M.A., Stams, A.J.M., Sousa, D.Z., Alves, M.M., Müller, V., 2019. Inhibition Studies with 2-Bromoethanesulfonate Reveal a Novel Syntrophic Relationship in Anaerobic Oleate Degradation. Appl. Environ. Microbiol. 85. https://doi.org/10.1128/AEM.01733-18

Salvador, A.F., Martins, G., Melle-Franco, M., Serpa, R., Stams, A.J.M., Cavaleiro, A.J., Pereira, M.A., Alves, M.M., 2017. Carbon nanotubes accelerate methane production in pure cultures of methanogens and in a syntrophic coculture. Environ. Microbiol. 19, 2727–2739. https://doi.org/10.1111/1462-2920.13774

Schink, B., Montag, D., Keller, A., Müller, N., 2017. Hydrogen or formate: Alternative key players in methanogenic degradation. Environ. Microbiol. Rep. 9, 189–202. https://doi.org/https://doi.org/10.1111/1758-2229.12524

Schmidt, A., Müller, N., Schink, B., Schleheck, D., 2013. A Proteomic View at the Biochemistry of Syntrophic Butyrate Oxidation in *Syntrophomonas wolfei*. PLoS One 8, e56905. https://doi.org/10.1371/journal.pone.0056905

Sequeira, J.C., Rocha, M., Alves, M.M., Salvador, A.F., 2022. UPIMAPI, reCOGnizer and KEGGCharter: Bioinformatics tools for functional annotation and visualization of (meta)-omics datasets. Comput. Struct. Biotechnol. J. 20, 1798–1810. https://doi.org/https://doi.org/10.1016/j.csbj.2022.03.042

Sequeira, J.C., Rocha, M., Alves, M.M., Salvador, A.F., 2018. MOSCA: An Automated Pipeline for Integrated Metagenomics and Metatranscriptomics Data Analysis. Adv. Intell. Syst. Comput. 803, 183–191. https://doi.org/10.1007/978-3-319-98702-6

Shen, L., Zhao, Q., Wu, X., Li, X., Li, Q., Wang, Y., 2016. Interspecies electron transfer in syntrophic methanogenic consortia: From cultures to bioreactors. Renew. Sustain. Energy Rev. 54, 1358–1367. https://doi.org/10.1016/j.rser.2015.10.102

Sieber, J.R., Crable, B.R., Sheik, C.S., Hurst, G.B., Rohlin, L., Gunsalus, R.P., McInerney, M.J., 2015. Proteomic analysis reveals metabolic and regulatory systems involved in the syntrophic and axenic lifestyle of *Syntrophomonas wolfei*. Front. Microbiol. 6, 1–9. https://doi.org/10.3389/fmicb.2015.00115

Sieber, J.R., Le, H.M., Mcinerney, M.J., 2014. The importance of hydrogen and formate transfer for syntrophic fatty , aromatic and alicyclic metabolism. Environ. Microbiol. 16, 177–188. https://doi.org/10.1111/1462-2920.12269

Sieber, J.R., Mcinerney, M.J., Gunsalus, R.P., 2012. Genomic Insights into Syntrophy: The Paradigm for

Anaerobic Metabolic Cooperation. Annu. Rev. Microbiol. 66, 429–452. https://doi.org/10.1146/annurev-micro-090110-102844

Sieber, J R, McInerney, M.J., Plugge, C.M., Schink, B., Gunsalus, R.P., 2010. Methanogenesis: Syntrophic Metabolism, in: Timmis, K.N. (Ed.), Handbook of Hydrocarbon and Lipid Microbiology. Springer Berlin Heidelberg, Berlin, Heidelberg, pp. 337–355. https://doi.org/10.1007/978-3-540-77587-4_22

Sieber, Jessica R., Sims, D.R., Han, C., Kim, E., Lykidis, A., Lapidus, A.L., McDonnald, E., Rohlin, L., Culley, D.E., Gunsalus, R., McInerney, M.J., 2010. The genome of *Syntrophomonas wolfei*: new insights into syntrophic metabolism and biohydrogen production. Environ. Microbiol. 12, 2289–2301. https://doi.org/https://doi.org/10.1111/j.1462-2920.2010.02237.x

Sikora, A., Detman, A., Mielecki, D., Chojnacka, A., Błaszczyk, M., 2018. Searching for Metabolic Pathways of Anaerobic Digestion: A Useful List of the Key Enzymes. https://doi.org/10.5772/intechopen.81256

Silva, A.R., Alves, M.M., Pereira, L., 2021a. Progress and prospects of applying carbon-based materials (and nanomaterials) to accelerate anaerobic bioprocesses for the removal of micropollutants. Microb. Biotechnol. 15, 1073–1100. https://doi.org/https://doi.org/10.1111/1751-7915.13822

Silva, A.R., Cavaleiro, A.J., Soares, O.S.G.P., Braga, C.S.N., Salvador, A.F., Pereira, M.F.R., Alves, M.M., Pereira, L., 2021b. Detoxification of Ciprofloxacin in an Anaerobic Bioprocess Supplemented with Magnetic Carbon Nanotubes: Contribution of Adsorption and Biodegradation Mechanisms. Int. J. Mol. Sci. 22, 2932. https://doi.org/10.3390/ijms22062932

Silva, A.R., Soares, O.S.G.P., Pereira, M.F.R., Alves, M.M., Pereira, L., 2020. Tailoring Carbon Nanotubes to Enhance their Efficiency as Electron Shuttle on the Biological Removal of Acid Orange 10 Under Anaerobic Conditions. Nanomaterials 10. https://doi.org/10.3390/nano10122496

Silva, R.M., Abreu, A.A., Salvador, A.F., Alves, M.M., Neves, I.C., Pereira, M.A., 2021. Zeolite addition to improve biohydrogen production from dark fermentation of C5/C6-sugars and Sargassum sp. biomass. Sci. Rep. 11, 16350. https://doi.org/10.1038/s41598-021-95615-1

Soares, O.S.G.P., Rocha, R.P., Órfão, J.J.M., Pereira, M.F.R., Figueiredo, J.L., 2019. Mechanothermal Approach for N-, S-, P-, and B-Doping of Carbon Nanotubes: Methodology and Catalytic Performance in Wet Air Oxidation. J. Carbon Res. 5. https://doi.org/10.3390/c5020030

Song, X., Liu, J., Jiang, Q., Zhang, P., Shao, Y., He, W., Feng, Y., 2019. Enhanced electron transfer and methane production from low-strength wastewater using a new granular activated carbon modified with nano-Fe3O4. Chem. Eng. J. 374, 1344–1352. https://doi.org/https://doi.org/10.1016/j.cej.2019.05.216

Sousa, D.Z., Salvador, A.F., Ramos, J., Guedes, A.P., Barbosa, S., Stams, A.J.M., Alves, M.M., Pereira, M.A., 2013. Activity and Viability of Methanogens in Anaerobic Digestion of Unsaturated and Saturated Long-Chain Fatty Acids. Appl. Environ. Microbiol. 79, 4239–4245. https://doi.org/10.1128/aem.00035-13

Sousa, D.Z., Smidt, H., Alves, M.M., Stams, A.J.M., 2009. Ecophysiology of syntrophic communities that degrade saturated and unsaturated long-chain fatty acids. FEMS - Fed. Eur. Microbiol. Soc. 68, 257–272. https://doi.org/10.1111/j.1574-6941.2009.00680.x

Sousa, D.Z., Smidt, H., Alves, M.M., Stams, A.J.M., 2007. *Syntrophomonas zehnderi* sp. nov., an anaerobe that degrades long-chain fatty acids in co-culture with *Methanobacterium formicicum*. Int. J. Syst. Evol. Microbiol. 57, 609–615. https://doi.org/10.1099/ijs.0.64734-0

Spadafora, E., 2011. Noncontact Atomic Force Microscopy and Kelvin Probe Force Microscopy investigations of model materials for organic photovoltaics.

Stams, A.J.M., 1994. Metabolic interactions between anaerobic bacteria in methanogenic environments. Antonie Van Leeuwenhoek 66, 271–294.

Stams, A.J.M., Dijk, J.B. Van, Dijkema, C., Plugge, C.M., 1993. Growth of syntrophic propionate-oxidizing bacteria with fumarate in the absence of methanogenic bacteria. Appl. Environ. Microbiol. 59, 1114–1119.

Stams, A.J.M., Plugge, C.M., 2009. Electron transfer in syntrophic communities of anaerobic bacteria and archaea. Nat. Rev. Microbiol. 7, 568–577. https://doi.org/10.1038/nrmicro2166

Stams, A.J.M., Worm, P., Souda, D.Z., Alves, M.M., Plugge, C.M., 2012. Syntrophic degradation of fatty acids by methanogenic communities, in: Hallenbeck, P.C. (Ed.), Microbial Technologies in Advanced Biofuels Production. Springer, pp. 127–142.

Summers, Z.M., Fogarty, H.E., Leang, C., Franks, A.E., Malvankar, N.S., Lovley, D.R., 2010. Direct Exchange of Electrons Within Aggregates of an Evolved Syntrophic Coculture of Anaerobic Bacteria. Science (80-.). 330, 1413–1415. https://doi.org/10.1126/science.1196526

Szerement, J., Szatanik-Kloc, A., Jarosz, R., Bajda, T., Mierzwa-Hersztek, M., 2021. Contemporary applications of natural and synthetic zeolites from fly ash in agriculture and environmental protection. J. Clean. Prod. 311, 127461. https://doi.org/https://doi.org/10.1016/j.jclepro.2021.127461

Tan, L.C., Lens, P.N.L., 2021. Addition of granular activated carbon during anaerobic oleate degradation overcomes inhibition and promotes methanogenic activity. Environ. Sci. Water Res. Technol. 7, 762–774. https://doi.org/10.1039/D0EW01093F

Tan, L.C., Lin, R., Murphy, J.D., Lens, P.N.L., 2021. Granular activated carbon supplementation enhances anaerobic digestion of lipid-rich wastewaters. Renew. Energy 171, 958–970. https://doi.org/https://doi.org/10.1016/j.renene.2021.02.087

Tessonnier, J.P., Rosenthal, D., Hansen, T.W., Hess, C., Schuster, M.E., Blume, R., Girgsdies, F., Pfänder, N., Timpe, O., Su, D.S., Schlögl, R., 2009. Analysis of the structure and chemical properties of some commercial carbon nanostructures. Carbon N. Y. 47, 1779–1798. https://doi.org/10.1016/j.carbon.2009.02.032

Thauer, R.K., Kaster, A.-K., Seedorf, H., Buckel, W., Hedderich, R., 2008. Methanogenic archaea: ecologically relevant differences in energy conservation. Nat. Rev. Microbiol. 6, 579–591. https://doi.org/10.1038/nrmicro1931

Van Bodegom, P.M., Scholten, J.C.M., Stams, A.J.M., 2004. Direct inhibition of methanogenesis by ferric iron. FEMS Microbiol. Ecol. 49, 261–268. https://doi.org/10.1016/j.femsec.2004.03.017

Van Steendam, C., Smets, I., Skerlos, S., Raskin, L., 2019. Improving anaerobic digestion via direct interspecies electron transfer requires development of suitable characterization methods. Curr. Opin. Biotechnol. 57, 183–190. https://doi.org/https://doi.org/10.1016/j.copbio.2019.03.018

Vanwonterghem, I., Jensen, P.D., Dennis, P.G., Hugenholtz, P., Rabaey, K., Tyson, G.W., 2014. Deterministic processes guide long-term synchronised population dynamics in replicate anaerobic digesters. ISME J. 8, 2015–2028. https://doi.org/10.1038/ismej.2014.50

Veiga, M.C., Jain, M.K., Wu, W., Hollingsworth, R.I., 1997. Composition and Role of Extracellular Polymers in Methanogenic Granules. Appl. Environ. Microbiol. 63, 403–407.

Wainaina, S., Lukitawesa, Awasthi, M.K., Taherzadeh, M.J., 2019. Bioengineering of anaerobic digestion for volatile fatty acids, hydrogen or methane production: A critical review. Bioengineered 10, 437–458. https://doi.org/10.1080/21655979.2019.1673937

Wainwright, M., Al-Wajeeh, K., Grayston, S.J., 1997. Effect of silicic acid and other silicon compounds on fungal growth in oligotrophic and nutrient-rich media. Mycol. Res. 101, 933–938. https://doi.org/https://doi.org/10.1017/S0953756297003560

Walker, D.J.F., Nevin, K.P., Holmes, D.E., Rotaru, A.-E., Ward, J.E., Woodard, T.L., Zhu, J., Ueki, T., Nonnenmann, S.S., McInerney, M.J., Lovley, D.R., 2020. *Syntrophus* conductive pili demonstrate that common hydrogen-donating syntrophs can have a direct electron transfer option. ISME J. 14, 837–846. https://doi.org/10.1038/s41396-019-0575-9

Wang, C., Liu, J., Xu, X., Zhu, L., 2022. Response of methanogenic granules enhanced by magnetite to ammonia stress. Water Res. 212, 118123. https://doi.org/https://doi.org/10.1016/j.watres.2022.118123

Wang, G., Li, Q., Li, Y., Xing, Y., Yao, G., Liu, Y., Chen, R., Wang, X.C., 2020. Redox-active biochar facilitates potential electron tranfer between syntrophic partners to enhance anaerobic digestion under high organic loading rate. Bioresour. Technol. 298, 122524. https://doi.org/https://doi.org/10.1016/j.biortech.2019.122524

Wang, H., Byrne, J.M., Liu, P., Liu, J., Dong, X., Lu, Y., 2020. Redox cycling of Fe(II) and Fe(III) in magnetite accelerates aceticlastic methanogenesis by *Methanosarcina mazei*. Environ. Microbiol. Rep. 12, 97–109. https://doi.org/https://doi.org/10.1111/1758-2229.12819

Wang, H., Xu, J., Sheng, L., Liu, X., Zong, M., Yao, D., 2019. Anaerobic Digestion Technology for Methane Production Using Deer Manure Under Different Experimental Conditions. Energies. https://doi.org/10.3390/en12091819

Wang, Z., Zhang, W., Xing, X., Li, X., Zheng, D., Bao, H., Xing, L., 2022. Effects of ferroferric oxide on propionate methanogenesis in sequencing batch reactors: Microbial community structure and metagenomic analysis. Bioresour. Technol. 363, 127909. https://doi.org/https://doi.org/10.1016/j.biortech.2022.127909

Weidenfeller, B., Höfer, M., Schilling, F., 2002. Thermal and electrical properties of magnetite filled polymers. Compos. Part A Appl. Sci. Manuf. 33, 1041–1053. https://doi.org/https://doi.org/10.1016/S1359-835X(02)00085-4

Whitman, W.B., Bowen, T.L., Boone, D.R., 2006. The Methanogenic Bacteria, in: Dworkin, M., Falkow, S., Rosenberg, E., Schleifer, K.-H., Stackebrandt, E. (Eds.), The Prokaryotes: Volume 3: Archaea. Bacteria: Firmicutes, Actinomycetes. Springer New York, New York, NY, pp. 165–207. https://doi.org/10.1007/0-387-30743-5_9

Wu, L., Jin, T., Chen, H., Shen, Z., Zhou, Y., 2023. Conductive materials as fantastic toolkits to stimulate direct interspecies electron transfer in anaerobic digestion: new insights into methanogenesis contribution, characterization technology, and downstream treatment. J. Environ. Manage. 326, 116732. https://doi.org/https://doi.org/10.1016/j.jenvman.2022.116732

Wu, Y.-W., Simmons, B.A., Singer, S.W., 2016. MaxBin 2.0: an automated binning algorithm to recover genomes from multiple metagenomic datasets. Bioinformatics 32, 605–607. https://doi.org/10.1093/bioinformatics/btv638

Wu, Y., Wang, S., Liang, D., Li, N., 2020. Conductive materials in anaerobic digestion: From mechanism to application. Bioresour. Technol. 298, 122403.

https://doi.org/https://doi.org/10.1016/j.biortech.2019.122403

Xia, X., Zhang, J., Song, T., 2019. Stimulation of Smithella -dominating propionate oxidation in a sediment enrichment by magnetite and carbon nanotubes. Environ. Microbiol. 11, 236–248. https://doi.org/10.1111/1758-2229.12737

Xiao, L., Liu, J., Senthil Kumar, P., Zhou, M., Yu, J., Lichtfouse, E., 2022. Enhanced methane production by granular activated carbon: A review. Fuel 320, 123903. https://doi.org/https://doi.org/10.1016/j.fuel.2022.123903

Xiao, L., Zheng, S., Lichtfouse, E., Luo, M., Tan, Y., Liu, F., 2020. Carbon nanotubes accelerate acetoclastic methanogenesis: From pure cultures to anaerobic soils. Soil Biol. Biochem. 150, 107938. https://doi.org/https://doi.org/10.1016/j.soilbio.2020.107938

Xu, H., Chang, J., Wang, H., Liu, Y., Zhang, X., Liang, P., Huang, X., 2019. Enhancing direct interspecies electron transfer in syntrophic-methanogenic associations with (semi)conductive iron oxides: Effects and mechanisms. Sci. Total Environ. 695, 133876. https://doi.org/https://doi.org/10.1016/j.scitotenv.2019.133876

Xu, J., Kumar Khanal, S., Kang, Y., Zhu, J., Huang, X., Zong, Y., Pang, W., Surendra, K.C., Xie, L., 2022. Role of interspecies electron transfer stimulation in enhancing anaerobic digestion under ammonia stress: Mechanisms, advances, and perspectives. Bioresour. Technol. 360, 127558. https://doi.org/https://doi.org/10.1016/j.biortech.2022.127558

Xu, S., Han, R., Zhang, Y., He, C., Liu, H., 2018. Differentiated stimulating effects of activated carbon on methanogenic degradation of acetate, propionate and butyrate. Waste Manag. 76, 394–403. https://doi.org/10.1016/j.wasman.2018.03.037

Yan, W., Mukherjee, M., Zhou, Y., 2020. Direct interspecies electron transfer (DIET) can be suppressed under ammonia-stressed condition – Reevaluate the role of conductive materials. Water Res. 183, 116094. https://doi.org/https://doi.org/10.1016/j.watres.2020.116094

Yan, W., Sun, F., Liu, J., Zhou, Y., 2018. Enhanced anaerobic phenol degradation by conductive materials via EPS and microbial community alteration. Chem. Eng. J. 352, 1–9. https://doi.org/https://doi.org/10.1016/j.cej.2018.06.187

Yang, Y., Zhang, Y., Li, Z., Zhao, Zhiqiang, Quan, X., Zhao, Zisheng, 2017. Adding granular activated carbon into anaerobic sludge digestion to promote methane production and sludge decomposition. J. Clean. Prod. 149, 1101–1108. https://doi.org/https://doi.org/10.1016/j.jclepro.2017.02.156

Yang, Z., Guo, R., Shi, X., Wang, C., Wang, L., 2016. Magnetite nanoparticles enable a rapid conversion of volatile fatty acids to methane. RSC Adv. 6, 25662–25668. https://doi.org/10.1039/C6RA02280D

Yee, M.O., Rotaru, A.-E., 2020. Extracellular electron uptake in *Methanosarcinales* is independent of multiheme c-type cytochromes. Sci. Rep. 10, 372. https://doi.org/10.1038/s41598-019-57206-z

Yee, M.O., Snoeyenbos-West, O.L.O., Thamdrup, B., Ottosen, L.D.M., Rotaru, A.-E., 2019. Extracellular electron uptake by two *Methanosarcina* species. bioRxiv. https://doi.org/10.1101/458091

Yimlamai, I., Niamlang, S., Chanthaanont, P., Kunanuraksapong, R., Changkhamchom, S., Sirivat, A., 2011. Electrical conductivity response and sensitivity of ZSM-5, Y, and mordenite zeolites towards ethanol vapor. Ionics (Kiel). 17, 607–615. https://doi.org/10.1007/s11581-011-0545-3

Yin, J., Li, J., Qiu, X., Zhou, Y., Wang, M., Feng, H., Li, Y., Chen, X., Chen, T., 2022. Effect of magnetite particle size on propionate degradation in the propionate-based anaerobic system. Sci. Total

Environ. 847, 157592. https://doi.org/https://doi.org/10.1016/j.scitotenv.2022.157592

Yin, Q., Gu, M., Hermanowicz, S.W., Hu, H., Wu, G., 2020. Potential interactions between syntrophic bacteria and methanogens via type IV pili and quorum-sensing systems. Environ. Int. 138, 105650. https://doi.org/https://doi.org/10.1016/j.envint.2020.105650

Yuan, H.Y., Ding, L.J., Zama, E.F., Liu, P.P., Hozzein, W.N., Zhu, Y.G., 2018. Biochar Modulates Methanogenesis through Electron Syntrophy of Microorganisms with Ethanol as a Substrate. Environ. Sci. Technol. 52, 12198–12207. https://doi.org/10.1021/acs.est.8b04121

Zabranska, J., Pokorna, D., 2018. Bioconversion of carbon dioxide to methane using hydrogen and hydrogenotrophic methanogens. Biotechnol. Adv. 36, 707–720. https://doi.org/https://doi.org/10.1016/j.biotechadv.2017.12.003

Zhang, J., Lu, Y., 2016. Conductive Fe3O4 Nanoparticles Accelerate Syntrophic Methane Production from Butyrate Oxidation in Two Different Lake Sediments. Front. Microbiol. 7, 1–9. https://doi.org/10.3389/fmicb.2016.01316

Zhang, Jingxin, Tian, H., Wang, X., Tong, Y.W., 2020. Effects of activated carbon on mesophilic and thermophilic anaerobic digestion of food waste: Process performance and life cycle assessment. Chem. Eng. J. 399, 125757. https://doi.org/https://doi.org/10.1016/j.cej.2020.125757

Zhang, Jing, Zhang, R., Wang, H., Yang, K., 2020. Direct interspecies electron transfer stimulated by granular activated carbon enhances anaerobic methanation efficiency from typical kitchen waste lipid-rapeseed oil. Sci. Total Environ. 704, 135282. https://doi.org/https://doi.org/10.1016/j.scitotenv.2019.135282

Zhang, J., Zhao, W., Zhang, H., Wang, Z., Fan, C., Zang, L., 2018. Recent achievements in enhancing anaerobic digestion with carbon- based functional materials. Bioresour. Technol. 266, 555–567. https://doi.org/https://doi.org/10.1016/j.biortech.2018.07.076

Zhang, S., Chang, J., Lin, C., Pan, Y., Cui, K., Zhang, X., Liang, P., Huang, X., 2017. Enhancement of methanogenesis via direct interspecies electron transfer between *Geobacteraceae* and *Methanosaetaceae* conducted by granular activated carbon. Bioresour. Technol. 245, 132–137. https://doi.org/10.1016/j.biortech.2017.08.111

Zhang, W., Zhang, J., Lu, Y., 2018. Stimulation of carbon nanomaterials on syntrophic oxidation of butyrate in sediment enrichments and a defined coculture. Sci. Rep. 8, 1–13. https://doi.org/10.1038/s41598-018-30745-7

Zhang, Y., Li, C., Yuan, Z., Wang, R., Angelidaki, I., Zhu, G., 2023. Syntrophy mechanism, microbial population, and process optimization for volatile fatty acids metabolism in anaerobic digestion. Chem. Eng. J. 452, 139137. https://doi.org/https://doi.org/10.1016/j.cej.2022.139137

Zhao, Z., Li, Y., Quan, X., Zhang, Y., 2017a. Towards engineering application: Potential mechanism for enhancing anaerobic digestion of complex organic waste with different types of conductive materials. Water Res. 115, 266–277. https://doi.org/10.1016/j.watres.2017.02.067

Zhao, Z., Li, Y., Yu, Q., Zhang, Y., 2018. Ferroferric oxide triggered possible direct interspecies electron transfer between *Syntrophomonas* and *Methanosaeta* to enhance waste activated sludge anaerobic digestion. Bioresour. Technol. 250, 79–85. https://doi.org/https://doi.org/10.1016/j.biortech.2017.11.003

Zhao, Z., Li, Y., Zhang, Y., Lovley, D.R., 2020. Sparking Anaerobic Digestion: Promoting Direct Interspecies Electron Transfer to Enhance Methane Production. iScience 23, 101794. https://doi.org/https://doi.org/10.1016/j.isci.2020.101794

Zhao, Z., Zhang, Y., Holmes, D.E., Dang, Y., Woodard, T.L., Nevin, K.P., Lovley, D.R., 2016. Potential enhancement of direct interspecies electron transfer for syntrophic metabolism of propionate and butyrate with biochar in up-flow anaerobic sludge blanket reactors. Bioresour. Technol. 209, 148–156. https://doi.org/10.1016/j.biortech.2016.03.005

Zhao, Z., Zhang, Y., Li, Y., Dang, Y., Zhu, T., Quan, X., 2017b. Potentially shifting from interspecies hydrogen transfer to direct interspecies electron transfer for syntrophic metabolism to resist acidic impact with conductive carbon cloth. Chem. Eng. J. 313, 10–18. https://doi.org/https://doi.org/10.1016/j.cej.2016.11.149

Zheng, H., Li, D., Stanislaus, M.S., Zhang, N., Zhu, Q., Hu, X., Yang, Y., 2015. Development of a bio-zeolite fixed-bed bioreactor for mitigating ammonia inhibition of anaerobic digestion with extremely high ammonium concentration livestock waste. Chem. Eng. J. 280, 106–114. https://doi.org/https://doi.org/10.1016/j.cej.2015.06.024

Zheng, S., Liu, F., Wang, B., Zhang, Y., Lovley, D.R., 2020. *Methanobacterium* Capable of Direct Interspecies Electron Transfer. Environ. Sci. \& Technol. 54, 15347–15354. https://doi.org/10.1021/acs.est.0c05525

Zhong, Y., He, J., Wu, F., Zhang, P., Zou, X., Pan, X., Zhang, J., 2022. Metagenomic analysis reveals the size effect of magnetite on anaerobic digestion of waste activated sludge after thermal hydrolysis pretreatment. Sci. Total Environ. 851, 158133. https://doi.org/https://doi.org/10.1016/j.scitotenv.2022.158133

Ziels, R.M., Nobu, M.K., Sousa, D.Z., 2019. Elucidating Syntrophic Butyrate-Degrading Populations in Anaerobic Digesters Using Stable-Isotope-Informed Genome-Resolved Metagenomics. mSystems 4, e00159-19. https://doi.org/10.1128/mSystems.00159-19